

11-2007

Development of the Midwest Guardrail System (MGS) W-beam to Thrie Beam Transition Element

Ronald K. Faller

University of Nebraska - Lincoln, rfaller1@unl.edu

John R. Rohde

jrohde1@unl.edu

Robert W. Bielenberg

University of Nebraska - Lincoln, rbielenberg2@unl.edu

Karla A. Polivka

University of Nebraska - Lincoln, kpolivka2@unl.edu

Dean L. Sicking

University of Nebraska - Lincoln, dsicking1@unl.edu

See next page for additional authors

Follow this and additional works at: <http://digitalcommons.unl.edu/ndor>



Part of the [Transportation Engineering Commons](#)

Faller, Ronald K.; Rohde, John R.; Bielenberg, Robert W.; Polivka, Karla A.; Sicking, Dean L.; Reid, John D.; Eller, Craig M.; and Allison, Erin M., "Development of the Midwest Guardrail System (MGS) W-beam to Thrie Beam Transition Element" (2007).

Nebraska Department of Transportation Research Reports. 39.

<http://digitalcommons.unl.edu/ndor/39>

This Article is brought to you for free and open access by the Nebraska LTAP at DigitalCommons@University of Nebraska - Lincoln. It has been accepted for inclusion in Nebraska Department of Transportation Research Reports by an authorized administrator of DigitalCommons@University of Nebraska - Lincoln.

Authors

Ronald K. Faller, John R. Rohde, Robert W. Bielenberg, Karla A. Polivka, Dean L. Sicking, John D. Reid, Craig M. Eller, and Erin M. Allison

*Midwest States' Regional Pooled Fund Research Program
Fiscal Years 2000-2002, 2005-2006 (Years 11-12, 16)
Research Project Number SPR-3(017)
NDOR Sponsoring Agency Codes RFPF-01-04, RFPF-02-05, RFPF-06-04*

DEVELOPMENT OF THE MIDWEST GUARDRAIL SYSTEM (MGS) W-BEAM TO THRIE BEAM TRANSITION ELEMENT

Submitted by

Craig M. Eller
Former Undergraduate Research Assistant

Ronald K. Faller, Ph.D., P.E.
Research Assistant Professor

John R. Rohde, Ph.D., P.E.
Associate Professor

Robert W. Bielenberg, M.S.M.E., E.I.T.
Research Associate Engineer

Karla A. Polivka, M.S.M.E., E.I.T.
Research Associate Engineer

Dean L. Sicking, Ph.D., P.E.
Professor and MwRSF Director

John D. Reid, Ph.D.
Professor

Erin M. Allison
Undergraduate Research Assistant

MIDWEST ROADSIDE SAFETY FACILITY

University of Nebraska-Lincoln
527 Nebraska Hall
Lincoln, Nebraska 68588-0529
(402) 472-6864

Submitted to

MIDWEST STATES' REGIONAL POOLED FUND PROGRAM

Nebraska Department of Roads
1500 Nebraska Highway 2
Lincoln, Nebraska 68502

MwRSF Research Report No. TRP-03-167-07

November 26, 2007

Technical Report Documentation Page

1. Report No. TRP-03-167-07	2.	3. Recipient's Accession No.	
4. Title and Subtitle Development of the Midwest Guardrail System (MGS) W-beam to Thrie Beam Transition Element		5. Report Date November 26, 2007	
		6.	
7. Author(s) Eller, C.M., Polivka, K.A., Faller, R.K., Sicking, D.L., Rhode, J.R., Reid, J.D., Bielenberg, R.W., and Allison, E.M.		8. Performing Organization Report No. TRP-03-167-07	
9. Performing Organization Name and Address Midwest Roadside Safety Facility (MwRSF) University of Nebraska-Lincoln 527 Nebraska Hall Lincoln, NE 68588-0529		10. Project/Task/Work Unit No.	
		11. Contract © or Grant (G) No. SPR-3(017)	
12. Sponsoring Organization Name and Address Midwest States' Regional Pooled Fund Program Nebraska Department of Roads 1500 Nebraska Highway 2 Lincoln, Nebraska 68502		13. Type of Report and Period Covered Final Report 2001-2007	
		14. Sponsoring Agency Code RPFP-01-04, RPFP-02-05, RPFP-06-04	
15. Supplementary Notes Prepared in cooperation with U.S. Department of Transportation, Federal Highway Administration			
16. Abstract (Limit: 200 words) <p>For longitudinal barriers, it is common practice to use standard W-beam guardrail along the required highway segments and to use a stiffened thrie beam guardrail in a transition region near the end of a bridge. As a result of the differences in rail geometries, a W-beam to thrie beam transition element is typically used to connect the two rail sections and to provide continuity in the barrier system. However, the W-beam to thrie beam transition element has not been evaluated according to current impact safety standards. Therefore, an approach guardrail transition system, including a W-beam to thrie beam transition element, was constructed and crash tested. The transition system was attached to Missouri's thrie beam and channel bridge railing system.</p> <p>The objective of the study was to evaluate the safety performance of a W-beam to thrie beam transition element according to the Test Level 3 (TL-3) criteria set forth in the NCHRP Report No. 350. The research study included four full-scale vehicle crash tests, three with a ¾-ton pickup truck and one with a small car. Due to vehicle rollover of the first pickup truck test, the W-beam to thrie beam transition was redesigned to consist of an asymmetrical W-beam to thrie beam transition element and an increase in W-beam height to the Midwest Guardrail System (MGS) height of 787 mm (31 in.). Following the successful redirection of the ¾-ton pickup truck and the small car, the safety performance of the assymetrical MGS W-beam to thrie beam transition element was determined to be acceptable according to the TL-3 evaluation criteria specified in NCHRP Report No. 350.</p>			
17. Document Analysis/Descriptors Highway Safety, Guardrail, Roadside Appurtenances, Longitudinal Barrier, Crash Test, Compliance Test, W-Thrie Beam Transition, Midwest Guardrail System		18. Availability Statement No restrictions. Document available from: National Technical Information Services, Springfield, Virginia 22161	
19. Security Class (this report) Unclassified	20. Security Class (this page) Unclassified	21. No. of Pages 276	22. Price

DISCLAIMER STATEMENT

The contents of this report reflect the views of the authors who are responsible for the facts and the accuracy of the data presented herein. The contents do not necessarily reflect the official views nor policies of the State Highway Departments participating in the Midwest States' Regional Pooled Fund Research Program nor the Federal Highway Administration. This report does not constitute a standard, specification, or regulation.

ACKNOWLEDGMENTS

The authors wish to acknowledge several sources that made a contribution to this project: (1) the Midwest States' Regional Pooled Fund Program funded by the California Department of Transportation, Connecticut Department of Transportation, Illinois Department of Transportation, Iowa Department of Transportation, Kansas Department of Transportation, Minnesota Department of Transportation, Missouri Department of Transportation, Montana Department of Transportation, Nebraska Department of Roads, New Jersey Department of Transportation, Ohio Department of Transportation, South Dakota Department of Transportation, Texas Department of Transportation, Wisconsin Department of Transportation, and Wyoming Department of Transportation for sponsoring this project; (2) MwRSF personnel for constructing the barriers and conducting the crash tests; and (3) GSI Highway Products, Inc. from Hutchins, TX, Mid-Park, Inc. from Leitchfield, KY, and IMH Products, Inc. from Indianapolis, IN for their help in prototyping the asymmetrical W-beam to three beam transition element.

A special thanks is also given to the following individuals who made a contribution to the completion of this research project.

Midwest Roadside Safety Facility

J.C. Holloway, M.S.C.E., E.I.T., Research Manager
C.L. Meyer, B.S.M.E., E.I.T., Research Engineer II
A.T. Russell, B.S.B.A., Laboratory Mechanic II
K.L. Krenk, B.S.M.A, Field Operations Manager
A.T. McMaster, Laboratory Mechanic I
Undergraduate and Graduate Assistants

California Department of Transportation

Gary Gauthier, Roadside Safety Research Specialist
Wes Lum, P.E., Office Chief National Liaison

Connecticut Department of Transportation

Dionysia Oliveira, Transportation Engineer 3

Illinois Department of Transportation

David Piper, P.E., Highway Policy Engineer

Iowa Department of Transportation

David Little, P.E., Assistant District Engineer

Deanna Maifield, Methods Engineer

Kansas Department of Transportation

Ron Seitz, P.E., Bureau Chief

Rod Lacy, P.E., Road Design Leader

Minnesota Department of Transportation

Jim Klessig, Implementation Liaison

Michael Elle, P.E., Design Standard Engineer

Missouri Department of Transportation

Daniel Smith, P.E., Research and Development Engineer

Montana Department of Transportation

Susan Sillick, Research Bureau Chief

Nebraska Department of Roads

Amy Starr, Research Engineer

Phil TenHulzen, P.E., Design Standards Engineer

Jodi Gibson, Research Coordinator

New Jersey Department of Transportation

Kiran Patel, P.E., P.M.P., C.P.M., Deputy State Transportation Engineer

Ohio Department of Transportation

Dean Focke, P.E., Standards Engineer

South Dakota Department of Transportation

David Huft, Research Engineer
Bernie Clocksin, Lead Project Engineer

Texas Department of Transportation

Mark Bloschock, P.E., Supervising Design Engineer
Mark Marek, P.E., Design Engineer

Wisconsin Department of Transportation

John Bridwell, Standards Development Engineer
Patrick Fleming, Standards Development Engineer

Wyoming Department of Transportation

William Wilson, P.E., Standards Engineer

Federal Highway Administration

John Perry, P.E., Nebraska Division Office
Danny Briggs, Nebraska Division Office

Dunlap Photography

James Dunlap, President and Owner

TABLE OF CONTENTS

	Page
TECHNICAL REPORT DOCUMENTATION PAGE	i
DISCLAIMER STATEMENT	ii
ACKNOWLEDGMENTS	iii
TABLE OF CONTENTS	vi
List of Figures	ix
List of Tables	xiv
1 INTRODUCTION	1
1.1 Background and Problem Statement	1
1.2 Research Objective	2
1.3 Scope	2
2 LITERATURE REVIEW	4
2.1 NCHRP 230 Systems	4
2.2 NCHRP 350 Systems	6
3 COMPUTER SIMULATION	9
3.1 Background	9
3.2 Critical Transition Angle	9
3.3 BARRIER VII Results	11
4 DESIGN DETAILS (DESIGN NO. 1)	12
5 TEST REQUIREMENTS AND EVALUATION CRITERIA	28
5.1 Test Requirements	28
5.2 Evaluation Criteria	28
6 TEST CONDITIONS	31
6.1 Test Facility	31
6.2 Vehicle Tow and Guidance System	31
6.3 Test Vehicles	31
6.4 Data Acquisition Systems	45
6.4.1 Accelerometers	45
6.4.2 Rate Transducers	45
6.4.3 High-Speed Photography	46
6.4.4 Pressure Tape Switches	47
7 CRASH TEST NO. 1	52

7.1 Test MWT-3	52
7.2 Test Description	52
7.3 Barrier Damage	53
7.4 Vehicle Damage	55
7.5 Occupant Risk Values	56
7.6 Discussion	57
8 ANALYSIS AND DISCUSSION OF TEST NO. MWT-3	77
9 DESIGN MODIFICATIONS (DESIGN NO. 2)	79
10 CRASH TEST NO. 2	94
10.1 Test MWT-4	94
10.2 Test Description	94
10.3 Barrier Damage	95
10.4 Vehicle Damage	97
10.5 Occupant Risk Values	97
10.6 Discussion	98
11 DISCUSSION AND COMPUTER SIMULATION	118
11.1 Analysis of Test No. MWT-4	118
11.2 Redesigned Asymmetrical Transition Element	118
11.3 BARRIER VII Results	119
12 DESIGN MODIFICATIONS (DESIGN NO. 3)	120
13 CRASH TEST NO. 3	138
13.1 Test MWT-5	138
13.2 Test Description	138
13.3 Barrier Damage	139
13.4 Vehicle Damage	141
13.5 Occupant Risk Values	142
13.6 Discussion	142
14 CRASH TEST NO. 4	162
14.1 Test MWT-6	162
14.2 Test Description	162
14.3 Barrier Damage	163
14.4 Vehicle Damage	164
14.5 Occupant Risk Values	165
14.6 Discussion	165
15 SUMMARY, CONCLUSIONS AND RECOMMENDATIONS	184

16 REFERENCES	188
17 APPENDICES	190
APPENDIX A	
English-Unit Design Details, Design No. 1	191
APPENDIX B	
Test Summary Sheets in English Units	203
APPENDIX C	
Occupant Compartment Deformation Data	208
APPENDIX D	
Accelerometer and Rate Transducer Data Analysis, Test MWT-3	216
APPENDIX E	
English-Unit Design Details, Design No. 2	224
APPENDIX F	
Accelerometer and Rate Transducer Data Analysis, Test MWT-4	236
APPENDIX G	
BARRIER VII Computer Model	244
APPENDIX H	
English-Unit Design Details, Design No. 3	250
APPENDIX I	
Accelerometer and Rate Transducer Data Analysis, Test MWT-5	264
APPENDIX J	
Accelerometer and Rate Transducer Data Analysis, Test MWT-6	272

List of Figures

	Page
1. Critical Pocketing Angle	10
2. Layout (Design No. 1)	15
3. Layout and Design Details (Design No .1)	16
4. Cap Rail and Post No. 18 Details (Design No. 1)	17
5. Post Nos. 16 and 17 Details (Design No. 1)	18
6. Post Nos. 12 through 15 Details (Design No. 1)	19
7. Post Nos. 3 through 11 Details (Design No. 1)	20
8. Channel Bridge Rail Design Details (Design No. 1)	21
9. Channel Bridge Rail Design Details, (Design No. 1)	22
10. Rail Detail (Design No. 1)	23
11. BCT Post and Tube Details (Design No. 1)	24
12. Cable Strut and Anchor Bracket Details (Design No. 1)	25
13. System and Transition Element (Design No. 1)	26
14. Anchor and Tarmac Connection Details (Design No. 1)	27
15. Test Vehicle, Test MWT-3	32
16. Vehicle Dimensions, Test MWT-3	33
17. Test Vehicle, Test MWT-4	35
18. Vehicle Dimensions, Test MWT-4	36
19. Test Vehicle, Test MWT-5	37
20. Vehicle Dimensions, Test MWT-5	38
21. Test Vehicle, Test MWT-6	39
22. Vehicle Dimensions, Test MWT-6	40
23. Vehicle Target Locations, Test MWT-3	41
24. Vehicle Target Locations, Test MWT-4	42
25. Vehicle Target Locations, Test MWT-5	43
26. Vehicle Target Locations, Test MWT-6	44
27. Locations of High-Speed Cameras, Test MWT-3	48
28. Locations of High-Speed Cameras, Test MWT-4	49
29. Locations of High-Speed Cameras, Test MWT-5	50
30. Locations of High-Speed Cameras, Test MWT-6	51
31. Summary of Test Results and Sequential Photographs, Test MWT-3	58
32. Additional Sequential Photographs, Test MWT-3	59
33. Additional Sequential Photographs, Test MWT-3	60
34. Additional Sequential Photographs, Test MWT-3	61
35. Documentary Photographs, Test MWT-3	62
36. Documentary Photographs, Test MWT-3	63
37. Impact Location, Test MWT-3	64
38. Vehicle Final Position and Trajectory Marks, Test MWT-3	65
39. System Damage, Test MWT-3	66
40. System Damage, Test MWT-3	67
41. Anchorage Damage, Test MWT-3	68

42. Post Nos. 9 and 10 Damage, Test MWT-3	69
43. Post Nos. 11 and 12 Damage, Test MWT-3	70
44. Post Nos. 13 and 14 Damage, Test MWT-3	71
45. Bridge Posts and Post No. 15 Damage, Test MWT-3	72
46. Vehicle Damage, Test MWT-3	73
47. Vehicle Damage, Test MWT-3	74
48. Vehicle Damage, Test MWT-3	75
49. Occupant Compartment and Windshield Damage, Test MWT-3	76
50. Layout (Design No. 2)	81
51. Layout and Design Details (Design No. 2)	82
52. Cap Rail and Post No. 18 Details (Design No. 2)	83
53. Post Nos. 16 and 17 Details (Design No. 2)	84
54. Post Nos. 12 through 15 Details (Design No. 2)	85
55. Post Nos. 3 through 11 Details (Design No. 2)	86
56. Channel Bridge Rail Design Details (Design No. 2)	87
57. Channel Bridge Rail Design Details (Design No. 2)	88
58. Rail and End BCT Details (Design No. 2)	89
59. BCT Post and Tube Details (Design No. 2)	90
60. Cable Strut and Anchor Bracket Details (Design No. 2)	91
61. System and Transition Element (Design No. 2)	92
62. Anchor and Tarmac Connection (Design No. 2)	93
63. Summary of Test Results and Sequential Photographs, Test MWT-4	100
64. Additional Sequential Photographs, Test MWT-4	101
65. Additional Sequential Photographs, Test MWT-4	102
66. Documentary Photographs, Test MWT-4	103
67. Documentary Photographs, Test MWT-4	104
68. Impact Location, Test MWT-4	105
69. Vehicle Final Position, Test MWT-4	106
70. System Damage, Test MWT-4	107
71. System Damage, Test No. MWT-4	108
72. Rail Rupture Damage, Test MWT-4	109
73. Post Nos. 1, 2, 5, and 6 Damage, Test MWT-4	110
74. Post Nos. 7 through 9 Damage, Test MWT-4	111
75. Post Nos. 10 through 15 Damage, Test MWT-4	112
76. Post Nos. 16 and 17 Damage, MWT-4	113
77. Vehicle Damage, Test MWT-4	114
78. Vehicle Damage, Test MWT-4	115
79. Undercarriage Damage, Test MWT-4	116
80. Occupant Compartment Damage, Test MWT-4	117
81. Layout (Design No. 3)	121
82. Layout and Design Details (Design No. 3)	122
83. Asymmetrical W-Beam to Thrie Beam Transition Element Details (Design No. 3)	123
84. Asymmetrical W-Beam to Thrie Beam Transition Element Prototype, Design No. 3	124
85. Cap Rail and Post No. 18 Details (Design No. 3)	125

86. Post Nos. 16 and 17 Details (Design No. 3)	126
87. Post Nos. 12 through 15 Details (Design No. 3)	127
88. Post Nos. 3 through 11 Details (Design No. 3)	128
89. Channel Bridge Rail Design Details (Design No. 3)	129
90. Channel Bridge Rail Design Details (Continued) (Design No. 3)	130
91. Rail and End BCT Details (Design No. 3)	131
92. BCT Post and Tube Details (Design No. 3)	132
93. Cable Strut and Anchor Bracket Details (Design No. 3)	133
94. Anchor Cable Details (Design No. 3)	134
95. System and Transition Element (Design No. 3)	135
96. Welded W-beam to Thrie Beam Transition Element, Design No. 3	136
97. Anchor and Tarmac Connection (Design No. 3)	137
98. Summary of Test Results and Sequential Photographs, Test MWT-5	144
99. Additional Sequential Photographs, Test MWT-5	145
100. Additional Sequential Photographs, Test MWT-5	146
101. Documentary Photographs, Test MWT-5	147
102. Documentary Photographs, Test MWT-5	148
103. Impact Location, Test MWT-5	149
104. Vehicle Final Position and Trajectory Marks, Test MWT-5	150
105. System Damage, Test MWT-5	151
106. System Damage, Test MWT-5	152
107. Anchorage System Damage, Test MWT-5	153
108. Post Nos. 5 through 7 Damage, Test MWT-5	154
109. Post Nos. 8 through 10 Damage, Test MWT-5	155
110. Post Nos. 10 through 13 Damage, Test MWT-5	156
111. Post Nos. 13 through 16 Damage, Test MWT-5	157
112. Post Nos. 16 through 21 Damage, Test MWT-5	158
113. Vehicle Damage, Test MWT-5	159
114. Vehicle Damage, Test MWT-5	160
115. Occupant Compartment Damage, Test MWT-5	161
116. Summary of Test Results and Sequential Photographs, Test MWT-6	168
117. Additional Sequential Photographs, Test MWT-6	169
118. Additional Sequential Photographs, Test MWT-6	170
119. Documentary Photographs, Test MWT-6	171
120. Documentary Photographs, Test MWT-6	172
121. Impact Location, Test MWT-6	173
122. Final Location and Trajectory Marks, Test MWT-6	174
123. System Damage, Test MWT-6	175
124. Post Nos. 1 and 5 Damage, Test MWT-6	176
125. Post Nos. 6 through 9 Damage, Test MWT-6	177
126. Post Nos. 10 and 11 Damage, Test MWT-6	178
127. Post Nos. 12 and 13 Damage, Test MWT-6	179
128. Post Nos. 14 through 19 Damage, Test MWT-6	180
129. Vehicle Damage, Test MWT-6	181

130. Vehicle Damage, Test MWT-6	182
131. Occupant Compartment Damage, Test MWT-6	183
A-1. Layout, Design No. 1 (English)	192
A-2. Layout and Design Details, Design No. 1 (English)	193
A-3. Cap Rail and Post No. 18 Details, Design No. 1 (English)	194
A-4. Post Nos. 16 and 17.Details, Design No. 1 (English)	195
A-5. Post Nos. 12 through 15 Details, Design No. 1 (English)	196
A-6. Post Nos. 3 through 11 Details, Design No. 1 (English)	197
A-7. Channel Bridge Rail Design Details, Design No. 1 (English)	198
A-8. Channel Bridge Rail Design Details (Continued), Design No. 1 (English)	199
A-9. Rail Details, Design No. 1 (English)	200
A-10. BCT Post and Tube Detail, Design No. 1 (English)	201
A-11. Cable Strut and Anchor Bracket Details, Design No. 1 (English)	202
B-1. Summary of Test Results and Sequential Photographs (English), Test MWT-3	204
B-2. Summary of Test Results and Sequential Photographs (English), Test MWT-4	205
B-3. Summary of Test Results and Sequential Photographs (English), Test MWT-5	206
B-4. Summary of Test Results and Sequential Photographs (English), Test MWT-6	207
C-1. Occupant Compartment Deformation Data, Test MWT-3	209
C-2. Occupant Compartment Deformation Data, Test MWT-4	210
C-3. Occupant Compartment Deformation Index (OCDI), Test MWT-4	211
C-4. Occupant Compartment Deformation Data - Set 1, Test MWT-5	212
C-5. Occupant Compartment Deformation Data - Set 2, Test MWT-5	213
C-6. Occupant Compartment Deformation Index (OCDI), Test MWT-5	214
C-7. Occupant Compartment Deformation Index (OCDI), Test MWT-6	215
D-1. Graph of Longitudinal Deceleration, Test MWT-3	217
D-2. Graph of Longitudinal Occupant Impact Velocity, Test MWT-3	218
D-3. Graph of Longitudinal Occupant Displacement, Test MWT-3	219
D-4. Graph of Lateral Deceleration, Test MWT-3	220
D-5. Graph of Lateral Occupant Impact Velocity, Test MWT-3	221
D-6. Graph of Lateral Occupant Displacement, Test MWT-3	222
D-7. Graph of Roll and Yaw Angular Displacements, Test MWT-3	223
E-1. Layout, Design No. 2 (English)	225
E-2. Layout and Design Details, Design No. 2 (English)	226
E-3. Cap Rail and Post No. 18 Details- Design No. 2 (English)	227
E-4. Post Nos. 16 and 17 Details- Design No. 2 (English)	228
E-5. Post Nos. 12 through 15 Details, Design No. 2 (English)	229
E-6. Post Nos. 3 through 11 Details, Design No. 2 (English)	230
E-7. Channel Bridge Rail Design Details, Design No. 2 (English)	231
E-8. Channel Bridge Rail Design Details, Design No. 2 (English)	232
E-9. Rail and End BCT Details, Design No. 2 (English)	233
E-10. BCT Post and Tube Details, Design No. 2 (English)	234
E-11. Cable Strut and Anchor Bracket Details, Design No. 2 (English)	235
F-1. Graph of Longitudinal Deceleration, Test MWT-4	237
F-2. Graph of Longitudinal Occupant Impact Velocity, Test MWT-4	238

F-3. Graph of Longitudinal Occupant Displacement, Test MWT-4	239
F-4. Graph of Lateral Deceleration, Test MWT-4	240
F-5. Graph of Lateral Occupant Impact Velocity, Test MWT-4	241
F-6. Graph of Lateral Occupant Displacement, Test MWT-4	242
F-7. Graph of Roll, Pitch and Yaw Angular Displacements, Test MWT-4	243
G-1. Model of the MGS W-Beam to Thrie Beam Transition	245
H-1. Layout, Design No. 3 (English)	251
H-2. Layout and Design Details, Design No. 3 (English)	252
H-3. Asymmetrical W-Beam to Thrie Beam Transition Rail Detail, Design No. 3 (English) ..	253
H-4. Cap Rail and Post No. 18 Details- Design No. 3 (English)	254
H-5. Post Nos. 16 and 17 Details, Design No. 3 (English)	255
H-6. Post Nos. 12 through 15 Details, Design No. 3 (English)	256
H-7. Post Nos. 3 through 11, Design No. 3 (English)	257
H-8. Channel Bridge Rail Design Details, Design No. 3 (English)	258
H-9. Channel Bridge Rail Design Details (Continued), Design No. 3 (English)	259
H-10. Rail and End BCT Details, Design No. 3 (English)	260
H-11. BCT Post and Tube Details, Design No. 3 (English)	261
H-12. Cable Strut and Anchor Bracket Details, Design No. 3 (English)	262
H-13. Anchor Cable Details, Design No. 3 (English)	263
I-1. Graph of Longitudinal Deceleration, Test MWT-5	265
I-2. Graph of Longitudinal Occupant Impact Velocity, Test MWT-5	266
I-3. Graph of Longitudinal Occupant Displacement, Test MWT-5	267
I-4. Graph of Lateral Deceleration, Test MWT-5	268
I-5. Graph of Lateral Occupant Impact Velocity, Test MWT-5	269
I-6. Graph of Lateral Occupant Displacement, Test MWT-5	270
I-7. Graph of Roll, Pitch and Yaw Angular Displacements, Test MWT-5	271
J-1. Graph of Longitudinal Deceleration, Test MWT-6	273
J-2. Graph of Longitudinal Occupant Impact Velocity, Test MWT-6	274
J-3. Graph of Longitudinal Occupant Displacement, Test MWT-6	275
J-4. Graph of Lateral Deceleration, Test MWT-6	276
J-5. Graph of Lateral Occupant Impact Velocity, Test MWT-6	277
J-6. Graph of Lateral Occupant Displacement, Test MWT-6	278
J-7. Graph of Roll, Pitch and Yaw Angular Displacements, Test MWT-6	279

List of Tables

	Page
1. NCHRP Report 350 Test Level 3 Crash Test Conditions.	29
2. NCHRP Report No. 350 Evaluation Criteria for Crash Tests.	30
3. Summary of Safety Performance Evaluation Results	187

1 INTRODUCTION

1.1 Background and Problem Statement

Throughout the United States, State Highway Departments commonly use standard strong-post, W-beam guardrail systems to prevent errant vehicles from leaving the roadway and encountering safety hazards beyond or near the roadway edge. One of the more common applications for this barrier is to shield traffic from the ends of bridge rails and their associated drop offs. Although the strong-post, W-beam barriers are generally considered to be “semi-rigid,” these barriers are much more flexible than most bridge railing systems. In order to eliminate the potential for vehicle pocketing or wheel snag at the point of attachment to a rigid bridge rail end, an approach guardrail transition region is added between the W-beam guardrail and the bridge rail to provide a more gradual change in lateral barrier stiffness.

Over the years, this change in lateral barrier stiffness has been accomplished by some combination of reduced post spacing, nesting of the guardrail, placing additional stiffening rails in the region, and incorporating a curb under the barrier. Many of these approach guardrail transition systems have incorporated three beam guardrail elements to help meet the increased stiffness requirements resulting from the bridge railing system. Therefore, a W-beam to three beam transition element is utilized near the beginning of the transition system to account for the differences in rail geometries and provide structural continuity between the two barrier systems.

Although the field experience of the W-beam to three beam section has generally been believed to be acceptable, previous crash testing efforts with passenger-size and small car sedans have been met with mixed results (1-3). While several crash tests on the W-beam to three beam section resulted in acceptable performance, other tests resulted in severe wheel snagging and even

vehicle rollover. Furthermore, all these crash testing efforts were conducted according to the guidelines set forth in the National Cooperative Highway Research Program (NCHRP) Report No. 230, *Recommended Procedures for the Safety Performance Evaluation of Highway Appurtenances* (4) and did not evaluate the transition element's performance with light truck vehicles. As a result, questions remained as to the performance of the W-beam to thrie beam transition element, including whether the element could prevent vehicle underride by mini-size vehicles and prevent pocketing, wheel snagging, or rollover during light truck impacts. Therefore, the safety performance of the W-beam to thrie beam transition element should be evaluated under the current guidelines set forth in the NCHRP Report No. 350, *Recommended Procedures for the Safety Performance Evaluation of Highway Features* (5) in order for its use to be continued on Federal-aid highways.

1.2 Research Objective

The objective of the research project was to investigate the safety performance of the W-beam to thrie beam transition element used in conjunction with an approach guardrail transition. The W-beam to thrie beam transition element was to be evaluated according to the Test Level 3 (TL-3) safety performance criteria set forth in NCHRP Report No. 350 (5). It is important to note that the performance of the transition element is somewhat dependent upon the stiffness of the transition system. Therefore, it is generally accepted that a stiffer transition element will increase the risk of pocketing, wheel snag, and vehicle underride. Accordingly, it was determined to examine the performance of the W-beam to thrie beam transition element when attached to a very stiff transition system, specifically Missouri's thrie beam and channel bridge railing system (6).

1.3 Scope

The research objective was achieved through the completion of several tasks. First, a

literature review was undertaken to review previous evaluations of W-beam to thrie beam transition sections. Second, a redesign phase utilizing BARRIER VII simulation was undertaken to resolve the unsatisfactory performance of the W-beam to thrie beam transition system. Third, a guardrail system consisting of a W-beam to thrie beam transition element was constructed adjacent to an approved approach guardrail transition system. After fabrication of the test installation, a full-scale vehicle crash test was performed according to the TL-3 impact conditions of NCHRP Report No. 350. The crash test utilized a ¾-ton pickup truck, weighing approximately 2,000 kg (4,409 lbs). The targeted impact conditions for this test were an impact speed and angle of 100.0 km/h (62.1 mph) and 25 degrees, respectively. Following the unsuccessful test results, a second redesign phase was undertaken utilizing BARRIER VII simulation. Next, the test installation was fabricated, and three full-scale vehicle crash tests were performed according to the TL-3 impact conditions of NCHRP Report No. 350. The first two crash tests utilized a ¾-ton pickup truck, weighing approximately 2,000 kg (4,409 lbs). The targeted impact conditions for these tests were an impact speed and angle of 100.0 km/h (62.1 mph) and 25 degrees, respectively. The final test utilized a small car, weighing approximately 820 kg (1808 lbs). The target impact conditions for this test were an impact speed and angle of 100.0 km/h (62.1 mph) and 20 degrees, respectively. Next, the test results were analyzed, evaluated, and documented. Finally, conclusions and recommendations were made that pertain to the safety performance of the W-beam to thrie beam transition element used in conjunction with an approach guardrail transition.

2 LITERATURE REVIEW

2.1 NCHRP 230 Systems

Previous testing on various W-beam to thrie beam transition sections was conducted by the New York State Department of Transportation (NYSDOT) and was met with mixed results. When the unsymmetrical designs were initially tested with full-size vehicles, the vehicles were forced down under the W-beam rail element, resulting in severe snagging on the lower thrie beam corrugation which included a taper (1-2). In the later tests on a symmetrical W-beam to thrie beam section, two out of the three test vehicles were successfully redirected. Crash testing of the W-beam to thrie beam transition systems previously conducted at NYSDOT were evaluated according to the criteria provided in NCHRP Report No. 230.

NYSDOT performed five full-scale vehicle crash tests on several W-beam to thrie beam transition configurations used to transition from a weak-post, W-beam guardrail system with reduced post spacing to a rigid thrie beam bridge railing. For the first design, an 1.27-m (50-in.) long asymmetrical section was placed between the W-beam and thrie beam rails. At the upstream end of the transition section, the lower corrugation terminated with a 305-mm (12-in.) long taper toward the rail's mid-height. A 2,041-kg (4,500 lb) passenger-size sedan (test no. 67) impacted the rail 2.67 m (105 in.) upstream from the tapered section at 94.6 km/h (58.8 mph) and 25 degrees. During the test, the right-front wheel and suspension snagged severely on the end of the lower thrie beam corrugation, and the test was determined to be unacceptable according to the NCHRP Report No. 230 requirements.

Following the failure of test no. 67, the transition section was modified in order to reduce the severe snagging at the end of the section. For the second design, an 1.90-m (75-in) long

asymmetrical section was placed between the W-beam and thrie beam rails. At the upstream end of the transition section, the lower corrugation terminated with an increased taper length of 914 mm (36 in.), as measured from the bottom of the rail to the rail's mid-height. A 2,041-kg (4,499-lb) passenger-size sedan (test no. 68) impacted the rail 1.40 m (55 in.) upstream from the tapered section at 95.8 km/h (59.5 mph) and 24 degrees. During the test, the right-front wheel and suspension once again snagged severely on the end of the lower thrie beam corrugation, and the test was determined to be unacceptable according to the NCHRP Report No. 230 requirements.

After the failure of test nos. 67 and 68, the NYSDOT realized that the termination of the lower tapered corrugation presented an insurmountable snag point. Therefore, the W-beam to thrie beam transition section was redesigned to include a symmetrical tapered section which could adapt W-beam rail directly to thrie beam rail. This transition section is the same design that now appears in the American Association of State Highway and Transportation Officials' (AASHTO's) *Standard Specifications for Transportation Materials and Methods of Sampling and Testing* (7).

Following the redesign of the symmetrical W-beam to thrie beam transition section, three additional full-scale crash tests were performed. For this design, a 2,087-kg (4,601-lb) passenger-size sedan (test no. 69) impacted the rail 2.07 m (82 in.) upstream from the tapered section at 87.5 km/h (54.4 mph) and 26 degrees. During the impact, the vehicle was smoothly redirected with only minor snagging on the posts, and the test was determined to be acceptable according to the NCHRP Report No. 230 requirements (4). A fourth test (test no. 70) was performed using an 898-kg (1980-lb) small car (Subaru station wagon) impacting the rail 1.07 m (42 in.) upstream from the tapered section at 93.0 km/h (57.8 mph) and 20 degrees. During the test, the right-front wheel and bumper snagged severely on the first W152x13.4 (W6x9) steel post which resulted in the vehicle yawing

rapidly away from the rail and rolling onto its side. As a result, the test was determined to be unacceptable according to the NCHRP Report No. 230 requirements.

After the failed small car test on the symmetric W-beam to thrie beam transition section, the depth of the steel wide-flange blockouts was increased from 152 to 356 mm (6 to 14 in.), and the small car crash test was rerun. This fifth test (test no. 71) was performed using an 816-kg (1,799-lb) small car (Honda) impacting the rail 0.85 m (34 in.) upstream from the tapered section at 97.0 km/h (60.3 mph) and 19 degrees. During the test, the vehicle was smoothly redirected, and the test was determined to be acceptable according to the NCHRP Report No. 230 requirements. Although the system was redesigned following the successful test with a passenger-size sedan, a retest with the large car was deemed unnecessary.

Thus, the symmetrical W-beam to thrie beam transition section, combined with 362-mm (14.25-in.) deep blockouts and used to connect weak-post W-beam guardrail to a thrie approach guardrail transition, met the requirements of NCHRP Report No. 230.

2.2 NCHRP 350 Systems

In 1999, the Midwest Roadside Safety Facility (MwRSF) conducted two full-scale vehicle crash tests on a symmetric W-beam to thrie beam transition section (8). The test installation consisted of four major structural components: (1) two nested 5,715-mm (225-in.) long by 2.67-mm (12-gauge) thick thrie beam rail sections; (2) an 1,905-mm (75-in.) long by 2.67-mm (12-gauge) thick W-beam to thrie beam transition section; (3) a 15,240-mm (600-in.) long by 2.67-mm (12-gauge) thick W-beam rail section attached to a simulated anchorage device; and (4) a 3,810-mm (150-in.) long thrie beam and channel bridge railing system with an attached simulated anchorage device. The tests were evaluated according to the safety performance criteria provided in NCHRP

Report No. 350.

For the first test, test no. MWT-1, an 821-kg (1,810-lb) small car impacted the system 1219 mm (48 in.) upstream from the first post of the W-beam to thrie beam transition at a speed of 99.5 km/h (61.8 mph) and an angle of 25.7 degrees. The vehicle was redirected smoothly, and the test was determined to be acceptable according to the NCHRP Report No. 350 requirements.

In the second test, test no. MWT-2, a 2,022-kg (4,458- lb) $\frac{3}{4}$ -ton pickup truck impacted the system 2,235 mm (88 in.) upstream from the first post of the W-beam to thrie beam transition at a speed of 98.3 km/h (61.1 mph) and an angle of 25.3 degrees. During this test on the approach guardrail transition, the guardrail upstream of the transition element began to deform laterally and the test vehicle slowly began to redirect. As the vehicle progressed into the barrier, a pocket began to develop at the downstream end of the transition element where it was connected to the nested thrie beam rail. As the test vehicle approached the nested thrie beam rails, a sharp kink developed at the end of the transition element and eventually ruptured at this point. When the front of the test vehicle contacted the end of the largely undeformed nested thrie beam elements, it was forced up into the air and rolled over the traffic side of the barrier. Therefore, this test was determined to be unacceptable according to the NCHRP Report No. 350 requirements, as the vehicle did not remain upright after collision with the W-beam to thrie beam transition element.

In 2002, the Materials Engineering and Testing Services of the California Department of Transportation (CALTRANS) designed and tested a Y-shaped W-beam to thrie beam transition section (9). The system consisted of nested thrie beam on the traffic-side face of the barrier and a single thrie beam on the backside. One of the thrie beams on the traffic side was 3.43 mm (10 gauge) thick, while the other one and the one on the backside were 2.67 mm (12 gauge) thick. A 3.43-mm

(10-gauge) thick symmetrical W-beam to thrie beam transition connected the W-beam to the thrie beam. The five posts closest to the bridge rail were 254-mm x 254-mm x 2.44-m long (10-in. x 10-in. x 96-in.) Douglas Fir posts with 203-mm x 203-mm x 559-mm (8-in. x 8-in. x 22-in.) blockouts. The sixth post was also 254 mm x 254 mm (10 in. x 10 in.) but only 1.83 m (72 in.) long.

In test no. 519, a 1,974-kg (4,352-lb) $\frac{3}{4}$ -ton pickup truck impacted the transition at the third post upstream from the end of the concrete bridge rail at a speed and angle of 100.0 km/h (62.1 mph) and 25.5 degrees, respectively. The vehicle was safely redirected without any incident of pocketing. Therefore, this test was considered acceptable according to the NCHRP Report No. 350 safety performance criteria.

In test no. 518, a 1996-kg (4,400-lb) $\frac{3}{4}$ -ton pickup truck impacted the transition 953 mm (37.5 in.) upstream from the sixth post upstream from the end of the concrete bridge rail at a speed and angle of 99.9 km/h (62.1 mph) and 25.0 degrees, respectively. The vehicle was safely redirected without any incident of pocketing. Therefore, this test was considered acceptable according to the NCHRP Report No. 350 safety performance criteria.

In test no. 514, a 8,011-kg (17,661-lb) single-unit truck impacted the transition midway between the second and third posts upstream from the end of the concrete bridge rail at a speed and angle of 75.5 km/h (46.9 mph) and 16.0 degrees, respectively. The vehicle was safely redirected without any tendency toward pocketing. Therefore, this test was considered acceptable according to the NCHRP Report No. 350 safety performance criteria.

3 COMPUTER SIMULATION

3.1 Background

Following the unacceptable performance of the initial 2000P test on the approach guardrail transition, it was necessary to determine the cause of the poor barrier performance and make design modifications to the barrier system in order to improve its overall performance (8). From an analysis of the test results, the test failed due to the abrupt stiffness change between the approach guardrail and the stiff transition system. Hence, it was determined that the W-beam to thrie beam transition element performed acceptably and that the approach to the transition element should be stiffened to eliminate the severe pocketing that was observed.

3.2 Critical Transition Angle

As a vehicle approaches the stiffened, semi-rigid approach guardrail transition region from the relatively flexible guardrail region, there is a potential for pocketing of the vehicle. Pocketing occurs when the lateral deflection of the transition region is much less than the abutting guardrail region, creating a sharp bend in the guardrail system before the transition region. This sharp bend produces a high longitudinal force on the vehicle that can create excessive deceleration, or in the case of test no. MWT-2, can force the vehicle to override the pocket and rollover.

Although BARRIER VII (10) can predict the creation of a sharp bend in a guardrail system that could lead to pocketing, there are no objective criteria with which to measure the risk of serious consequences associated with pocketing. After reviewing crash tests of many guardrail systems, it was theorized that at a critical pocketing angle, θ_p , could be defined such that at angles smaller than θ_p , the bend in the guardrail would not cause serious pocketing. However, at angles more severe than θ_p , where the difference between the guardrail and transition regions was more abrupt, the vehicle

would not be able to escape from the pocket and an undesirable vehicle response could be expected. The critical pocketing angle is defined as the angle between the guardrail region just in front of the impacting vehicle and the downstream section of rail. Note that this definition of θ_p is only applicable where there is a sharp bend in the guardrail, and the pocketing angle is essentially a measure of the magnitude of that angle. It should also be noted that the depth of the pocket may also have a significant impact on the performance of a guardrail system. However, for the purposes of using BARRIER VII to design a guardrail stiffness transition, the authors have assumed that the depth of the pocket will always be sufficient to create a problem, provided the critical pocketing angle is reached, as shown in Figure 1.

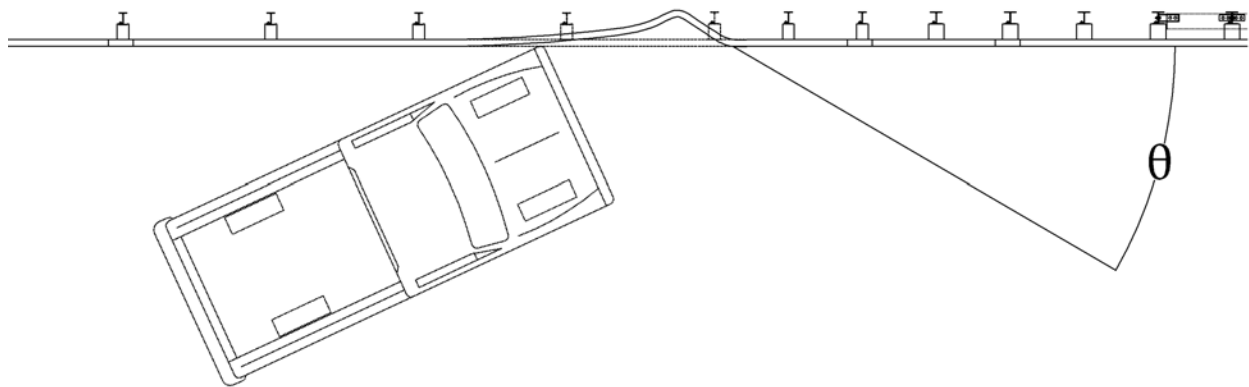


Figure 1. Critical Pocketing Angle

Many guardrail and approach guardrail transition tests involving 2000P vehicles were carefully reviewed in order to identify the critical pocketing angle. Based upon this analysis, the critical pocketing angle was estimated to be approximately 23 degrees. Every test that exhibited a pocketing angle of 23 degrees or less resulted in a successful redirection of the 2000P vehicle,

whereas most tests with pocketing angles greater than 23 degrees exhibited significant pocketing and corresponding adverse vehicle behavior. For example, the pocketing angle from test no. MWT-2 was estimated to be 45 degrees. As a result of the pocketing, the rail ruptured and the test vehicle rolled over during the test.

3.3 BARRIER VII Results

In order to determine the critical transition angle, computer simulations were conducted using BARRIER VII (10). BARRIER VII was first calibrated against test no. MWT-2 to assure that it could accurately predict pocketing in advance of the guardrail transition section. Following the successfully calibrated model, BARRIER VII was used to analyze the stiffening of the guardrail upstream of the W-beam to thrie beam transition element to reduce the pocketing angle below the critical value of 23 degrees.

In order to reduce the predicted pocketing angle to 23 degrees or less, it was necessary to alter the stiffness differential between the transition and guardrail sections. This was achieved by changing the post sizes and depths which resulted in weakening the transition region and strengthening the guardrail region.

4 DESIGN DETAILS (DESIGN NO. 1)

The 26.67-m (87-ft 6-in.) test installation, as shown in Figure 2, consisted of five major structural components: (1) a 3,810-mm (12-ft 6-in.) long thrie beam and channel bridge railing system; (2) 3,810 mm (12 ft - 6 in.) of nested 2.67-mm (12-gauge) thick thrie beam guardrail; (3) 1,905 mm (6 ft - 3 in.) of standard 2.67-mm (12-gauge) thick thrie beam guardrail; (4) a 1,905-mm (6-ft 3-in.) long, 2.67-mm (12-gauge) thick W-beam to thrie beam transition section; and (5) 15.24 m (50 ft) of standard 2.67-mm (12-gauge) thick W-beam to thrie beam rail attached to a simulated anchorage device. Design details are shown in Figures 2 through 12. The corresponding English-unit drawings are shown in Appendix A.

The barrier system was constructed with three bridge posts and eighteen guardrail posts. Post nos. 1 and 2 were timber posts measuring 140 mm wide x 190 mm deep x 1,156 mm long (5.5 in. x 7.5 in. x 45.5 in.) and were placed in 1,829-mm (6-ft) long steel foundation tubes. The timber posts and foundation tubes were part of an anchorage system used to develop the required tensile capacity of a tangent guardrail terminal. Post nos. 3 through 15 were galvanized ASTM A36 Steel W152 x 13.4 (W6x9) sections. Post nos. 3 through 8 measured 1,829 mm (6 ft) long, while post nos. 9 through 15 measured 2,134 mm (7 ft) long. Post nos. 16 through 18 were galvanized ASTM A36 steel W152x22.3 (W6x15) sections measuring 2,134 mm (7 ft) long. Bridge post nos. 19 through 21 were galvanized ASTM A36 steel W152x29.8 (W6x20) sections measuring 752 mm (29.625 in.) long.

Post nos. 1 through 7 were spaced 1,905 mm (75 in.) on center, while post nos. 7 through 19 were spaced 953 mm (37.5 in.) on center, as shown in Figure 2. Post nos. 19 through 21 were spaced 1,905 mm (75 in.) on center. The soil embedment depths for post nos. 3 through 18 were 1,099 mm

(43.25 in.), 1,403 mm (55.25 in.), 1,343 mm (52.875 in.), 1,308 mm (51.5 in.), and 1,374 mm (54.125 in.), respectively, as shown in Figures 4 through 7. The steel posts were placed in a compacted coarse, crushed limestone material that met Grading B of AASHTO M147-65 (1990) as found in NCHRP Report 350.

For post nos. 3 through 11, 152-mm wide x 203-mm deep x 362-mm long (6-in. x 8-in. x 14.25-in.) wood spacer blockouts were used to block the rail away from the front face of the steel posts. For post no. 12, a 152-mm wide x 203-mm deep x 483-mm long (6-in. x 8-in. x 19-in.) wood spacer blockout was used to block the rail away from the front face of the steel post. For post nos. 13 through 15, a 152-mm wide x 203-mm deep x 559-mm long (6-in. x 8-in. x 22-in.) wood spacer blockout was used to block the rail away from the front face of the steel post. For post nos. 16 through 18, 203-mm wide x 203-mm deep (8-in. x 8-in.) wood spacer blockouts were used to block the rail away from the front face of the steel posts. The wood spacer blockouts for post nos. 16 and 17 were 483 mm (19 in.) long, while the wood spacer blockout for post no. 18 was 381 mm (15 in.) long. For post nos. 19 through 21, a galvanized ASTM A36 steel W152x22.3 (W6x15) section spacer blockout measuring 346 mm (13.625 in.) long was used to block the rail away from the front face of the steel bridge post.

Standard 2.67-mm (12-gauge) thick W-beam rails were placed between post nos. 1 and 11, as shown in Figure 2. The W-beam's top rail height was 706 mm (27.75 in.) with a 550-mm (21.625-in.) center mounting height. A standard 2.67-mm (12-gauge) thick W-beam to thrie beam transition section was placed between post nos. 11 and 13. Standard 2.67-mm (12-gauge) thick thrie beam rail was placed between post nos. 13 and 15 and also between post nos. 19 and 21. Two nested 2.67-mm (12-gauge) thick thrie beams were placed between post nos. 15 and 19, as shown in Figure 3. The

thrie beam's top rail height was 803 mm (31.625 in.) with a 550-mm (21.625-in.) center mounting height. All lap-splice connections between the rail sections were configured to reduce vehicle snag at the splice during the crash test. The thrie beam channel bridge railing system was rigidly attached to the concrete tarmac located at the MwRSF's outdoor test site, as shown in Figures 13 and 14.

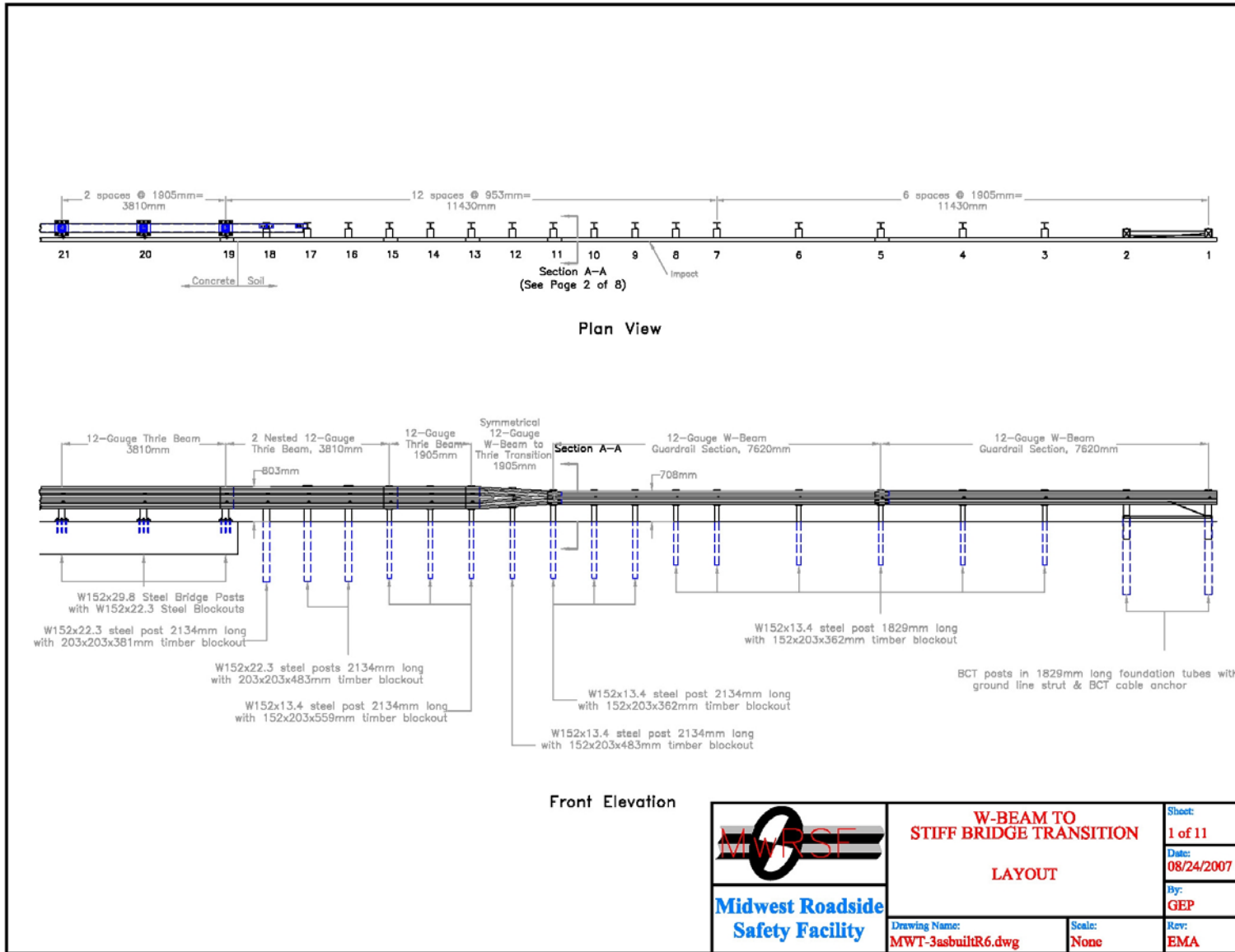


Figure 2. Layout (Design No. 1)

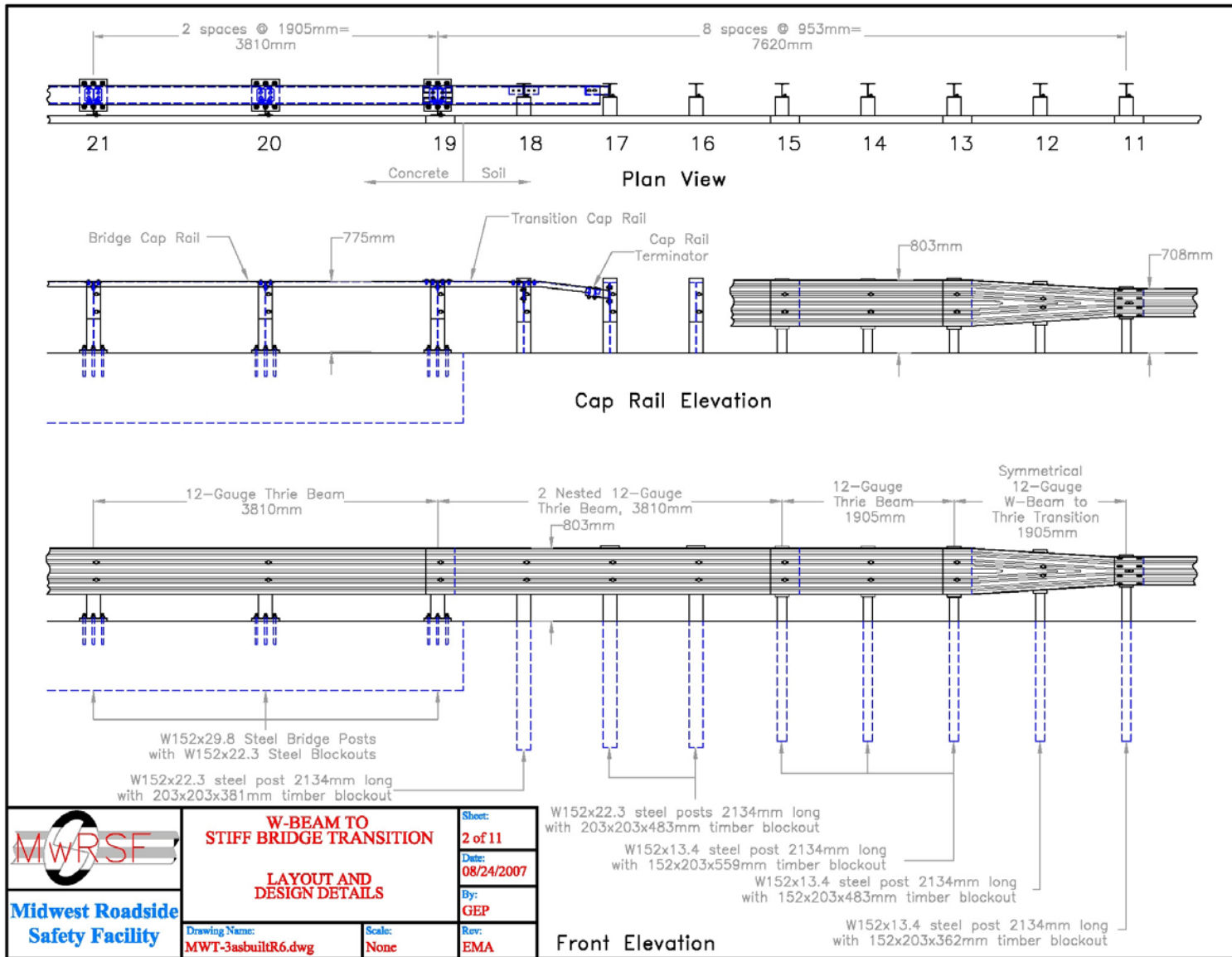


Figure 3. Layout and Design Details (Design No .1)

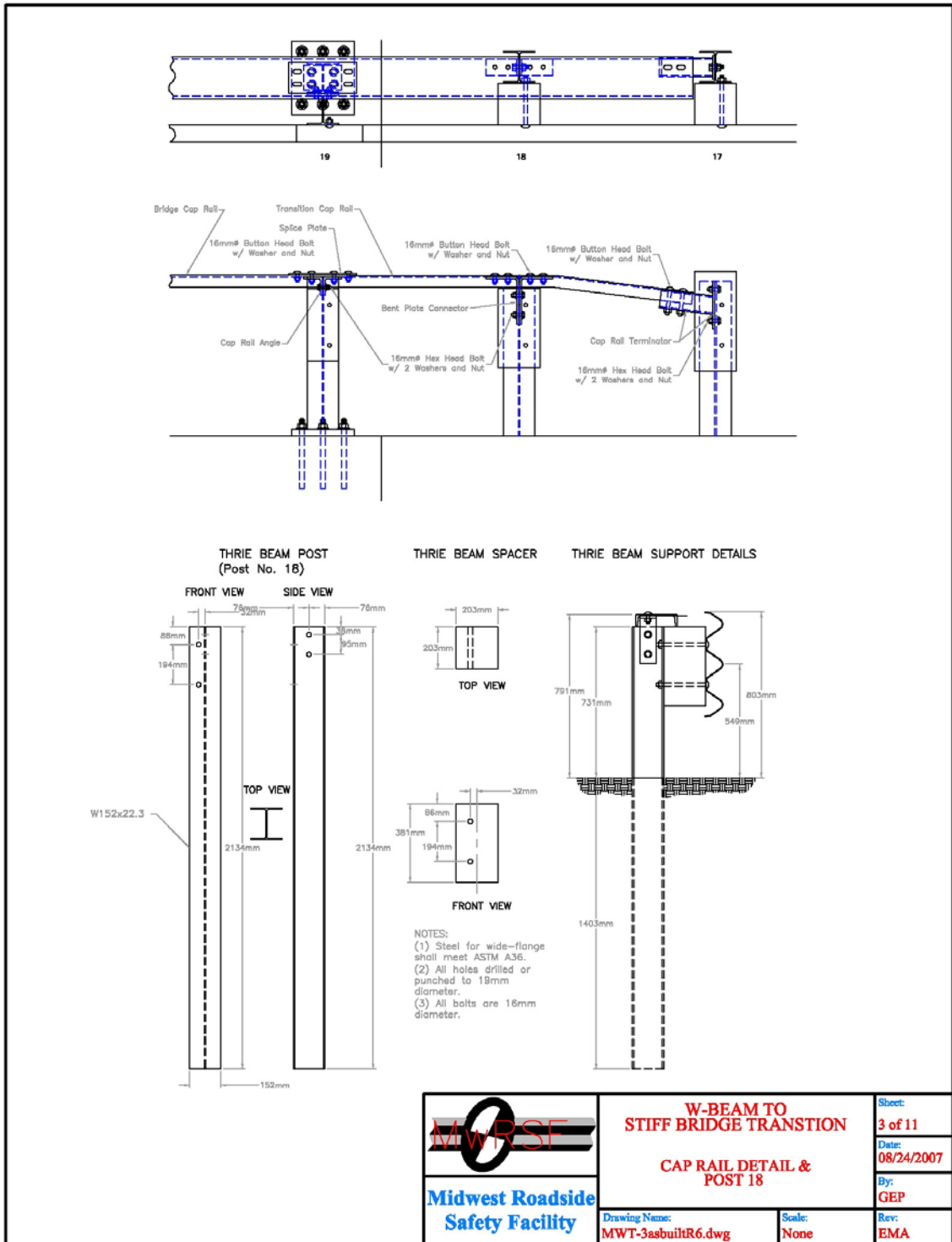


Figure 4. Cap Rail and Post No. 18 Details (Design No. 1)

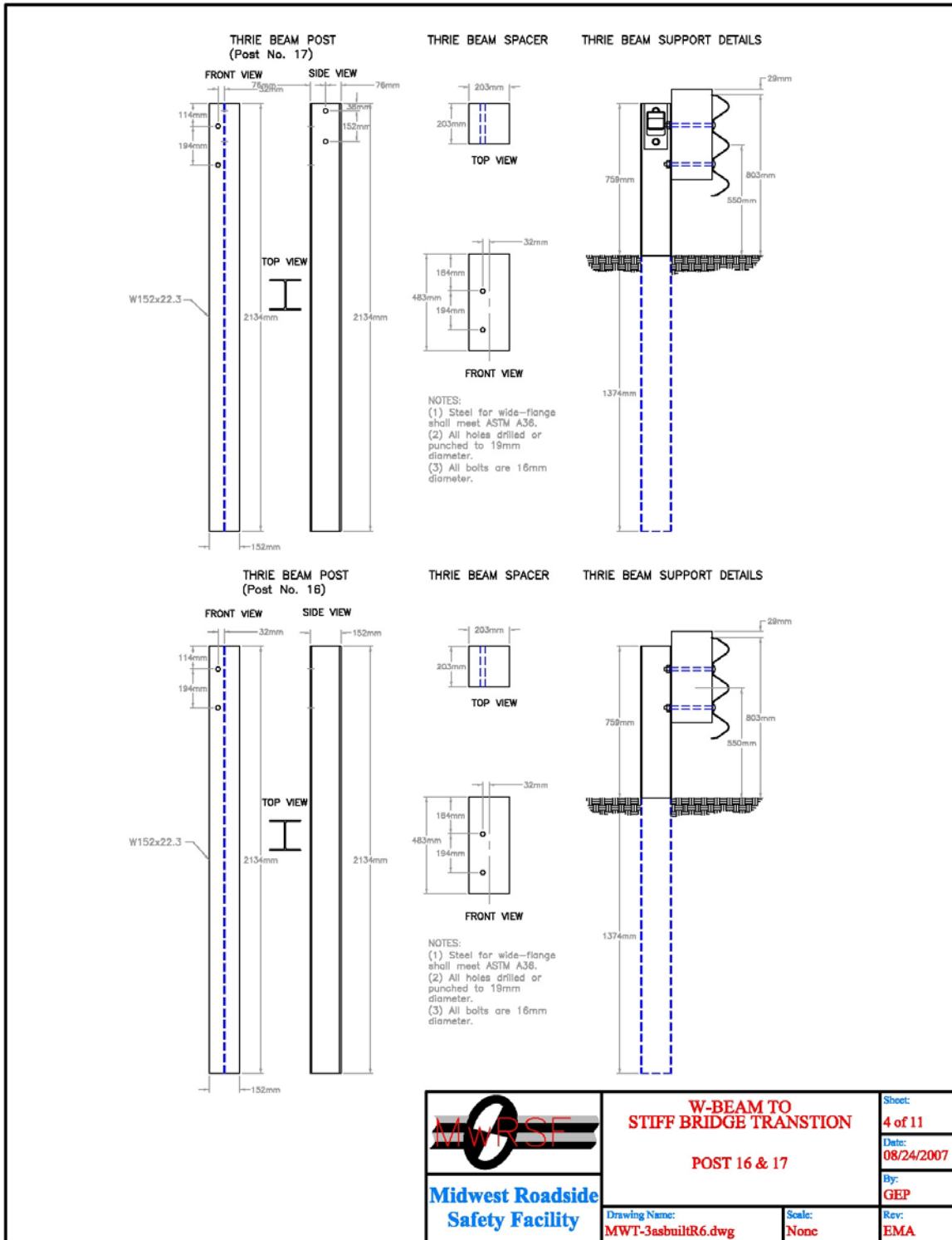


Figure 5. Post Nos. 16 and 17 Details (Design No. 1)

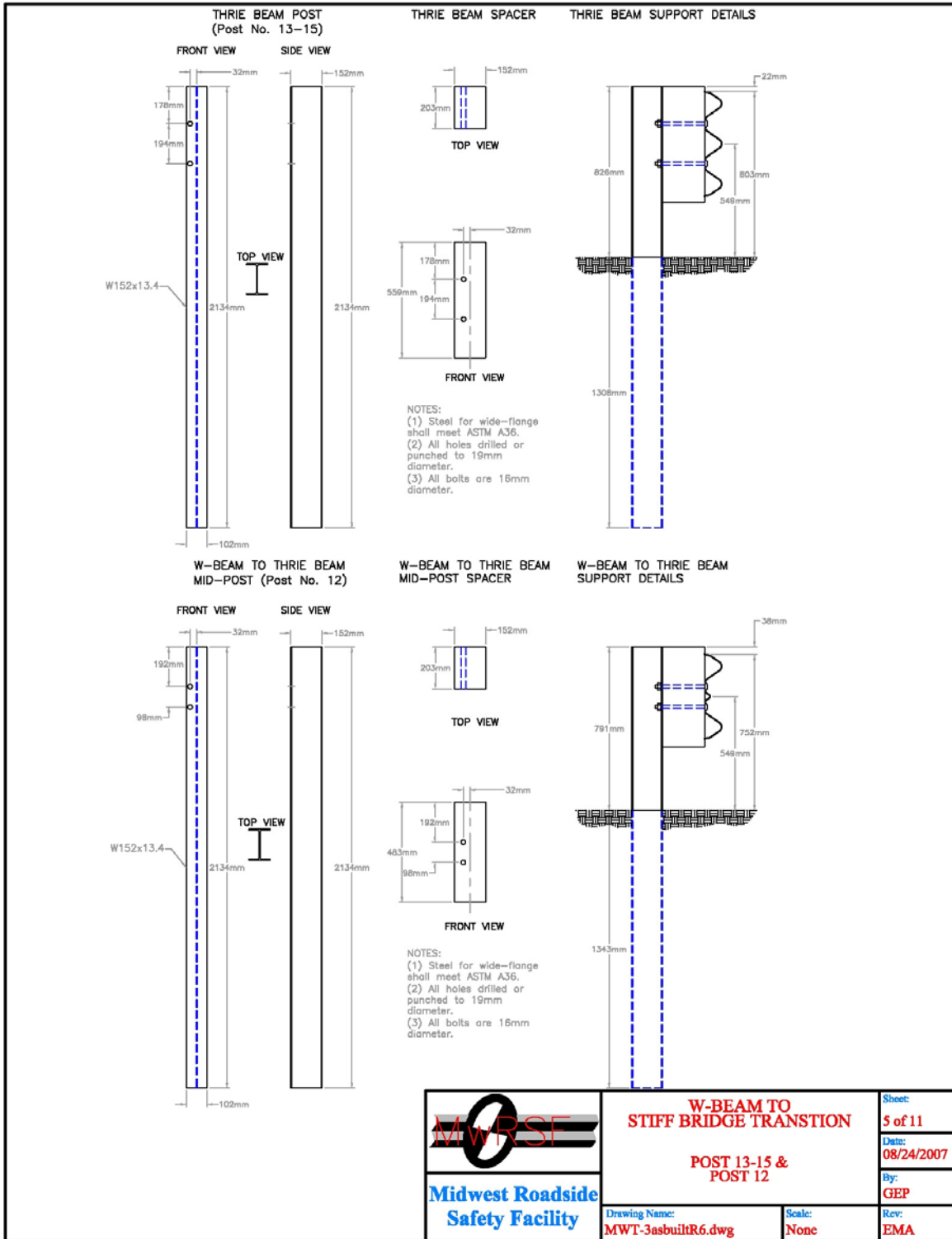


Figure 6. Post Nos. 12 through 15 Details (Design No. 1)

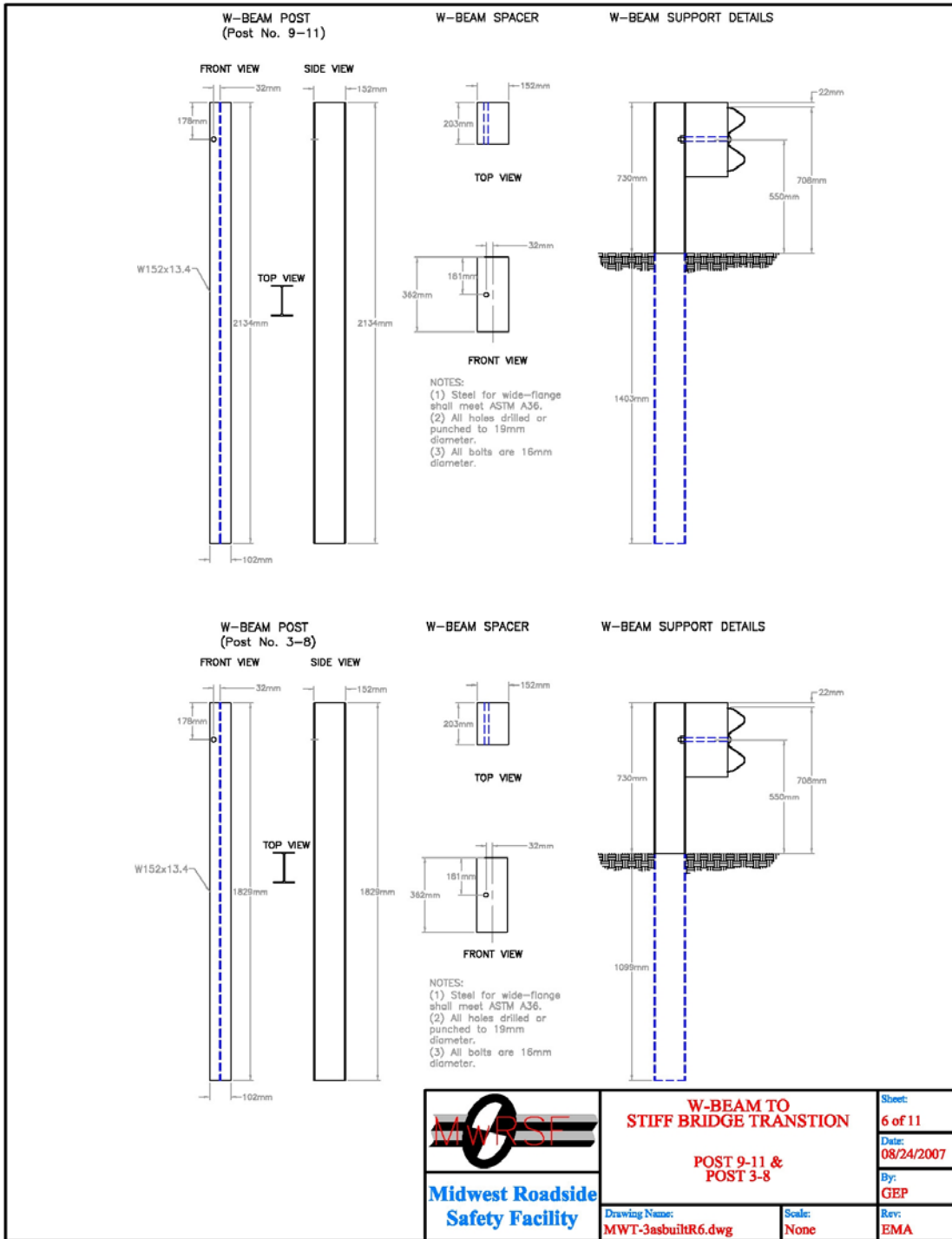


Figure 7. Post Nos. 3 through 11 Details (Design No. 1)

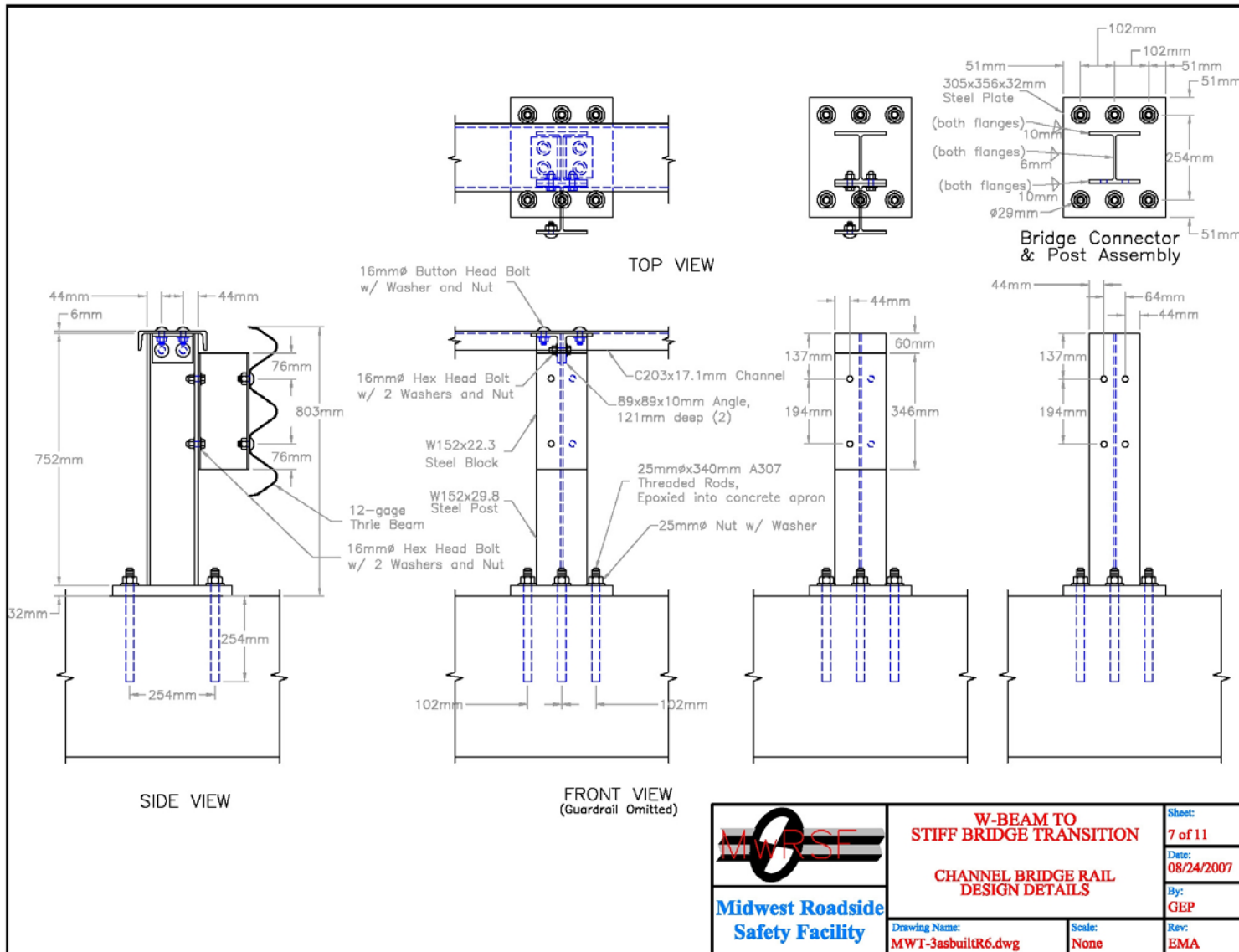


Figure 8. Channel Bridge Rail Design Details (Design No. 1)

	W-BEAM TO STIFF BRIDGE TRANSITION	Sheet: 7 of 11
	CHANNEL BRIDGE RAIL DESIGN DETAILS	Date: 08/24/2007
Drawing Name: MWT-3asbuiltR6.dwg	Scale: None	By: GEP
		Rev: EMA

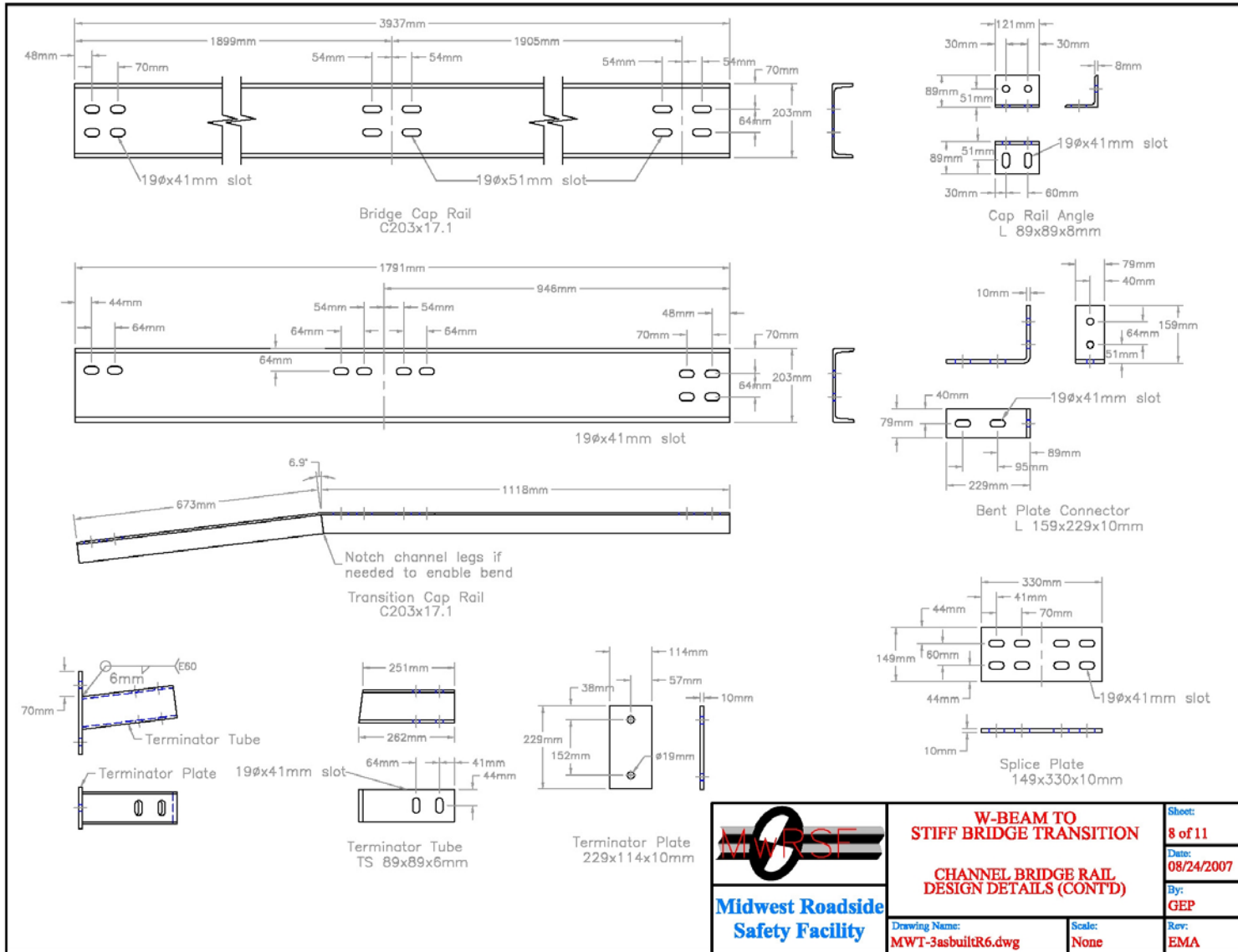


Figure 9. Channel Bridge Rail Design Details, (Design No. 1)

	W-BEAM TO STIFF BRIDGE TRANSITION	Sheet: 8 of 11
	CHANNEL BRIDGE RAIL DESIGN DETAILS (CONTD)	Date: 08/24/2007
Midwest Roadside Safety Facility	Drawing Name: MWT-3asbuiltR6.dwg	By: GEP
	Scale: None	Rev: EMA

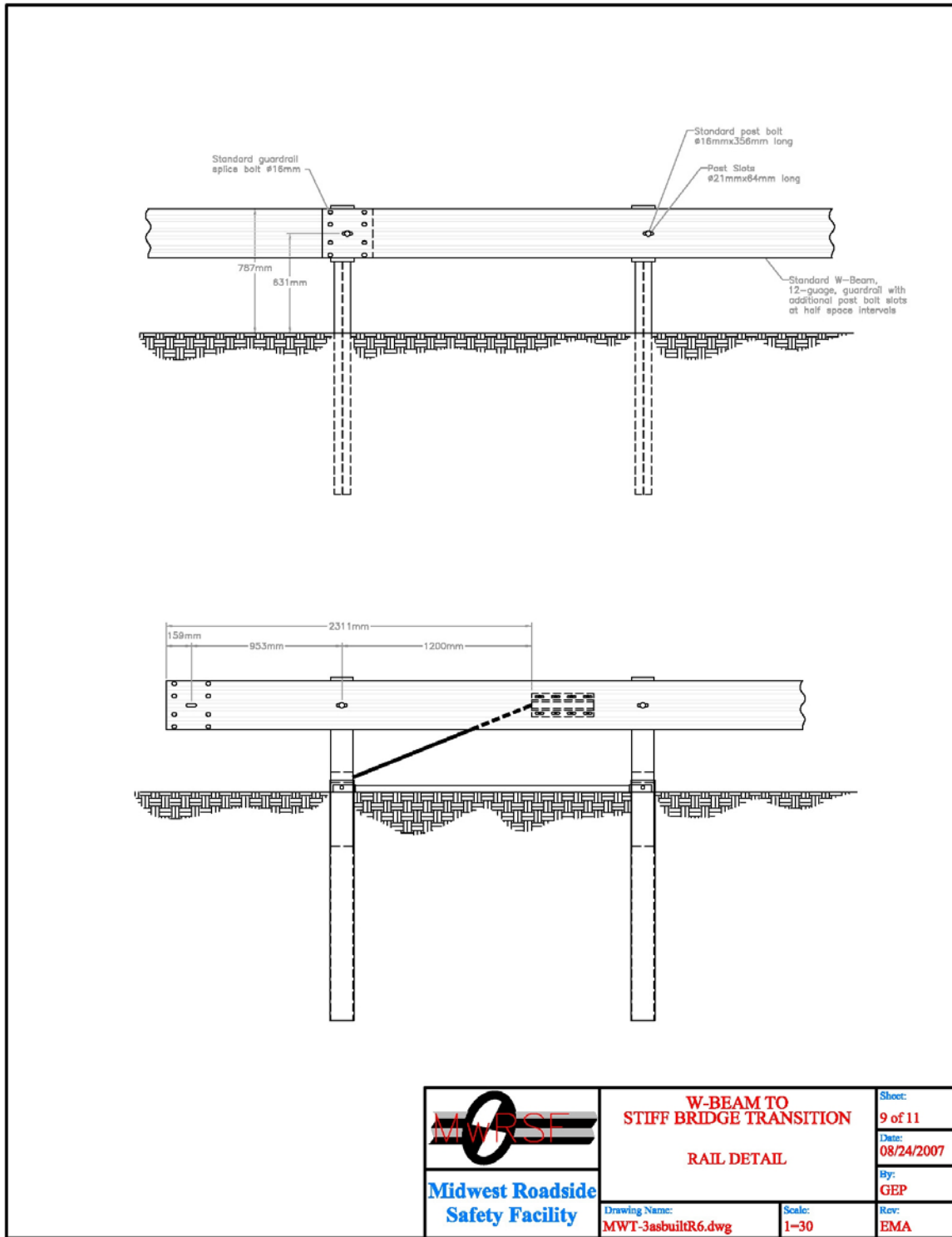


Figure 10. Rail Detail (Design No. 1)

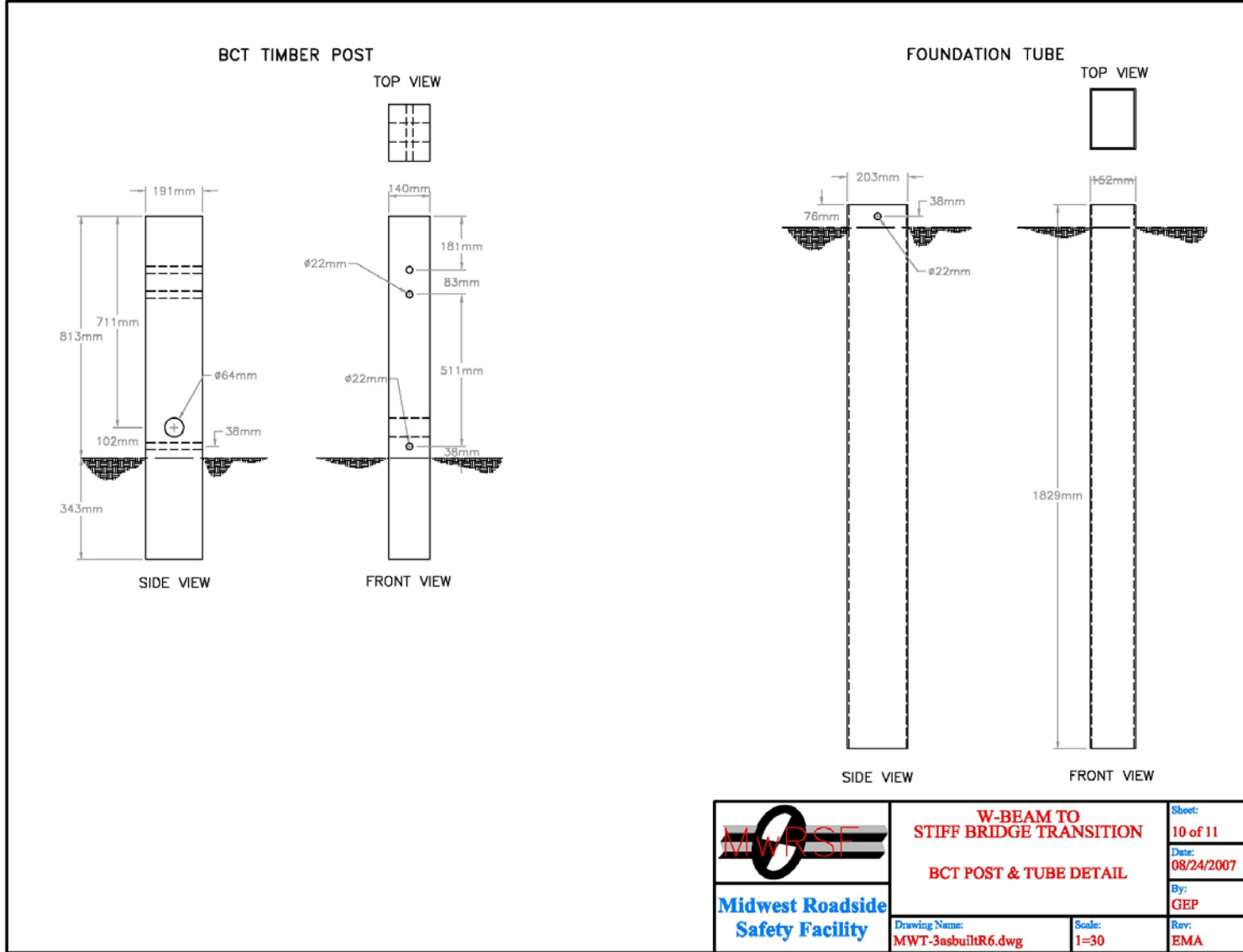


Figure 11. BCT Post and Tube Details (Design No. 1)

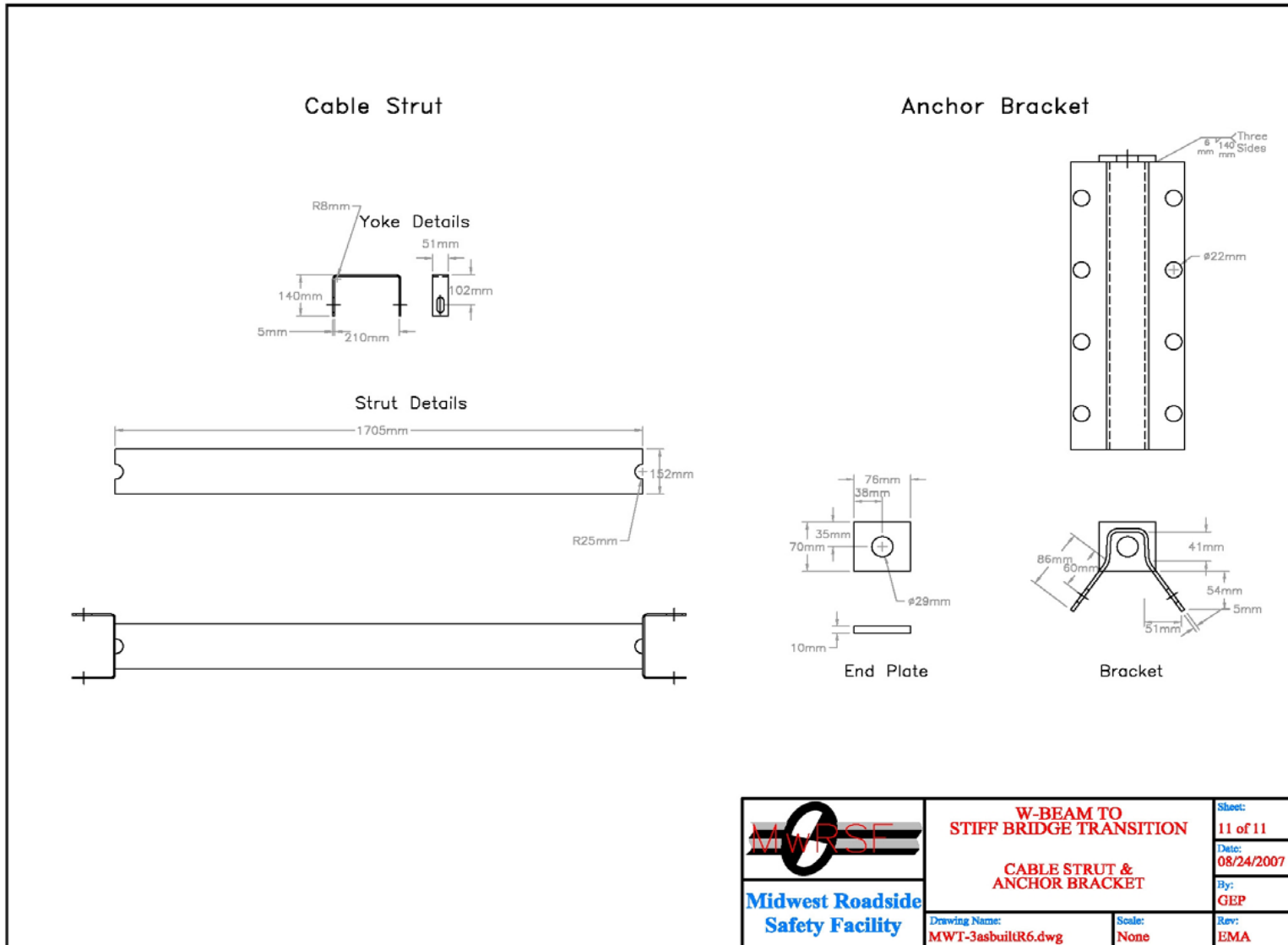


Figure 12. Cable Strut and Anchor Bracket Details (Design No. 1)



Figure 13. System and Transition Element (Design No. 1)



Figure 14. Anchor and Tarmac Connection Details (Design No. 1)

5 TEST REQUIREMENTS AND EVALUATION CRITERIA

5.1 Test Requirements

Longitudinal barriers, such as W-beam to thrie beam transitions, must satisfy impact safety standards provided in NCHRP Report No. 350 in order to be accepted by the Federal Highway Administration (FHWA) for use on National Highway Systems (NHS) new construction projects or as a replacement for existing transition designs not meeting current safety standards. According to TL-3 of NCHRP Report No. 350, W-beam to thrie beam transition systems must be subjected to two full-scale vehicle crash tests. The two crash tests are as follows:

1. Test Designation 3-20, consisting of an 820-kg (1,808-lb) small car impacting the W-beam to thrie beam transition system at a nominal speed and angle of 100.0 km/h (62.1 mph) and 20 degrees, respectively.
2. Test Designation 3-21, consisting of a 2,000-kg (4,409-lb) pickup truck impacting the W-beam to thrie beam transition system at a nominal speed and angle of 100.0 km/h (62.1 mph) and 25 degrees, respectively.

The test conditions for TL-3 longitudinal barriers are summarized in Table 1.

5.2 Evaluation Criteria

According to NCHRP Report No. 350, the evaluation criteria for full-scale vehicle crash testing are based on three appraisal areas: (1) structural adequacy; (2) occupant risk; and (3) vehicle trajectory after collision. Criteria for structural adequacy are intended to evaluate the ability of the barrier to contain, redirect, or allow controlled vehicle penetration in a predictable manner. Occupant risk evaluates the degree of hazard to occupants in the impacting vehicle. Vehicle trajectory after collision is a measure of the potential for the post-impact trajectory of the vehicle to cause subsequent multi-vehicle accidents. This criterion also indicates the potential safety hazard for the occupants of

other vehicles or the occupants of the impacting vehicle when subjected to secondary collisions with other fixed objects. These three evaluation criteria are summarized in Table 2 and defined in greater detail in NCHRP Report No. 350. The full-scale vehicle crash tests were conducted and reported in accordance with the procedures provided in NCHRP Report No. 350.

Table 1. NCHRP Report 350 Test Level 3 Crash Test Conditions.

Test Article	Test Designation	Test Vehicle	Impact Conditions			Evaluation Criteria ¹
			Speed		Angle (degrees)	
			(km/h)	(mph)		
Longitudinal Barrier Transition	3-20	820C	100	62.1	20	A,D,F,H,I,K,M
	3-21	2000P	100	62.1	25	A,D,F,K,L,M

¹ - Evaluation criteria explained in Table 2.

Table 2. NCHRP Report No. 350 Evaluation Criteria for Crash Tests.

Structural Adequacy	A. Test article should contain and redirect the vehicle; the vehicle should not penetrate, underride, or override the installation although controlled lateral deflection of the test article is acceptable.
Occupant Risk	D. Detached elements, fragments or other debris from the test article should not penetrate or show potential for penetrating the occupant compartment, or present an undue hazard to other traffic, pedestrians, or personnel in a work zone. Deformations of, or intrusions into, the occupant compartment that could cause serious injuries should not be permitted.
	F. The vehicle should remain upright during and after collision although moderate roll, pitching, and yawing are acceptable.
	H. Longitudinal and lateral occupant impact velocities should fall below the preferred value of 9 m/s (29.5 ft/s), or at least below the maximum allowable value of 12 m/s (39.4 ft/s).
	I. Longitudinal and lateral occupant ridedown accelerations should fall below the preferred value of 15 Gs, or at least below the maximum allowable value of 20 Gs.
Vehicle Trajectory	K. After collision it is preferable that the vehicle's trajectory not intrude into adjacent traffic lanes.
	L. The occupant impact velocity in the longitudinal direction should not exceed 12 m/s (39.4 ft/s) and the occupant ridedown acceleration in the longitudinal direction should not exceed 20 Gs.
	M. The exit angle from the test article preferably should be less than 60 percent of test impact angle, measured at time of vehicle loss of contact with test device.

6 TEST CONDITIONS

6.1 Test Facility

The testing facility is located at the Lincoln Air Park on the northwest side of the Lincoln Municipal Airport and is approximately 8.0 km (5 mi.) northwest of the University of Nebraska-Lincoln.

6.2 Vehicle Tow and Guidance System

A reverse cable tow system with a 1:2 mechanical advantage was used to propel the test vehicle. The distance traveled and the speed of the tow vehicle were one-half that of the test vehicle. The test vehicle was released from the tow cable before impact with the barrier system. A digital speedometer was located on the tow vehicle to increase the accuracy of the test vehicle impact speed.

A vehicle guidance system developed by Hinch (11) was used to steer the test vehicle. A guide-flag, attached to the front-left wheel and the guide cable, was sheared off before impact with the barrier system. The 9.5-mm (0.375-in.) diameter guide cable was tensioned to approximately 15.6 kN (3,500 lbf), and supported laterally and vertically every 30.48 m (100 ft) by hinged stanchions. The hinged stanchions stood upright while holding up the guide cable, but as the vehicle was towed down the line, the guide-flag struck and knocked each stanchion to the ground. For tests MWT-3, MWT-4, MWT-5, and MWT-6, the vehicle guidance systems were 297 m (975 ft), 302 m (990 ft), 299-m (981 ft), and 137 m (451 ft) long, respectively.

6.3 Test Vehicles

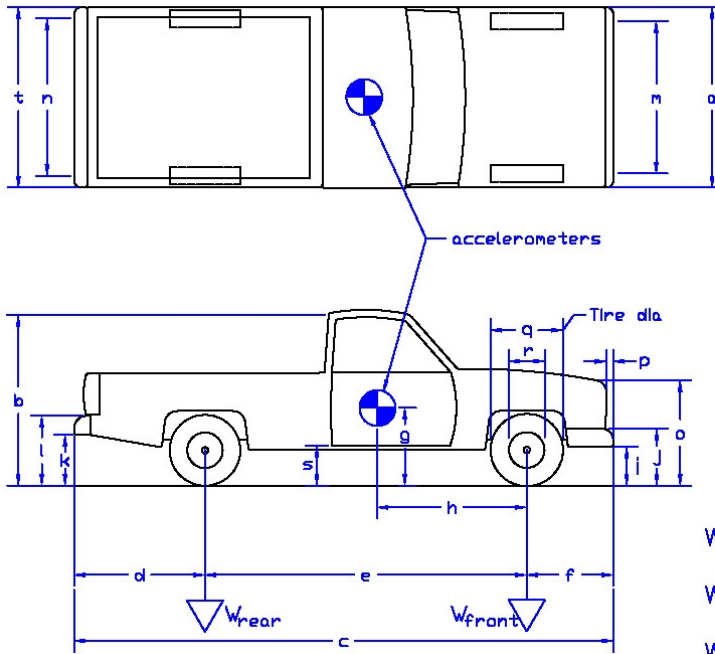
For test MWT-3, a 1997 GMC 2500 ¾-ton pickup truck was used as the test vehicle. The test inertial and gross static weights were 2,021 kg (4,456 lbs). The test vehicle is shown in Figure 15, and vehicle dimensions are shown in Figure 16.



Figure 15. Test Vehicle, Test MWT-3

Date: 6/18/03 Test Number: MWT-3 Model: 2000P
 Make: GMC Vehicle I.D.#: 1GDGC24R9VZ535854
 Tire Size: LT 245/75 R16 Year: 1997 Odometer: 280808

*(All Measurements Refer to Impacting Side)



Vehicle Geometry – mm

a	<u>1905 (75.0)</u>	b	<u>1832 (72.125)</u>
c	<u>5537 (218.0)</u>	d	<u>1461 (51.5)</u>
e	<u>3327 (131)</u>	f	<u>1257 (49.5)</u>
g	<u>667 (26.25)</u>	h	<u>1384 (54.5)</u>
i	<u>457 (18.0)</u>	j	<u>679 (26.75)</u>
k	<u>603 (23.75)</u>	l	<u>806 (31.75)</u>
m	<u>1594 (62.75)</u>	n	<u>1626 (64.0)</u>
o	<u>1372 (54.0)</u>	p	<u>89 (3.5)</u>
q	<u>610 (29.0)</u>	r	<u>445 (17.5)</u>
s	<u>483 (19.0)</u>	t	<u>1829 (72.0)</u>

Wheel Center Height Front	<u>365 (14.365)</u>
Wheel Center Height Rear	<u>375 (14.75)</u>
Wheel Well Clearance (FR)	<u>902 (35.5)</u>
Wheel Well Clearance (RR)	<u>968 (38.125)</u>

Weights	– kg	Curb	Test Inertial	Gross Static
W_{front}	<u>1146 (2522)</u>	<u>1181 (2604)</u>	<u>1181 (2604)</u>	<u>1181 (2604)</u>
W_{rear}	<u>841 (1853)</u>	<u>840 (1852)</u>	<u>840 (1852)</u>	<u>840 (1852)</u>
W_{total}	<u>1984 (4379)</u>	<u>2021 (4456)</u>	<u>2021 (4456)</u>	<u>2021 (4456)</u>

Engine Type 8 CYL. GAS

Engine Size 5.7 L 350 GI

Transmission Type:

Automatic or Manual

FWD or RWD or 4WD

Note any damage prior to test: None

Figure 16. Vehicle Dimensions, Test MWT-3

For test MWT-4, a 1998 GMC 2500 ¾-ton pickup truck was used as the test vehicle. The test inertial and gross static weights were 2,018 kg (4,448 lbs). The test vehicle is shown in Figure 17, and vehicle dimensions are shown in Figure 18.

For test MWT-5, a 2000 GMC 2500 ¾-ton pickup truck was used as the test vehicle. The test inertial and gross static weights were 2,010 kg (4,431 lbs). The test vehicle is shown in Figure 19, and vehicle dimensions are shown in Figure 20.

For test MWT-6, a 1997 Geo Metro was used as the test vehicle. The test inertial and gross static weights were 828 kg (1,826 lbs) and 904 kg (1,992 lbs), respectively. The test vehicle is shown in Figure 21, and vehicle dimensions are shown in Figure 22.

The Suspension Method (12) was used to determine the vertical component of the center of gravity (c.g.) for the pickup trucks. This method is based on the principle that the c.g. of any freely suspended body is in the vertical plane through the point of suspension. The vehicle was suspended successively in three positions, and the respective planes containing the c.g. were established. The intersection of these planes pinpointed the location of the c.g. The longitudinal component of the c.g. was determined using the measured axle weights. The location of the final centers of gravity are shown in Figures 16, 18, 20, and 22.

Square black and white-checked targets were placed on the vehicle to aid in the analysis of the high-speed film and E/cam, Photron, and AOS videos, as shown in Figures 23 through 26. Checkered targets were placed on the c.g., on the driver's side door, on the passenger's side door, and on the roof of the vehicle. The remaining targets were located for reference so that they could be viewed from the high-speed cameras for film analysis.

The front wheels of the test vehicle were aligned for camber, caster, and toe-in values of zero



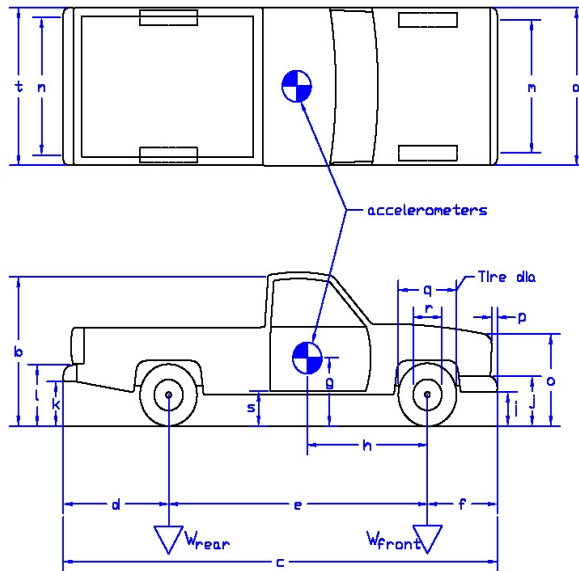
Figure 17. Test Vehicle, Test MWT-4

Date: 7/29/04 Test Number: MWT-4 Model: 2000P

Make: GMC Vehicle I.D.#: 1GDGC24R7W2534929

Tire Size: LT 245/75 r16 Year: 1998 Odometer: 237989

*(All Measurements Refer to Impacting Side)



Vehicle Geometry – mm (in.)

- a 1883 (74.125) b 1838 (72.375)
- c 5528 (217.625) d 1495 (58.875)
- e 3346 (131.75) f 889 (35.0)
- g 667 (26.25) h 1372 (54.0)
- i 464 (18.25) j 679 (26.75)
- k 591 (23.25) l 781 (30.75)
- m 1594 (62.75) n 1657 (65.25)
- o 1048 (41.25) p 83 (3.25)
- q 768 (30.25) r 292 (11.5)
- s 495 (19.5) t 1861 (73.25)
- Wheel Center Height Front 371 (14.625)
- Wheel Center Height Rear 371 (14.625)
- Wheel Well Clearance (FR) 918 (36.125)
- Wheel Well Clearance (RR) 953 (37.5)
- Frame Height (FR) 429 (16.875)
- Frame Height (RR) 673 (26.5)

Weights	Curb	Test Inertial	Gross Static
W_{front}	<u>1131 (2494)</u>	<u>1170 (2579)</u>	<u>1170 (2579)</u>
W_{rear}	<u>845 (1864)</u>	<u>848 (1869)</u>	<u>848 (1869)</u>
W_{total}	<u>1977 (4358)</u>	<u>2018 (4448)</u>	<u>2018 (4448)</u>

Engine Type 8 CYL. GAS

Engine Size 350 CI / 5.7 L

Transmission Type:

Automatic or Manual

FWD or RWD or 4WD

Note any damage prior to test: None

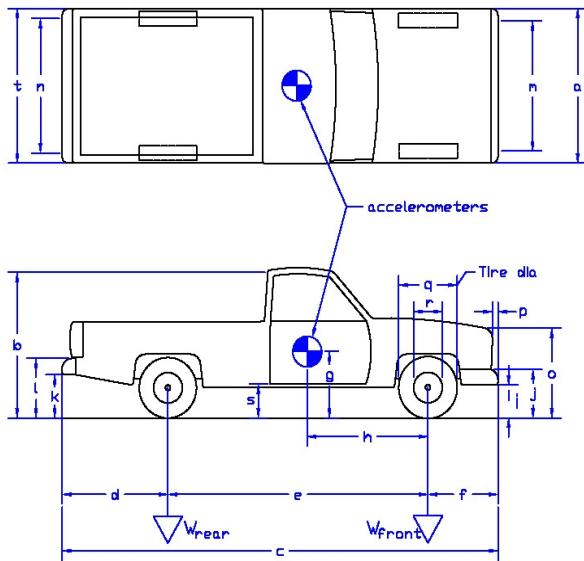
Figure 18. Vehicle Dimensions, Test MWT-4



Figure 19. Test Vehicle, Test MWT-5

Date: 11/10/05 Test Number: MWT-5 Model: 2000P/C2500
 Make: GMC Vehicle I.D.#: IGDGC24R8YF420426
 Tire Size: LT 245/75 R16 Year: 2000 Odometer: 222729

*(All Measurements Refer to Impacting Side)



Vehicle Geometry – mm (in.)

- a 1892 (74.5) b 1842 (72.5)
- c 5537 (218.0) d 1289 (50.75)
- e 3334 (131.25) f 914 (36.0)
- g 667 (26.25) h 1394 (54.75)
- i 457 (18.0) j 667 (26.25)
- k 572 (22.5) l 775 (30.5)
- m 1594 (62.75) n 1626 (64.0)
- o 1035 (40.75) p 76 (3.0)
- q 762 (30.0) r 495 (19.5)
- s 464 (18.25) t 1867 (73.5)
- Wheel Center Height Front 368 (14.5)
- Wheel Center Height Rear 371 (14.625)
- Wheel Well Clearance (FR) 918 (36.125)
- Wheel Well Clearance (RR) 959 (37.75)

- Frame Height (FR) 413 (16.25)
- Frame Height (RR) 673 (26.5)

Weights kg (lbs)	Curb	Test Inertial	Gross Static
W_{front}	<u>1133 (2497)</u>	<u>1170 (2579)</u>	<u>1170 (2579)</u>
W_{rear}	<u>817 (1801)</u>	<u>840 (1852)</u>	<u>840 (1852)</u>
W_{total}	<u>1950 (4298)</u>	<u>2010 (4431)</u>	<u>2010 (4431)</u>

- Engine Type 8 CYL. GAS
- Engine Size 5.7 L 350c.i.

Transmission Type:

- Automatic or Manual
- FWD or RWD or 4WD

GVWR Ratings	Front	Rear	Total
	<u>1860 (4100)</u>	<u>2722 (6000)</u>	<u>3901 (8600)</u>

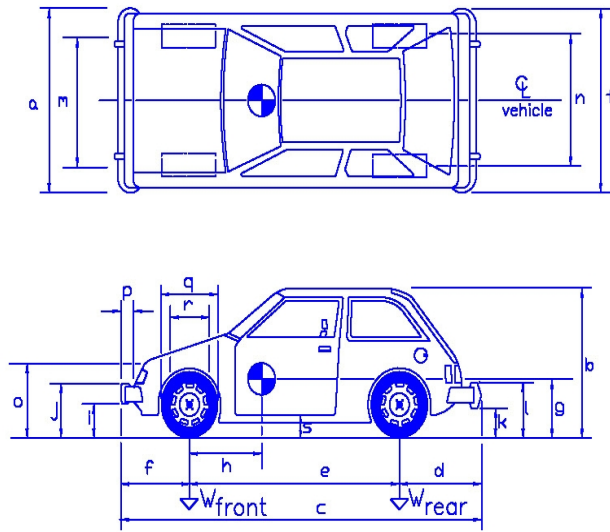
Note any damage prior to test: Small dent – center of front bumper
Left rear box dent – beat out

Figure 20. Vehicle Dimensions, Test MWT-5



Figure 21. Test Vehicle, Test MWT-6

Date: 11/22/2005 Test Number: MWT-6 Model: 820C Metro
 Make: Chevrolet Vehicle I.D.#: 2C1MR2296V6758290
 Tire Size: P155/80 R13 Year: 1997 Odometer: 88356



Vehicle Geometry - mm (in.)

- a 1556 (61.25) b 1403 (55.25)
- c 3791 (149.25) d 603 (23.75)
- e 2362 (93.0) f 826 (32.5)
- g 546 (21.5) h 864 (34.0)
- i 254 (10.0) j 508 (20.0)
- k 337 (13.25) l 648 (25.5)
- m 1380 (54.375) n 1353 (53.25)
- o 546 (21.5) p 89 (3.5)
- q 578 (22.75) r 362 (14.25)
- s 311 (12.25) t 1530 (60.25)

Wheel Center Height 260 (10.25)

Engine Type 4 CYL. GAS

Engine Size 1.3 L

Transmission Type:

Automatic or Manual

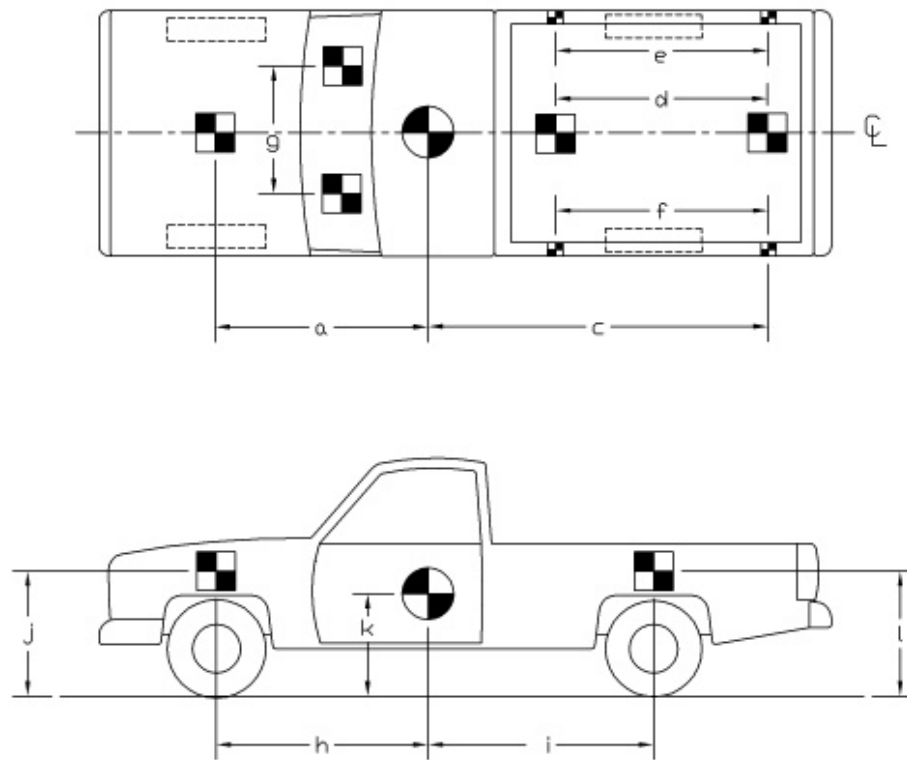
FWD or RWD or 4WD

GVWR F 650 (1433)
 GVWR R 560 (1235)
 GVWR Tot. 1210 (2668)

Weights kg (lbs)	Stripped	Test Inertial	Gross Static
W_{front}	<u>503 (1108)</u>	<u>525 (1158)</u>	<u>562 (1238)</u>
W_{rear}	<u>288 (636)</u>	<u>303 (668)</u>	<u>342 (754)</u>
W_{total}	<u>791 (1744)</u>	<u>828 (1826)</u>	<u>904 (1992)</u>

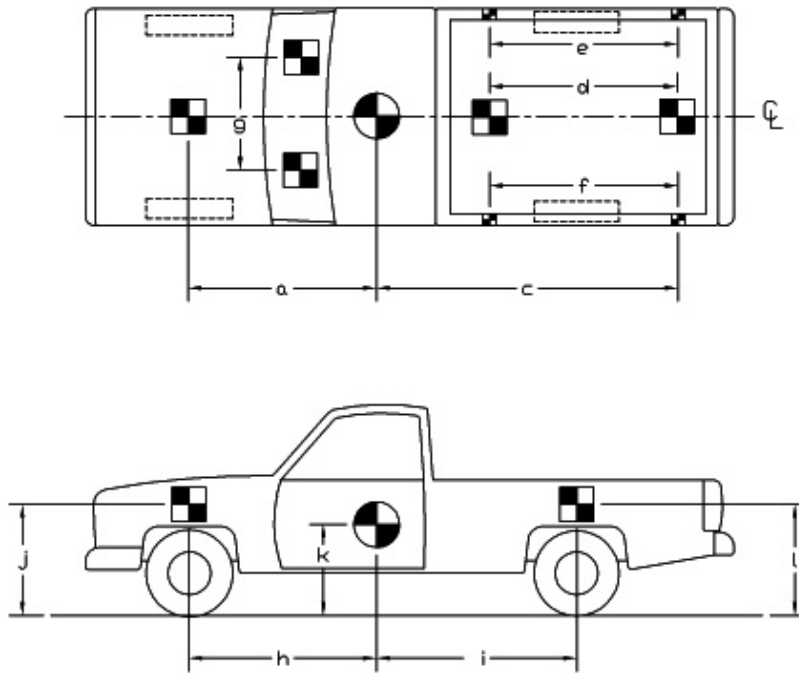
Note any damage prior to test: None

Figure 22. Vehicle Dimensions, Test MWT-6



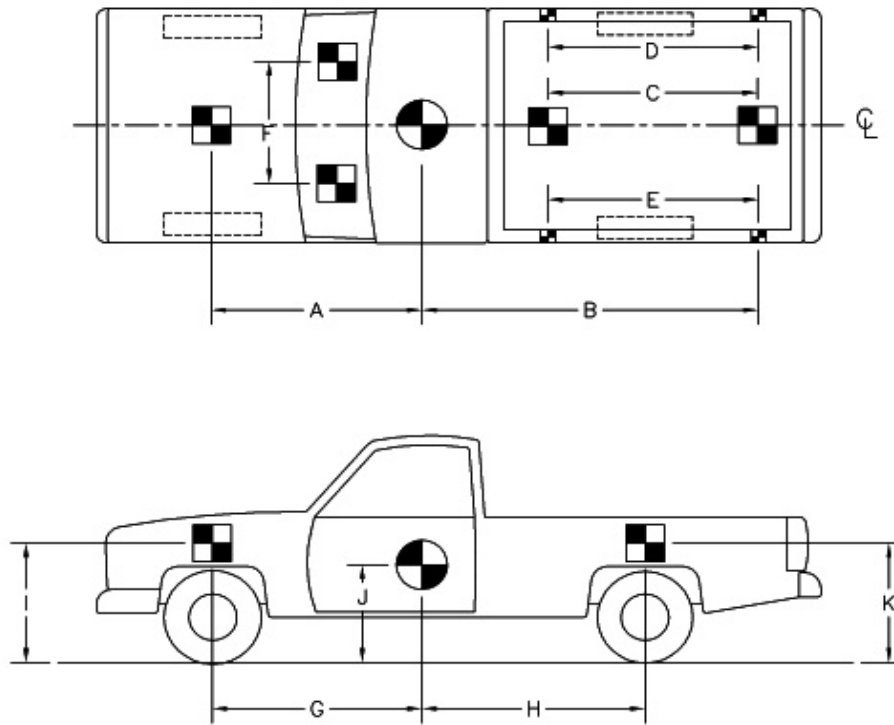
TEST #: <u>MWT-3</u>							
TARGET GEOMETRY (mm - in)							
a	<u>1565 (61.625)</u>	d	<u>1664 (65.5)</u>	g	<u>1362 (53.625)</u>	j	<u>1010 (39.75)</u>
b	<u>N/A</u>	e	<u>2153 (84.75)</u>	h	<u>1384 (54.5)</u>	k	<u>667 (26.25)</u>
c	<u>2635 (103.75)</u>	f	<u>2153 (84.75)</u>	i	<u>1943 (76.5)</u>	l	<u>1070 (42.125)</u>

Figure 23. Vehicle Target Locations, Test MWT-3



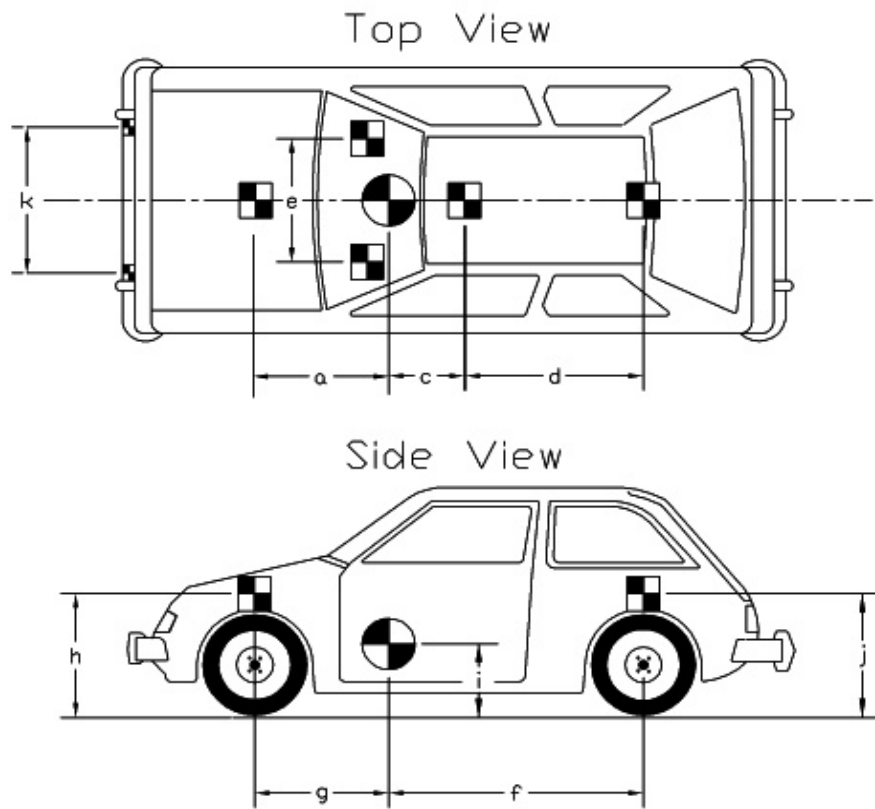
TEST #: <u>MWT-4</u>											
TARGET GEOMETRY -- mm (in.)											
a	<u>1549</u>	(61.0)	d	<u>1470</u>	(57.875)	g	<u>886</u>	(34.875)	j	<u>1026</u>	(40.375)
b	-		e	<u>2156</u>	(84.875)	h	<u>1391</u>	(54.75)	k	<u>667</u>	(26.25)
c	<u>2610</u>	(102.75)	f	<u>2156</u>	(84.875)	i	<u>2191</u>	(86.25)	l	<u>1051</u>	(41.375)

Figure 24. Vehicle Target Locations, Test MWT-4



TEST #: <u> MWT-5 </u>			
TARGET GEOMETRY -- mm (in.)			
A	<u>1588 (62.5)</u>	D	<u>2149 (84.625)</u>
B	<u>4477 (176.25)</u>	E	<u>2153 (84.75)</u>
C	<u>1641 (64.625)</u>	F	<u>886 (34.875)</u>
		G	<u>1391 (54.75)</u>
		H	<u>1943 (76.5)</u>
		I	<u>1016 (40.0)</u>
		J	<u>1060 (41.75)</u>
		K	<u>667 (26.25)</u>

Figure 25. Vehicle Target Locations, Test MWT-5



TEST #: <u> MWT-6 </u>			
TARGET GEOMETRY -- mm (in.)			
a	<u> 1041 (41.0)</u>	b	<u> NA </u>
c	<u> 229 (9.0)</u>	d	<u> 1048 (41.25)</u>
e	<u> 781 (30.75)</u>	f	<u> 1499 (59.0)</u>
g	<u> 864 (34.0)</u>	h	<u> 730 (28.75)</u>
i	<u> 546 (21.5)</u>	j	<u> 781 (30.75)</u>
k	<u> NA </u>		

Figure 26. Vehicle Target Locations, Test MWT-6

so that the vehicles would track properly along the guide cable. Two 5B flash bulbs were mounted on both the hood and roof of the vehicles to pinpoint the time of impact with the barrier system on the high-speed film, E/cam video, Photron video, and AOS video. The flash bulbs were fired by a pressure tape switch mounted on the front face of the bumper. A remote controlled brake system was installed in the test vehicle so the vehicle could be brought safely to a stop after the test.

6.4 Data Acquisition Systems

6.4.1 Accelerometers

One triaxial piezoresistive accelerometer system with a range of ± 200 Gs was used to measure the acceleration in the longitudinal, lateral, and vertical directions at a sample rate of 10,000 Hz. The environmental shock and vibration sensor/recorder system, Model EDR4M6, was developed by Instrumented Sensor Technology (IST) of Okemos, Michigan and includes three differential channels as well as three single-ended channels. The EDR-4 was configured with 6 MB of RAM memory and a 1,500 Hz lowpass filter. Computer software, “DynaMax 1 (DM-1)” and “DADiSP”, was used to analyze and plot the accelerometer data.

Another triaxial piezoresistive accelerometer system with a range of ± 200 Gs was also used to measure the acceleration in the longitudinal, lateral, and vertical directions at a sample rate of 3,200 Hz. The environmental shock and vibration sensor/recorder system, Model EDR-3, was developed by Instrumented Sensor Technology (IST) of Okemos, Michigan. The EDR-3 was configured with 256 kB of RAM memory and a 1,120 Hz lowpass filter. Computer software, “DynaMax1 (DM-1)” and “DADiSP”, was used to analyze and plot the accelerometer data.

6.4.2 Rate Transducers

An Analog Systems 3-axis rate transducer with a range of 1,200 degrees/sec in each of the three directions (pitch, roll, and yaw) was used to measure the rates of motion of the test vehicles.

The rate transducer was mounted inside the body of the EDR-4M6 and recorded data at 10,000 Hz to a second data acquisition board inside the EDR-4M6 housing. The raw data measurements were then downloaded, converted to the proper Euler angles for analysis, and plotted. Computer software, “DynaMax 1” and “DADiSP”, was used to analyze and plot the rate transducer data.

6.4.3 High-Speed Photography

For test no. MWT-3, two high-speed 16-mm Red Lake Locam cameras, with operating speed of approximately 500 frames/sec, were used to film the crash test. Five high-speed Red Lake E/cam video cameras, with operating speeds of 500 frames/sec, and five Canon digital video cameras with a standard operating speed of 29.97 frames/sec, were also used to film the crash test. Camera details and a schematic of all twelve camera locations for test no. MWT-3 is shown in Figure 27.

For test no. MWT-4, one high-speed 16-mm Red Lake Locam camera, with operating speed of approximately 500 frames/sec, was used to film the crash test. Two high-speed Photron video cameras and four high-speed Red Lake E/cam video cameras, all with operating speeds of 500 frames/sec, and six Canon digital video cameras, with a standard operating speed of 29.97 frames/sec, were also used to film the crash test. Camera details and a schematic of all thirteen camera locations for test no. MWT-4 is shown in Figure 28.

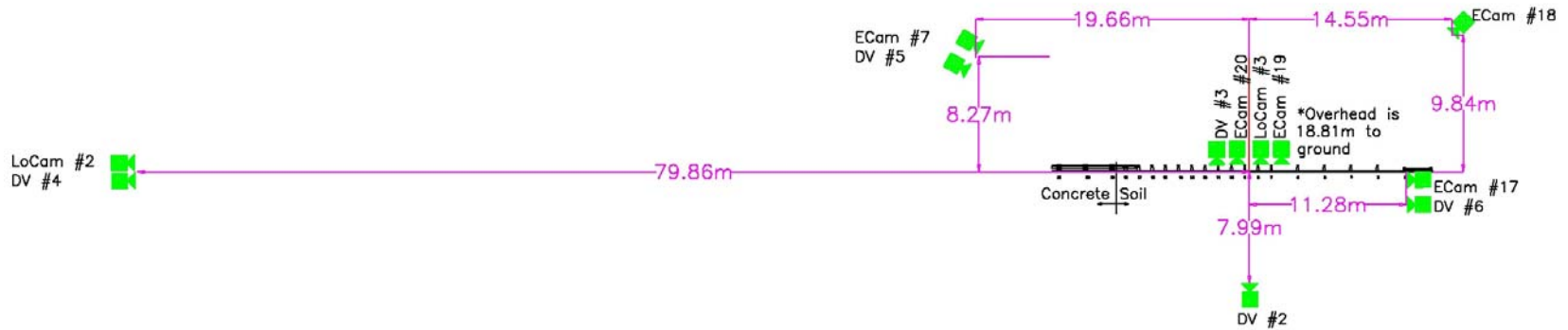
For test nos. MWT-5 and MWT-6, four high-speed AOS VITcam video cameras, all with operating speeds of 500 frames/sec, were used to film the crash test. Five Canon digital video cameras and one JVC digital video camera, with standard operating speeds of 29.97 frames/sec, were also used to film the crash test. Camera details and a schematic of all ten camera locations for test nos. MWT-5 and MWT-6 are shown in Figure 29 and 30, respectively.

The Locam films, Photron and AOS videos, and E/cam videos were analyzed using the Vanguard Motion Analyzer, ImageExpress MotionPlus software, and Redlake Motion Scope

software, respectively. Actual camera speed and camera divergence factors were considered in the analysis of the high-speed films and videos.

6.4.4 Pressure Tape Switches

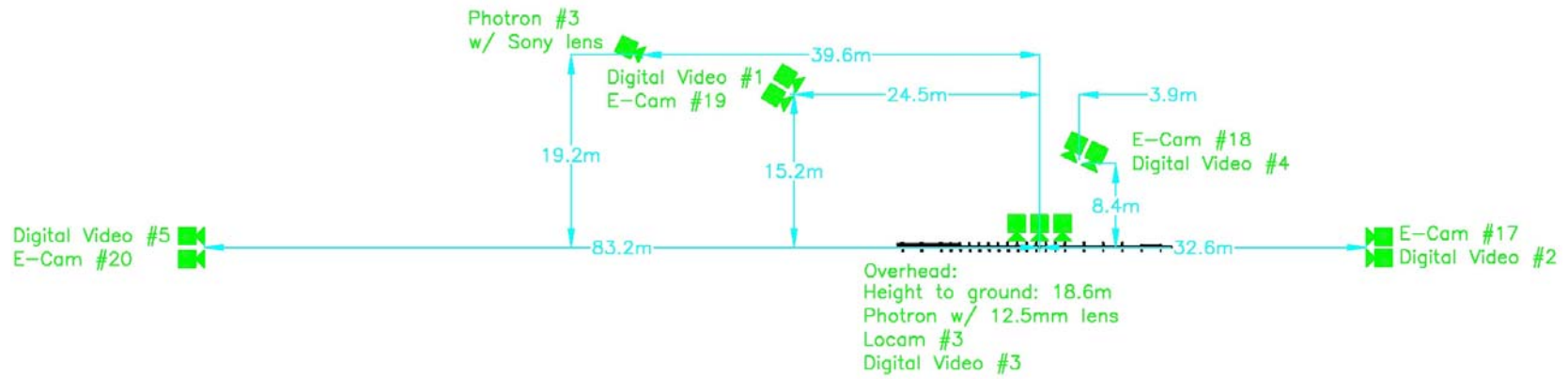
For test nos. MWT-3 through MWT-6, five pressure-activated tape switches, spaced at 2-m (6.56-ft) intervals, were used to determine the speed of the vehicle before impact. Each tape switch fired a strobe light which sent an electronic timing signal to the data acquisition system as the right-front tire of the test vehicle passed over it. Test vehicle speeds were determined from electronic timing mark data recorded using TestPoint software. Strobe lights and high-speed film analysis are used only as a backup in the event that vehicle speeds cannot be determined from the electronic data.



MWT-3 Camera Summary

	No.	Type	Operating Speed (frames/sec)
High-Speed Video	2	Redlake Locam	~500
	3	Redlake Locam	~500
	7	Redlake E/cam Camera	500
	17	Redlake E/cam Camera	500
	18	Redlake E/cam Camera	500
	19	Redlake E/cam Camera	500
Digital Video	20	Redlake E/cam Camera	500
	2	Canon-ZR10	29.97
	3	Canon	29.97
	4	Canon-ZR30	29.97
	5	Canon	29.97
	6	Canon-ZR25	29.97

Figure 27. Locations of High-Speed Cameras, Test MWT-3

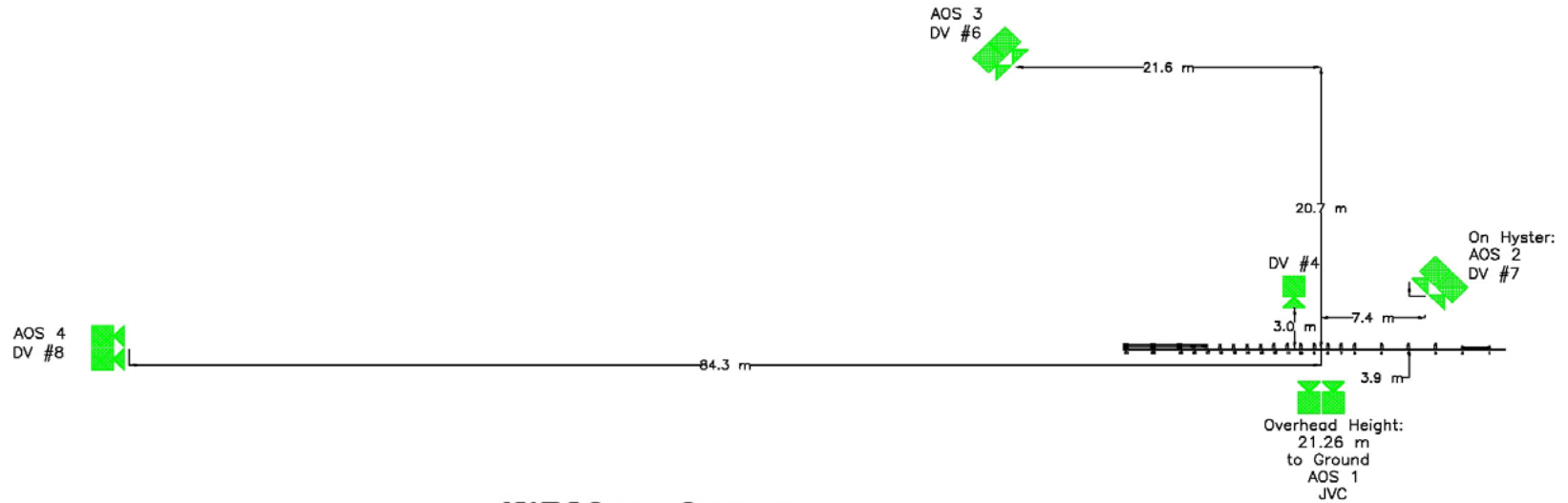


MWT-4 Camera Summary

	No.	Type	Operating Speed (frames/sec)	Lens
High-Speed Video	3	Redlake Locam	~500	
	1	Photron	500	12.5 mm fixed
	3	Photron	500	Sony
	17	Redlake E/cam Camera	500	
	18	Redlake E/cam Camera	500	
	19	Redlake E/cam Camera	500	
	20	Redlake E/cam Camera	500	
Digital Video	1	Canon	29.97	
	2	Canon-ZR10	29.97	
	3	Canon	29.97	
	4	Canon-ZR30	29.97	
	5	Canon	29.97	
	6	Canon-ZR25	29.97	

Digital Video #6
(Panning approx. dist 61m)
Digital Video #3

Figure 28. Locations of High-Speed Cameras, Test MWT-4



MWT-5 Camera Summary

	No.	Type	Operating Speed (frames/sec)	Lens	Lens Setting
High-Speed Video	1	AOS Vitcam CTM	500	12.5 mm fixed	
	2	AOS Vitcam CTM	500	Sigma 24-135	40
	3	AOS Vitcam CTM	500	Sigma 28-70	70
	4	AOS Vitcam CTM	500	Sigma 70-200	200
Digital Video	2	Canon-ZR10	29.97		
	4	Canon-ZR30	29.97		
	6	Canon-ZR25	29.97		
	7	Canon-ZR90	29.97		
	8	Canon-ZR90	29.97		
	1	JVC - GZ-MC500 (Enverio)	29.97		

DV #2 Panning


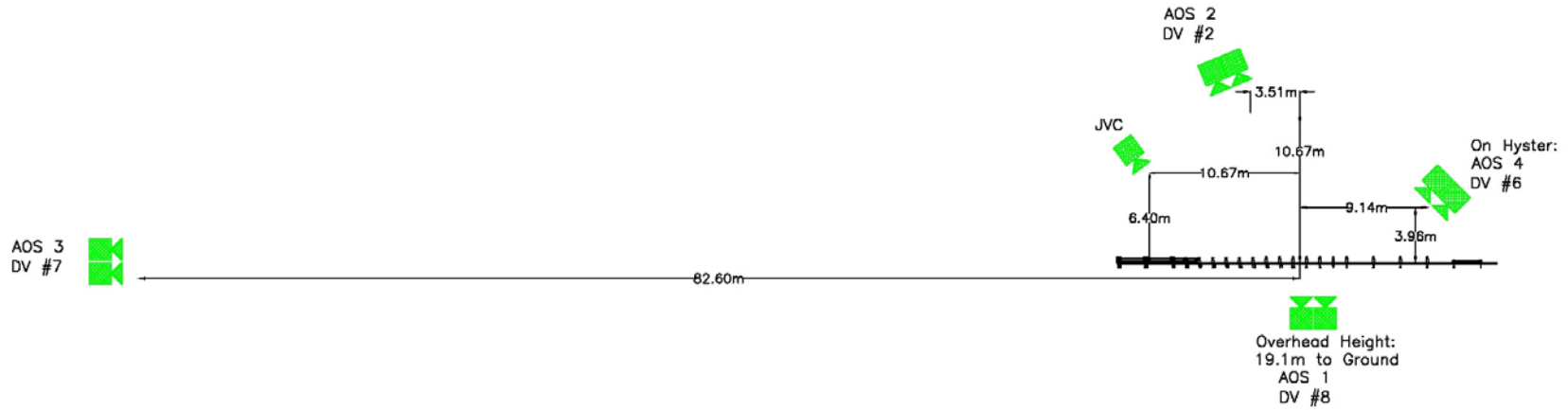


Figure 29. Locations of High-Speed Cameras, Test MWT-5



MWT-6 Camera Summary

	No.	Type	Operating Speed (frames/sec)	Lens	Lens Setting
High-Speed Video	1	AOS Vitcam CTM	500	20 mm fixed	
	2	AOS Vitcam CTM	500	TeleMacro(124) 100-300	100
	3	AOS Vitcam CTM	500	Sigma 70-200	200
	4	AOS Vitcam CTM	500	Sigma 24-135	70-100
Digital Video	2	Canon-ZR10	29.97		
	4	Canon-ZR30	29.97		
	6	Canon-ZR25	29.97		
	7	Canon-ZR90	29.97		
	8	Canon-ZR90	29.97		
	1	JVC - GZ-MC500 (Everio)	29.97		



Figure 30. Locations of High-Speed Cameras, Test MWT-6

7 CRASH TEST NO. 1

7.1 Test MWT-3

The 2,021-kg (4,456-lb) pickup truck impacted the guardrail system (Design No. 1) upstream from the W-beam to thrie beam transition element at a speed of 102.9 km/h (63.9 mph) and at an angle of 24.8 degrees. A summary of the test results and sequential photographs are shown in Figure 31. The summary of the test results and sequential photographs in English units are shown in Appendix B. Additional sequential photographs are shown in Figures 32 through 34. Documentary photographs are shown in Figures 35 and 36.

7.2 Test Description

Initial vehicle impact was to occur between post nos. 8 and 9, or 330 mm (13 in.) upstream from the centerline of post no. 9, as shown in Figure 37. Actual vehicle impact occurred 203 mm (8 in.) upstream from the centerline of post no. 9. At 0.010 sec after impact, the right-front corner of the vehicle was located at post no. 9 and began to crush inward. At 0.022 sec, the rail deformed at post nos. 8, 9, and 10. At this same time, the soil around post no. 9 began to fail, and the right-front corner of the hood protruded over the rail. At 0.050 sec, the right-front corner of the hood was positioned over post no. 10, rail deflection continued downstream to post no. 11, and large amounts of soil damage were evident. At 0.093 sec, the right-side door became ajar at the top, and the right-front corner of the hood, which was crushed inward to the centerline of the truck with bumper completely under the hood, was positioned over post no. 11. At this same time, post no. 9 rotated clockwise slightly, and post nos. 12 and 13 began to deflect. At 0.097 sec, the body of the truck began to redirect while the truck continued along its same direction and encountered positive roll toward the system. At 0.145 sec, post no. 10 rotated clockwise. At this same time, the left-front edge of the hood separated from the quarter panel, and the front edge of the right-side door crushed into the rail. At

0.174 sec, the truck continued to redirect. At this same time, the left-side tires became airborne as the truck continued to encounter roll toward the system. At 0.238 sec, the right-rear corner of the truck bed contacted the rail slightly downstream of post no. 9, and the front of the hood was located near post no. 15, which encountered slight deflection. At 0.280 sec, the truck became parallel to the system. At this same time, the vehicle began to roll clockwise, and the right-rear corner of the bed mounted the system. At 0.311 sec, the right-front corner of the hood was located at post no. 16 and was no longer protruding over the system. At 0.360 sec, the right-front tire was airborne, and the truck continued to roll clockwise. At 0.533 sec, the right-front tire contacted the ground as the vehicle continued to roll. At this same time, the truck exited the system at an angle of 16.6 degrees and a resultant velocity of 59.2 km/h (36.7 mph). At approximately 1.010 sec, the truck rolled onto its right-front corner as it continued to roll. By 1.650 sec, the truck rolled completely over onto its roof and slid along the ground on its roof. The vehicle came to rest on its roof 35.8 m (117 ft - 5 in.) downstream from impact and 11.4 m (37 ft - 5 in.) laterally away from the traffic-side face of the guardrail system. The trajectory and final position of the pickup are shown in Figures 31 and 38.

7.3 Barrier Damage

Damage to the barrier was moderate, as shown in Figures 39 through 45. Barrier damage consisted of deformed guardrail and posts, contact marks on a guardrail section, and fractured wooden spacer blockouts. The length of vehicle contact along the approach guardrail system was approximately 5.7 m (18.75 ft), which spanned from 203 mm (8 in.) upstream from the centerline of post no. 9 through 203 mm (8 in.) upstream from the centerline of post no. 15.

Buckling in the upper and lower portions of the rail was found 102 mm (4 in.) upstream of post no. 8. Two buckle points were evident on the top portion of the rail at the leading edges of the blockouts at post nos. 16 and 17. Between post nos. 9 and 12, the bottom portion of the W-beam was

flattened, and the top portion encountered buckling but retained its shape. Severe scraping occurred on the upper and lower portions of the W-beam guardrail between post nos. 9 and 11. A tire contact mark occurred 279 mm (11 in.) upstream of post no. 9. A significant tire contact mark along the bottom portion of the W-beam started at post no. 10 and continued through post no. 14. A third tire contact mark on the upper portion of the W-beam to thrie beam transition section began 178 mm (7 in.) upstream of post no. 12 and continued through 102 mm (4 in.) upstream of post no. 14. Another tire mark began on the middle portion of the W-beam to thrie beam transition section between post nos. 11 and 12 and continued to 203 mm (8 in.) upstream of post no. 15. Slight rail damage was visible between post nos. 14 and 15.

Guardrail to post bolt pullout occurred at post nos. 10 through 14. At post no. 11, the guardrail bolt pulled through both layers of the W-beam rail. Both bolts pulled out of the guardrail at post nos. 12 and 14, while only the top bolt pulled out of the guardrail at post no. 13. The blockouts at post nos. 12 and 13 were split.

Post nos. 1 and 2 deflected downstream slightly causing soil cracks to radiate from both soil foundation tubes. The soil became amassed on the upstream side of post no. 1. Soil gaps were visible on the upstream and downstream sides of post nos. 1 and 2. Post nos. 3 through 7 twisted approximately 25 mm (1 in.) at the back of the rail and were rotated downstream. Minor soil gaps occurred around post nos. 3 through 7. Post no. 8 remained undamaged with no major twisting nor deflection. Soil gaps of 3 mm (0.125 in) and 6 mm (0.25 in.) were evident on the traffic and back sides of post no. 8, respectively. Post no. 9 encountered 19 mm ($\frac{3}{4}$ in.) of twist. Soil gaps of 25.4 mm (1 in.) were found on both the traffic and back sides of post no. 9. Post no. 10 encountered severe deflections backward and downstream. Post no. 10 also twisted approximately 30 degrees counter-clockwise. A tire mark was visible on post no. 10 beginning on the upstream corner 102 mm (4 in.)

from the ground and continuing for 203 mm (8 in.) downstream. Post no. 11 was severely bent, twisted, and deflected backward. Post no. 11 was twisted 20 to 30 degrees counter-clockwise from its original position. Post no. 12 bent backwards and twisted 45 degrees counter-clockwise. Post no. 13 bent backward and downstream but not as severe as post nos. 11 and 12. Post no. 13 twisted 10 to 20 degrees counter-clockwise and large soil gaps of 152 mm (6 in.) and 64 mm (2.5 in.) formed on the traffic and back sides of the post, respectively. Post no. 14 bent downstream 30 degrees from the vertical, bent backward slightly, and an 89 mm (3.5 in.) soil gap formed on the traffic side of the post. Soil gaps of 25 mm (1 in.) and 19 mm (0.75 in.) formed on the traffic and back sides of post no. 15, respectively. A 13-mm (0.5-in.) soil gap on the traffic side of post no. 16. Post nos. 17 through 21 remained in their original positions and were undamaged.

The permanent set of the barrier system is shown in Figure 39. The maximum lateral permanent set rail and post deflections were 389 mm (15.3 in.) at the centerline of post no. 12 and 556 mm (21.9 in.) at the centerline of post no. 11, respectively, as measured in the field. The maximum lateral dynamic rail and post deflections were 620 mm (24.4 in.) at the centerline of post no. 12 and 649 mm (25.5 in.) at the centerline of post no. 11, respectively, as determined from the high-speed film analysis. The working width of the system was found to be 785 mm (30.9 in.).

7.4 Vehicle Damage

Exterior and interior damage to the vehicle was extensive, as shown in Figures 46 through 49. Occupant compartment deformations to the roof were severe due to vehicle rollover. However, the floorboard and firewall deformations were minimal. Complete occupant compartment deformations and the corresponding locations are provided in Appendix C.

Most of the damage was concentrated on the front, both the left and right sides, and the roof of the vehicle due to rollover, as shown in Figure 46. The right-front corner of the vehicle was

crushed inward toward the engine with the bumper buckling near its center. The roof of the vehicle was crushed downwards due to vehicle roll. The right-front tire was deflated and removed from the steel rim, and the inside of the steel rim encountered deformations. The right-front outer tie rod was disengaged, while the ball joints, stabilizer bar, and shock mount remained intact. The right-side A-frame was deformed. The right-rear fender behind the tire, the right-side end of the rear bumper, and the tail pipe encountered significant damage.

The damage to the frame was minimal and focused mainly around the bumper bracket and frame horns. Deformations to the vehicle's body were evident on the right side in the shape of the guardrail. Left-side damage was limited to light scraping and box deformations due to rollover. The windshield was shattered but remained intact due to the safety layer, as shown in Figure 48. All other window glass shattered and was removed from the system.

7.5 Occupant Risk Values

The longitudinal and lateral occupant impact velocities were determined to be 7.81 m/s (25.64 ft/s) and 5.69 m/s (18.65 ft/sec), respectively. The maximum 0.010-sec average occupant ridedown decelerations in the longitudinal and lateral directions were 7.96 Gs and 15.77 Gs, respectively. It is noted that the occupant impact velocities (OIVs) and occupant ridedown decelerations (ORDs) were within the suggested limits provided in NCHRP Report No. 350. The results of the occupant risk, as determined from the accelerometer data, are summarized in Figure 31. Results are shown graphically in Appendix D. The results from the rate transducer are shown graphically in Appendix D.

7.6 Discussion

The analysis of the test results for test no. MWT-3 showed that the W-beam to thrie beam transition element, used in conjunction with an approach guardrail transition system, did not meet safety performance criteria established in NCHRP Report No. 350. The system adequately contained

but did not safely redirect the vehicle, since the vehicle rolled over after collision with the barrier. There were no detached elements nor fragments which showed potential for penetrating the occupant compartment nor presented undue hazard to other traffic. Deformations of, or intrusion into, the occupant compartment that could have caused serious injury did occur with the crushing of the roof. The test vehicle did not penetrate nor ride over the barrier system; however, the vehicle did not remain upright after the collision. Vehicle roll, pitch, and yaw angular displacements were noted. After collision, the vehicle's trajectory revealed minimum intrusion into adjacent traffic lanes. Therefore, test no. MWT-3 conducted on the W-beam to three beam transition element used in conjunction with an approach guardrail transition system was determined to be unacceptable according to the TL-3 safety performance criteria found in NCHRP Report No. 350 due to vehicle rollover.



0.000 sec

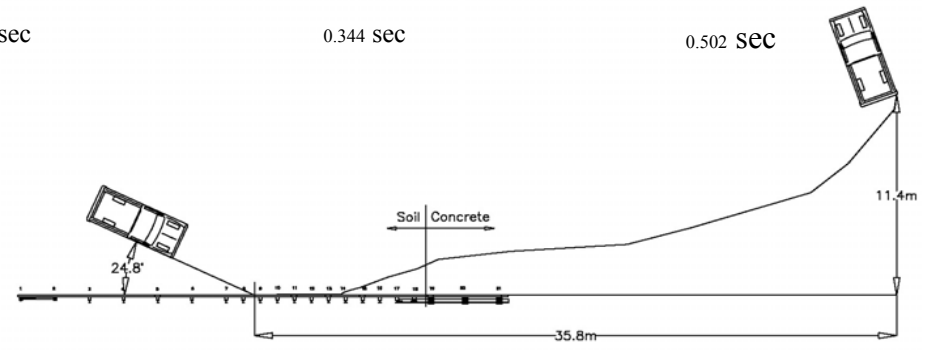
0.134 sec

0.226 sec

0.344 sec

0.502 sec

- Test Agency MwRSF
- Test Number MWT-3
- Date 6/18/03
- NCHRP 350 Test Designation 3-21
- Appurtenance W-beam to Thrie Beam Transition Element used with Approach Guardrail Transition
- Total Length 26.67 m
- Key Elements - Steel Thrie Beam Guardrail
 - Thickness 2.67 mm
 - Top Mounting Height 803 mm
- Key Elements - Steel W-Beam to Thrie Beam Transition
 - Thickness 2.67 mm
 - Shape Symmetrical
- Key Elements - Steel W-Beam Guardrail
 - Thickness 2.67 mm
 - Top Mounting Height 706 mm
- Key Elements - Steel Posts
 - Post Nos. 3 - 8 W152x13.4 by 1,829 mm long
 - Post Nos. 9 - 15 W152x13.4 by 2,134 mm long
 - Post Nos. 16 - 18 W152x22.3 by 2,134 mm long
 - Post Nos. 19 - 21 W152x29.8 by 752 mm long
- Key Elements - Post Spacing
 - Post Nos. 1 - 7, 19 - 21 1,905 mm
 - Post Nos. 7 - 19 953 mm
- Key Elements - Wood Spacer Blocks
 - Post Nos. 3 - 11 152 mm x 203 mm x 356 mm long
 - Post No 12 152 mm x 203 mm x 483 mm long
 - Post Nos. 13 - 15 152 mm x 203 mm x 559 mm long
 - Post Nos. 16 - 17 203 mm x 203 mm x 483 mm long
 - Post No. 18 203 mm x 203 mm x 381 mm long
- Key Elements - Steel Spacer Blocks
 - Post Nos. 19 - 21 W152 x 22.3 by 346 mm long
- Type of Soil Grading B - AASHTO M 147-65 (1990)
- Test Vehicle
 - Type/Designation 2000P
 - Make and Model 1998 GMC 2500 3/4-ton pickup
 - Curb 1,986 kg
 - Test Inertial 2,021 kg
 - Gross Static 2,021 kg



- Impact Conditions
 - Speed 102.9 km/h
 - Angle 24.8 degrees
 - Impact Location 203 mm upstream centerline post no. 9
- Exit Conditions
 - Speed 59.2 km/h
 - Angle 16.6 degrees
- Post-Impact Trajectory
 - Vehicle Stability Unsatisfactory
 - Stopping Distance 35.8 m downstream
11.4 m traffic-side face
- Occupant Impact Velocity
 - Longitudinal 7.81 m/s < 12 m/s
 - Lateral (not required) 5.69 m/s
- Occupant Ridedown Deceleration (10 msec avg.)
 - Longitudinal 7.96 Gs < 20 Gs
 - Lateral (not required) 15.77 Gs
- THIV (not required) NA
- PHD (not required) NA
- Test Article Damage Moderate
- Test Article Deflections
 - Permanent Set 556 mm
 - Dynamic 649 mm
 - Working Width 785 mm
- Vehicle Damage Extensive
 - VDS¹³ 01-R&T-4
 - CDC¹⁴ 01-RDAO9
 - Maximum Deformation NA

58

Figure 31. Summary of Test Results and Sequential Photographs, Test MWT-3



0.000 sec



0.100 sec



0.200 sec



0.300 sec



0.434 sec



0.667 sec



0.000 sec



0.048 sec



0.128 sec



0.228 sec



0.288 sec



0.348 sec

Figure 32. Additional Sequential Photographs, Test MWT-3



0.000 sec



0.048 sec



0.096 sec



0.138 sec



0.230 sec



0.418 sec



0.000 sec



0.046 sec



0.088 sec



0.144 sec

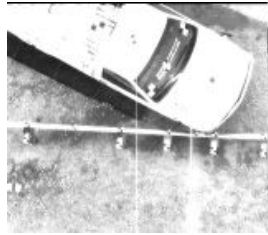


0.318 sec

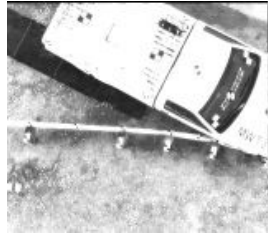


1.004 sec

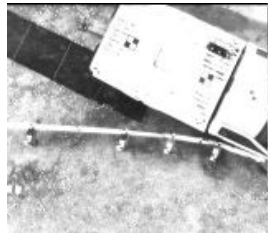
Figure 33. Additional Sequential Photographs, Test MWT-3



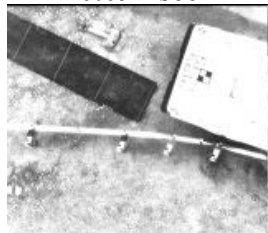
0.000 sec



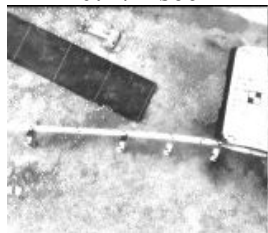
0.050 sec



0.094 sec



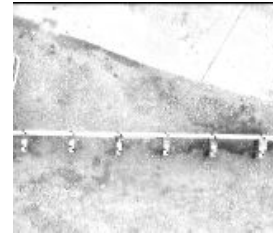
0.172 sec



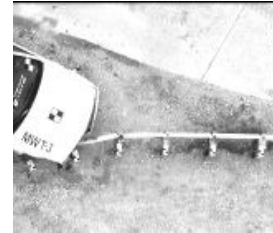
0.232 sec



0.274 sec



0.000 sec



0.066 sec



0.098 sec



0.162 sec



0.278 sec



0.414 sec

Figure 34. Additional Sequential Photographs, Test MWT-3

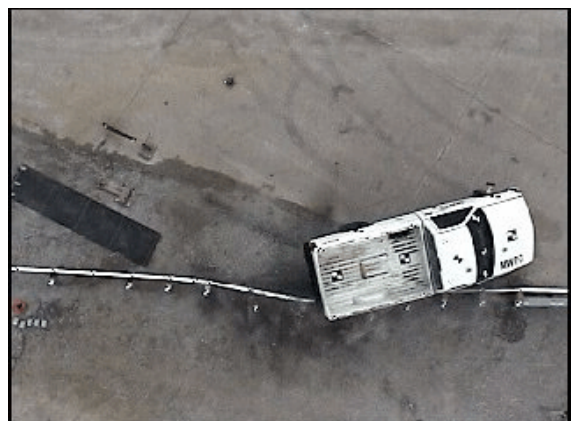
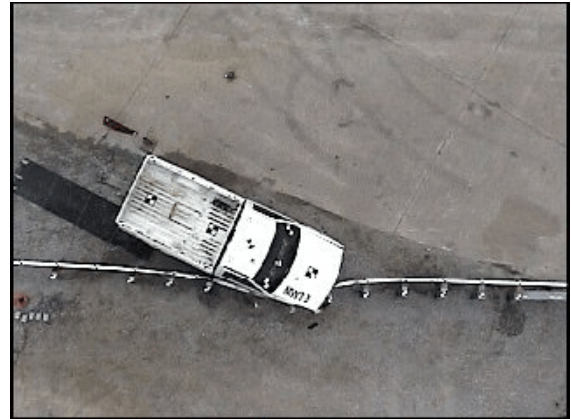


Figure 35. Documentary Photographs, Test MWT-3



Figure 36. Documentary Photographs, Test MWT-3



Figure 37. Impact Location, Test MWT-3



Figure 38. Vehicle Final Position and Trajectory Marks, Test MWT-3



Figure 39. System Damage, Test MWT-3



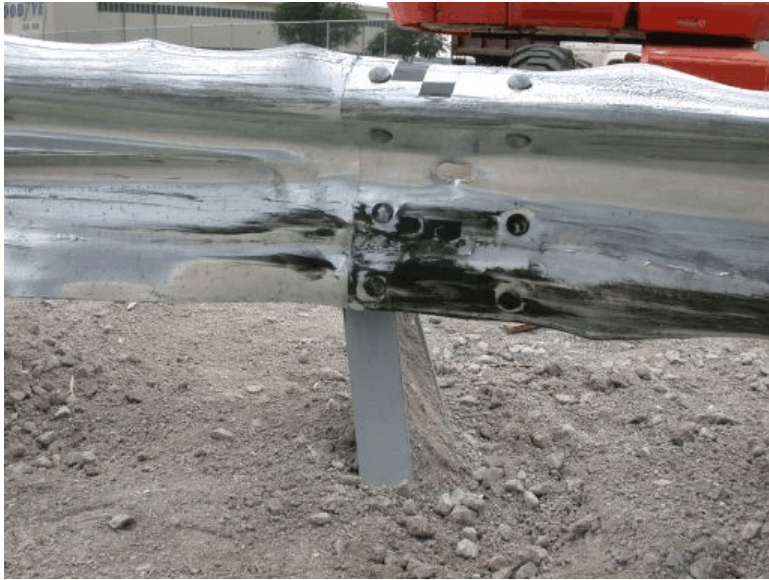
Figure 40. System Damage, Test MWT-3



Figure 41. Anchorage Damage, Test MWT-3



Figure 42. Post Nos. 9 and 10 Damage, Test MWT-3



70

Figure 43. Post Nos. 11 and 12 Damage, Test MWT-3



Figure 44. Post Nos. 13 and 14 Damage, Test MWT-3



Figure 45. Bridge Posts and Post No. 15 Damage, Test MWT-3



Figure 46. Vehicle Damage, Test MWT-3



74

Figure 47. Vehicle Damage, Test MWT-3



75

Figure 48. Vehicle Damage, Test MWT-3



Figure 49. Occupant Compartment and Windshield Damage, Test MWT-3

8 ANALYSIS AND DISCUSSION OF TEST NO. MWT-3

Following test no. MWT-3, a safety performance evaluation was conducted, and the W-beam to thrie beam transition element, used in conjunction with an approach guardrail transition system, was determined to be unacceptable according to the NCHRP Report No. 350 criteria. Due to the unsuccessful crash test, it was necessary to determine the cause of the poor barrier performance so that design modifications could be made to the barrier system in order to improve its overall safety performance.

As a result of the increased stiffness, the significant pocketing observed in test no. MWT-2 was not present in test no. MWT-3. However, the increased system stiffness caused the vehicle to begin to roll over the top of the guardrail. This roll behavior was a result of the effects of the relatively high center of gravity of the 2000P vehicle combined with the relatively low height for the 706 mm (27.75 in.) tall standard guardrail.

The rapid vehicle roll velocity induced during the early stages of test no. MWT-3 highlights a fundamental problem associated with standard metric height guardrail. This barrier is very near its performance limit when installed at its design height, and any further stiffening of the guardrail is likely to cause light trucks to rollover. Further, guardrail deflections observed during test no. MWT-3 were very similar to that predicted by the BARRIER VII analysis used in the design process. Therefore, it was concluded that the guardrail stiffening designed to prevent vehicle pocketing had achieved its purpose, and that the vehicle instability observed in test no. MWT-3 could not be effectively resolved without raising the height of the W-beam guardrail.

The Midwest Guardrail System (MGS) utilizes a 787 mm (31 in.) mounting height, 305-mm (12-in.) deep blockouts, and midspan splices, all of which improve the barrier's capacity to contain

and redirect light truck vehicles without inducing rollover (15-19). The MGS guardrail has demonstrated greatly improved performance with light truck impacts as well as a greater capacity to tolerate stiffening and other design variations without inducing rollover. In view of the improved performance of the MGS guardrail, it was decided to utilize this barrier on the approach to the transition system.

9 DESIGN MODIFICATIONS (DESIGN NO. 2)

Following the simulation analysis, converting the W-beam guardrail to the MGS guardrail was not as simple as replacing the upstream barrier since the height of the top of the MGS is approximately the same as the top of the thrie beam transition system. Hence, the standard symmetrical W-beam to thrie beam transition element could not be utilized to attach the two barrier systems. Instead, an asymmetrical transition element had to be utilized that would extend the bottom of the W-beam downward to meet the thrie beam element.

The modified approach guardrail transition system was identical to the previous system except for the conversion to the MGS guardrail, as shown in Figures 50 through 60. For this installation, the W-beam's top guardrail height was 787 mm (31 in.) with a 632-mm (24.875-in.) center mounting height. Additionally, the post embedment depth for post nos. 3 through 8, 9 through 15, 16 and 17, and 18 were 1,019 mm (40.125 in.), 1,324 mm (52.125 in.), 1,391 mm (54.75 in.), and 1,420 mm (56 in.), respectively, as shown in Figures 52 through 55.

Additionally, the only asymmetrical W-beam to thrie beam transition element available was a segment fabricated by cutting a triangular piece from the bottom of a standard 2.67-mm (12-gauge) thick thrie beam rail. A 3.43-mm (10-gauge) thick flat plate was welded along a portion of the cut region to reduce the risk of the exposed edge slicing through the sheet metal on an impacting vehicle, as shown in Figure 61. Although, this element clearly included some undesirable stress concentrations, it was the only readily available alternative.

Once again, the 26.67-m (87-ft 6-in.) test installation consisted of five major structural components: (1) a thrie beam channel bridge railing system; (2) nested 2.67-mm (12-gauge) thick thrie beam guardrail; (3) standard 2.67-mm (12-gauge) thick thrie beam guardrail; (4) a 2.67-mm

(12-gauge) thick asymmetrical W-beam to thrie beam transition section; and (5) standard 2.67-mm (12-gauge) thick W-beam rail attached to a simulated anchorage device. The corresponding English-unit drawings are shown in Appendix E. Photographs of the test installation are shown in Figures 61 and 62.

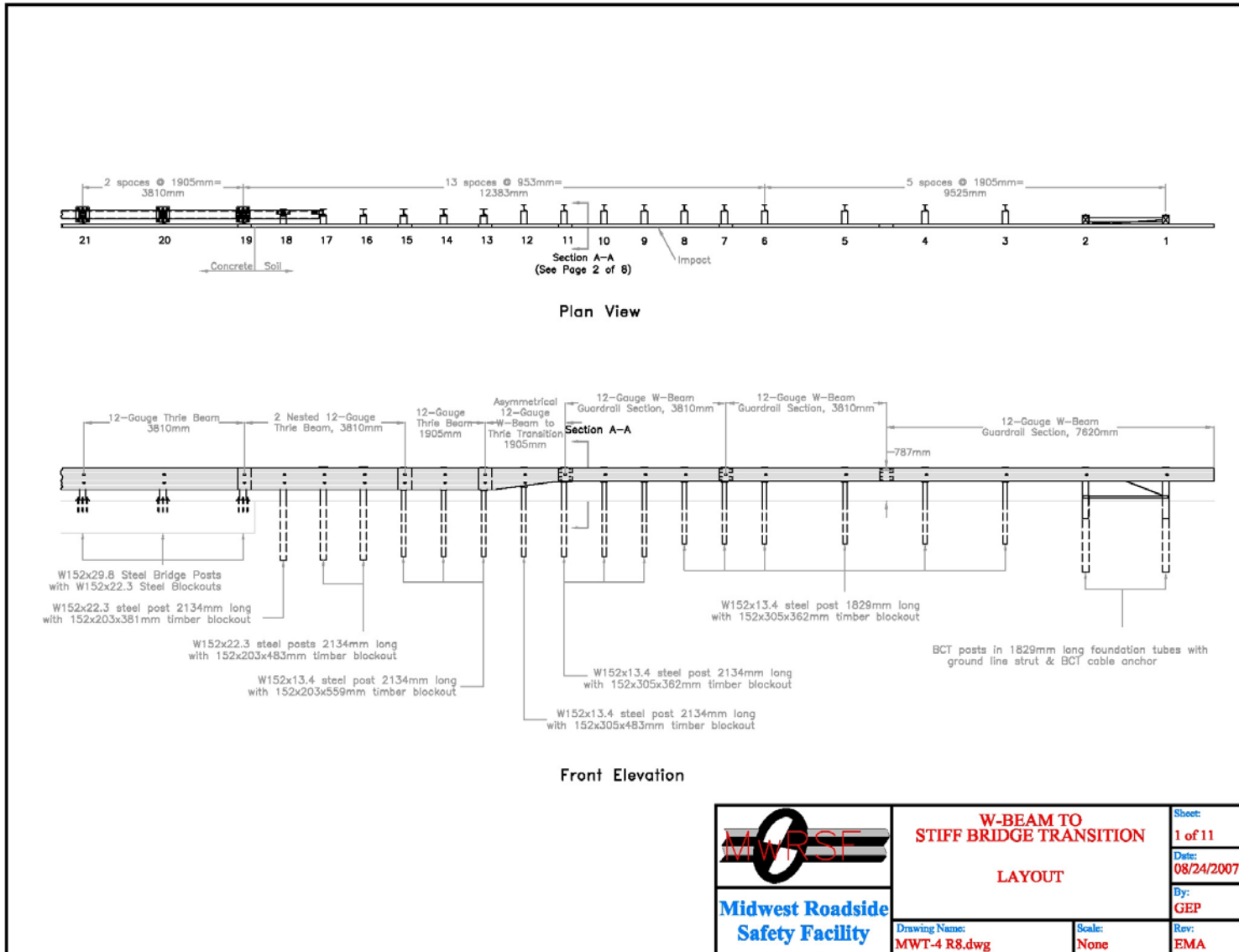


Figure 50. Layout (Design No. 2)

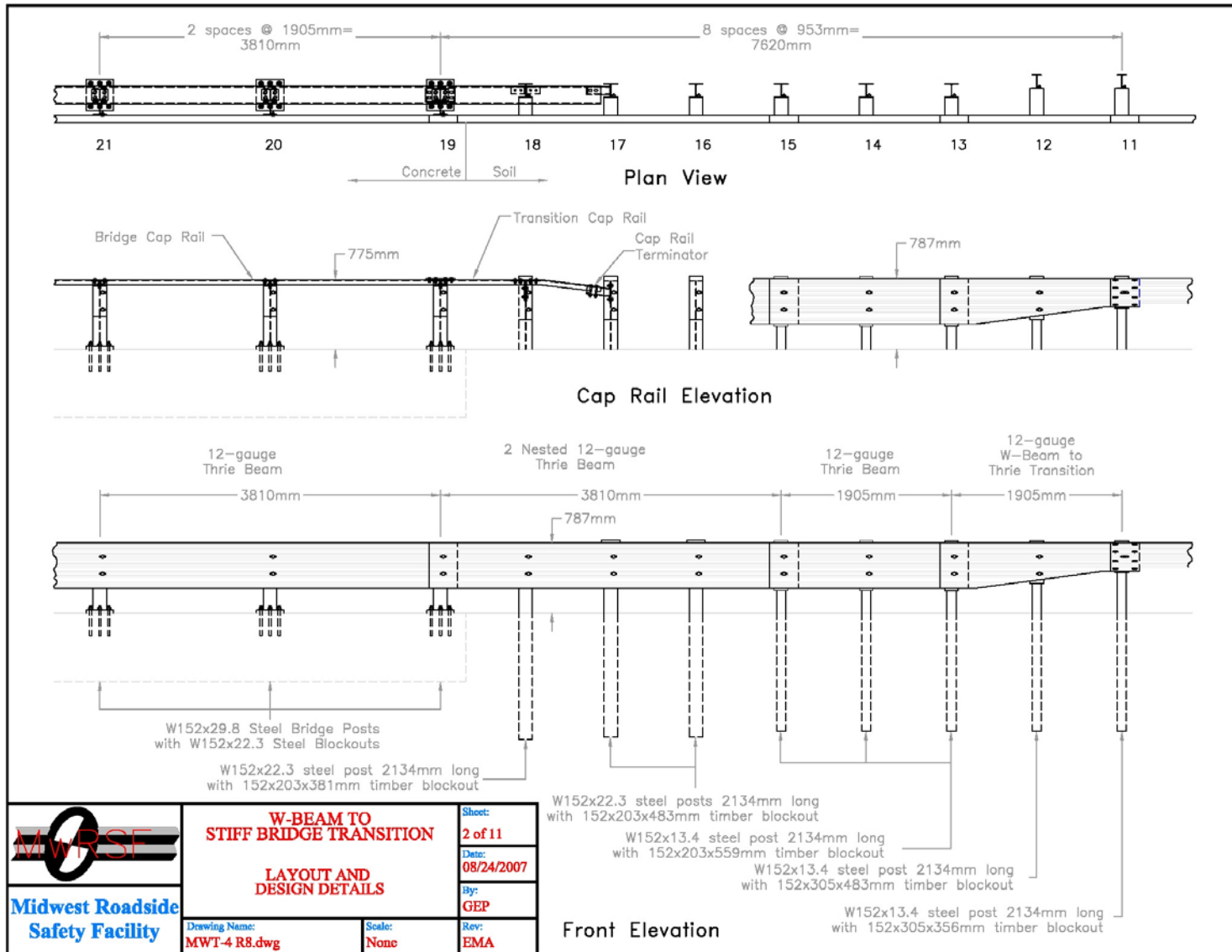


Figure 51. Layout and Design Details (Design No. 2)

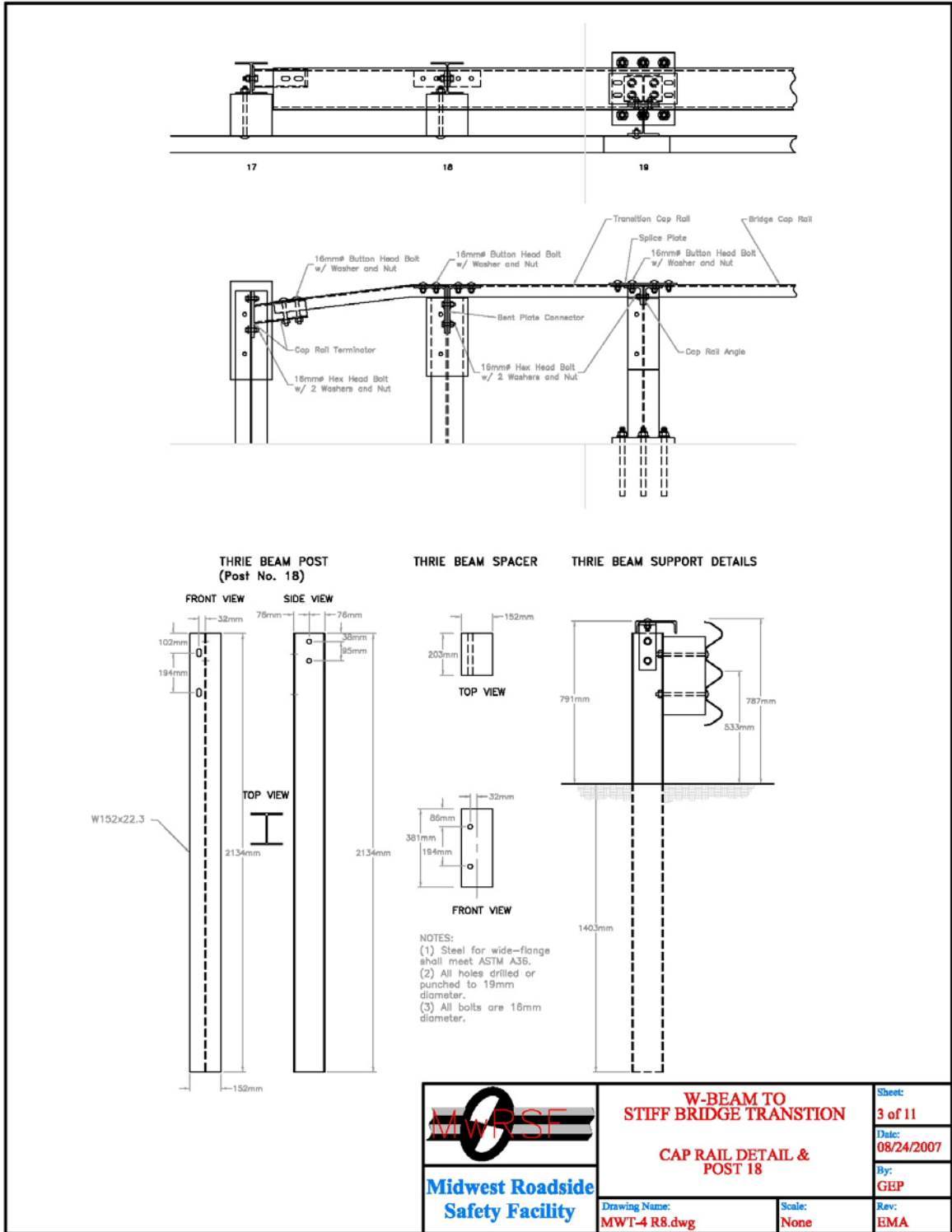


Figure 52. Cap Rail and Post No. 18 Details (Design No. 2)

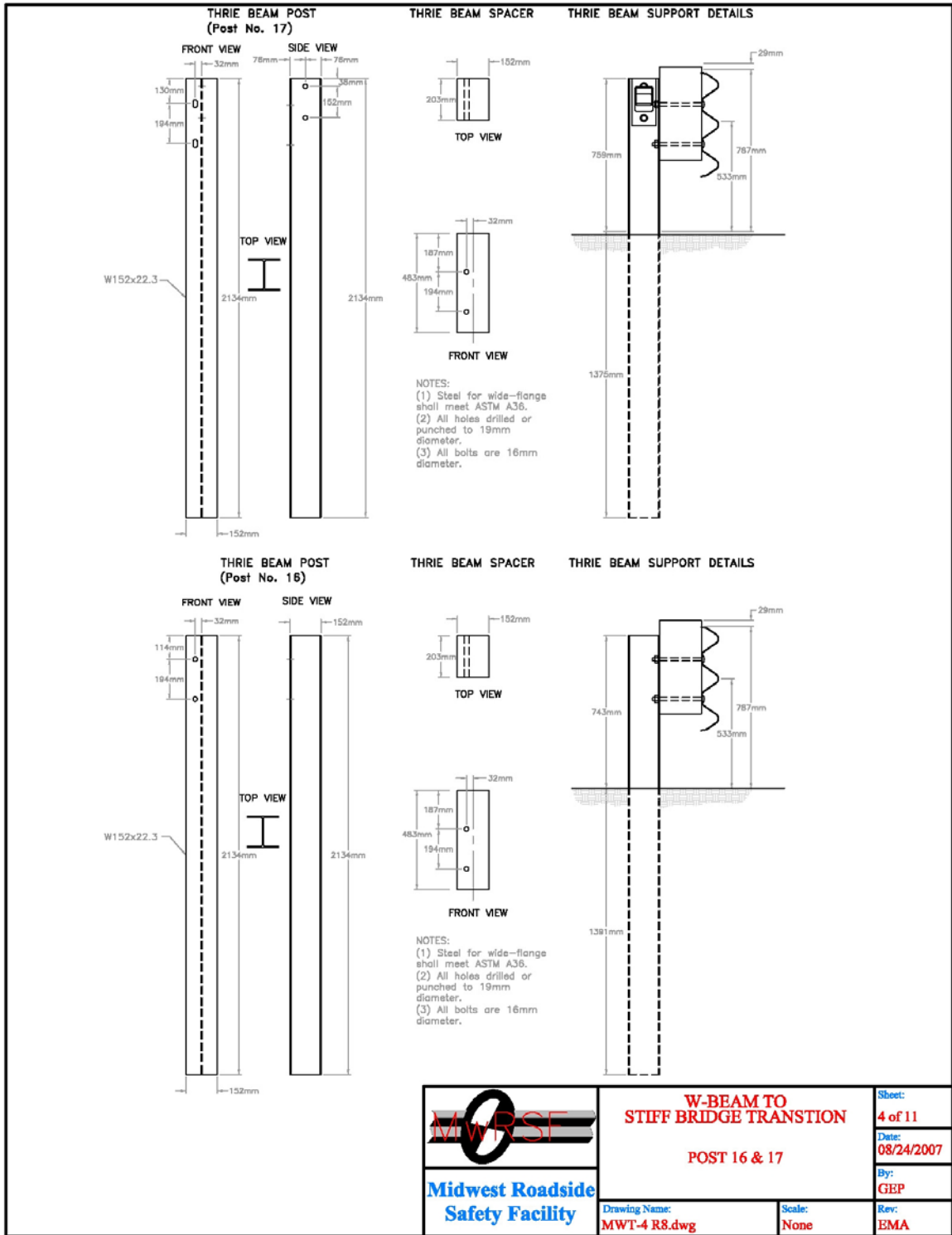


Figure 53. Post Nos. 16 and 17 Details (Design No. 2)

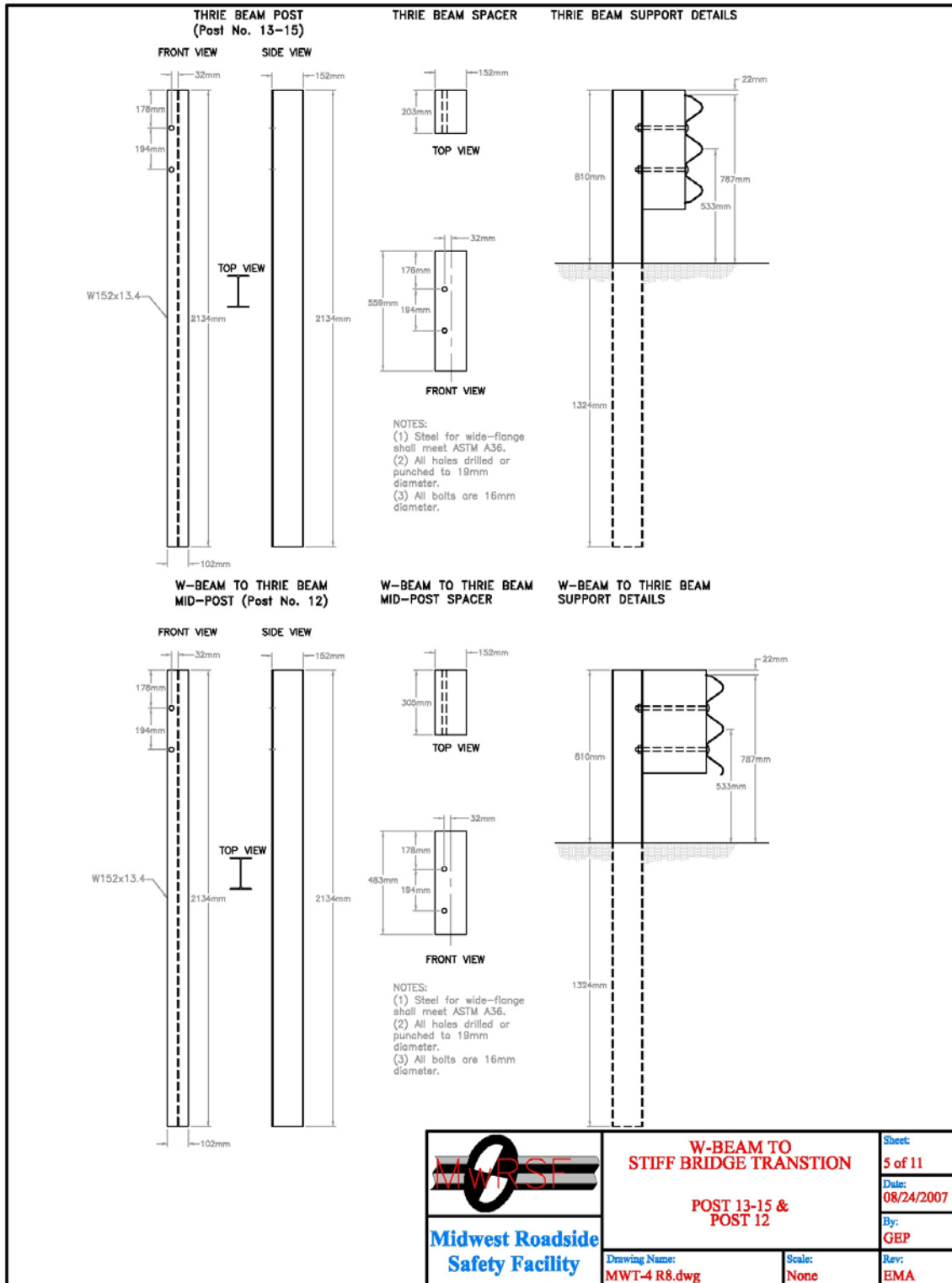


Figure 54. Post Nos. 12 through 15 Details (Design No. 2)

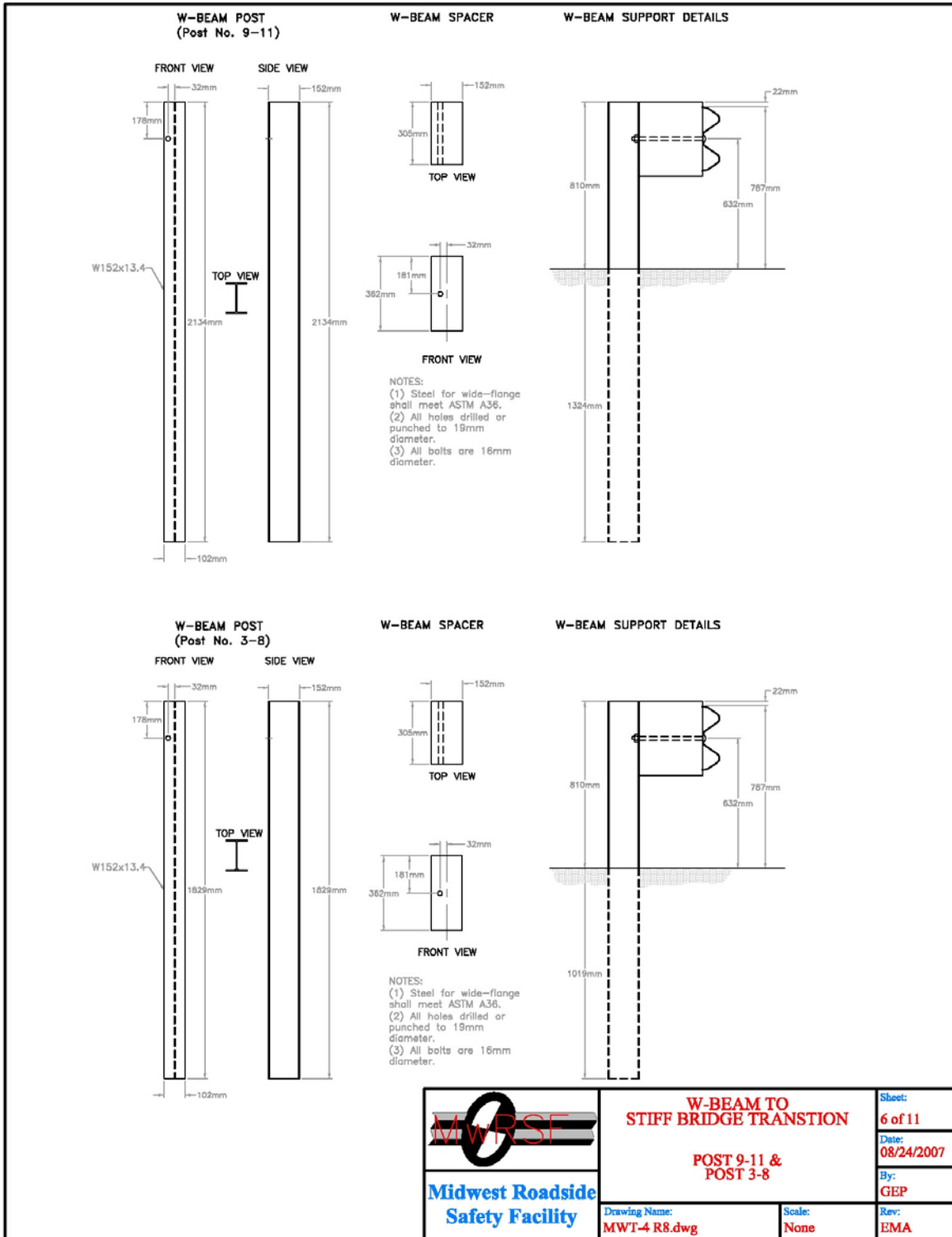


Figure 55. Post Nos. 3 through 11 Details (Design No. 2)

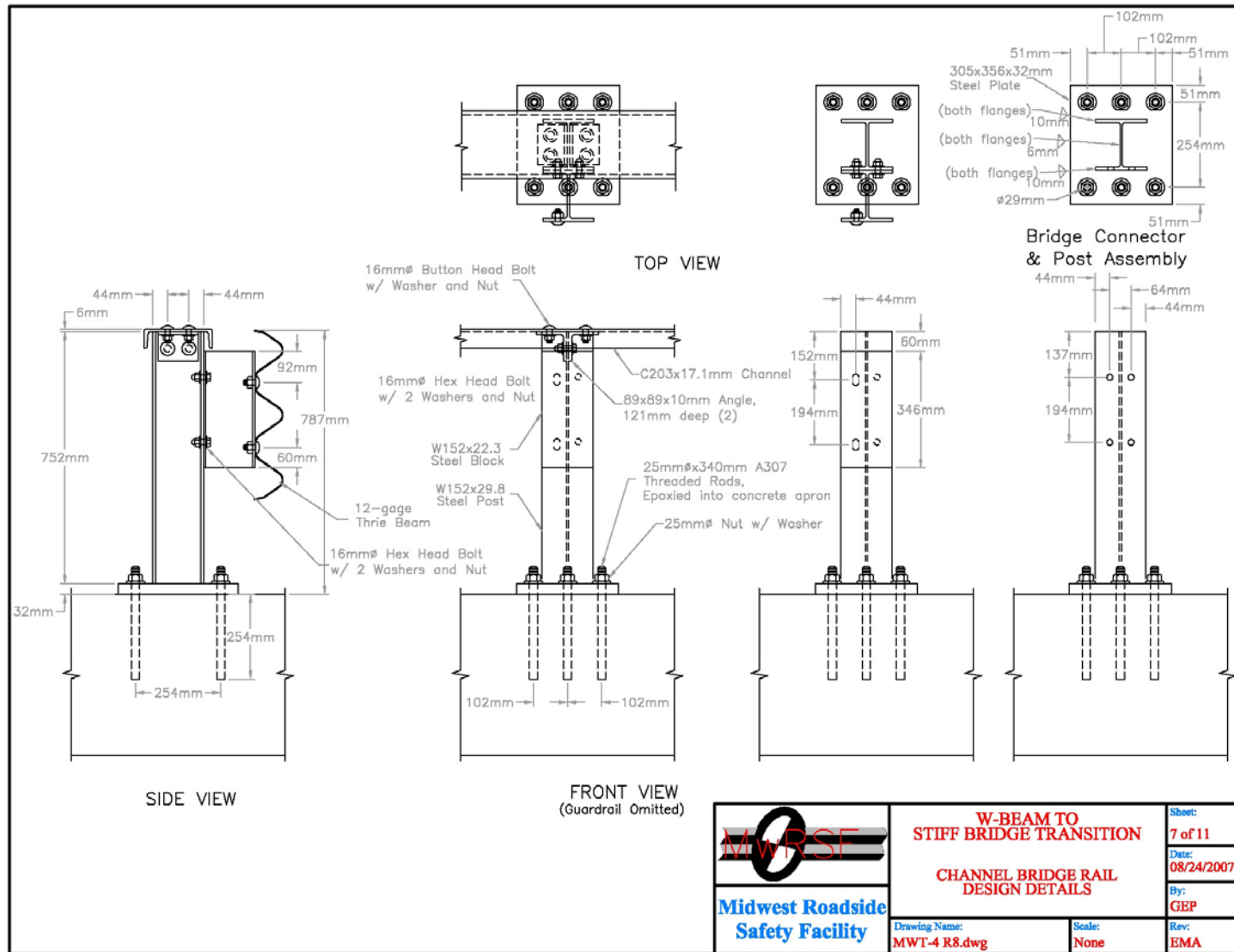
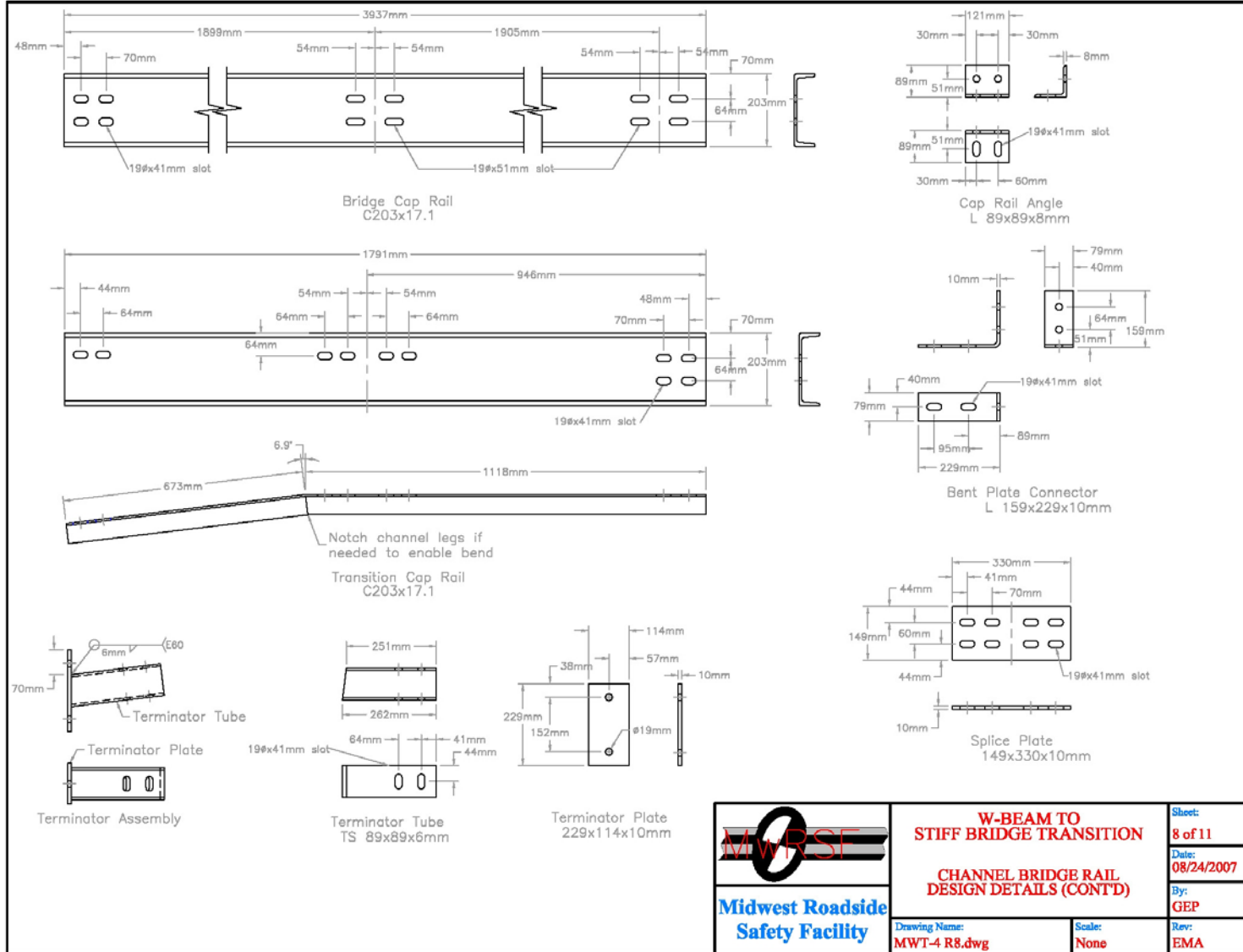


Figure 56. Channel Bridge Rail Design Details (Design No. 2)



<p>Midwest Roadside Safety Facility</p>	<p>W-BEAM TO STIFF BRIDGE TRANSITION</p>		<p>Sheet:</p> <p>8 of 11</p>
	<p>CHANNEL BRIDGE RAIL DESIGN DETAILS (CONT'D)</p>		<p>Date:</p> <p>08/24/2007</p>
	<p>Drawing Name:</p> <p>MWT-4 R8.dwg</p>		<p>By:</p> <p>GEP</p>
	<p>Scale:</p> <p>None</p>		<p>Rev:</p> <p>EMA</p>

Figure 57. Channel Bridge Rail Design Details (Design No. 2)

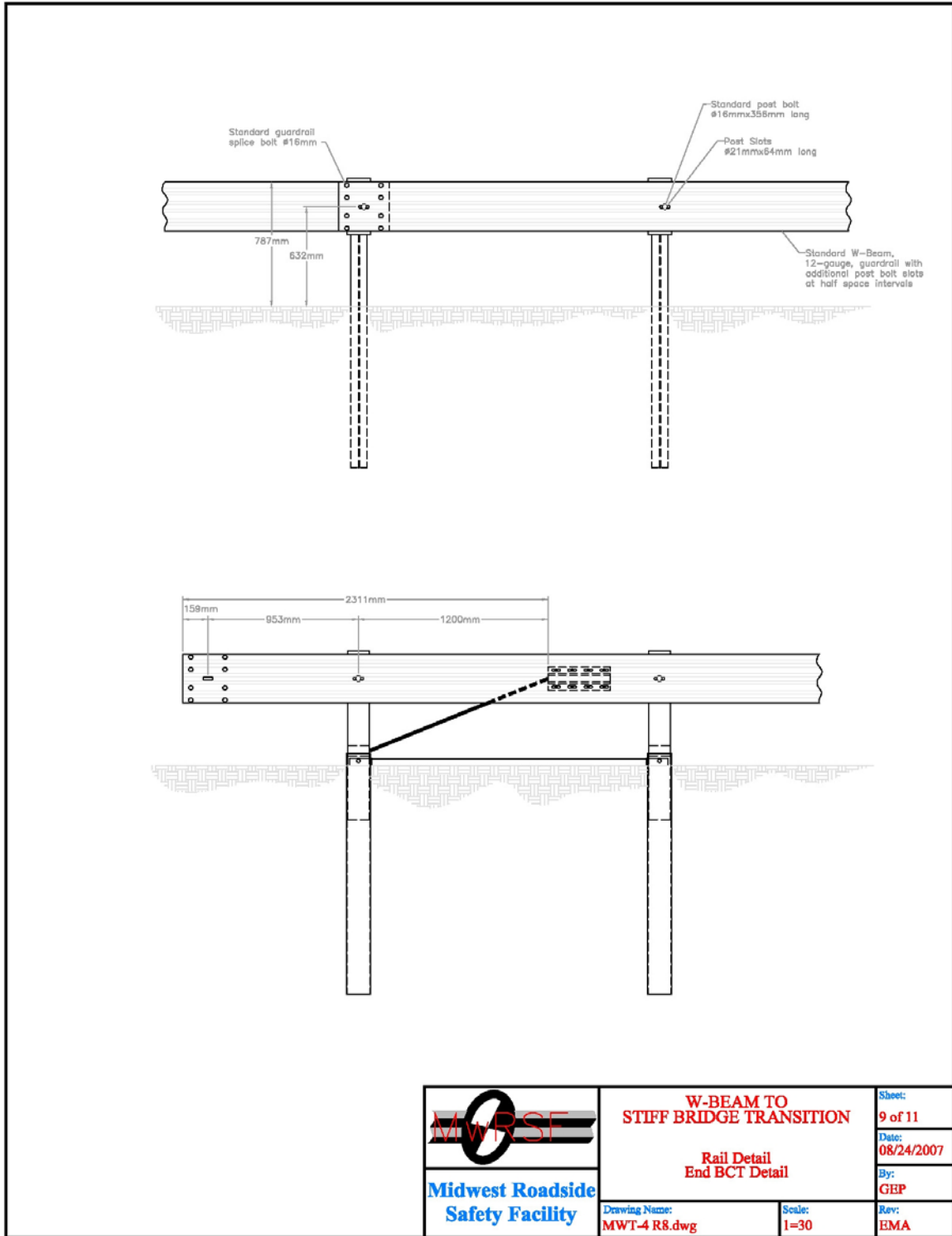


Figure 58. Rail and End BCT Details (Design No. 2)

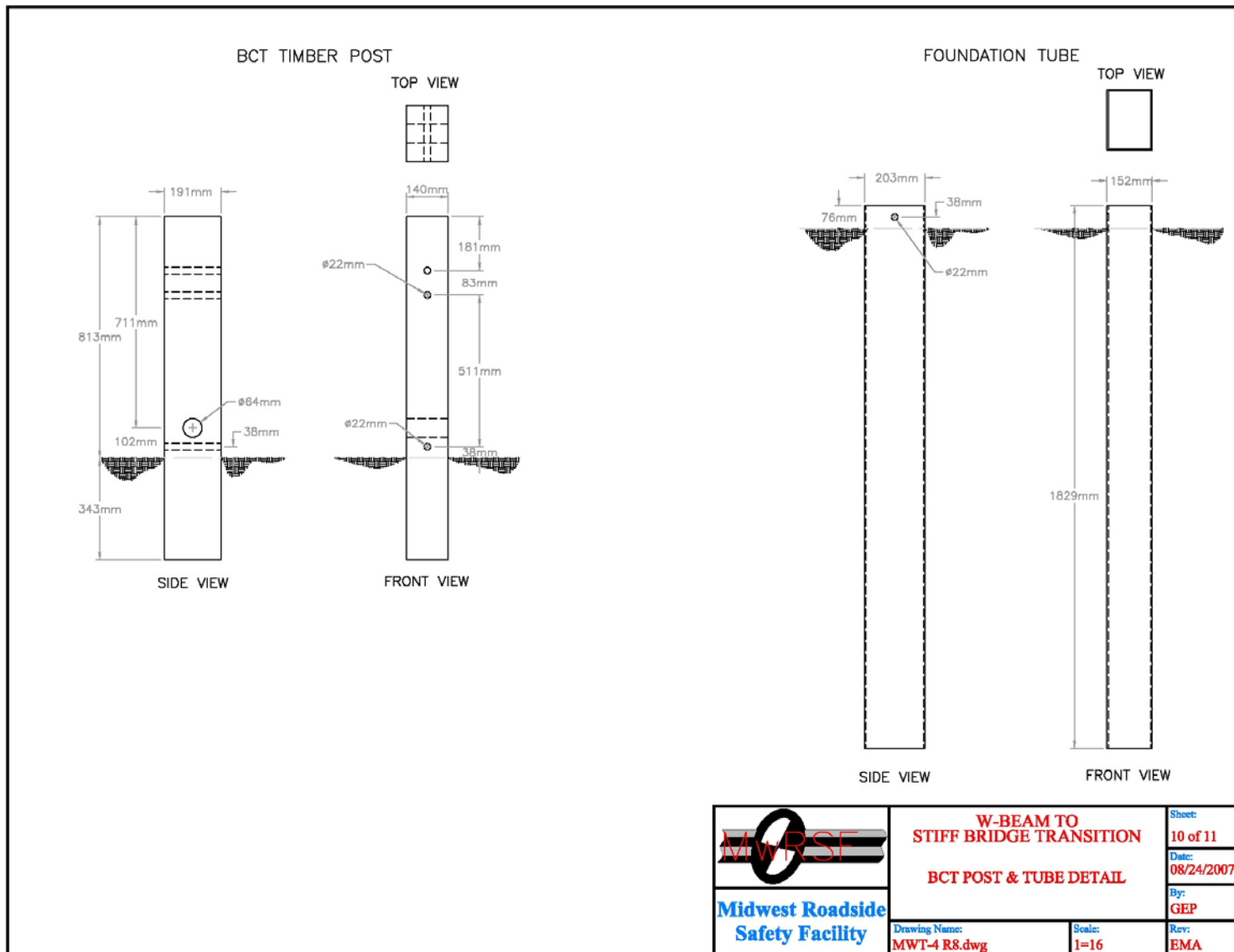


Figure 59. BCT Post and Tube Details (Design No. 2)

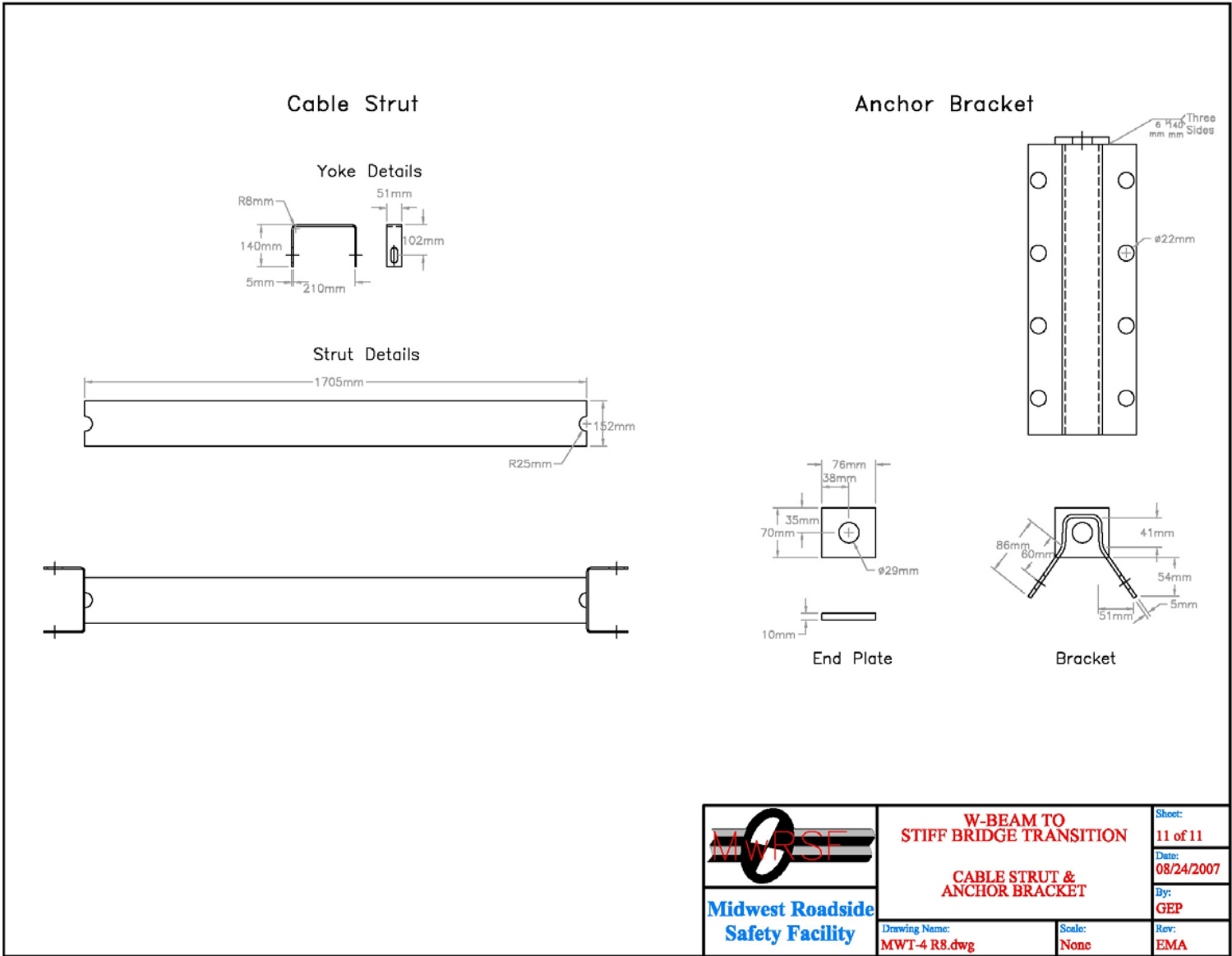


Figure 60. Cable Strut and Anchor Bracket Details (Design No. 2)



Figure 61. System and Transition Element (Design No. 2)



Figure 62. Anchor and Tarmac Connection (Design No. 2)

10 CRASH TEST NO. 2

10.1 Test MWT-4

The 2,018-kg (4,448lb) pickup truck impacted the guardrail system upstream from the W-beam to thrie beam transition element at a speed of 98.1 km/h (61.0 mph) and at an angle of 25.3 degrees. A summary of the test results and sequential photographs are shown in Figure 63. The summary of the test results and sequential photographs in English units are shown in Appendix B. Additional sequential photographs are shown in Figures 64 and 65. Documentary photographs of the crash test are shown in Figures 66 and 67.

10.2 Test Description

Initial vehicle impact was to occur between post nos. 8 and 9, or 330 mm (13 in.) upstream from the centerline of post no. 9, as shown in Figure 68. Actual vehicle impact occurred 229 mm (9 in.) upstream from the centerline of post no. 9. At 0.010 sec after impact, the right-front corner of the truck began to crush inward. At this same time, the bumper buckled at its midpoint, and the right-front quarter panel buckled outward. At 0.020 sec, the right-front corner of the truck protruded over the rail. At 0.040 sec, post nos. 5 through 9 deflected and rotated as the right-front corner of the truck continued to deform. At 0.086 sec, post no. 10 separated from the rail. At 0.100 sec, the truck began to redirect, and the right-front corner of the truck, up through the wheel well, extended over the rail. At this same time, post no. 11 disengaged from the rail, and the right-front tire contacted the post. At 0.188 sec, post nos. 11 and 12 continued to rotate and pull away from the rail as the truck yawed. By 0.196 sec, the rail had fractured and the downstream end of the fracture was located near the right-front corner of the truck. At 0.254 sec, the truck twisted and the front of the truck pitched downward with the rear end rising into the air. At 0.292 sec, the truck bowed along

its length near its midpoint. At this same time, the front of the vehicle had been captured by the rail, and the rear end continued to rise into the air. At 0.384 sec, the right- rear tire contacted the rail. At 0.408 sec, the truck rolled counterclockwise away from the system. At 0.476 sec, the right-rear tire lost contact with the rail. At 0.512 sec, the truck yawed counterclockwise away from the rail with the rear of the truck rotating over the rail. At 0.668 sec, pitching of the truck ceased and the rear end of the truck began to drop back down toward the ground. At 0.796 sec, the truck continued to yaw counterclockwise as it approached parallel. At 1.034 sec, both rear wheels contacted the ground. At 1.182 sec, the truck rolled clockwise toward the system. By 1.658 sec, the truck movement has ceased except for the continued rocking back and forth along its longitudinal axis. The vehicle came to rest on top of the system 5.0 m (16 ft - 4.5 in.) downstream from impact and 0.6 m (2 ft) laterally behind the traffic-side face of the guardrail system. The trajectory and final position of the truck are shown in Figures 63 and 69.

10.3 Barrier Damage

Barrier damage was extensive as shown in Figures 70 through 76. Barrier damage consisted of deformed guardrail and posts, ruptured guardrail, fractured blockouts, and contact marks on a guardrail section. The length of vehicle contact along the approach guardrail system was approximately 5.9 m (19.5 ft), which spanned from 229 mm (9 in.) upstream from the centerline of post no. 9 through the centerline of post no. 15.

The guardrail damage consisted of significant contact marks and moderate deformation and flattening of the impacted section of W-beam and thrie beam rail between post nos. 9 and 14. The guardrail buckled at post nos. 8, 9, 14, 15, and 16 and 89 mm (3.5 in.) downstream of post no. 10. The guardrail bent around the blockouts at post nos. 9 and 10. The W-beam guardrail was torn

through the cross section, beginning at the bottom of the W-beam to the beam transition element 476 mm (18.75 in.) downstream of the centerline of post no. 11, propagating up vertically 267 mm (10.5 in.), then horizontally 305 mm (12 in.), and then vertically once again ending at the top of the W-beam rail at the centerline of post no. 12 as shown in Figure 72. The W-beam was pulled off of post nos. 6, 10, and 13. The W-beam guardrail sustained significant yielding around the post bolt slots at post nos. 3 through 5 and 7 through 12, and the post bolt slot at post no. 8 also sustained small tears. The three beam guardrail sustained significant yielding around the post bolt slots at post nos. 14 through 18. No significant guardrail damage occurred downstream of post no. 16.

Steel post nos. 3 through 7 twisted and rotated slightly downstream. Post nos. 8 through 10 rotated backward slightly and bent longitudinally downstream. Post nos. 11 through 14 rotated backwards and bent longitudinally downstream. Post nos. 11 and 12 also encountered contact marks on the upstream front flange and rear flange, respectively. Post nos. 15 through 21 bent slightly downstream, and post nos. 15 through 18 also rotated backward slightly. The upstream anchorage system moved slightly longitudinally, but the posts were not damaged.

The wooden blockouts at post nos. 9 and 15 through 17 encountered minor deformations due to rail interaction, while the wooden blockout at post no. 10 encountered more significant deformations. The wooden blockout at post no. 14 encountered moderate damage due to the post bolt pulling partially through the blockout. The wooden blockouts at post nos. 13 and 18 were fractured but remained attached to the post. The wooden blockouts at post nos. 11 and 12 disengaged from the system. The steel blockouts at post nos. 19 through 21 twisted slightly downstream. The blockouts at post nos. 3 through 8 remained undamaged.

10.4 Vehicle Damage

Exterior vehicle damage was moderate, as shown in Figures 77 and 80. Extensive occupant compartment deformations occurred with the penetration of the center of the floorboard, as shown in Figure 80. The drive shaft U-joint penetrated through and caused a 178-mm (7-in.) slice in the floorboard. A 64-mm (2.5-in.) dent was also found in the floorboard. Complete occupant compartment deformations and the corresponding locations are provided in Appendix C.

Damage was concentrated on the front third of the vehicle. The front of the vehicle through the front quarter panels buckled inward. The right-front and left-front quarter panels and right-side door encountered significant contact and scratch marks along with buckling and numerous dents. The right-side frame rail buckled near the cab portion. The hood deformed downward and inward under itself. The front bumper encountered significant tears, dents, and buckling. The front grill was fractured and removed from the vehicle. The radiator encountered contact marks and was punctured. Contact marks were visible on the right side of the rear bumper. The right-front and left-front wheel wells sustained contact and scratch marks, and the right-front wheel well also encountered significant dents. Both of the front wheel assemblies were severely deformed and damaged.

10.5 Occupant Risk Values

The longitudinal and lateral occupant impact velocities were determined to be 6.77 m/s (22.22 ft/s) and 4.79 m/s (15.71 ft/s), respectively. The maximum 0.010-sec average occupant ridedown decelerations in the longitudinal and lateral directions were 19.00 Gs and 13.34 Gs, respectively. It is noted that the occupant impact velocities (OIVs) and occupant ridedown decelerations (ORDs) were within the suggested limits provided in NCHRP Report No. 350. The THIV and PHD values were determined to be 8.53 m/s (27.99 ft/s) and 20.22 Gs, respectively. The

results of the occupant risk, as determined from the accelerometer data, are summarized in Figure 63. Results are shown graphically in Appendix F. The results from the rate transducer are shown graphically in Appendix F.

10.6 Discussion

The analysis of the test results for test no. MWT-4 showed that the W-beam to thrie beam transition element, used in conjunction with an approach guardrail transition system, did not safely contain nor redirect the vehicle since the vehicle penetrated the system. There were no detached elements nor fragments which showed potential for penetrating the occupant compartment nor presented undue hazard to other traffic. Deformations of, or intrusion into the occupant compartment that could have caused serious injury did occur with the penetration of the floorboard. The vehicle did remain upright during and after the collision. The vehicle penetrated the guardrail due to rail rupture. The vehicle's trajectory did not intrude into adjacent traffic lanes, but the penetration of the vehicle through the system was unacceptable. Therefore, test no. MWT-4 conducted on the W-beam to thrie beam transition element used in conjunction with an approach guardrail transition system was determined to be unacceptable according to the TL-3 safety performance criteria found in NCHRP Report No. 350 due to vehicle penetration through the system and the deformation of, and penetration into, the occupant compartment.



0.000 sec

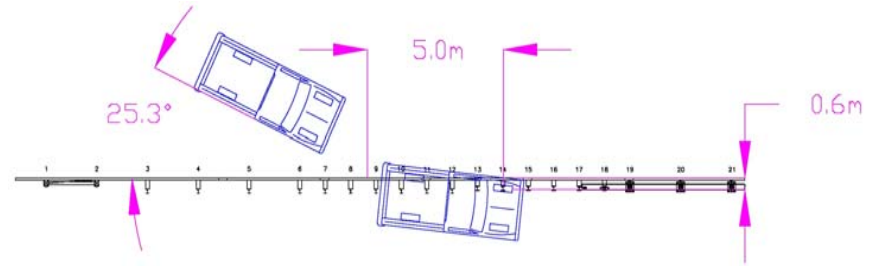
0.100 sec

0.196 sec

0.512 sec

1.658 sec

- Test Agency MwRSF
- Test Number MWT-4
- Date 7/29/03
- NCHRP 350 Test Designation 3-21
- Appurtenance W-beam to Thrie Beam Transition Element used with Approach Guardrail Transition
- Total Length 26.67 m
- Key Elements - Steel Thrie Beam Guardrail
 - Thickness 2.67 mm
 - Top Mounting Height 787 mm
- Key Elements - Steel W-Beam to Thrie Beam Transition
 - Thickness 2.67 mm
 - Shape Asymmetrical
- Key Elements - Steel W-Beam Guardrail
 - Thickness 2.67 mm
 - Top Mounting Height 787 mm
- Key Elements - Steel Posts
 - Post Nos. 3 - 8 W152x13.4 by 1,829 mm long
 - Post Nos. 9 - 15 W152x13.4 by 2,134 mm long
 - Post Nos. 16 - 18 W152x22.3 by 2,134 mm long
 - Post Nos. 19 - 21 W152x29.8 by 752 mm long
- Key Elements - Post Spacing
 - Post Nos. 1 - 6, 19 - 21 1,905 mm
 - Post Nos. 6 - 19 953 mm
- Key Elements - Wood Spacer Blocks
 - Post Nos. 3 - 11 152 mm x 305 mm x 362 mm long
 - Post No 12 152 mm x 305 mm x 483 mm long
 - Post Nos. 13 - 15 152 mm x 203 mm x 559 mm long
 - Post Nos. 16 - 17 152 mm x 203 mm x 483 mm long
 - Post No. 18 152 mm x 203 mm x 381 mm long
- Key Elements - Steel Spacer Blocks
 - Post Nos. 19 - 21 W152 x 22.3 by 346 mm long
- Type of Soil Grading B - AASHTO M 147-65 (1990)
- Test Vehicle
 - Type/Designation 2000P
 - Make and Model 1998 GMC 2500 3/4-ton pickup
 - Curb 1,977 kg
 - Test Inertial 2,018 kg
 - Gross Static 2,018 kg



- Impact Conditions
 - Speed 98.1 km/h
 - Angle 25.3 degrees
 - Impact Location 229 mm upstream centerline post no. 9
- Exit Conditions
 - Speed NA
 - Angle NA
- Post-Impact Trajectory
 - Vehicle Stability Satisfactory
 - Stopping Distance 5.0 m downstream
0.6 m laterally behind
- Occupant Impact Velocity
 - Longitudinal 6.77 m/s < 12 m/s
 - Lateral (Not Required) 4.79 m/s
- Occupant Ridedown Deceleration (10 msec avg.)
 - Longitudinal 19.00 Gs < 20 Gs
 - Lateral (Not Required) 13.34 Gs
- THIV 8.53 m/s
- PHD 20.22 Gs
- Test Article Damage Extensive (rail rupture)
- Test Article Deflections
 - Permanent Set NA
 - Dynamic NA
 - Working Width NA
- Vehicle Damage Moderate
 - VDS¹³ 01-RFQ-6
 - CDC¹⁴ 01-RYEW9
 - Maximum Deformation 165 mm

Figure 63. Summary of Test Results and Sequential Photographs, Test MWT-4



0.000 sec



0.060 sec



0.196 sec



0.496 sec



0.730sec



1.052 sec



0.000 sec



0.086 sec



0.204 sec



0.340 sec



0.554 sec



0.948 sec

Figure 64. Additional Sequential Photographs, Test MWT-4



0.000 sec



0.076 sec



0.174 sec



0.384 sec



0.750 sec



1.000 sec



0.000 sec



0.133 sec



0.334 sec



0.667 sec



1.135 sec



2.169 sec

Figure 65. Additional Sequential Photographs, Test MWT-4



Figure 66. Documentary Photographs, Test MWT-4



Figure 67. Documentary Photographs, Test MWT-4



Figure 68. Impact Location, Test MWT-4



Figure 69. Vehicle Final Position, Test MWT-4



Figure 70. System Damage, Test MWT-4



Figure 71. System Damage, Test No. MWT-4



Figure 72. Rail Rupture Damage, Test MWT-4



Figure 73. Post Nos. 1, 2, 5, and 6 Damage, Test MWT-4



Figure 74. Post Nos. 7 through 9 Damage, Test MWT-4



Figure 75. Post Nos. 10 through 15 Damage, Test MWT-4



Figure 76. Post Nos. 16 and 17 Damage, MWT-4



Figure 77. Vehicle Damage, Test MWT-4



Figure 78. Vehicle Damage, Test MWT-4



Figure 79. Undercarriage Damage, Test MWT-4



Figure 80. Occupant Compartment Damage, Test MWT-4

11 DISCUSSION AND COMPUTER SIMULATION

11.1 Analysis of Test No. MWT-4

Following test no. MWT-4, a safety performance evaluation was conducted, and the W-beam to thrie beam transition element, used in conjunction with an approach guardrail transition system, was determined to be unacceptable according to the NCHRP Report No. 350 criteria. Due to the unsuccessful crash test, it was necessary to determine the cause of the poor barrier performance so that design modifications could be made to the barrier system in order to improve its overall safety performance.

As the truck progressed into the guardrail during test no. MWT-4, vehicle redirection continued until the front bumper contacted the point of the flat plate extension on the bottom of the transition element. The start of the weldment proved to be a stress concentrator that produced a tear in the W-beam to thrie beam transition section. The tear quickly propagated through the entire segment and ruptured the rail system. Thereafter, all redirection stopped, and the test vehicle moved forward into the end of the stiff transition section where it was brought to an abrupt stop. Although the performance of the guardrail system initially looked promising and the rapid roll velocity associated with test no. MWT-3 was eliminated, the premature failure of the only available transition piece caused this test to be unsuccessful.

11.2 Redesigned Asymmetrical Transition Element

Test no. MWT-4 indicated that the basic transition design showed potential for meeting the safety performance criteria established in NCHRP Report No. 350, but the fabricated asymmetrical W-beam to thrie beam transition element that was available at the time of testing was unacceptable for use in the system. MwRSF researchers undertook an effort to develop a more acceptable W-beam

to three beam transition element. The new design incorporated the same basic philosophy utilized in the symmetrical transition piece, i.e., gradually introducing a new peak between the two existing peaks in a W-beam. The new component was to be manufactured from a 3.43-mm (10-gauge) plate conforming to AASHTO M-180 material specifications.

Three guardrail component producers (GSI Highway Products, Inc., Mid-Park, Inc., and IMH Products, Inc.) were contacted in an attempt to produce prototypes of the new transition element. GSI and Mid-Park collaborated to produce a welded part while IMH attempted to produce a component by creating a complicated bending operation to produce the component from a single flat plate. After obtaining both sets of components, the welded part was found to have fewer stress concentrations and was selected for use in the full-scale crash test program.

11.3 BARRIER VII Results

Following a review of test no. MWT-4, the pocketing observed in the guardrail system prior to the rupture was deemed significant and warranted further analysis. Therefore, BARRIER VII analysis was conducted on the system converted to MGS guardrail with an asymmetrical W-beam to three beam transition element. The BARRIER VII finite element model of the W-beam to three beam transition and a typical computer simulation input data file is shown in Appendix G.

In order to reduce the predicted pocketing angle, it was necessary to alter the stiffness between the transition and guardrail sections. This was achieved by changing the post sizes and depths in order to strengthen the transition and guardrail sections.

12 DESIGN MODIFICATIONS (DESIGN NO. 3)

The simulation analysis showed that increasing the post size and embedment depth for the posts within the transition region as well as the beginning of the MGS guardrail helped to eliminate the significant pocketing observed in the transition section during test no. MWT-4. The modified approach guardrail transition system was identical to the previous system, except for increasing the post size and embedment depth for post nos. 9 through 15 and the incorporating the prototype asymmetrical W-beam to thrie beam transition element in place of the available component, as shown in Figures 81 through 94. For this installation, post nos. 9 through 15 were galvanized ASTM A36 steel W152x17.9 (W6x12) sections measuring 2,286 mm (7.5 ft) long. Additionally, the post embedment depth for post nos. 9 through 15 was 1,473 mm (58 in.), as shown in Figures 86 through 88. The fabricated asymmetrical W-beam to thrie beam transition element was also replaced with the new 3.43-mm (10-gauge) MGS asymmetrical transition element, as shown in Figures 95 through 97.

The 26.67-m (87-ft 6-in.) test installation consisted of five major structural components: (1) a thrie beam channel bridge railing system; (2) nested 2.67-mm (12-gauge) thick thrie beam guardrail; (3) standard 2.67-mm (12-gauge) thick thrie beam guardrail; (4) a 3.43-mm (10-gauge) thick asymmetrical W-beam to thrie beam transition section; and (5) standard 2.67-mm (12-gauge) thick W-beam rail attached to a simulated anchorage device. The corresponding English-unit drawings are shown in Appendix G. Photographs of the test installation are shown in Figures 95 and 97.

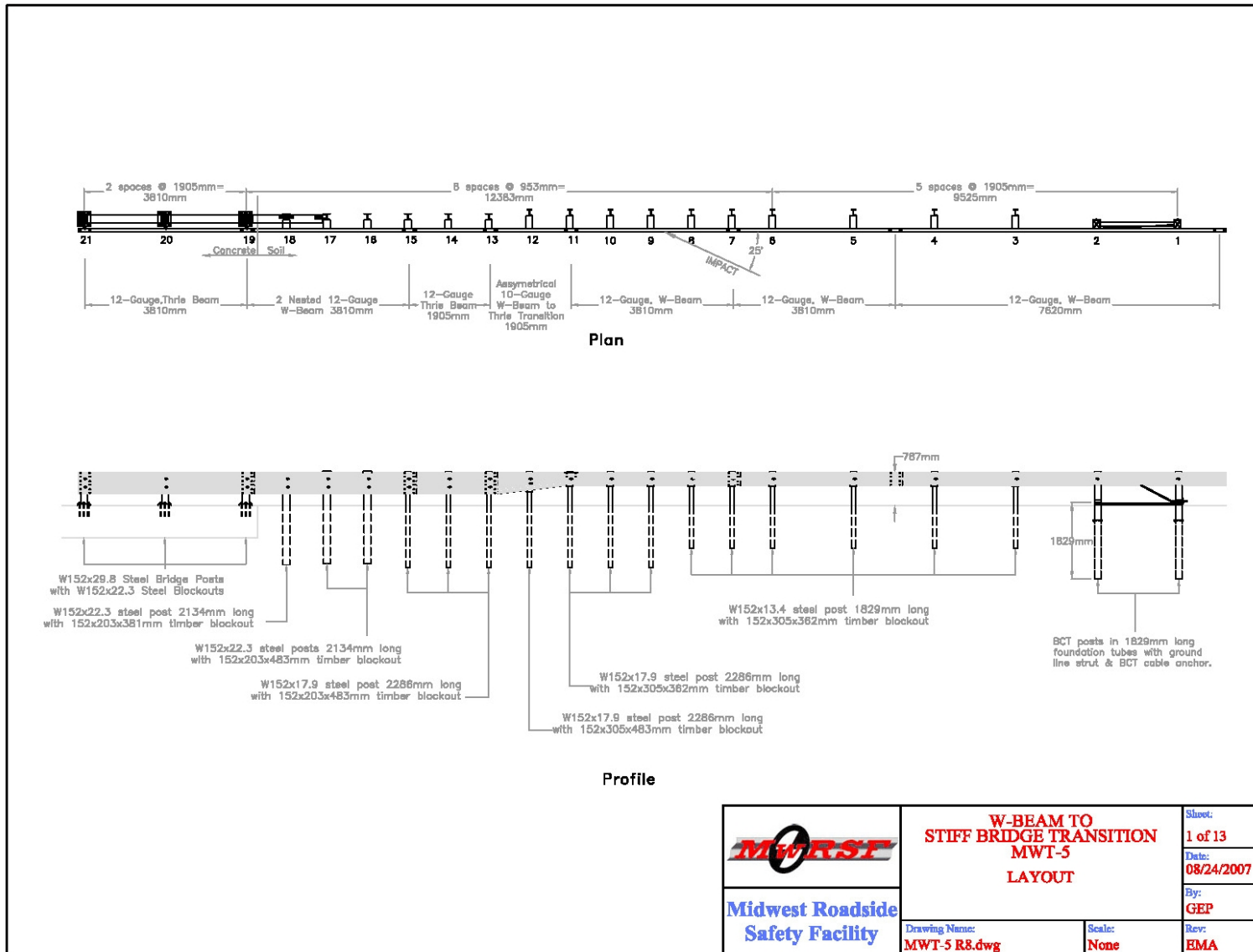


Figure 81. Layout (Design No. 3)

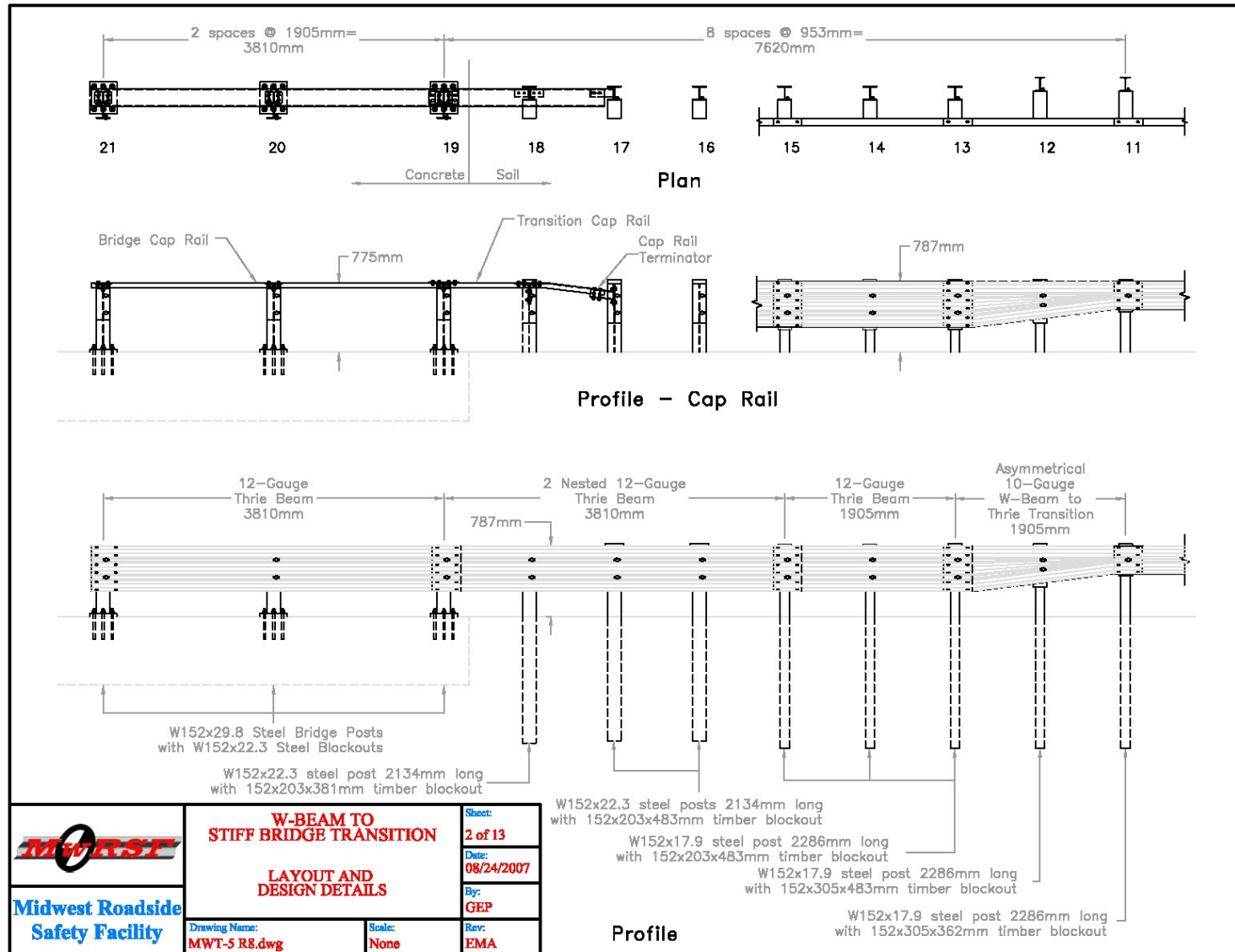
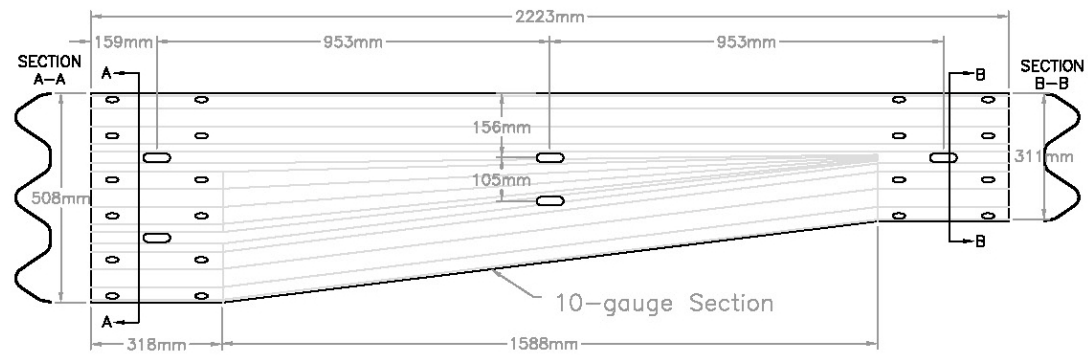


Figure 82. Layout and Design Details (Design No. 3)




	W-BEAM TO STIFF BRIDGE TRANSITION	Sheet: 3 of 13
	Asymmetrical W-Beam to Thrie Beam Transition Rail Detail	Date: 08/24/2007
Drawing Name: MWT-5 R8.dwg	Scale: 1=10	By: GEP
		Rev: EMA

Figure 83. Asymmetrical W-Beam to Thrie Beam Transition Element Details (Design No. 3)

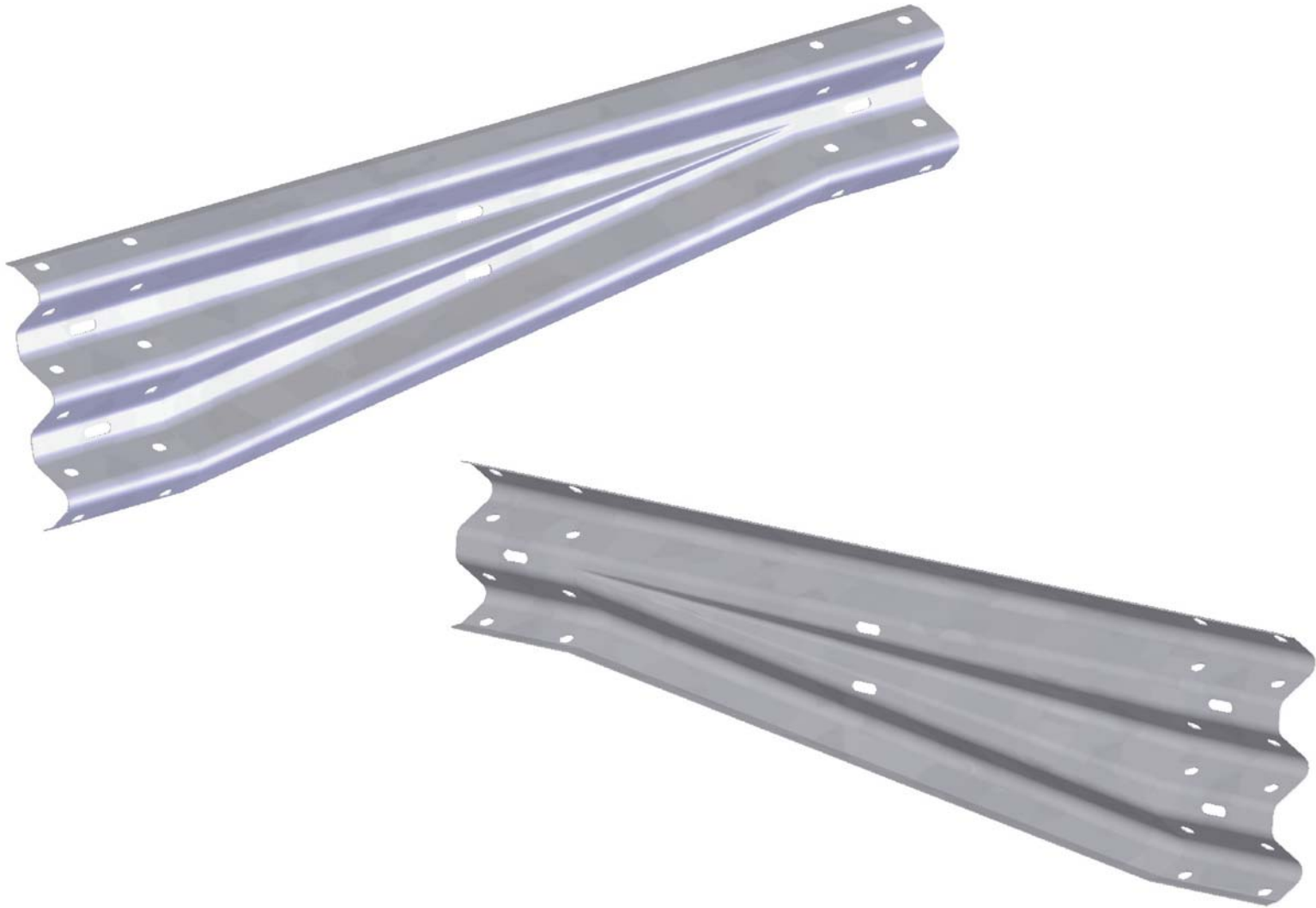


Figure 84. Asymmetrical W-Beam to Thrie Beam Transition Element Prototype, Design No. 3

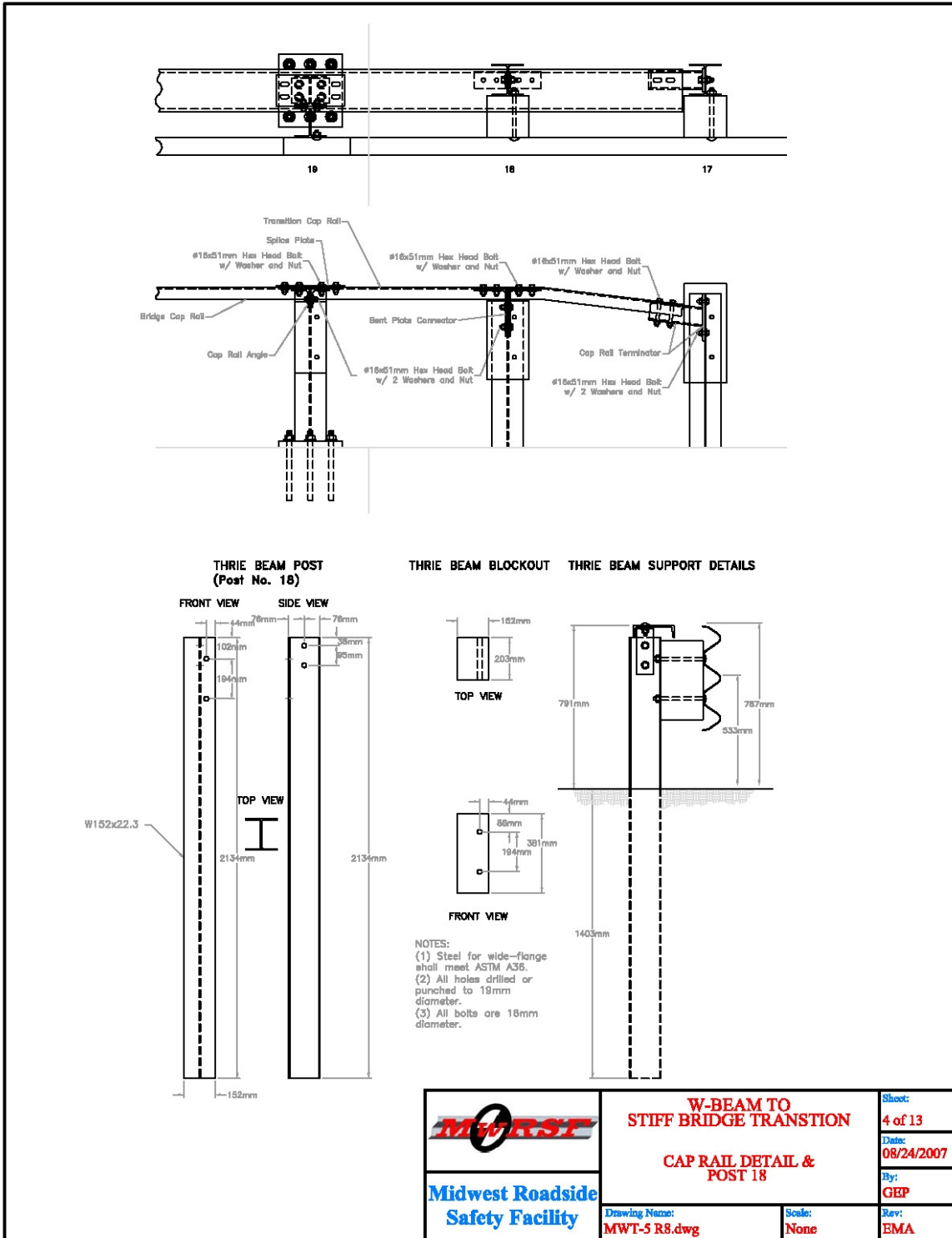


Figure 85. Cap Rail and Post No. 18 Details (Design No. 3)

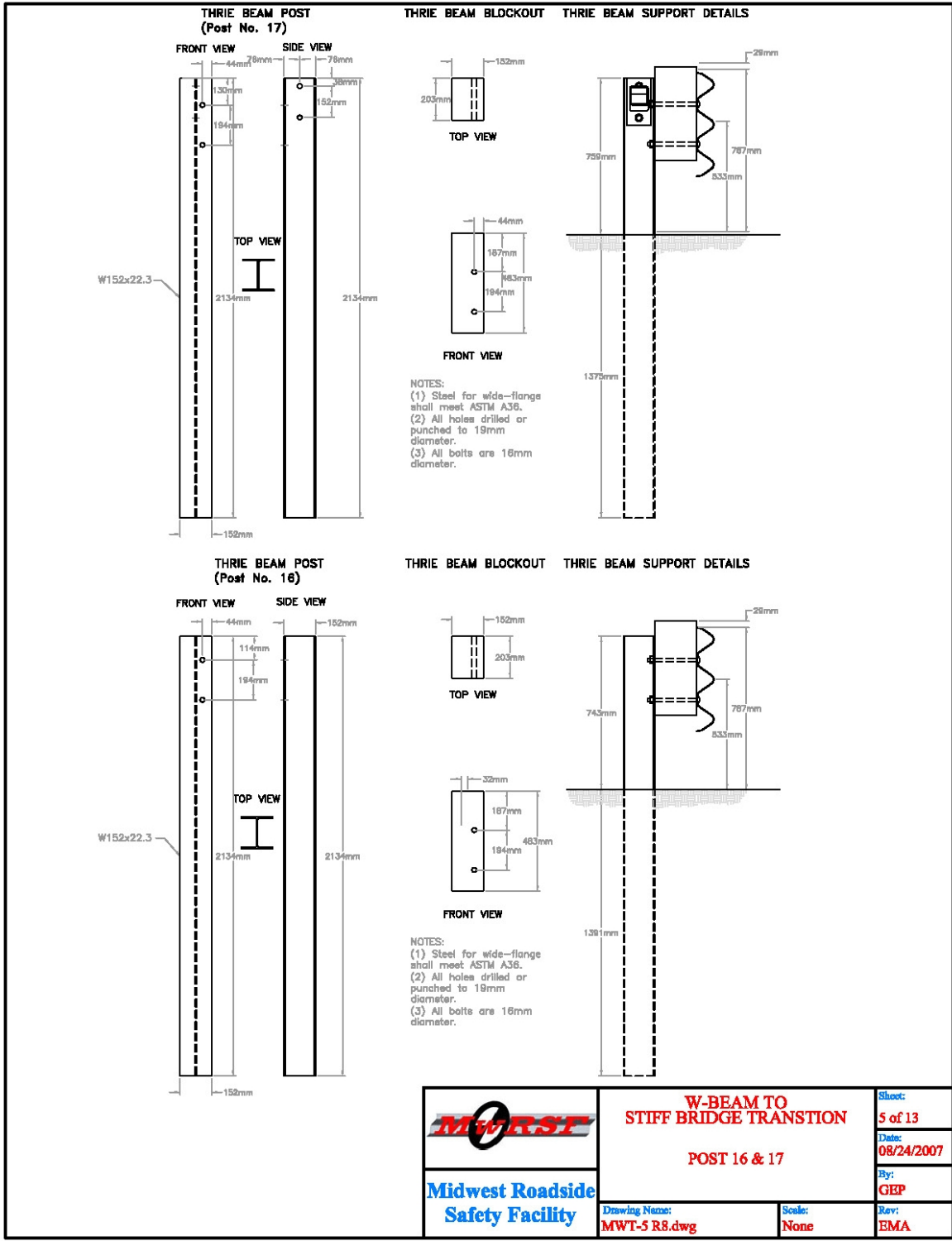


Figure 86. Post Nos. 16 and 17 Details (Design No. 3)

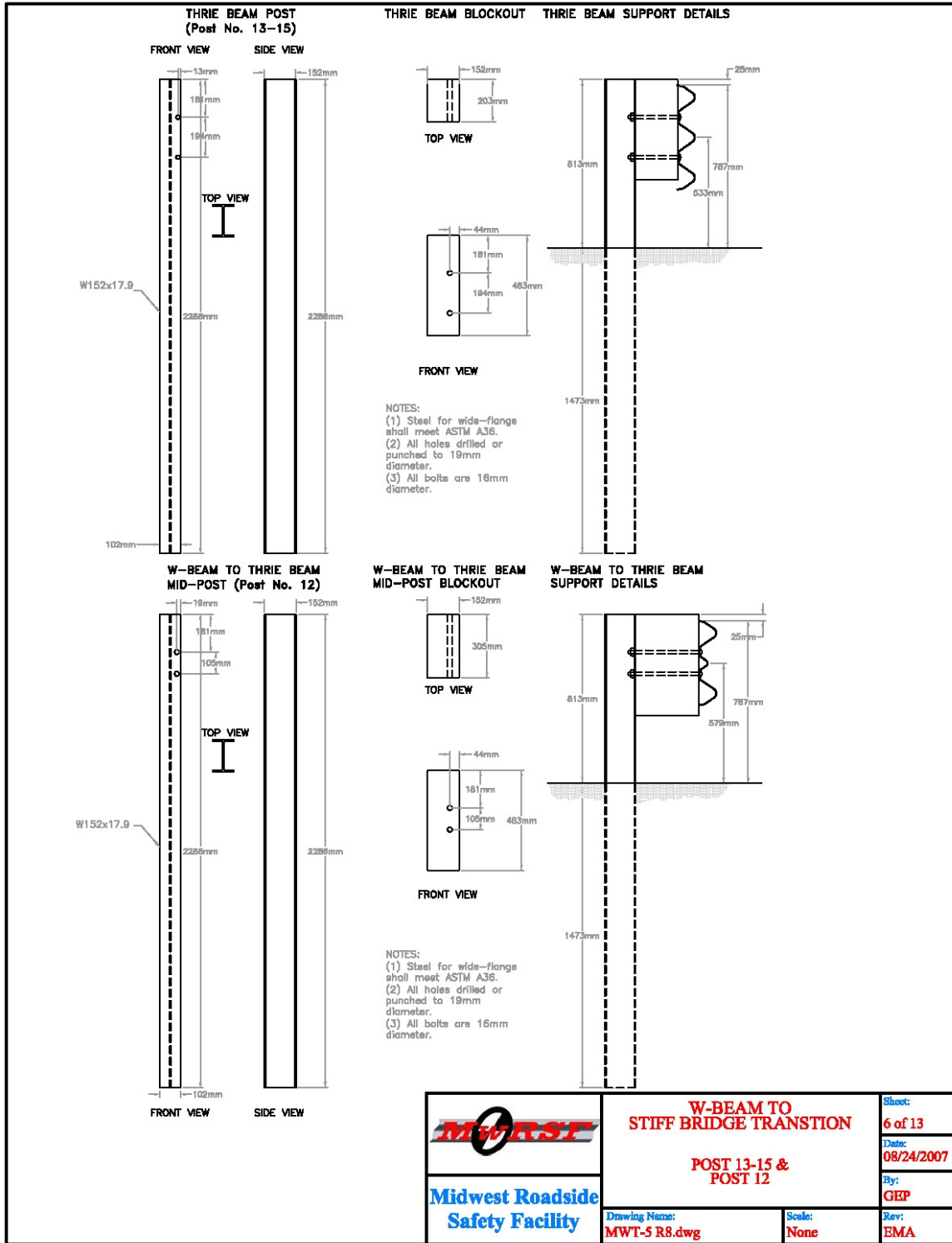


Figure 87. Post Nos. 12 through 15 Details (Design No. 3)

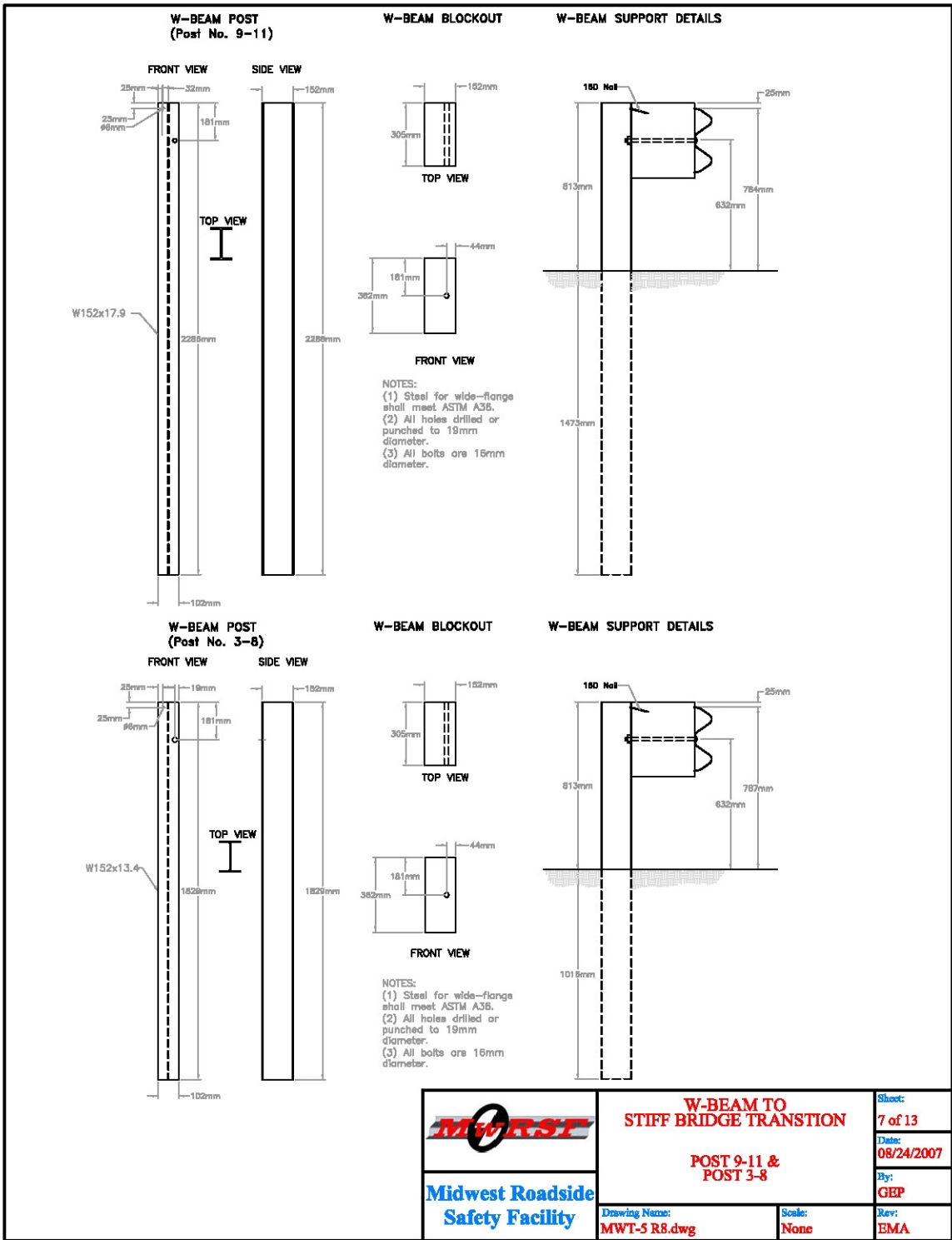


Figure 88. Post Nos. 3 through 11 Details (Design No. 3)

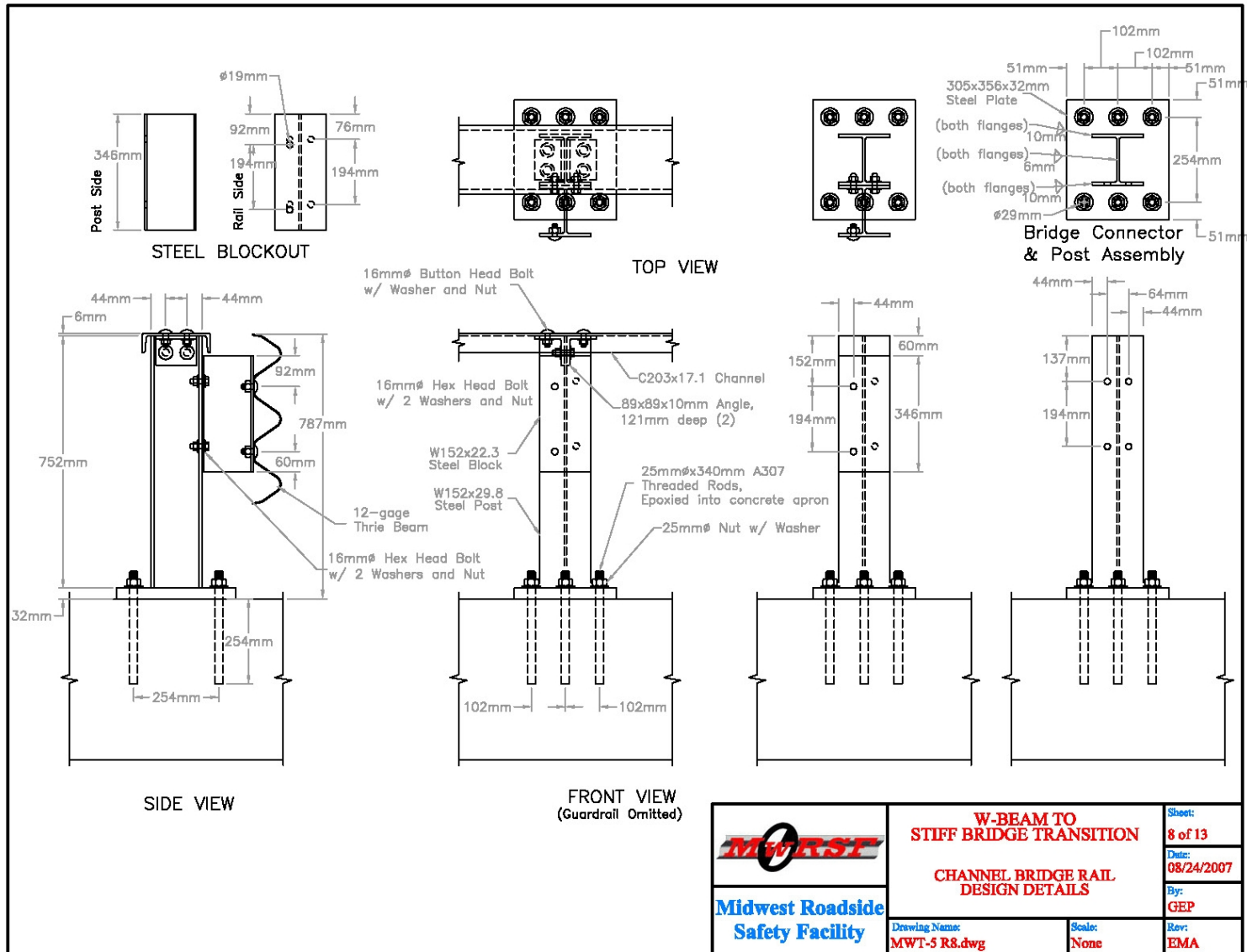
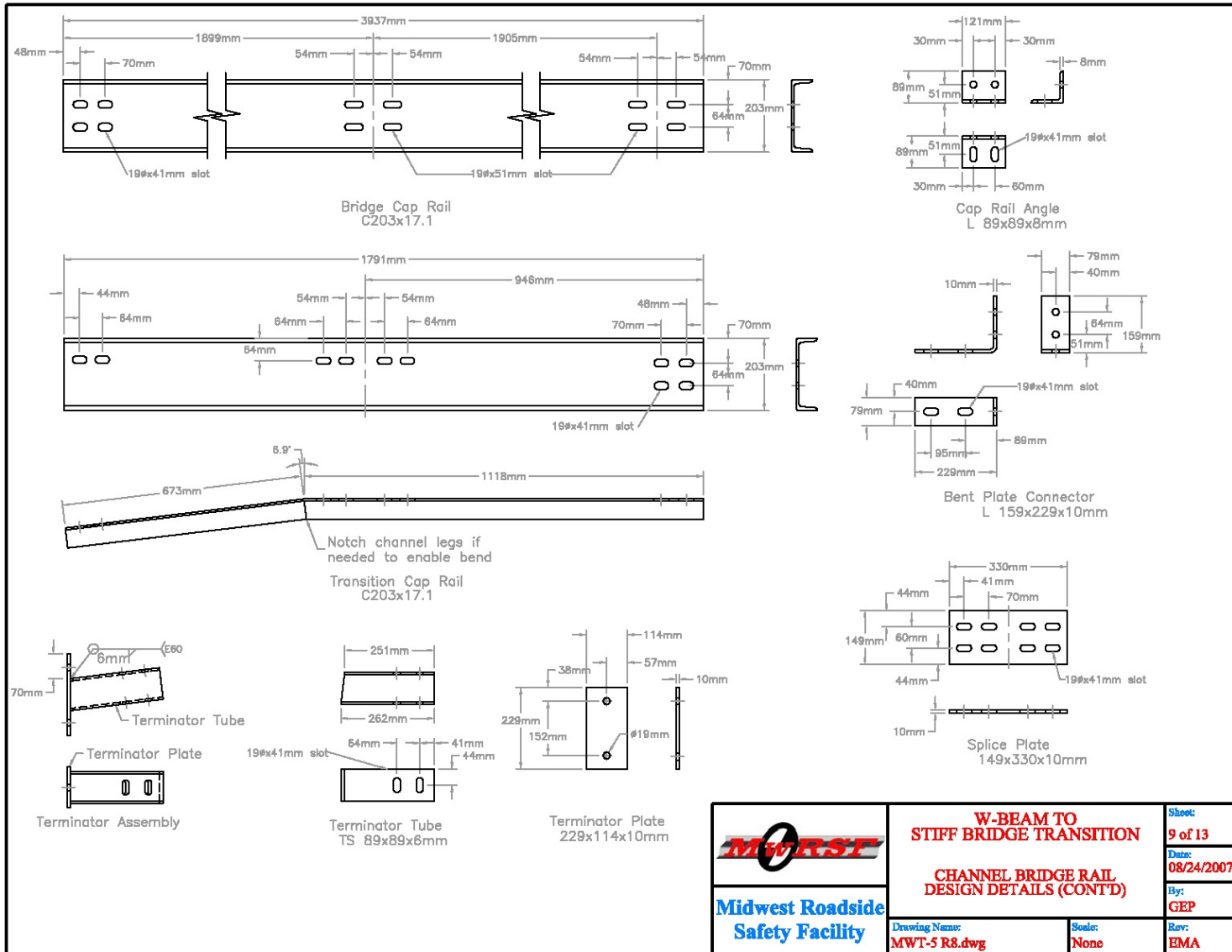


Figure 89. Channel Bridge Rail Design Details (Design No. 3)



	W-BEAM TO STIFF BRIDGE TRANSITION	Sheet: 9 of 13
	CHANNEL BRIDGE RAIL DESIGN DETAILS (CONTD)	Date: 08/24/2007
Drawing Name: MWT-5 R8.dwg	Scale: None	By: GEP
		Rev: EMA

Figure 90. Channel Bridge Rail Design Details (Continued) (Design No. 3)

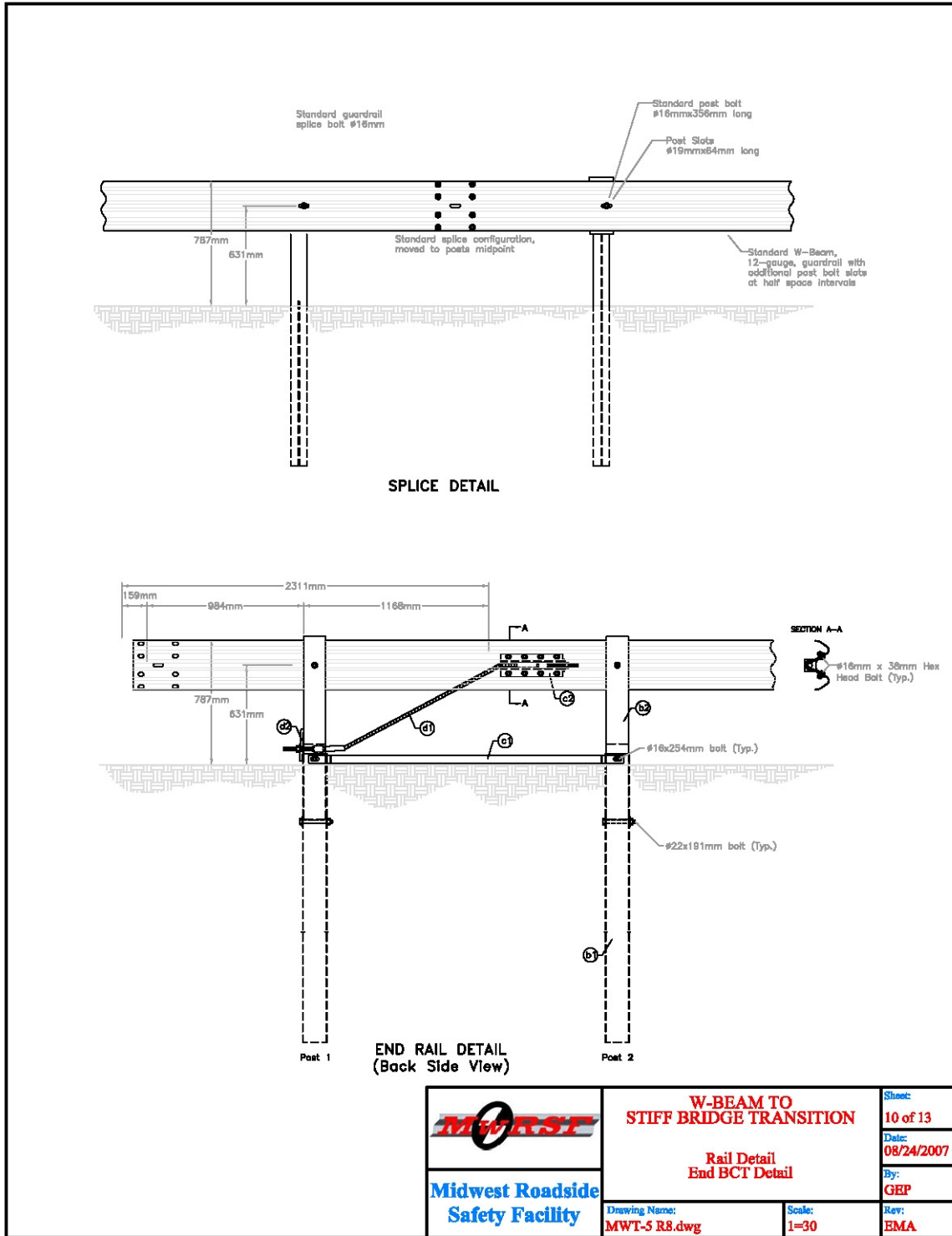


Figure 91. Rail and End BCT Details (Design No. 3)

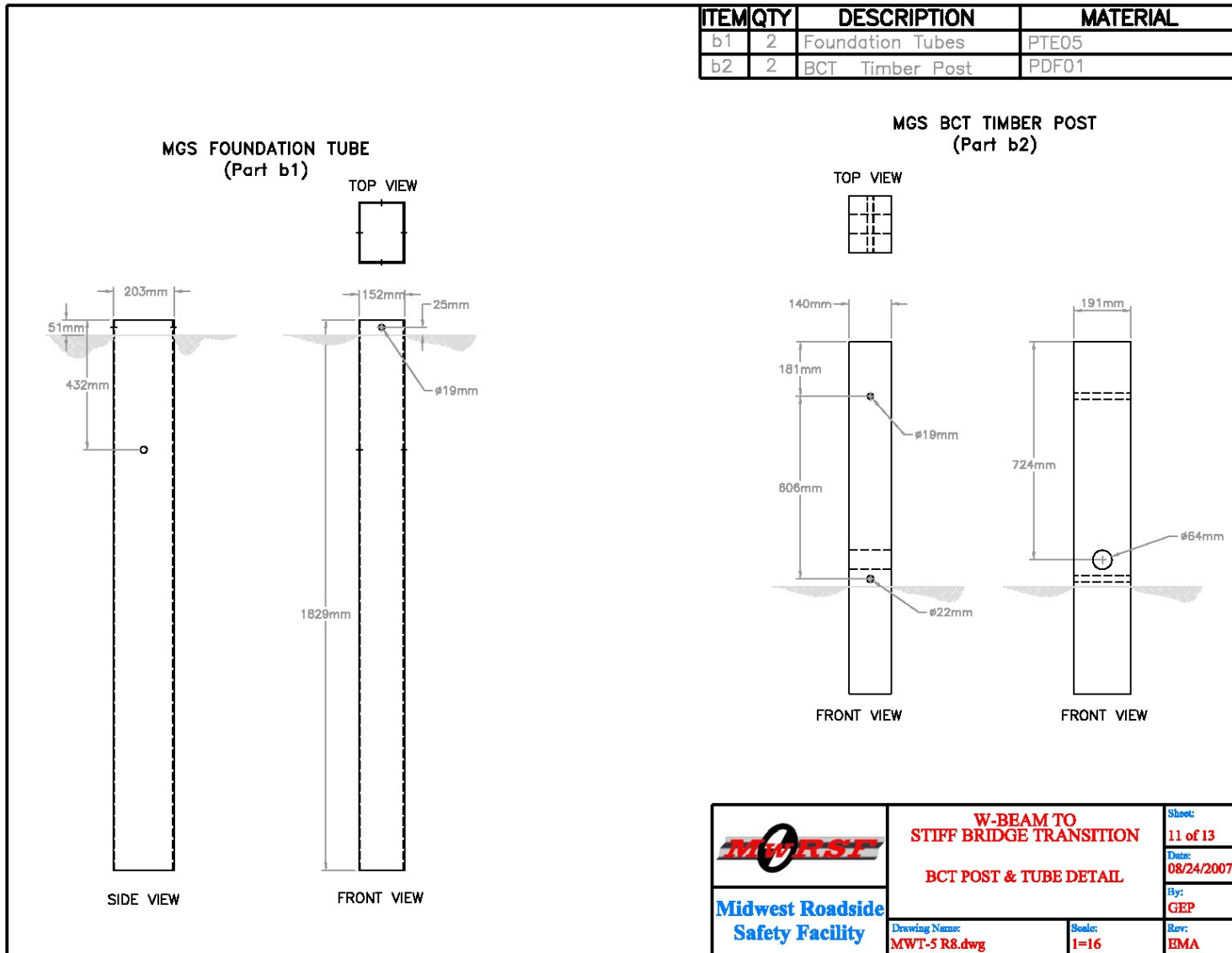


Figure 92. BCT Post and Tube Details (Design No. 3)

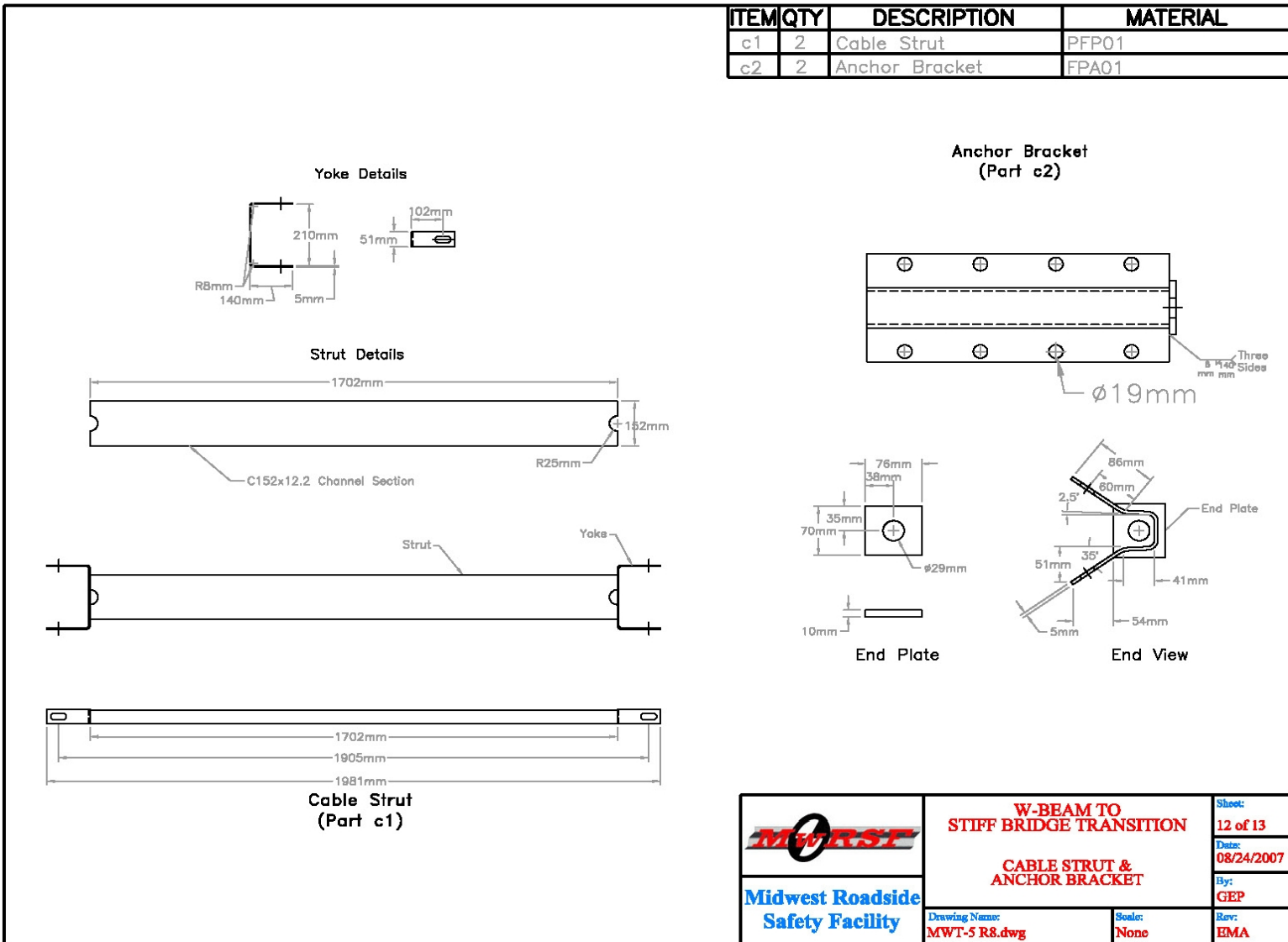


Figure 93. Cable Strut and Anchor Bracket Details (Design No. 3)

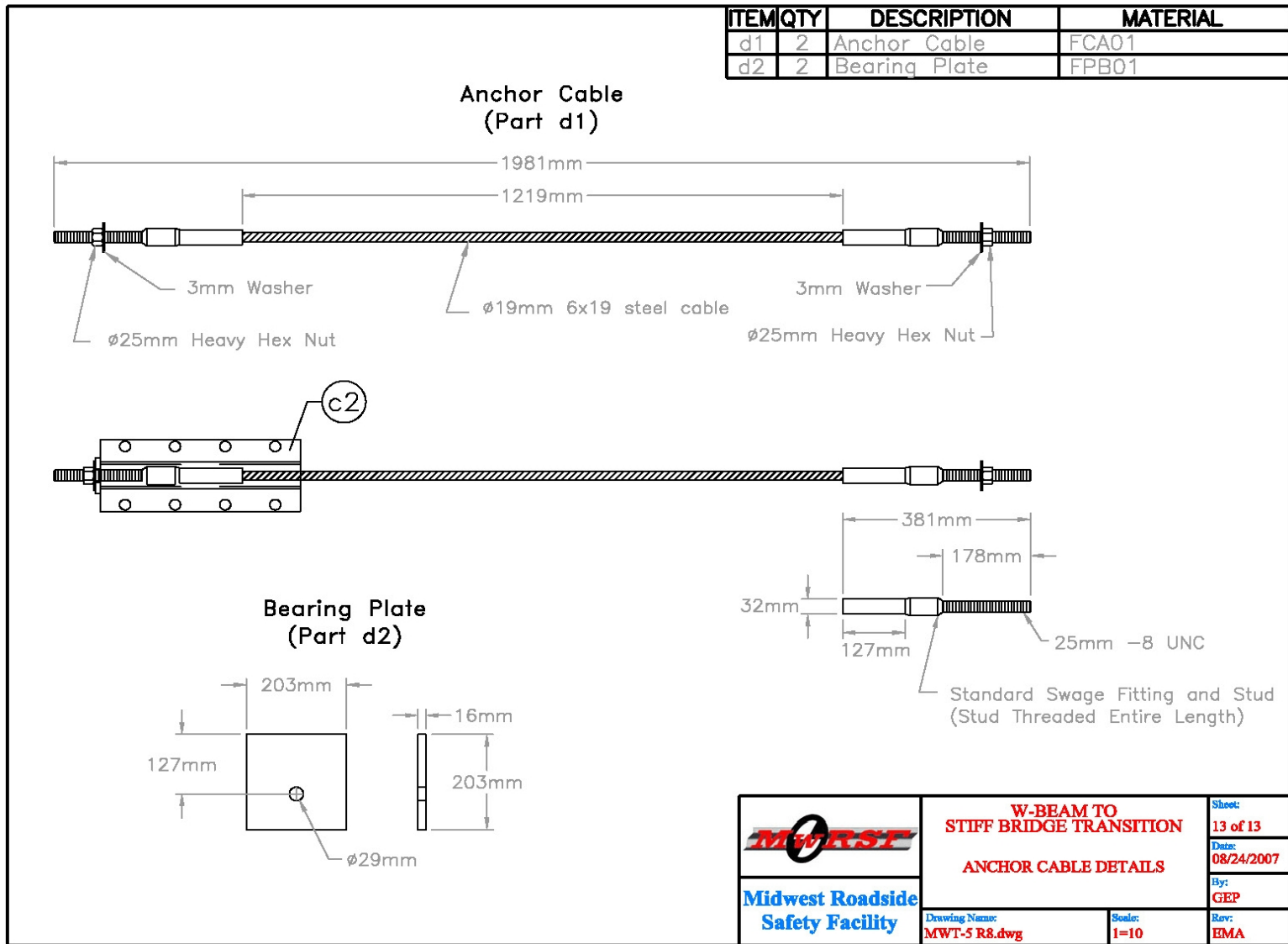


Figure 94. Anchor Cable Details (Design No. 3)



Figure 95. System and Transition Element (Design No. 3)

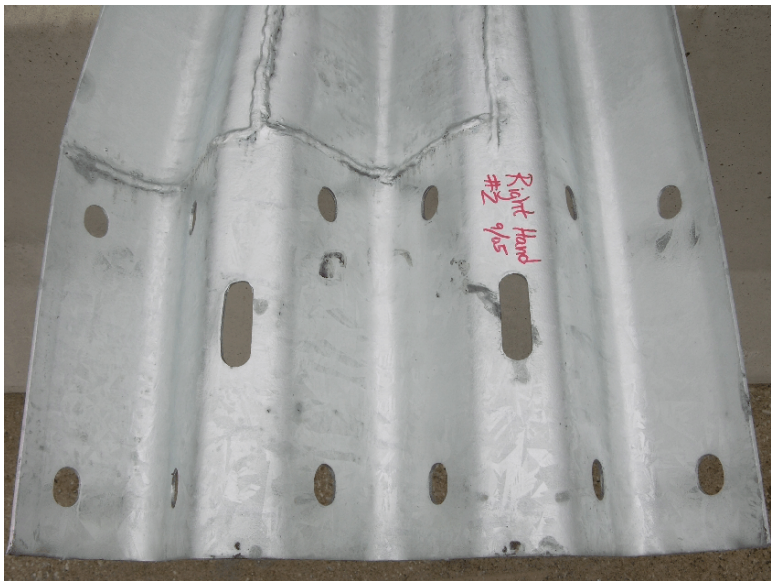


Figure 96. Welded W-beam to Thrie Beam Transition Element, Design No. 3



Figure 97. Anchor and Tarmac Connection (Design No. 3)

13 CRASH TEST NO. 3

13.1 Test MWT-5

The 2,010-kg (4,431-lb) pickup truck impacted the guardrail system upstream from the W-beam to thrie beam transition element at a speed of 99.0 km/h (61.5 mph) and at an angle of 24.9 degrees. A summary of the test results and sequential photographs are shown in Figure 98. The summary of the test results and sequential photographs in English units are provided in Appendix B. Additional sequential photographs are shown in Figures 99 and 100. Documentary photographs of the crash test are shown in Figures 101 and 102.

13.2 Test Description

Initial vehicle impact was to occur between post nos. 8 and 9, or 330 mm (13 in.) upstream of the centerline of post no. 9, as shown in Figure 101. Actual vehicle impact occurred at the targeted impact location. At 0.016 sec after impact, the pickup bumper and the right-front quarter panel crushed inward towards the engine compartment. At 0.042 sec, post nos. 9 through 11 rotated backwards slightly, and the right-front right quarter panel crushed inward under the hood. At 0.066 sec, post nos. 11 through 13 rotated backward, and the guardrail flattened around the right-front quarter panel of the truck. At this same time, the hood protruded over the rail. At 0.082 sec, the rail buckled at post no. 12, and post nos. 10 and 11 continued to rotate backwards. At 0.096 sec, post nos. 10 and 11 deflected downstream, while post nos. 12 through 14 deflected upstream and rotated backwards. At this same time, the rail continued to flatten around the front of the vehicle. At 0.124 sec, the blackout at post no. 11 disengaged from the system and traveled downstream. By this time, the front bumper was located at post no. 12, and the right-front side of the vehicle continued to crush inwards. At 0.174 sec, the blackout at post no. 12 disengaged from the system and fell to the ground. At this same time, post no. 13 rotated backwards, and a buckle in the rail appeared at post

no. 10. At 0.194 sec, the pickup was sliding along the rail between post nos. 13 and 14 and was redirecting towards parallel. At 0.234 sec, deflections and rotations of post nos. 3 through 10 reached their maximum. At this same time, the rear of the truck yawed toward the system. At 0.298 sec, the rail buckle at post no. 10 intensified, and another buckle formed at the midspan between post nos. 9 and 10. At 0.348 sec, the truck became parallel to the system with a resultant velocity of 48.6 km/h (30.2 mph). However, the rear of the truck had yet to contact the system. At this same time, the front of the truck was located at post no. 14, and the blockout on post no. 14 split down the center. At 0.430 sec, the rear of the truck pitched upward, and the vehicle redirected away from the system. At 0.478 sec, the rear half of the pickup was positioned over the guardrail, and the right-rear tire contacted the rail. At 0.570 sec, the vehicle continued to redirect away from the system with the rear of the vehicle yawing toward the system. By 0.648 sec, vehicle yaw ceased, and the vehicle rolled slightly toward the right side. At this same time, the rear of the vehicle was located at post no. 15, and the vehicle continued to move longitudinally. At 0.710 sec, only the rear of the vehicle was in contact with the system at post no. 16. At this same time, vehicle roll ceased, and the rear of the vehicle descended toward the ground. At 0.878 sec, the vehicle exited the system at an angle of 23.9 degrees and a resultant velocity of 37.7 km/h (23.4 mph). At 1.180 sec, the vehicle yawed clockwise due to a bent right-side rim and continued on this path until its final resting place. The vehicle came to rest 23.9 m (78 ft - 3 in.) downstream from impact and 2.8 m (9 ft - 1 in.) laterally behind the traffic-side face of the barrier, as shown in Figures 98 and 104.

13.3 Barrier Damage

System damage was moderate as shown in Figures 105 through 112. System damage consisted mostly of deformed guardrail and posts, soil damage, fractured wooden spacer blockouts, and contact marks on a guardrail section. The length of vehicle contact along the approach guardrail

system was approximately 5.9 m (19.2 ft), which spanned from 330 mm (13 in.) upstream from the centerline of post no. 9 through 191 mm (7.5 in.) upstream from the centerline of post no. 15.

Contact marks on the lower corrugation of the rail began 330 mm (13 in.) upstream of post no. 9 and continued through 762 mm (30 in.) downstream of post no. 14. Slight buckling of the rail was visible between post nos. 8 and 9. Flattening of the rail was found between post nos. 9 and 10. Slight rail buckling also occurred at the rail splice at post no. 13. The rail between post nos. 10 and 13 was deformed upward from vehicle contact. The rail was also deformed at the guardrail to post bolt at post no. 14, but the bolt did not pull through the rail. Slight deformation was visible at the rail splice at post no. 15. Guardrail to post bolt pullout occurred at post no. 11.

Minor soil gaps were visible around post nos. 1, 2, and 8 through 14. Post nos. 3 through 8 rotated slightly downstream. Post nos. 9 and 10 rotated backward. Post no. 11 rotated backward and downstream to approximately 60 degrees. Post nos. 12 through 14 also deflected downstream and backward, but to a lesser extent than post no. 11. Post nos. 15 through 21 were not visibly damaged. The wooden blockouts at post nos. 10 and 14 were fractured but remained attached to the post and rails. The wooden blockouts at post nos. 11 through 13 fractured and disengaged from the system.

The permanent set of the barrier system is shown in Figures 105 and 106. The maximum lateral permanent set rail and post deflections were 375 mm (14.75 in.) at the centerline of post no. 11 and 318 mm (12.5 in.) at the centerline of post no. 12, respectively, as measured in the field. The maximum lateral dynamic rail and post deflections were 605 mm (23.8 in.) at the midspan between post nos. 11 and 12 and 557 mm (21.9 in.) at the centerline of post no. 11, respectively, as determined from high-speed video analysis. The working width of the system was found to be 1,021 mm (40.2 in.).

13.4 Vehicle Damage

Exterior vehicle damage was minimal, as shown in Figures 113 through 115. Occupant compartment deformations to the right side and center of the floorboard were judged insufficient to cause serious injury to the vehicle occupants, as shown in Figure 115. Maximum longitudinal deflections of 13 mm (0.5 in.) were located near the left-front side of the right-side floorboard. Maximum lateral deflections of 44 mm (1.75 in.) were located near the front center of the floorboard. Maximum vertical deflections of 32 mm (1.25 in.) were located at the front of the floorboard. Complete occupant compartment deformations and the corresponding locations are provided in Appendix C.

The minor damage was concentrated on the right-front corner of the vehicle. The right-front corner of the bumper was pushed backward into the radiator. The left-front corner of the bumper pulled away from the truck due to the right-side damage. The right-front quarter panel buckled and deformed inward under the hood. Scraping and sheet metal tearing was found on the rear portion of the right-front quarter panel. The top of the right-side door was twisted and ajar. The back of the left-side door was deformed. The grill was fractured and detached from the truck. The hood twisted clockwise and lodged in place to prevent opening. The right-front tire and rim were severely deformed and bent backward into the wheel well with the bumper resting on the tire. The windshield encountered a minor crack at the center for the length of the windshield. The roof, box, and rear of vehicle, left-side rims and tires, and all other window glass remained undamaged.

13.5 Occupant Risk Values

The longitudinal and lateral occupant impact velocities were determined to be 6.70 m/s (22.00 ft/s) and 5.58 m/s (18.32 ft/s), respectively. The maximum 0.010-sec average occupant ridedown decelerations in the longitudinal and lateral directions were 13.24 Gs and 8.67 Gs,

respectively. It is noted that the occupant impact velocities (OIVs) and occupant ridedown decelerations (ORDs) were within the suggested limits provided in NCHRP Report No. 350. The THIV and PHD values were determined to be 8.48 m/s (12.82 ft/s) and 13.76 Gs, respectively. The results of the occupant risk, as determined from the accelerometer data, are summarized in Figure 98. Results are shown graphically in Appendix H. The results from the rate transducer are shown graphically in Appendix I.

13.6 Discussion

The analysis of the test results for test no. MWT-5 showed that the MGS W-beam to thrie beam transition element, used in conjunction with an approach guardrail transition system, adequately contained and redirected the vehicle with controlled lateral displacements of the barrier system. There were no detached elements nor fragments which showed potential for penetrating the occupant compartment nor presented undue hazard to other traffic. Deformations of, or intrusion into, the occupant compartment that could have caused serious injury did not occur. The test vehicle did not penetrate nor ride over the barrier system and remained upright during and after the collision. Vehicle roll, pitch, and yaw angular displacements were noted, but they were deemed acceptable because they did not adversely influence occupant risk safety criteria nor cause rollover. After collision, the vehicle's trajectory revealed minimum intrusion into adjacent traffic lanes. Therefore, test no. MWT-5 conducted on the W-beam to thrie beam transition element, used in conjunction with an approach guardrail transition system, was determined to be acceptable according to the TL-3 safety performance criteria found in NCHRP Report No. 350.



0.000 sec

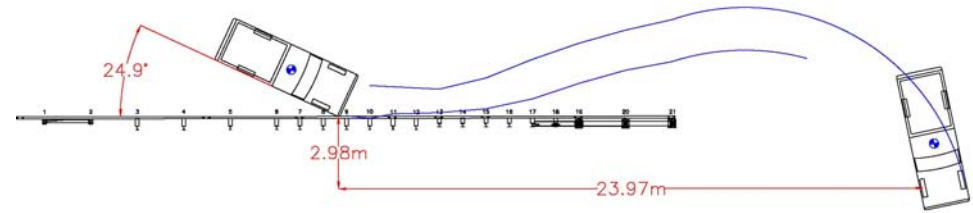
0.134 sec

0.234 sec

0.478 sec

0.874 sec

- Test Agency MwRSF
- Test Number MWT-5
- Date 11/10/05
- NCHRP 350 Test Designation 3-21
- Appurtenance W-beam to Thrie Beam Transition Element used with Approach Guardrail Transition
- Total Length 26.67 m
- Key Elements - Steel Thrie Beam Guardrail
 - Thickness 2.67 mm
 - Top Mounting Height 787 mm
- Key Elements - Steel W-Beam to Thrie Beam Transition
 - Thickness 3.43 mm
 - Top Mounting Height 787 mm
 - Shape Asymmetrical
- Key Elements - Steel W-Beam Guardrail
 - Thickness 2.67 mm
 - Top Mounting Height 787 mm
- Key Elements - Steel Posts
 - Post Nos. 3 - 8 W152x13.4 by 1,829 mm long
 - Post Nos. 9 - 15 W152x17.9 by 2,286 mm long
 - Post Nos. 16 - 18 W152x22.3 by 2,134 mm long
 - Post Nos. 19 - 21 W152x29.8 by 752 mm long
- Key Elements - Post Spacing
 - Post Nos. 1 - 6, 19-21 1,905 mm
 - Post Nos. 6 - 19 953 mm
- Key Elements - Wood Spacer Blocks
 - Post Nos. 3 - 11 152 mm x 305 mm x 362 mm long
 - Post No 12 152 mm x 305 mm x 483 mm long
 - Post Nos. 13 - 17 152 mm x 203 mm x 483 mm long
 - Post No. 18 152 mm x 203 mm x 381 mm long
- Key Elements - Steel Spacer Blocks
 - Post Nos. 19 - 21 W152 x 22.3 by 346 mm long
- Type of Soil Grading B - AASHTO M 147-65 (1990)
- Test Vehicle
 - Type/Designation 2000P
 - Make and Model 2000 GMC 2500 3/4-ton pickup
 - Curb 1,950 kg
 - Test Inertial 2,010 kg
 - Gross Static 2,010 kg



- Impact Conditions
 - Speed 99.0 km/h
 - Angle 24.9 degrees
 - Impact Location 330 mm upstream centerline post no. 9
- Exit Conditions
 - Speed 37.7 km/h
 - Angle 23.9 degrees
- Post-Impact Trajectory
 - Vehicle Stability Satisfactory
 - Stopping Distance 23.9 m downstream, 2.8 m behind traffic-side face
- Occupant Impact Velocity
 - Longitudinal 6.70 m/s < 12 m/s
 - Lateral (Not Required) 5.58 m/s
- Occupant Ridedown Deceleration (10 msec avg.)
 - Longitudinal 13.24 Gs < 20 Gs
 - Lateral (Not Required) 8.67 Gs
- THIV 8.48 m/s
- PHD 13.76 Gs
- Test Article Damage Moderate
- Test Article Deflections
 - Permanent Set 375 mm
 - Dynamic 605 mm
 - Working Width 1,021 mm
- Vehicle Damage Minimal
 - VDS¹³ 01-RFQ-4
 - CDC¹⁴ 01-RFEW6
 - Maximum Deformation 32 mm

Figure 98. Summary of Test Results and Sequential Photographs, Test MWT-5



0.000 sec



0.046 sec



0.158 sec



0.290 sec



0.646 sec



0.964 sec



0.000 sec



0.064 sec



0.098 sec



0.154 sec



0.248 sec



0.488 sec

Figure 99. Additional Sequential Photographs, Test MWT-5



0.000 sec



0.066 sec



0.116 sec



0.290



0.646 sec



0.964 sec



0.000 sec



0.067 sec



0.100 sec



0.167 sec



0.300 sec



0.400 sec

Figure 100. Additional Sequential Photographs, Test MWT-5



Figure 101. Documentary Photographs, Test MWT-5



Figure 102. Documentary Photographs, Test MWT-5



Figure 103. Impact Location, Test MWT-5



Figure 104. Vehicle Final Position and Trajectory Marks, Test MWT-5



Figure 105. System Damage, Test MWT-5

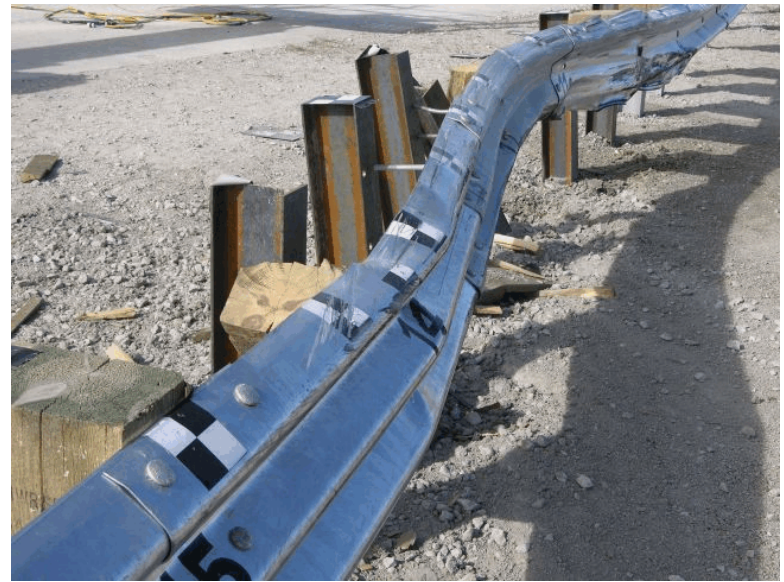


Figure 106. System Damage, Test MWT-5



Figure 107. Anchorage System Damage, Test MWT-5



Figure 108. Post Nos. 5 through 7 Damage, Test MWT-5



Figure 109. Post Nos. 8 through 10 Damage, Test MWT-5



Figure 110. Post Nos. 10 through 13 Damage, Test MWT-5



Figure 111. Post Nos. 13 through 16 Damage, Test MWT-5



Figure 112. Post Nos. 16 through 21 Damage, Test MWT-5



Figure 113. Vehicle Damage, Test MWT-5



Figure 114. Vehicle Damage, Test MWT-5



Figure 115. Occupant Compartment Damage, Test MWT-5

14 CRASH TEST NO. 4

14.1 Test MWT-6

The 904-kg (1,992-lb) small car impacted the guardrail system upstream from the W-beam to thrie beam transition element at a speed of 105.3 km/h (65.5 mph) and at an angle of 20.4 degrees. A summary of the test results and sequential photographs are shown in Figure 116. The summary of the test results and sequential photographs in English units are shown in Appendix B. Additional sequential photographs are shown in Figures 117 and 118. Documentary photographs of the crash test are shown in Figures 119 and 120.

14.2 Test Description

Initial vehicle impact was to occur between post nos. 9 and 10, or 318 mm (12.5 in.) upstream of the centerline of post no. 10, as shown in Figure 121. Actual vehicle impact occurred 235 mm (9.25 in.) upstream from the centerline of post no. 10. At 0.024 sec after impact, the right-front corner of the vehicle was located at the midspan between post nos. 10 and 11. At this same time, post nos. 10 and 11 deflected away from the vehicle. At 0.052 sec, the blockout at post no. 11 fractured, and the rail continued to deflect. At this same time, the front of the vehicle pitched downward. At 0.066 sec, the right-front corner of the vehicle was located at post no. 12. At this same time, the system continued to deflect through post no. 13. At 0.084 sec, the right-side window fractured, and the right-front tire protruded under the rail. At 0.116 sec, the right-front tire was located at post no. 13. At 0.128 sec, the right side of the hood was pushed back toward the windshield, and the system reached its maximum deflection. At 0.160 sec, the front of the vehicle was located at post no. 14. At this same time, the vehicle redirected toward parallel, and the right-front tire was no longer protruding under the rail. At 0.188 sec, the right-rear side of the vehicle

came in contact with the rail. At 0.260 sec, the vehicle became parallel to the system with a resultant velocity of 68.3 km/h (42.4 mph). At 0.275 sec, the rear of the vehicle became airborne. At 0.276 sec, the vehicle exited the system at an angle of 6.6 degrees and a resultant velocity of 58.6 km/h (36.4 mph). At 0.532 sec, the vehicle continued to travel away from the system with only the front of the vehicle in contact with the ground. At this same time, the rear of the car began to descend back toward the ground. At 0.617 sec, all wheels of the vehicle regained contact with the ground. At 1.050 sec, the vehicle redirected back toward the system. The vehicle came to rest 41.9 m (137 ft - 5 in.) downstream from impact and 5.3 (17 ft - 5 in.) behind the traffic-side face of the guardrail system. The trajectory and final position of the small car are shown in Figure 116 and 122.

14.3 Barrier Damage

Barrier damage was minimal, as shown in Figures 121 through 126. Barrier damage consisted of deformed guardrail and posts, damaged blockouts, and contact marks on a guardrail section. The length of vehicle contact along the approach guardrail system was approximately 4.5 m (14.8 ft), which spanned from 235 mm (9.25 in.) upstream from the centerline of post no. 10 through the midspan between post nos. 14 and 15.

Post nos. 3 through 8 encountered slight downstream twist of approximately 5 degrees. Post nos. 9 and 10 deflected backward slightly but did not twist laterally. Post no. 11 rotated slightly upstream but did not deflect. Post no. 12 deflected backward approximately 10 degrees and also twisted and rotated slightly downstream. Post no. 13 twisted slightly downstream. Both post nos. 13 and 14 deflected slightly backwards. Minor soil gaps were visible at post nos. 9 through 14.

The blockout at post no. 11 fractured and was removed from the system. The blockout at post no. 12 rotated around its bolt but remained attached to the post. No other blockout damage occurred.

The guardrail bolt at post no. 11 was bent but remained connected to the rail and post.

Minor buckling occurred at the downstream edge of the blockout at post no. 9. Rail buckling occurred around the top and bottom edges of the blockout at post no. 10. Moderate buckling occurred at post nos. 11, 14, and 15. Buckling also occurred at the midspan between post nos. 13 and 14. Minor flattening of the rail occurred between post nos. 10 and 13. The bottom of the rail between post nos. 10 and 11 and along the entire W-beam to thrie beam element was folded under.

A contact mark on the top corrugation of the W-beam began 235 mm (9.25 in.) upstream of post no. 10 and continued through the midspan of post nos. 14 and 15. A 3,658-mm (12-ft) long contact mark was found on the lower corrugation and began 235 mm (9.25 in.) upstream of post no. 10. Another contact mark on the middle corrugation on the transition piece began 235 mm (9.25 in.) upstream of post no. 10 and extended to post no. 14.

The permanent set of the barrier is shown in Figure 121. The maximum lateral permanent set rail and post deflections were 314 mm (12.375 in.) at the centerline of post no. 11 and 298 mm (11.75 in.) at post no. 12, respectively, as measured in the field. The maximum lateral dynamic rail and post deflections were 314.3 mm (12.375 in.) at the midspan between post nos. 11 and 23 and 307 mm (12.1 in.) at post no. 12, respectively, as determined from high-speed digital video analysis. The working width of the system was found to be 847 mm(33.3 in.).

14.4 Vehicle Damage

Exterior vehicle damage was moderate, as shown in Figures 127 and 128. Occupant compartment deformations to the right side and center of the floorboard were judged insufficient to cause serious injury to the vehicle occupants, as shown in Figure 129. Occupant compartment deformations and the corresponding locations are provided in Appendix C.

Damage to the test vehicle was concentrated to the right side of the vehicle. The bumper cover was torn off on the right side and rotated forward on the left side. The hood deformed upward and was dented in center. The entire front bumper was deformed downward from impact. The right-front headlight disengaged. The grill and radiator fan were broken. The right-front quarter panel was crushed inward, scratched, and torn. The right-front tire was torn and deflated, and the steel rim was bent and deformed. The right-side frame was torn. The right-side suspension bar and control arm were bent outwards. The right-side shocks were dislodged. The right-side door frame was ajar at the top. Dents were found on the right side of the vehicle. A 610-mm (24-in.) long scratch was found on the right-side door. The left-side wheel well was fractured. The windshield was cracked and the right-side door window was shattered. All other window glass remained undamaged.

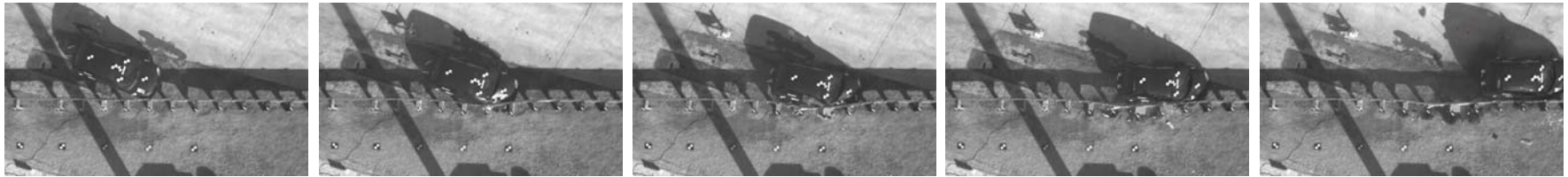
14.5 Occupant Risk Values

The longitudinal and lateral occupant impact velocities were determined to be -6.07 m/s (-19.91 ft/s) and 6.89 m/s (22.60 ft/s), respectively. The maximum 0.010-sec average occupant ridedown decelerations in the longitudinal and lateral directions were -18.53 Gs and 10.97 Gs, respectively. It is noted that the occupant impact velocities (OIVs) and occupant ridedown decelerations (ORDs) were within the suggested limits provided in NCHRP Report No. 350. The THIV and PHD values were determined to be 8.96 m/s (29.40 ft/s) and 19.93 Gs, respectively. The results of the occupant risk, as determined from the accelerometer data, are summarized in Figure 114. Results are shown graphically in Appendix I. The results from the rate transducer are shown graphically in Appendix J.

14.6 Discussion

The analysis of the test results for test no. MWT-6 showed that the W-beam to thrie beam

transition element, used in conjunction with an approach guardrail transition system, adequately contained and redirected the vehicle with controlled lateral displacements of the barrier system. There were no detached elements nor fragments which showed potential for penetrating the occupant compartment nor presented undue hazard to other traffic. Deformations of, or intrusion into, the occupant compartment that could have caused serious injury did not occur. The test vehicle did not penetrate nor ride over the guardrail system and remained upright during and after the collision. Vehicle roll, pitch, and yaw angular displacements were noted, but they were deemed acceptable because they did not adversely influence occupant risk safety criteria nor cause rollover. After collision, the vehicle's trajectory revealed minimum intrusion into adjacent traffic lanes. Therefore, test no. MWT-6 conducted on the W-beam to thrie beam transition element, used in conjunction with an approach guardrail transition system, was determined to be acceptable according to the TL-3 safety performance criteria found in NCHRP Report No. 350.



0.000 sec

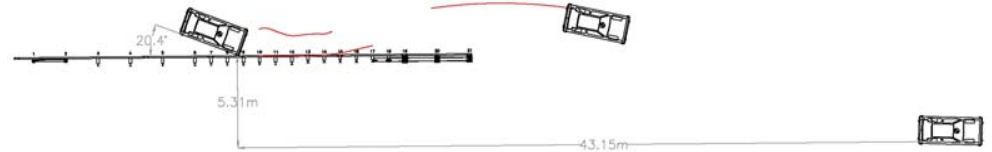
0.066 sec

0.116 sec

0.188 sec

0.302 sec

- Test Agency MwRSF
- Test Number MWT-6
- Date 11/22/05
- NCHRP 350 Test Designation 3-20
- Appurtenance W-beam to Thrie Beam Transition
Element used with Approach
Guardrail Transition
- Total Length 26.67 m
- Key Elements - Steel Thrie Beam Guardrail
 - Thickness 2.67 mm
 - Top Mounting Height 787 mm
- Key Elements - Steel W-Beam to Thrie Beam Transition
 - Thickness 2.67 mm
 - Top Mounting Height 787 mm
 - Shape Assymetrical
- Key Elements - Steel Posts
 - Post Nos. 3 - 11 W152 x 13.4 by 1,829 mm long
 - Post Nos. 9 - 15 W152 x 17.9 by 2,286 mm long
 - Post Nos. 16 - 18 W152 x 22.3 by 2,134 mm long
 - Post Nos. 19 - 21 W152 x 29.8 by 752 mm long
- Key Elements - Post Spacing
 - Post Nos. 1 - 6, 19 - 21 1,905 mm
 - Post Nos. 6 - 19 953 mm
- Key Elements - Wood Spacer Blocks
 - Post Nos. 3 - 11 152 mm x 305 mm x 362 mm long
 - Post No. 12 152 mm x 305 mm x 483 mm long
 - Post Nos. 13 - 17 152 mm x 203 mm x 483 mm long
 - Post No. 18 152 mm x 203 mm x 381 mm long
- Key Elements - Steel Spacer Blockouts
 - Post Nos. 19-21 W152 mm x 22.3 by 346 mm long
- Test Vehicle
 - Type/Designation 820C
 - Make and Model 1997 Geo Metro
 - Curb 791 kg
 - Test Inertial 828 kg
 - Gross Static 904 kg



- Impact Conditions
 - Speed 105.3 km/h
 - Angle 20.4 degrees
 - Impact Location 235 mm upstream centerline
post no. 10
- Exit Conditions
 - Speed 58.6 km/h
 - Angle 6.6 degrees
- Post-Impact Trajectory
 - Vehicle Stability Satisfactory
 - Stopping Distance 41.9 m downstream,
5.3 m laterally behind
- Occupant Impact Velocity
 - Longitudinal -6.07 m/s < 12 m/s
 - Lateral 6.89 m/s < 12 m/s
- Occupant Ridedown Deceleration (10 msec avg.)
 - Longitudinal -18.53 Gs < 20 Gs
 - Lateral 10.97 Gs < 20 Gs
- THIV 8.96 m/s
- PHD (not required) 19.93 Gs
- Test Article Damage Minimal
- Test Article Deflections
 - Permanent Set 247 mm
 - Dynamic 307 mm
 - Working Width 844 mm
- Vehicle Damage Moderate
 - VDS¹³ 01-RFQ-5
 - CDC¹⁴ 01-RYEW7
 - Maximum Deformation NA

Figure 116. Summary of Test Results and Sequential Photographs, Test MWT-6



0.062 sec



0.126 sec



0.180 sec



0.316 sec



0.532 sec



1.050 sec



0.000 sec



0.067 sec



0.100 sec



0.133 sec



0.234 sec



0.334 sec

Figure 117. Additional Sequential Photographs, Test MWT-6



0.000 sec



0.033 sec



0.067 sec



0.100 sec



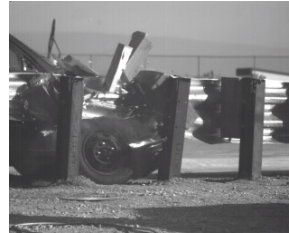
0.133 sec



0.200 sec



0.070 sec



0.086 sec



0.122 sec



0.154 sec



0.210 sec



0.250 sec

Figure 118. Additional Sequential Photographs, Test MWT-6



Figure 119. Documentary Photographs, Test MWT-6



Figure 120. Documentary Photographs, Test MWT-6



Figure 121. Impact Location, Test MWT-6



Figure 122. Final Location and Trajectory Marks, Test MWT-6



Figure 123. System Damage, Test MWT-6



Figure 124. Post Nos. 1 and 5 Damage, Test MWT-6



Figure 125. Post Nos. 6 through 9 Damage, Test MWT-6



Figure 126. Post Nos. 10 and 11 Damage, Test MWT-6



Figure 127. Post Nos. 12 and 13 Damage, Test MWT-6



177

Figure 128. Post Nos. 14 through 19 Damage, Test MWT-6



Figure 129. Vehicle Damage, Test MWT-6



Figure 130. Vehicle Damage, Test MWT-6



Figure 131. Occupant Compartment Damage, Test MWT-6

15 SUMMARY, CONCLUSIONS AND RECOMMENDATIONS

This study set out to examine the safety performance of the symmetrical W-beam to thrie beam transition element commonly used in conjunction with approach guardrail transitions. Two full-scale crash tests conducted on the transition system revealed that: (1) the symmetrical transition element performed acceptably for small car impacts and (2) rapid changes in lateral barrier stiffness from conventional metric height guardrail to a transition system can lead to pocketing, rail rupture, and vehicle rollover during a light truck impact (8).

From these test results, it is reasonable to conclude that some widely used thrie beam transition systems that incorporate a W-beam to thrie beam transition element attached to standard metric height guardrail may not meet NCHRP Report No. 350 safety performance evaluation criteria. Therefore, it is recommended that whenever new transition designs are developed in the future, the stiffness change at the end of the approach guardrail should be investigated as well as the stiffness change near the attachment to the rigid bridge railing.

In an attempt to produce a more gradual change in guardrail stiffness in front of the transition design, additional posts were added to the standard metric height guardrail. Although the resulting design eliminated the pocketing problem observed previously, full-scale crash testing showed that the stiffening of the standard W-beam guardrail induced a roll velocity that ultimately led to vehicle rollover. Based upon BARRIER VII simulation, test no. MWT-3, and prior full-scale tests (3 and 19), it can be concluded that standard metric height guardrail is likely to induce rollover whenever it is stiffened in transition systems or when additional posts are added to reduce deflections in front of fixed objects. It is important to verify this finding and/or identify ways to eliminate this problem if standard strong-post guardrail is to continue to be stiffened in order to reduce deflections in front

of fixed objects by adding extra posts.

One full-scale crash test, test nos. MWT-4, was conducted with an asymmetrical W-beam to thrie beam transition piece fabricated by cutting off the bottom corner of a 2.67-mm (12-gauge) thick thrie beam element and welding a flat plate across the cut section. Due to stress concentrations in the fabricated transition element, the rail ruptured. Thus, this test showed that the current design is unsafe and should not be used on high-speed roadways.

Finally, a stiffening system for the Midwest Guardrail System (MGS) and a new asymmetrical W-beam to thrie beam transition element were developed. The stiffening system and new transition element were attached to a very stiff thrie beam approach guardrail transition design and subjected to two full-scale crash tests, test nos. MWT-5 and MWT-6. These tests verified that the new design satisfied the safety performance evaluation criteria contained in NCHRP Report No. 350. The new guardrail stiffening system and transition element is recommended for use whenever the MGS barrier system must be attached to a thrie beam approach guardrail transition. Since a very stiff thrie beam approach guardrail transition design was used in the full-scale crash testing, the upstream guardrail stiffening system developed herein should be applicable to most other thrie beam transition designs.

Furthermore, this transition design represents the final component needed for full implementation of the MGS barrier system. The full-scale crash testing reported herein and in references (16-19) have demonstrated that implementation of the MGS guardrail will offer dramatic safety improvements for high-speed highways by reducing rollovers for light truck impacts, guardrail penetrations, and the incidence of secondary impacts after a vehicle is successfully redirected by the guardrail system.

This W-beam to thrie transition system has been crash tested using a system length of approximately 21.91 m (71 ft - 11 in.). For this length, it has been demonstrated that the barrier system will meet impact safety standards and allow the designer/researcher to gain knowledge on dynamic barrier performance. Thus, a minimum of 3.81 m (12 ft - 6 in.) of W-beam adjacent to the 12.83 m (42 ft - 1 in.) transition should be used prior to an acceptable TL-3 end terminal. However, the researchers recommend 7.62 m (25 ft) of W-beam adjacent to the transition.

However, a couple of issues need to be noted with regards to the new transition and existing transitions. First, it is unknown whether guardrails without offset blockouts will perform adequately when installed in the new transition design. Therefore, the performance of using a guardrail without a blockout in conjunction with the transition can only be verified through the use of full-scale crash testing. Second, the problems identified with a standard W-beam approach to a stiff approach guardrail transition are likely to be common to many existing transition designs. Therefore, all approach guardrail transition designs should be evaluated to assess the risk of poor performance during impacts on the “transition to transition”.

Finally, it should be noted that the new asymmetrical W-beam to thrie beam transition section was fabricated as a welded prototype and successfully used in test nos. MWT-5 and MWT-6. Although crash testing of the welded parts were successful, it is recommended that production parts be manufactured using stamping technology. It is believed that stamped transition sections will be more economical and reduce concerns with the quality control of welded sections and the associated stress concentrations.

Table 3. Summary of Safety Performance Evaluation Results

Evaluation Factors	Evaluation Criteria	Test MWT-3	Test MWT-4	Test MWT-5	Test MWT-6
Structural Adequacy	A. Test article should contain and redirect the vehicle; the vehicle should not penetrate, underide, or override the installation although controlled lateral deflections of the test article is acceptable.	U	U	S	S
Occupant Risk	D. Detached elements, fragments or other debris from the test article should not penetrate or show potential for penetrating the occupant compartment, or present an undue hazard to other traffic, pedestrians, or personnel in a work zone. Deformations of, or intrusions into, the occupant compartment that could cause serious injuries should not be permitted.	S	S	S	S
	F. The vehicle should remain upright during and after collision although moderate roll, pitching, and yawing are acceptable.	U	S	S	S
	H. Longitudinal and lateral occupant impact velocities should fall below the preferred value of 9 m/s (29.5 ft/s), or at least below the maximum allowable value of 12 m/s (39.4 ft/s).	NA	NA	NA	S
	I. Longitudinal and lateral occupant ridedown accelerations should fall below the preferred value of 15 Gs, or at least below the maximum allowable value of 20 Gs.	NA	NA	NA	S
Vehicle Trajectory	K. After collision it is preferable that the vehicle's trajectory not intrude into adjacent traffic lanes.	S	S	S	S
	L. The occupant impact velocity in the longitudinal direction should not exceed 12 m/s (39.4 ft/s), and the occupant ridedown acceleration in the longitudinal direction should not exceed 20 Gs.	S	S	S	NA
	M. The exit angle from the test article preferably should be less than 60 percent of test impact angle measured at time of vehicle loss of contact with test device.	S	S	S	S

S - Satisfactory U - Unsatisfactory
M - Marginal NA - Not Available

16 REFERENCES

1. Bryden, J.E. and Phillips, R.G., *Performance of a Thrie beam Steel-Post Bridge-Rail System*, Report No. FHWA/NY/RR-85/118, Submitted to the Office of Research, Development, and Technology, Federal Highway Administration, Performed by New York State Department of Transportation, February 1985.
2. Bryden, J.E. and Phillips, R.G., *Performance of a Thrie beam Steel-Post Bridge-Rail System*, Transportation Research Record No. 1024, Transportation Research Board, Washington, D.C., 1985.
3. Mak, K.K. and Menges, W.L. *Testing and Evaluation of the W-Beam Transition (on Steel Posts with Timber Blockouts) to the Vertical Flared-Back Concrete Bridge Parapet*, Turner-Fairbank Highway Research Center, Texas Transportation Institute, 1997.
4. Michie, J.D., *Recommended Procedures for the Safety Performance Evaluation of Highway Appurtenances*, National Cooperative Highway Research Program (NCHRP) Report No. 230, Transportation Research Board, Washington, D.C., March 1981.
5. Ross, H.E., Sicking, D.L., Zimmer, R.A. and Michie, J.D., *Recommended Procedures for the Safety Performance Evaluation of Highway Features*, National Cooperative Research Program (NCHRP) Report No. 350, Transportation Research Board, Washington, D.C., 1993.
6. Polivka, K.A., Faller, R.K., Reid, J.D., Sicking, D.L., Rohde, J.R., Keller, E.A., and Holloway, J.C., *Development of an Approach Guardrail Transition Attached to a Thrie Beam and Channel Bridge Railing*, Draft Report to the Midwest States' Regional Pooled Fund Program, Project SPR-3(017), Transportation Report No. TRP-03-91-99, Midwest Roadside Safety Facility, University of Nebraska-Lincoln, October 14, 1999.
7. *Standard Specifications for Transportation Materials and Methods of Sampling and Testing*, Seventeenth Edition, Part I Specifications, American Association of State Highway and Transportation Officials (AASHTO), Washington, D.C., 1995.
8. Polivka, K.A., Faller, R.K., Sicking, D.L., Reid, J.D., Rohde, J.R., and Holloway, J.C., *Crash Testing of Missouri's W-Beam to Thrie beam Transition Element*, Final Report to the Midwest States' Regional Pooled Fund Program, Transportation Research Report No. TRP-03-94-00, Project No. SPR-3(017)-Year 9, Midwest Roadside Safety Facility, University of Nebraska-Lincoln, Lincoln, NE, September 12, 2000.
9. Speer, D., Peter, R., Jewell, J., Clark, N., *Vehicular Crash Tests of a Nested Thrie Beam Transition Barrier*, Report No. FHWA/CA/TL-2001/09, Materials Engineering and Testing Services, California Department of Transportation, Sacramento, CA, May, 2002.

10. Powell, G.H., *Barrier VII: A Computer Program For Evaluation of Automobile Barrier Systems*, Prepared for: Federal Highway Administration, Report No. FHWA RD-73-51, April 1973.
11. Hinch, J., Yang, T-L, and Owings, R., *Guidance Systems for Vehicle Testing*, ENSCO, Inc., Springfield, VA 1986.
12. Center of Gravity Test Code - SAE J874 March 1981, SAE Handbook Vol. 4, Society of Automotive Engineers, Inc., Warrendale, Pennsylvania, 1986.
13. *Vehicle Damage Scale for Traffic Investigators*, Second Edition, Technical Bulletin No. 1, Traffic Accident Data (TAD) Project, National Safety Council, Chicago, Illinois, 1971.
14. *Collision Deformation Classification - Recommended Practice J224 March 1980*, Handbook Volume 4, Society of Automotive Engineers (SAE), Warrendale, Pennsylvania, 1985.
15. Polivka, K.A., Faller, R.K., Sicking, D.L., Rohde, J.R., Reid, J.D., and Holloway, J.C. *Guardrail and Guardrail Terminals Installed Over Curbs - Phase II*, Final Report to the Midwest States' Regional Pooled Fund Program, Transportation Research Report No. TRP-03-105-00, Project No. SPR-3(017)-Year 10, Midwest Roadside Safety Facility, University of Nebraska-Lincoln, November 5, 2001.
16. Sicking, D.L., Reid, J.D., and Rohde, J.R. *Development of the Midwest Guardrail System*, *Transportation Research Record 1797*, Transportation Research Board, Washington, D.C., January 2002.
17. Faller, R.K., Polivka, K.A., Kuipers, B.D., Bielenberg, B.W., Reid, J.D., Rohde, J.R. and Sicking, D.L. *Midwest Guardrail System for Standard and Special Applications* *Transportation Research Record No. 1890*, Transportation Research Board, Washington D.C., January 2004, pp 19-33.
18. Faller, R.K., Sicking, D.L., Bielenberg, B.W., Rohde, J.R., Polivka, K.A., and Reid, J.D. *Performance of Steel-Post, W-Beam Guardrail Systems*, Paper submitted for publication and presentation at the Transportation Research Board meeting, Washington, D.C., January 2007.
19. Polivka, K.A., Faller, R.K., Sicking, D.L., Reid, J.D., Rohde, J.R., Holloway, J.C., Bielenberg, B.W., and Kuipers, B.D. *Development of the Midwest Guardrail System (MGS) for Standard and Reduced Post Spacing and in Combination with Curbs*, Final Report to the Midwest States' Regional Pooled Fund Program, Transportation Research Report No. TRP-03-139-04, Project No. SPR-3(017)-Years 10, 12, and 13, Project Code: RFPF-00-02, 02-01, and 03-05, Midwest Roadside Safety Facility, University of Nebraska-Lincoln, September 1, 2004.

17 APPENDICES

APPENDIX A

English-Unit Design Details, Design No. 1

Figure A-1. Layout, Design No. 1 (English)

Figure A-2. Layout and Design Details, Design No. 1 (English)

Figure A-3. Cap Rail and Post No. 18 Details, Design No. 1 (English)

Figure A-4. Post Nos. 16 and 17. Details, Design No. 1 (English)

Figure A-5. Post Nos. 12 through 15 Details, Design No. 1 (English)

Figure A-6. Post Nos. 3 through 11 Details, Design No. 1 (English)

Figure A-7. Channel Bridge Rail Design Details, Design No. 1 (English)

Figure A-8. Channel Bridge Rail Design Details (Continued), Design No. 1 (English)

Figure A-9. Rail Details, Design No. 1 (English)

Figure A-10. BCT Post and Tube Detail, Design No. 1 (English)

Figure A-11. Cable Strut and Anchor Bracket Details, Design No. 1 (English)

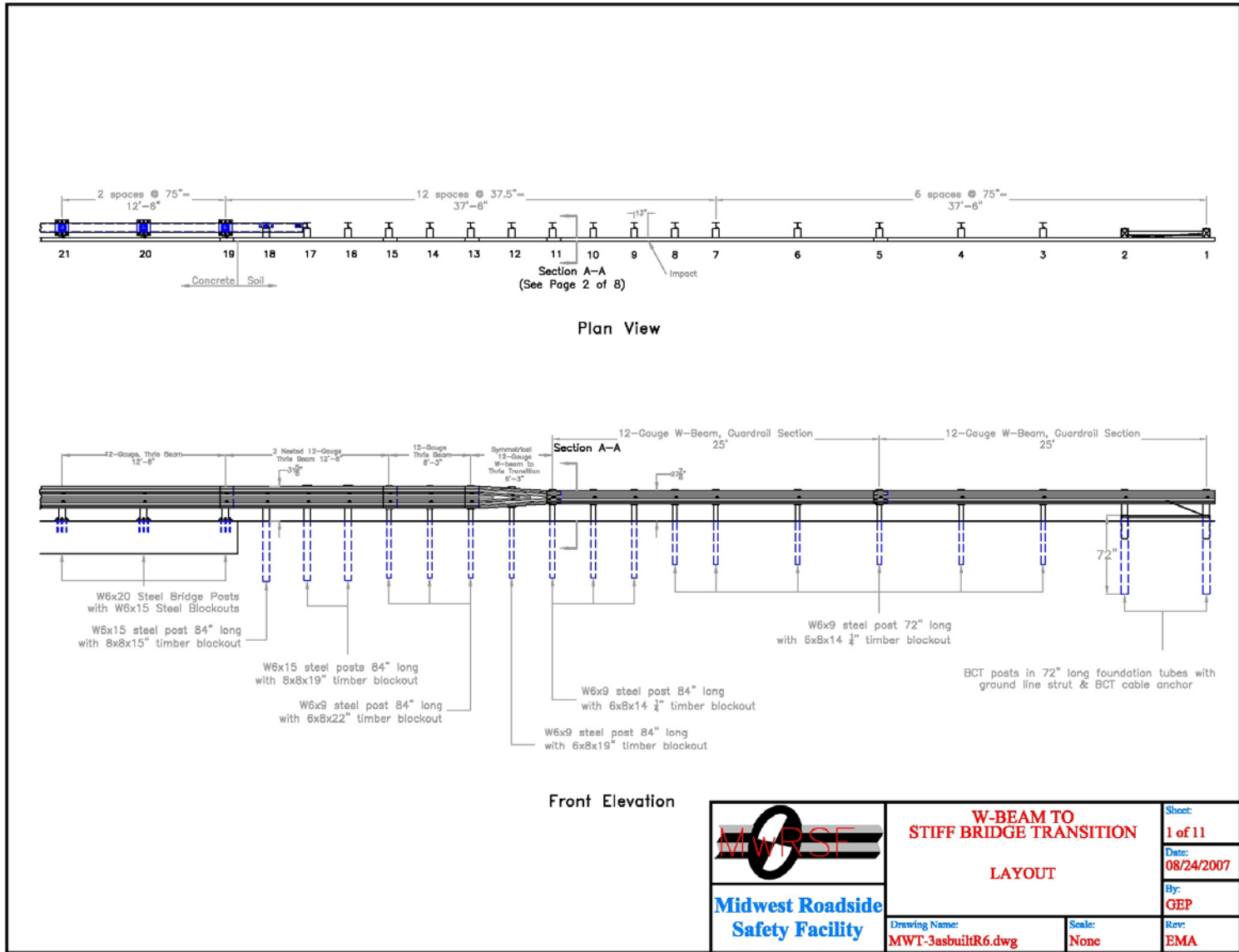


Figure A-1. Layout, Design No. 1 (English)

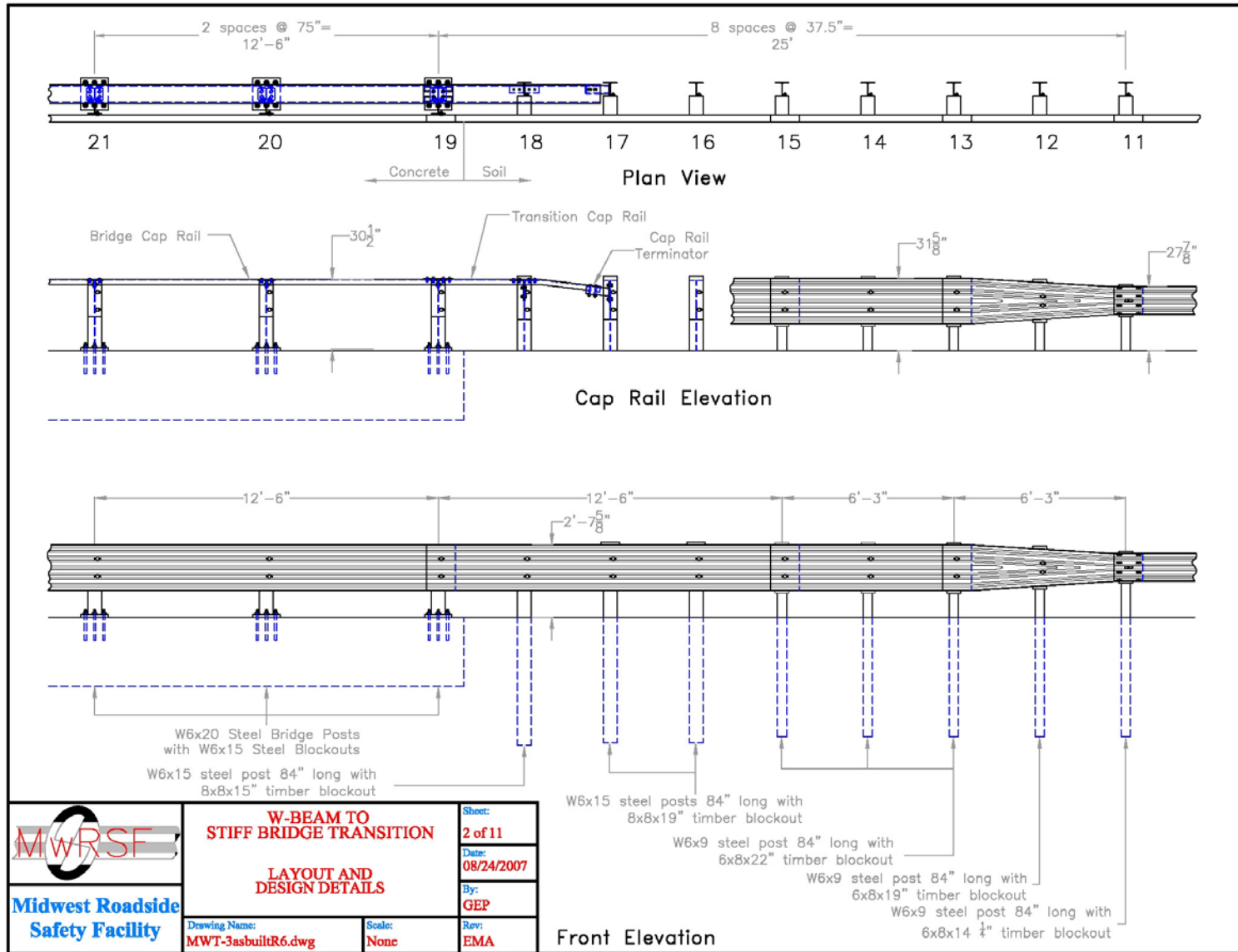


Figure A-2. Layout and Design Details, Design No. 1 (English)

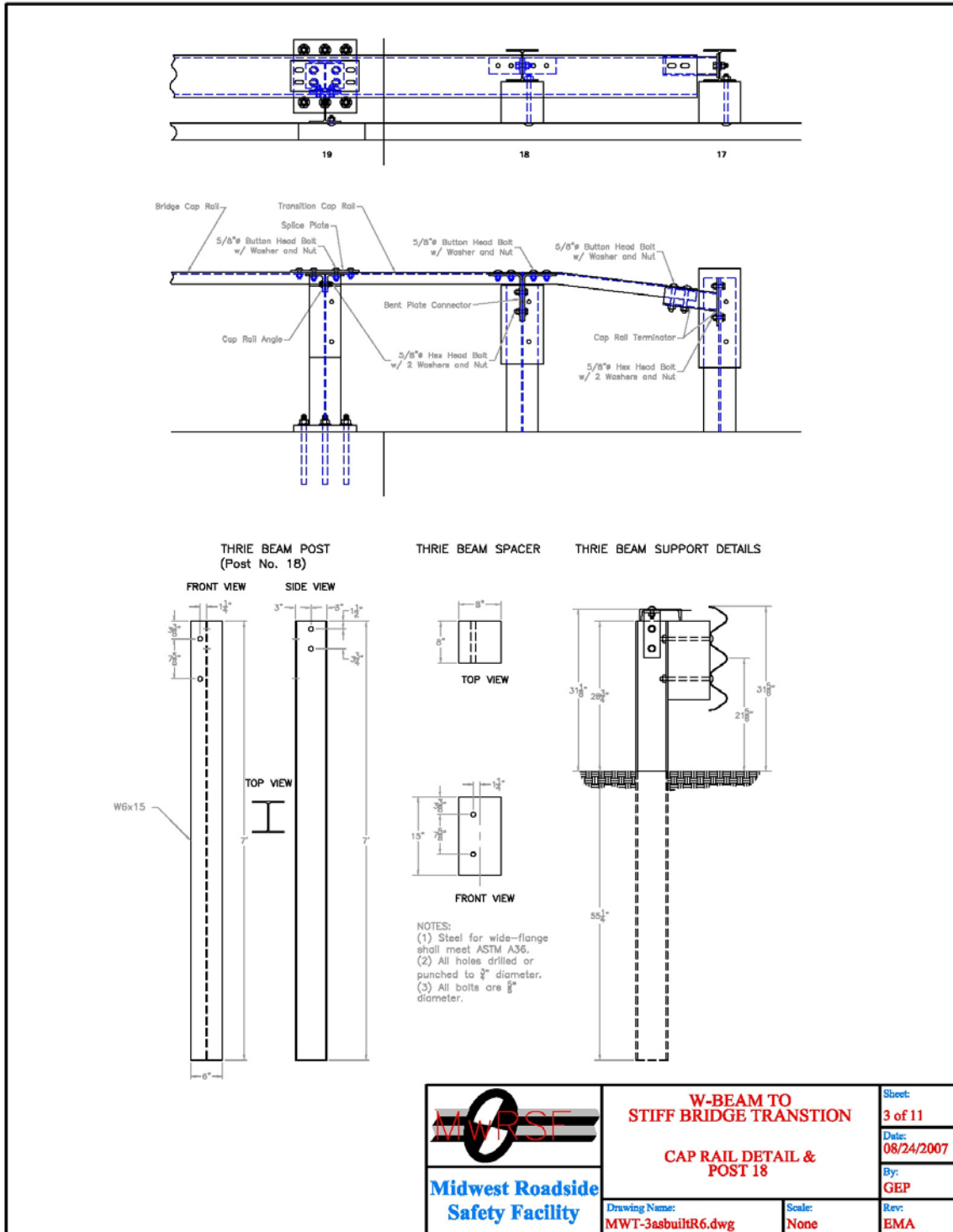


Figure A-3. Cap Rail and Post No. 18 Details, Design No. 1 (English)

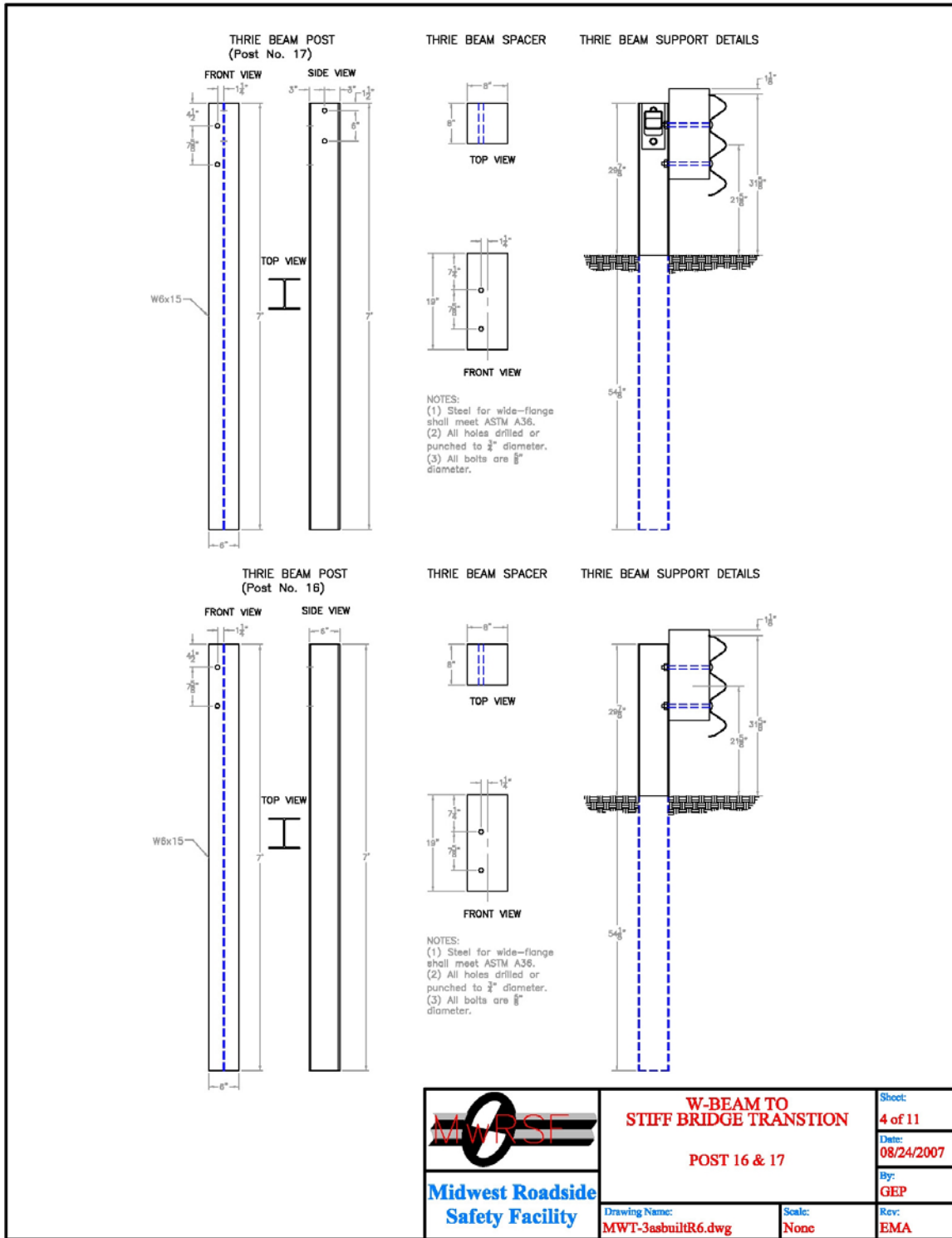


Figure A-4. Post Nos. 16 and 17.Details, Design No. 1 (English)

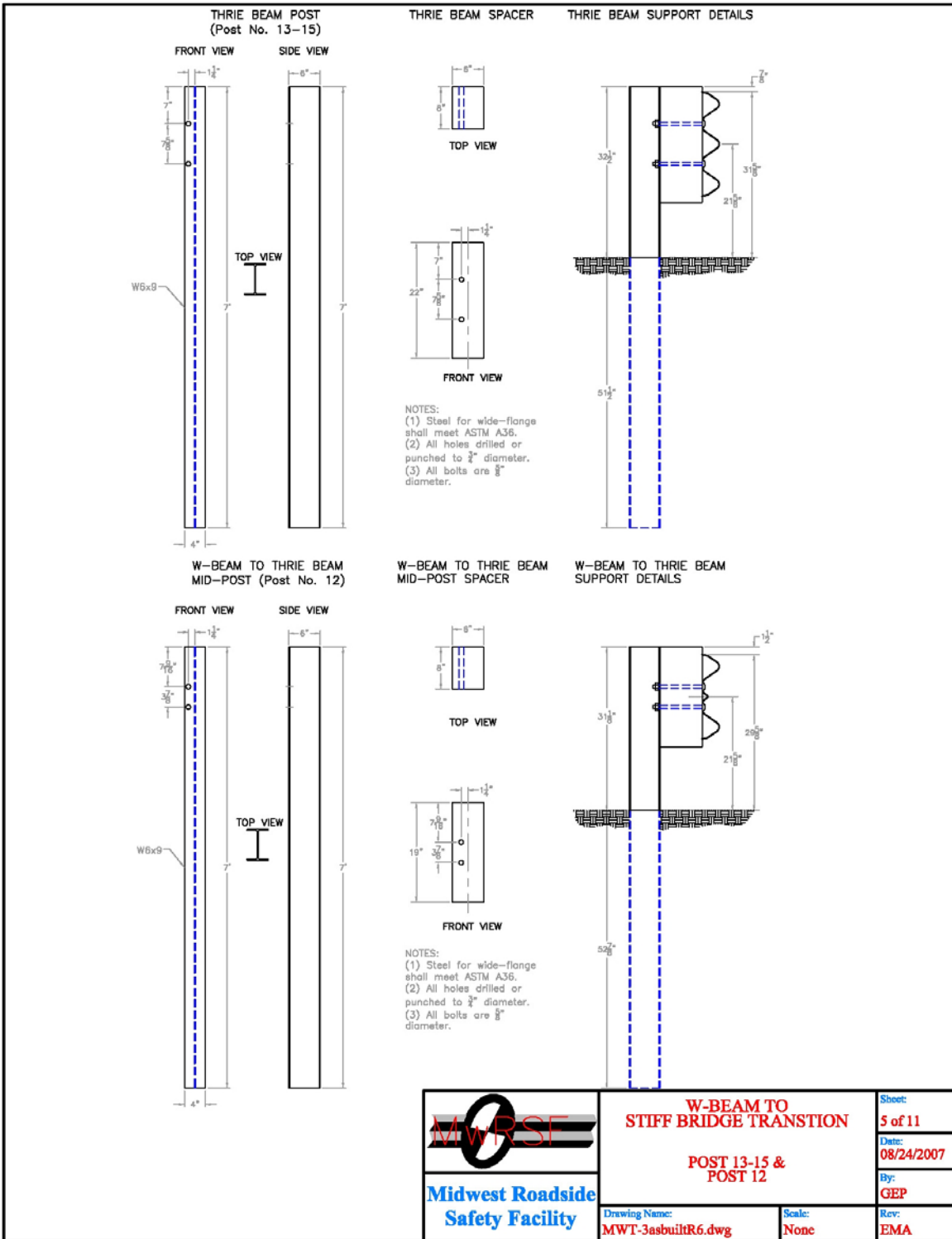


Figure A-5. Post Nos. 12 through 15 Details, Design No. 1 (English)

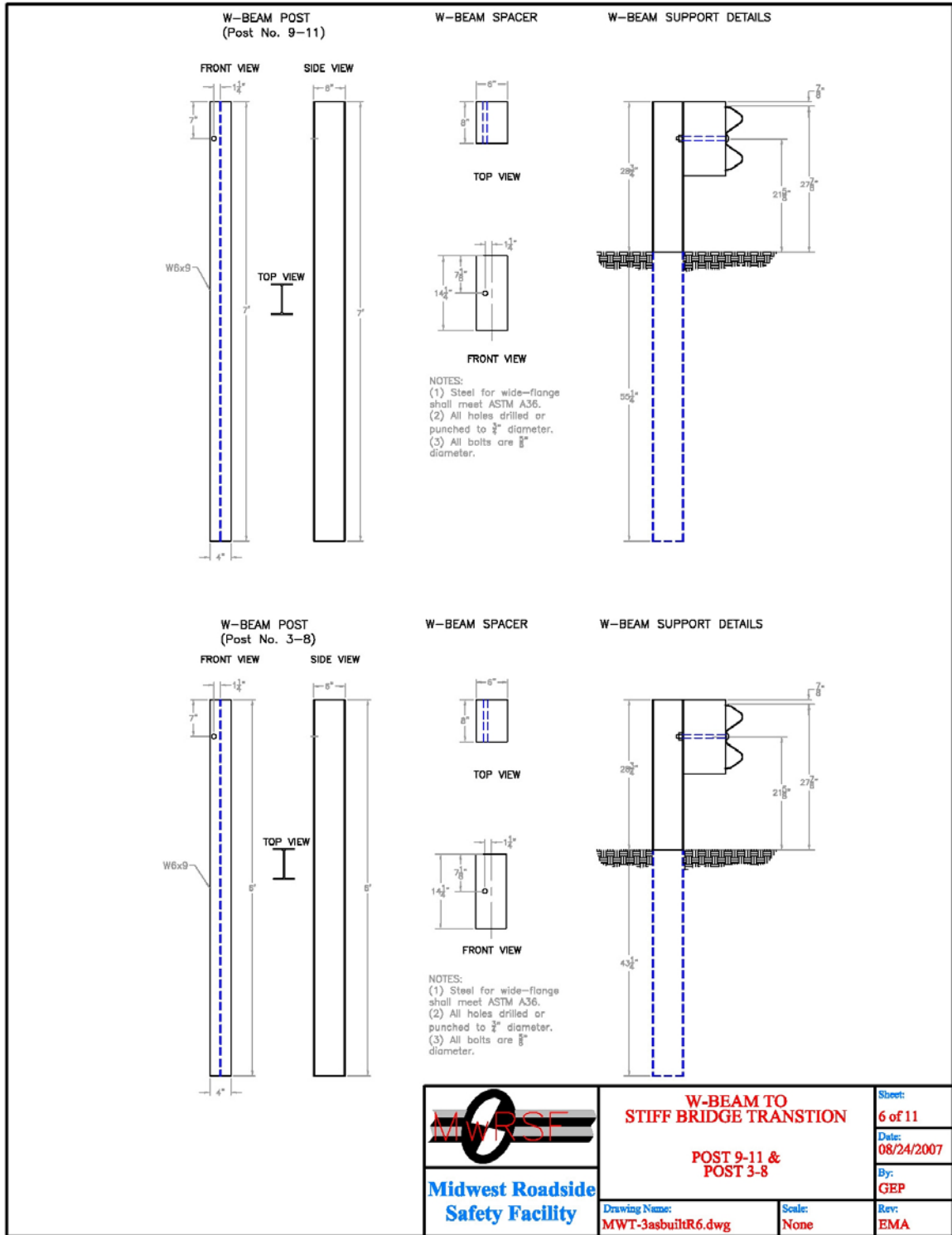
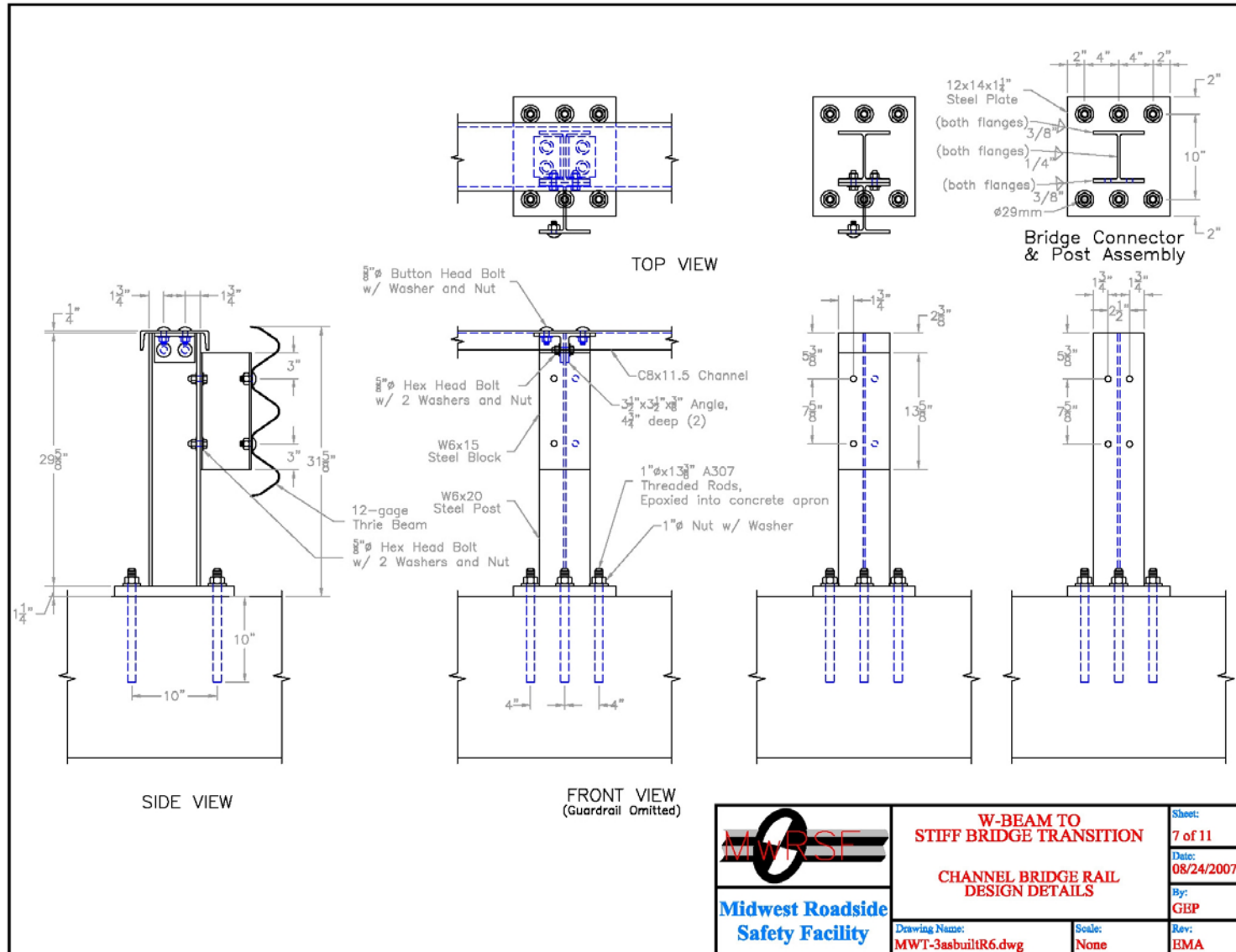


Figure A-6. Post Nos. 3 through 11 Details, Design No. 1 (English)



	W-BEAM TO STIFF BRIDGE TRANSITION	Sheet: 7 of 11
	CHANNEL BRIDGE RAIL DESIGN DETAILS	Date: 08/24/2007
Drawing Name: MWT-3asbuiltR6.dwg	Scale: None	By: GEP
		Rev: EMA

Figure A-7. Channel Bridge Rail Design Details, Design No. 1 (English)

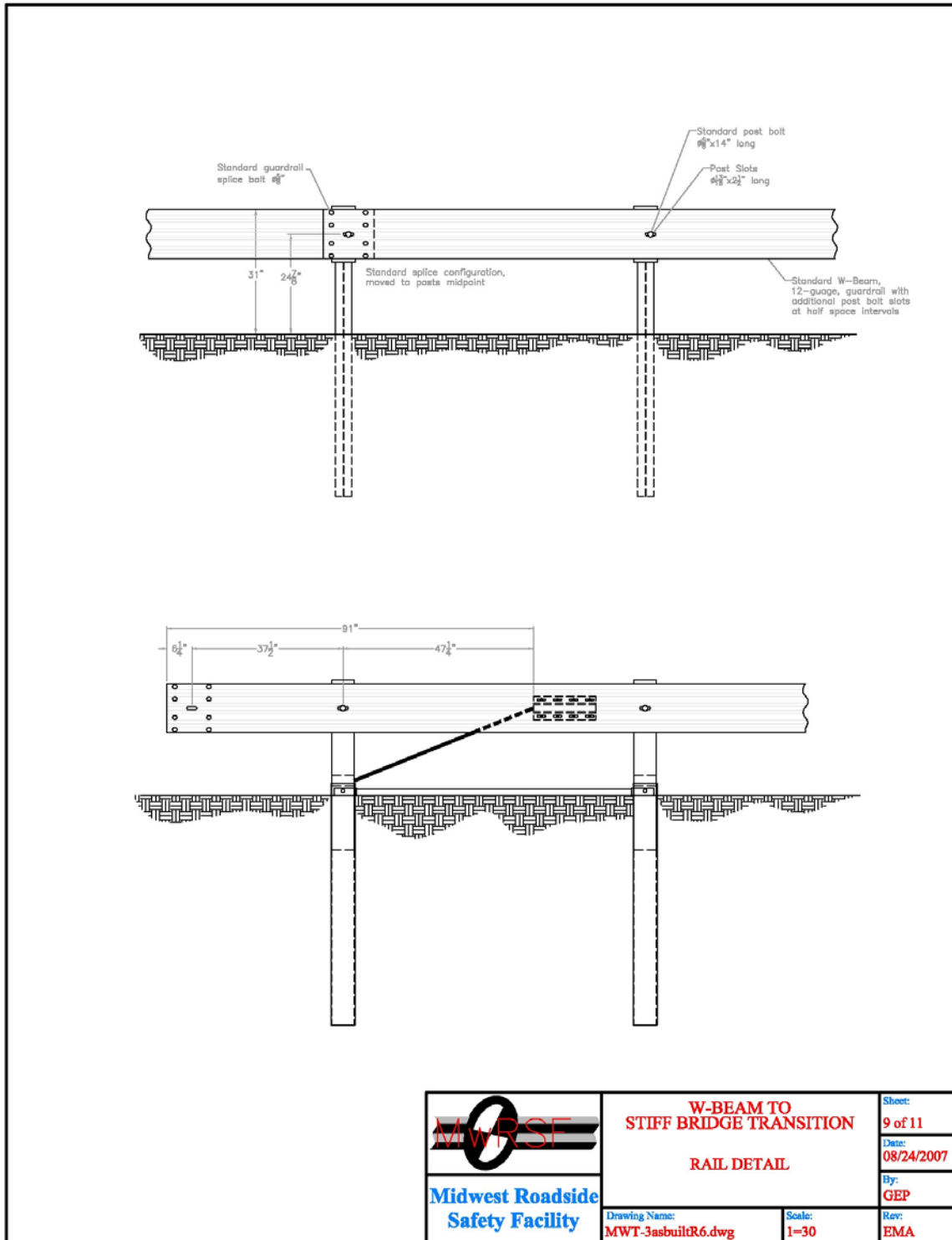


Figure A-9. Rail Details, Design No. 1 (English)

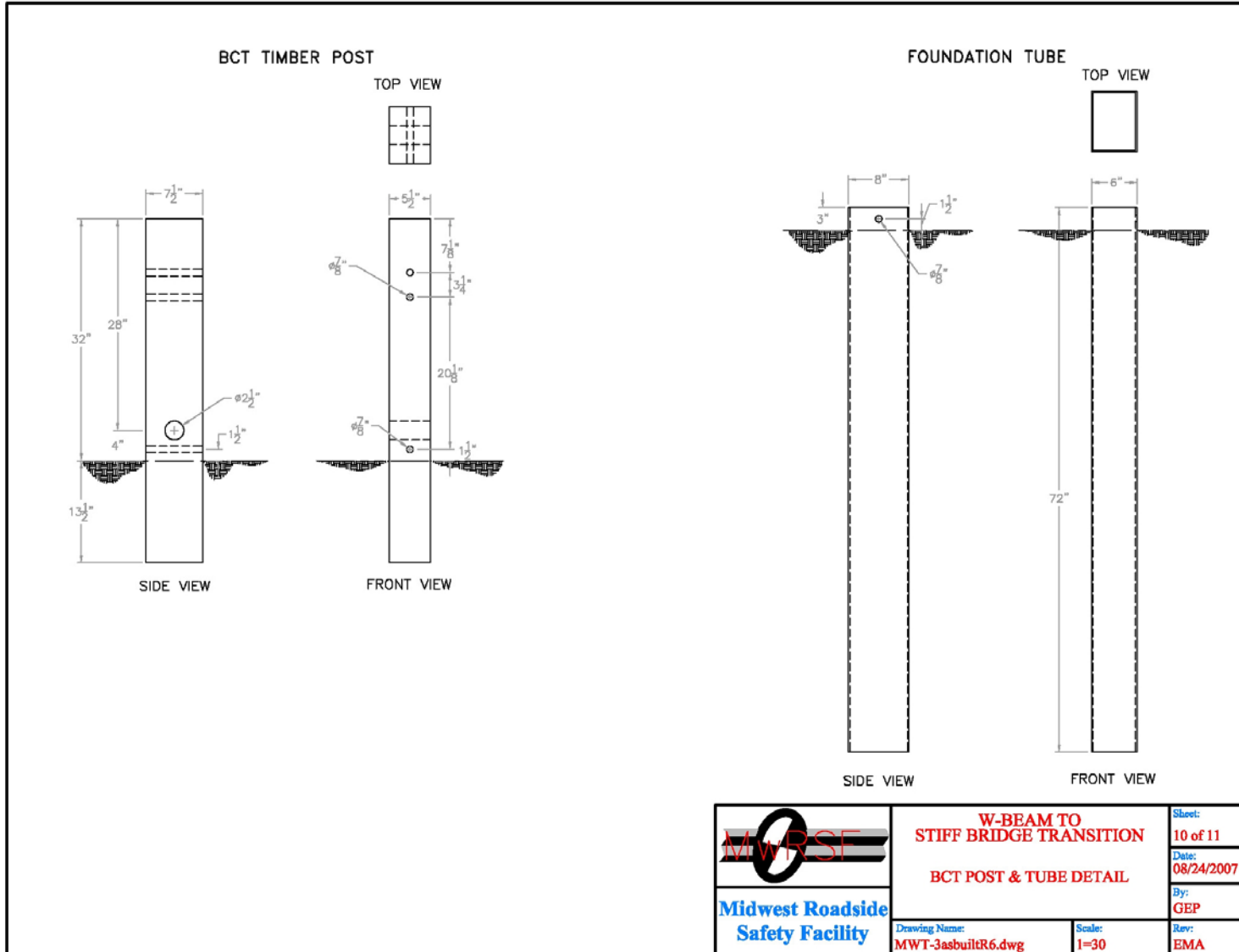


Figure A-10. BCT Post and Tube Detail, Design No. 1 (English)

APPENDIX B

Test Summary Sheets in English Units

Figure B-1. Summary of Test Results and Sequential Photographs (English), Test MWT-3

Figure B-2. Summary of Test Results and Sequential Photographs (English), Test MWT-4

Figure B-3. Summary of Test Results and Sequential Photographs (English), Test MWT-5

Figure B-4. Summary of Test Results and Sequential Photographs (English), Test MWT-6



0.000 SEC

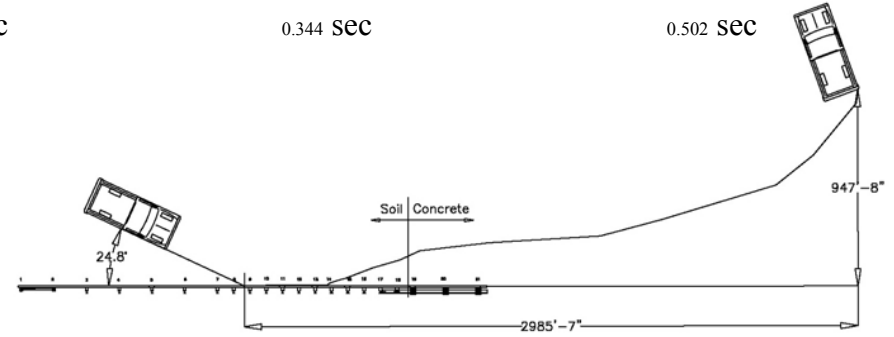
0.134 SEC

0.226 SEC

0.344 SEC

0.502 SEC

- Test Agency MwRSF
- Test Number MWT-3
- Date 6/18/03
- NCHRP 350 Test Designation 3-21
- Appurtenance W-beam to Thrie Beam Transition Element used with Approach Guardrail Transition
- Total Length 87 ft-6 in.
- Key Elements - Steel Thrie Beam Guardrail
 - Thickness 12 gauge
 - Top Mounting Height 31.625 in.
- Key Elements - Steel W-Beam to Thrie Beam Transition
 - Thickness 12 gauge
 - Shape Symmetrical
- Key Elements - Steel W-Beam Guardrail
 - Thickness 12 gauge
 - Top Mounting Height 27.8 in.
- Key Elements - Steel Posts
 - Post Nos. 3 - 8 W6x9 by 72 in. long
 - Post Nos. 9 - 15 W6x9 by 84 in. long
 - Post Nos. 16 - 18 W6x15 by 84 in. long
 - Post Nos. 19 - 21 W6x20 by 29.625 in. long
- Key Elements - Post Spacing
 - Post Nos. 1 - 7 75 in.
 - Post Nos. 7 - 19 37.5 in.
- Key Elements - Wood Spacer Blocks
 - Post Nos. 3 - 11 6 in. x 8 in. x 14 in. long
 - Post No 12 6 in. x 8 in. x 19 in. long
 - Post Nos. 13 - 15 6 in. x 8 in. x 22 in. long
 - Post Nos. 16 - 17 8 in. x 8 in. x 19 in. long
 - Post No. 18 8 in. x 8 in. x 15 in. long
- Key Elements - Steel Spacer Blocks
 - Post Nos. 19 - 21 W6x15 by 13.625 in. long
- Type of Soil Grading B - AASHTO M 147-65 (1990)
- Test Vehicle
 - Type/Designation 2000P
 - Make and Model 1998 GMC 2500 3/4-ton pickup
 - Curb 4,379 lbs
 - Test Inertial 4,456 lbs
 - Gross Static 4,456 lbs



- Impact Conditions
 - Speed 63.9 mph
 - Angle 24.8 degrees
 - Impact Location 8 in. upstream centerline post no. 9
- Exit Conditions
 - Speed 36.8 mph
 - Angle 16.6 degrees
- Post-Impact Trajectory
 - Vehicle Stability Unsatisfactory
 - Stopping Distance 117 ft - 7 in. downstream
 - 37 ft - 4 in. traffic-side face
- Occupant Impact Velocity
 - Longitudinal 23.29 ft/s < 39.37 ft/s
 - Lateral (not required) 17.85 ft/s
- Occupant Ridedown Deceleration (10 msec avg.)
 - Longitudinal 7.27 Gs < 20 Gs
 - Lateral (not required) 8.25 Gs
- THIV (not required) NA
- PHD (not required) NA
- Test Article Damage Moderate
- Test Article Deflections
 - Permanent Set 21.875 in.
 - Dynamic 25.6 in.
 - Working Width 30.9 in.
- Vehicle Damage Extensive
 - VDS¹³ 01-R&T-4
 - CDC¹⁴ 01-RDAO9
 - Maximum Deformation NA

Figure B-1. Summary of Test Results and Sequential Photographs (English), Test MWT-3



0.000 sec

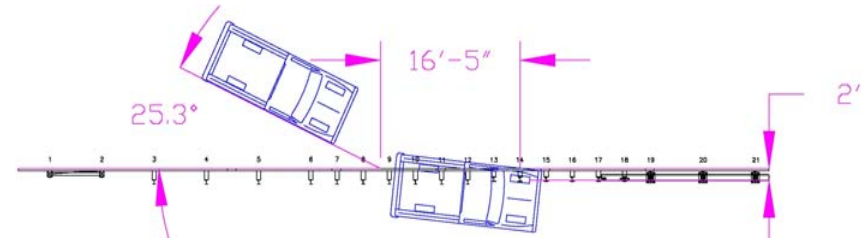
0.100 sec

0.196 sec

0.512 sec

1.658 sec

- Test Agency MwRSF
- Test Number MWT-4
- Date 7/29/03
- NCHRP 350 Test Designation 3-21
- Appurtenance W-beam to Thrie Beam Transition Element used with Approach Guardrail Transition
- Total Length 84 ft - 6in.
- Key Elements - Steel Thrie Beam Guardrail
 - Thickness 12 gauge
 - Top Mounting Height 31 in.
- Key Elements - Steel W-Beam to Thrie Beam Transition
 - Thickness 12 gauge
 - Shape Asymmetrical
- Key Elements - Steel W-Beam Guardrail
 - Thickness 12 gauge
 - Top Mounting Height 31 in.
- Key Elements - Steel Posts
 - Post Nos. 3 - 8 W6x9 by 72 in. long
 - Post Nos. 9 - 15 W6x9 by 84 in. long
 - Post Nos. 16 - 18 W6x15 by 84 in. long
 - Post Nos. 19 - 21 W6x20 by 29.625 in long
- Key Elements - Post Spacing
 - Post Nos. 1 - 6, 19 - 21 75 in.
 - Post Nos. 6 - 19 37.5 in.
- Key Elements - Wood Spacer Blocks
 - Post Nos. 3 - 11 6 in. x 12 in. x 14.25 in. long
 - Post No 12 6 in. x 12 in. x 19 in. long
 - Post Nos. 13 - 15 6 in. x 8 in. x 22 in. long
 - Post Nos. 16 - 17 8 in. x 8 in. x 19 in. long
 - Post No. 18 8 in. x 8 in. x 15 in. long
- Key Elements - Steel Spacer Blocks
 - Post Nos. 19 - 21 W6x15 by 13.625 in. long
- Type of Soil Grading B - AASHTO M 147-65 (1990)
- Test Vehicle
 - Type/Designation 2000P
 - Make and Model 1998 GMC 2500 3/4-ton pickup
 - Curb 4,359 lbs
 - Test Inertial 4,448 lbs
 - Gross Static 4,448 lbs



- Impact Conditions
 - Speed 61.0 mph
 - Angle 25.3 degrees
 - Impact Location 9 in. upstream centerline post no. 9
- Exit Conditions
 - Speed NA
 - Angle NA
- Post-Impact Trajectory
 - Vehicle Stability Satisfactory
 - Stopping Distance 16 ft - 4.5 in. downstream
2 ft laterally behind
- Occupant Impact Velocity
 - Longitudinal 22.22 ft/s < 39.37 ft/s
 - Lateral (not required) 15.71 ft/s
- Occupant Ridedown Deceleration (10 msec avg.)
 - Longitudinal 19.00 Gs < 20 Gs
 - Lateral (not required) 13.34 Gs
- THIV (not required) 27.99 ft/s
- PHD (not required) 20.22 Gs
- Test Article Damage Extensive (rail rupture)
- Test Article Deflections
 - Permanent Set NA
 - Dynamic NA
 - Working Width NA
- Vehicle Damage Moderate
 - VDS¹³ 01-RFQ-6
 - CDC¹⁴ 01-RYEW9
 - Maximum Deformation 6.5 in.

Figure B-2. Summary of Test Results and Sequential Photographs (English), Test MWT-4



0.000 sec



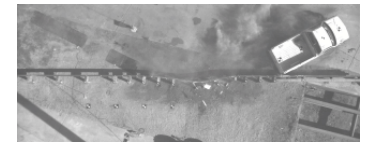
0.134 sec



0.234 sec

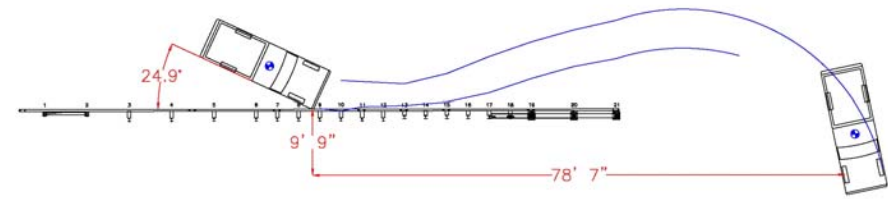


0.478 sec



0.874 sec

- Test Agency MwRSF
- Test Number MWT-5
- Date 11/10/05
- NCHRP 350 Test Designation 3-21
- Appurtenance Assymetrical W-beam to Thrie Beam Transition Element used with Approach Guardrail Transition
- Total Length 87 ft - 6 in.
- Key Elements - Steel Thrie Beam Guardrail
 - Thickness 12 gauge
 - Top Mounting Height 31 in.
- Key Elements - Steel W-Beam to Thrie Beam Transition
 - Thickness 10 gauge
 - Top Mounting Height 31 in.
 - Shape Asymmetrical
- Key Elements - Steel W-Beam Guardrail
 - Thickness 12 gauge
 - Top Mounting Height 31 in.
- Key Elements - Steel Posts
 - Post Nos. 3 - 8 W6x9 by 72 in. long
 - Post Nos. 9 - 15 W6x12 by 90 in. long
 - Post Nos. 16 - 18 W6x15 by 84 in. long
 - Post Nos. 19 - 21 W6x20 by 29.625 in. long
- Key Elements - Post Spacing
 - Post Nos. 1 - 6, 19 - 21 75 in.
 - Post Nos. 6 - 19 37.5 in.
- Key Elements - Wood Spacer Blocks
 - Post Nos. 3 - 11 6 in. x 12 in. x 14.25 in. long
 - Post No 12 6 in. x 12 in. x 19 in. long
 - Post Nos. 13 - 17 6 in. x 8 in. x 19 in. long
 - Post No. 18 6 in. x 8 in. x 15 in. long
- Key Elements - Steel Spacer Blocks
 - Post Nos. 19 - 21 W6x15 by 13.625 in. long
- Type of Soil Grading B - AASHTO M 147-65 (1990)
- Test Vehicle
 - Type/Designation 2000P
 - Make and Model 2000 GMC 2500 3/4-ton pickup
 - Curb 4,298 lbs
 - Test Inertial 4,431 lbs
 - Gross Static 4,431 lb



- Impact Conditions
 - Speed 61.5 mph
 - Angle 24.9 degrees
 - Impact Location 13 in. upstream centerline post no. 9
- Exit Conditions
 - Speed 23.4 mph
 - Angle 23.9 degrees
- Post-Impact Trajectory
 - Vehicle Stability Satisfactory
 - Stopping Distance 78 ft - 3 in. downstream
9 ft - 1 in. laterally behind
- Occupant Impact Velocity
 - Longitudinal 22.00 ft/s < 39.37 ft/s
 - Lateral (not required) 18.32 ft/s
- Occupant Ridedown Deceleration (10 msec avg.)
 - Longitudinal 13.24 Gs < 20 Gs
 - Lateral (not required) 8.67 Gs
- THIV 27.82 ft/s
- PHD 13.76 Gs
- Test Article Damage Moderate
- Test Article Deflections
 - Permanent Set 14.75 in
 - Dynamic 23.8 in.
 - Working Width 40.2 in.
- Vehicle Damage Minimal
 - VDS¹³ 01-RFW-4
 - CDC¹⁴ 01-RFEW6
 - Maximum Deformation 1.25 in.

Figure B-3. Summary of Test Results and Sequential Photographs (English), Test MWT-5



0.000 sec

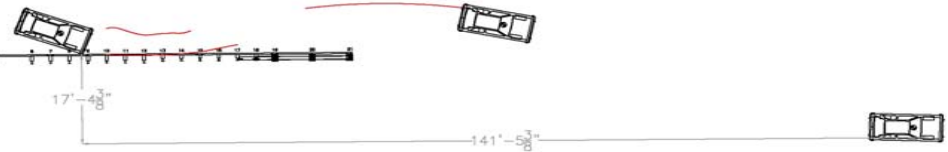
0.066 sec

0.116 sec

0.188 sec

0.302 sec

- Test Agency MwRSF
- Test Number MWT-6
- Date 11/22/05
- NCHRP 350 Test Designation 3-20
- Appurtenance Asymmetrical W-beam to Thrie Beam Transition Element used with Approach Guardrail Transition
- Total Length 87 ft 6 in.
- Key Elements - Steel Thrie Beam Guardrail
 - Thickness 12 gauge
 - Top Mounting Height 31 in.
- Key Elements - Steel W-Beam to Thrie Beam Transition
 - Thickness 10 gauge
 - Top Mounting Height 31 in.
 - Shape Asymmetrical
- Key Elements - Steel W-Beam Guardrail
 - Thickness 12 gauge
 - Top Mounting Height 31 in.
- Key Elements - Steel Posts
 - Post Nos. 3 - 8 W6x9 by 72 in. long
 - Post Nos. 9 - 15 W6x12 by 90 in. long
 - Post Nos. 16 - 18 W6x15 by 84 in. long
 - Post Nos. 19 - 21 W6x20 by 29.625 in. long
- Key Elements - Post Spacing
 - Post Nos. 1 - 6, 19 - 21 75 in.
 - Post Nos. 6 - 19 37.5 in.
- Key Elements - Wood Spacer Blocks
 - Post Nos. 3 - 11 6 in. x 12 in. x 14.25 in. long
 - Post No 12 6 in. x 12 in. x 19 in. long
 - Post Nos. 13 - 17 6 in. x 8 in. x 19 in. long
 - Post No. 18 6 in. x 8 in. x 15 in. long
- Key Elements - Steel Spacer Blocks
 - Post Nos. 19 - 21 W6x15 by 13.625 in long
- Type of Soil Grading B - AASHTO M 147-65 (1990)
- Test Vehicle
 - Type/Designation 820C
 - Make and Model 1997 Geo Metro
 - Curb 1,744 lbs
 - Test Inertial 1,826 lbs
 - Gross Static 1,992 lbs



- Impact Conditions
 - Speed 65.5 mph
 - Angle 20.4 degrees
 - Impact Location 9.25 in. upstream centerline post no. 10
- Exit Conditions
 - Speed 36.4 mph
 - Angle 6.6 degrees
- Post-Impact Trajectory
 - Vehicle Stability Satisfactory
 - Stopping Distance 137 ft - 5 in. downstream
17 ft - 5 in. laterally behind
- Occupant Impact Velocity
 - Longitudinal -19.91 ft/s < 39.37 ft/s
 - Lateral 22.60 ft/s < 39.37 ft/s
- Occupant Ridedown Deceleration (10 msec avg.)
 - Longitudinal -18.53 Gs < 20 Gs
 - Lateral 10.97 Gs < 20 Gs
- THIV 29.40 ft/s
- PHD 19.93 Gs
- Test Article Damage Minimal
- Test Article Deflections
 - Permanent Set 9.7 in
 - Dynamic 12.1 in.
 - Working Width 33.2 in.
- Vehicle Damage Moderate
 - VDS¹³ 01-RFQ-5
 - CDC¹⁴ 01-RYEW7
 - Maximum Deformation NA

Figure B-4. Summary of Test Results and Sequential Photographs (English), Test MWT-6

APPENDIX C

Occupant Compartment Deformation Data

Figure C-1. Occupant Compartment Deformation Data, Test MWT-3

Figure C-2. Occupant Compartment Deformation Data, Test MWT-4

Figure C-3. Occupant Compartment Deformation Index (OCDI), Test MWT-4

Figure C-4. Occupant Compartment Deformation Data - Set 1, Test MWT-5

Figure C-5. Occupant Compartment Deformation Data - Set 2, Test MWT-5

Figure C-6. Occupant Compartment Deformation Index (OCDI), Test MWT-5

Figure C-7. Occupant Compartment Deformation Index (OCDI), Test MWT-6

VEHICLE PRE/POST CRUSH INFO

TEST: MWT-3
 VEHICLE: 1997/GMC/2500/WHITE

POINT	X	Y	Z	X'	Y'	Z'	DEL X	DEL Y	DEL Z
1	53	5.75	-1.5	53	5.5	-1.75	0	-0.25	-0.25
2	56.5	10.5	-0.25	56.75	10	1	0.25	-0.5	1.25
3	58.25	14	0	59	13.75	1.5	0.75	-0.25	1.5
4	59	19.5	0.75	58.75	18	2.5	-0.25	-1.5	1.75
5	59.75	23.5	0	58.5	22.25	1.25	-1.25	-1.25	1.25
6	58	28.75	-1	58	28.25	1.5	0	-0.5	2.5
7	50.5	6.5	0.5	50.5	6.5	0.75	0	0	0.25
8	52.75	9.75	2.5	53	9	3	0.25	-0.75	0.5
9	54.5	13	4	54.25	11.25	5	-0.25	-1.75	1
10	54.75	17.75	4	54.5	16.75	5.75	-0.25	-1	1.75
11	54.5	23.5	4.5	54.25	22.25	6.25	-0.25	-1.25	1.75
12	54.75	28.75	4	54.25	27	6.75	-0.5	-1.75	2.75
13	46.75	6.5	0.5	46.75	6.25	0.75	0	-0.25	0.25
14	49.25	10	4	49.5	9.5	4.25	0.25	-0.5	0.25
15	51.25	14.5	6.5	51	13.25	7.25	-0.25	-1.25	0.75
16	51.25	19	6.5	51	12.5	7.5	-0.25	-6.5	1
17	50.75	24.5	6.5	50.5	23	7.5	-0.25	-1.5	1
18	50	29.75	6.5	50	28	7.75	0	-1.75	1.25
19	40.25	6	1	40.25	6.25	0.5	0	0.25	-0.5
20	42.25	13.25	6.25	42.25	13.5	6.25	0	0.25	0
21	42.75	21	6.25	42.75	20.25	6.5	0	-0.75	0.25
22	42.75	29.75	7	42.75	29	8.75	0	-0.75	1.75
23	31.5	12	6	31.5	11.25	5.75	0	-0.75	-0.25
24	32.25	25.75	6.25	32.25	25.75	6.75	0	0	0.5
25	10	17	2	10	17	2	0	0	0
26	42.5	10.25	-25.25	42	10.25	-24.5	-0.5	0	0.75
27	40.25	17.5	-25.25	41.25	17.5	-24.5	1	0	0.75
28	40.25	24.5	-25.5	41	24.5	-23.75	0.75	0	1.75
29	18	30	-14	18.5	31	-13.5	0.5	1	0.5
30									

ORIENTATION AND REFERENCE INFO

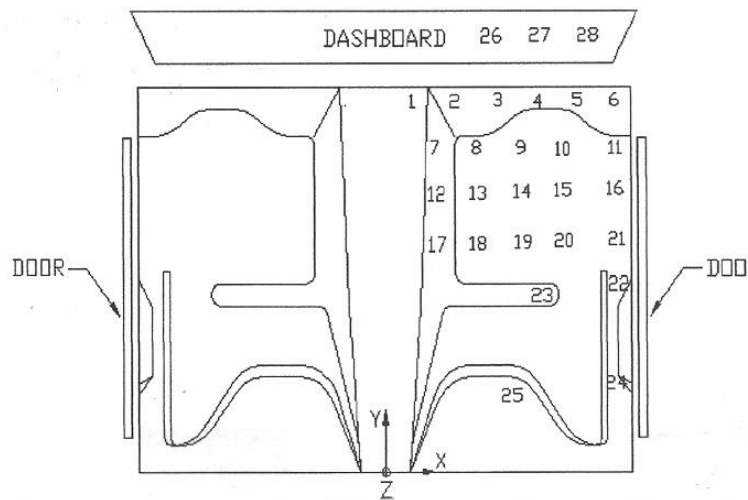


Figure C-1. Occupant Compartment Deformation Data, Test MWT-3

VEHICLE PRE/POST CRUSH INFO

TEST: MWT-4
VEHICL 1998/GMC/white

SECONDARY POINTS

POINT	X	Y	Z	X'	Y'	Z'	DEL X	DEL Y	DEL Z	Z2	Z2'	Del Z2
1	53.5	6.25	-1	53.5	6.25	N/A	0	0	N/A	2.5	4.5	2
2	55.25	9.75	-1.75	54.75	10.5	2.25	-0.5	0.75	4	0.5	2.5	2
3	56.75	16	-2.75	54.5	15.25	1.5	-2.25	-0.75	4.25	-2.25	1	3.25
4	56.75	21.75	-3.75	55	21	0.5	-1.75	-0.75	4.25	-3.25	-0.5	2.75
5	56.25	26	-3	55.5	25	0	-0.75	-1	3	-3.75	-1.75	2
6	56.5	29	-2.75	56	27.5	0	-0.5	-1.5	2.75	-4	-2.25	1.75
7	48	8.75	-3.5	48	8.5	0.25	0	-0.25	3.75	-2.25	-1	1.25
8	48.75	15.25	-7.25	48.75	14.5	-4.25	0	-0.75	3	-6.75	-4.5	2.25
9	48.75	19.75	-7.25	48.75	19	-4	0	-0.75	3.25	-7.25	-5.5	1.75
10	48	25	-7	48	24.25	-5	0	-0.75	2	-7.75	-6	1.75
11	48.5	28.5	-6.75	48	28	-4.25	-0.5	-0.5	2.5	-8	-6.5	1.5
12	41.5	8.75	-5.75	41.5	8.5	-4.25	0	-0.25	1.5	-3.35	-0.75	2.6
13	42	15.25	-7.75	42	14.5	-1.25	0	-0.75	6.5	-7.25	-5	2.25
14	42	19.5	-7.5	42	19.5	-4.75	0	0	2.75	-7.75	-5.75	2
15	41.5	25	-7.5	41.5	25	-4.75	0	0	2.75	-8.5	-6.75	1.75
16	42	28.5	-7.75	41.5	28.75	-5.25	-0.5	0.25	2.5	-9	-7.5	1.5
17	35.25	8.5	-5.5	5.25	8.25	-2.75	-30	-0.25	2.75	-4.25	-2	2.25
18	35	14.75	-7.75	35	14.5	-5	0	-0.25	2.75	-7.5	-5.5	2
19	34.75	19.5	-7.5	34.75	19	-5	0	-0.5	2.5	-8	-6.25	1.75
20	34	24.5	-7.75	33.75	24.25	-5.5	-0.25	-0.25	2.25	-9	-7.5	1.5
21	34.25	28.5	-7.75	33.75	28	-5.75	-0.5	-0.5	2	-9.5	-8.25	1.25
22	26.5	27.75	-7.75	26	27.5	-6	-0.5	-0.25	1.75	-9.5	-8.75	0.75
23	26.5	19.5	-7.75	26.5	19.25	-5.75	0	-0.25	2	-8.25	-7	1.25
24	16.75	27.75	-8	16.25	27.5	-6.75	-0.5	-0.25	1.25	-10.25	-10	0.25
25	10.75	16	-5.25	11	16	-4.5	0.25	0	0.75	-5.5	-5.25	0.25
26	42.75	0.25	23.75	43.25	0.25	25.5	0.5	0	1.75	26		N/A
27	41.25	14.75	24	41.75	15	26.5	0.5	0.25	2.5	24.25	26.25	2
28	40.75	24.75	24	41.25	24.75	26.75	0.5	0	2.75	23	25	2
29												
30												

ORIENTATION AND REFERENCE INFO

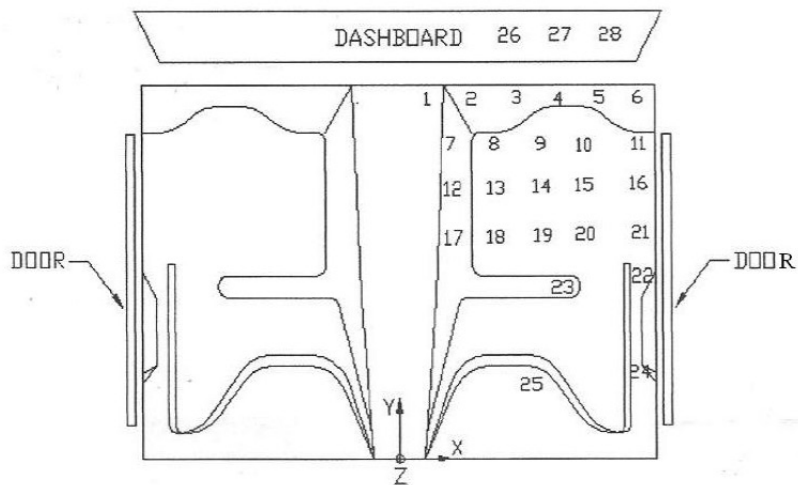


Figure C-2. Occupant Compartment Deformation Data, Test MWT-4

Occupant Compartment Deformation Index (OCDI)

Test No. MWT-4
 Vehicle Type: 2000p

OCDI = XXABCDEFGHI

XX = location of occupant compartment deformation

A = distance between the dashboard and a reference point at the rear of the occupant compartment, such as the top of the rear seat or the rear of the cab on a pickup

B = distance between the roof and the floor panel

C = distance between a reference point at the rear of the occupant compartment and the motor panel

D = distance between the lower dashboard and the floor panel

E = interior width

F = distance between the lower edge of right window and the upper edge of left window

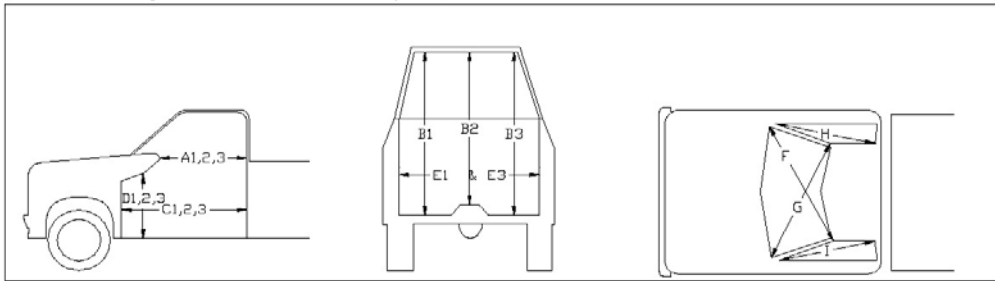
G = distance between the lower edge of left window and the upper edge of right window

H = distance between bottom front corner and top rear corner of the passenger side window

I = distance between bottom front corner and top rear corner of the driver side window

Severity Indices

- 0 - If the reduction is less than 3%
- 1 - If the reduction is greater than 3% and less than or equal to 10 %
- 2 - If the reduction is greater than 10% and less than or equal to 20 %
- 3 - If the reduction is greater than 20% and less than or equal to 30 %
- 4 - If the reduction is greater than 30% and less than or equal to 40 %



where,
 1 = Passenger Side
 2 = Middle
 3 = Driver Side

Location:

Measurement	Pre-Test (in.)	Post-Test (in.)	Change (in.)	% Difference	Severity Index
A1	38.75	39.00	0.25	0.65	0
A2	39.75	39.75	0.00	0.00	0
A3	39.00	39.50	0.50	1.28	0
B1	46.00	45.75	-0.25	-0.54	0
B2	42.50	40.75	-1.75	-4.12	1
B3	47.25	47.00	-0.25	-0.53	0
C1	59.00	59.25	0.25	0.42	0
C2	52.75	52.75	0.00	0.00	0
C3	58.25	57.00	-1.25	-2.15	0
D1	16.00	16.00	0.00	0.00	0
D2	9.00	7.25	-1.75	-19.44	2
D3	15.75	15.50	-0.25	-1.59	0
E1	62.50	61.75	-0.75	-1.20	0
E3	63.88	63.75	-0.13	-0.20	0
F	61.50	61.00	-0.50	-0.81	0
G	61.50	61.50	0.00	0.00	0
H	39.75	39.00	-0.75	-1.89	0
I	39.75	39.50	-0.25	-0.63	0

[Note: Maximum severity index for each variable (A-I) is used for determination of final OCDI value]

Final OCDI: RF A B C D E F G H I
 0 1 0 2 0 0 0 0 0

Figure C-3. Occupant Compartment Deformation Index (OCDI), Test MWT-4

VEHICLE PRE/POST CRUSH INFO
Set-1

TEST: MWT-5
VEHICLE: 2000p/C2500

Note: If impact is on driver side need to enter negative number for Y.

POINT	X	Y	Z	X'	Y'	Z'	DEL X	DEL Y	DEL Z
1	53.25	5.75	0	53.25	5.75	1	0	0	1
2	56.5	11.25	-1.25	57	10.25	-0.5	0.5	-1	0.75
3	58.5	17.25	-1.75	59	15.75	-1.5	0.5	-1.5	0.25
4	58.25	23.75	-1	58	22	-0.5	-0.25	-1.75	0.5
5	57.25	28.5	0	57	27	0.25	-0.25	-1.5	0.25
6	46.75	6.5	-2.25	46.75	6.75	-1.5	0	0.25	0.75
7	53	12.75	-6.75	53.25	11.25	-6.25	0.25	-1.5	0.5
8	53.25	17.75	-6	53.5	16.5	-6	0.25	-1.25	0
9	53.25	24.25	-5.25	53.25	22.75	-5	0	-1.5	0.25
10	53.25	29.5	-4.25	53	28	-4.25	-0.25	-1.5	0
11	47.5	11.5	-8	47.5	10.5	-7.5	0	-1	0.5
12	47.5	17.25	-7.5	47.5	16	-7	0	-1.25	0.5
13	47	23.75	-6.75	47	22.5	-6.25	0	-1.25	0.5
14	48.25	29	-6.25	48.25	27.5	-6.25	0	-1.5	0
15	44	11.5	-8	44	10.5	-7.5	0	-1	0.5
16	44.75	16.75	-7.75	44.75	16	-7.25	0	-0.75	0.5
17	44.25	24	-7	44.25	23.75	-6.25	0	-0.25	0.75
18	44.5	28	-6.75	44.5	27.75	-6.75	0	-0.25	0
19	40.75	11	-8	40.5	10	-7.5	-0.25	-1	0.5
20	41.25	16.75	-7.75	41.25	16	-7.25	0	-0.75	0.5
21	41.25	23.75	-7	41.25	23.5	-6.5	0	-0.25	0.5
22	41.5	29.5	-6.75	41.75	29	-7	0.25	-0.5	-0.25
23	37	10.5	-8	37	9.75	-7.75	0	-0.75	0.25
24	38	16.75	-7.75	38	16.25	-7.25	0	-0.5	0.5
25	38	24.25	-7	38	23.75	-6.5	0	-0.5	0.5
26	38.25	29.5	-7	38.25	29	-7	0	-0.5	0
27	31.75	14.5	-8.25	31.75	14	-8	0	-0.5	0.25
28	31.75	25.25	-7	31.75	24.5	-6.75	0	-0.75	0.25
29									
30									

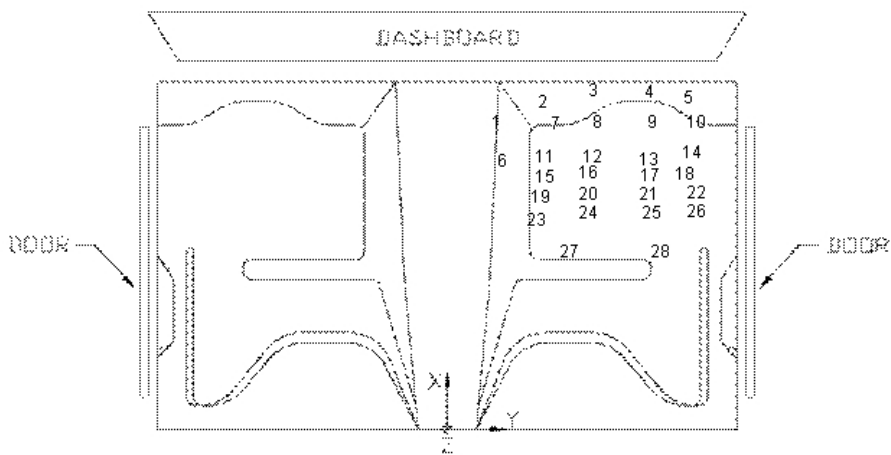


Figure C-4. Occupant Compartment Deformation Data - Set 1, Test MWT-5

VEHICLE PRE/POST CRUSH INFO
Set-2

TEST: MWT-5
VEHICLE: 2000p/C2500

Note: If impact is on driver side need to enter negative number for Y.

POINT	X	Y	Z	X'	Y'	Z'	DEL X	DEL Y	DEL Z
1	46.75	14.25	0	46.25	14.25	1.25	-0.5	0	1.25
2	50	19.75	-1.5	50	18.75	-0.5	0	-1	1
3	52	25.75	-2	52.25	24.25	-1.5	0.25	-1.5	0.5
4	51.75	32.25	-1.5	51.5	30.5	-0.75	-0.25	-1.75	0.75
5	50.75	37	-0.5	50.5	35.5	0	-0.25	-1.5	0.5
6	40.25	15	-2.75	39.75	15.25	-1.5	-0.5	0.25	1.25
7	46.5	21.25	-7	46.25	19.75	-6	-0.25	-1.5	1
8	46.75	26.25	-6.25	46.75	25	-6	0	-1.25	0.25
9	46.75	32.75	-5.5	46.75	31.25	-5.25	0	-1.5	0.25
10	46.75	38	-4.5	46.5	36.5	-4.25	-0.25	-1.5	0.25
11	41	20	-8	40.75	19	-7.25	-0.25	-1	0.75
12	41	25.75	-7.75	41	24.5	-7	0	-1.25	0.75
13	40.5	32.25	-7	40.5	31	-6.5	0	-1.25	0.5
14	41.75	37.5	-6.25	41.75	36	-6.25	0	-1.5	0
15	37.5	20	-8	37.25	19	-7.25	-0.25	-1	0.75
16	38.25	25.25	-7.75	38	24.5	-7.25	-0.25	-0.75	0.5
17	37.75	32.5	-7	37.5	32.25	-6.5	-0.25	-0.25	0.5
18	38	36.5	-6.75	38	36.25	-6.75	0	-0.25	0
19	34.25	19.5	-8	33.75	18.5	-7.5	-0.5	-1	0.5
20	34.75	25.25	-7.75	34.5	24.5	-7.25	-0.25	-0.75	0.5
21	34.75	32.25	-7.25	34.75	32	-6.5	0	-0.25	0.75
22	35	38	-7	35.25	37.5	-7	0.25	-0.5	0
23	30.5	19	-8	30.25	18.25	-7.25	-0.25	-0.75	0.75
24	31.5	25.25	-7.75	31.25	24.75	-7.25	-0.25	-0.5	0.5
25	31.5	32.75	-7.25	31.5	32.25	-6.5	0	-0.5	0.75
26	31.75	38	-7	32	37.5	-7	0.25	-0.5	0
27	25.25	23	-8.25	25	22.5	-7.75	-0.25	-0.5	0.5
28	25.25	33.75	-7.25	25.25	33	-6.5	0	-0.75	0.75
29									
30									

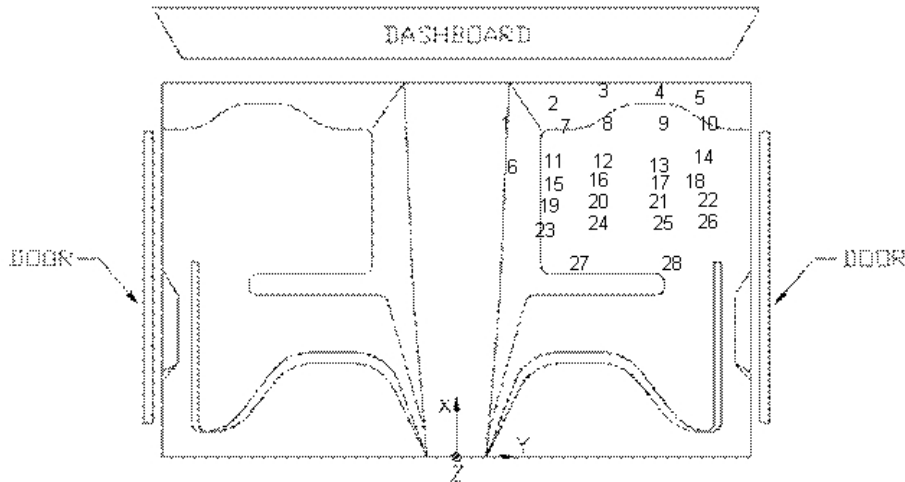


Figure C-5. Occupant Compartment Deformation Data - Set 2, Test MWT-5

Occupant Compartment Deformation Index (OCDI)

Test No. MWT-5
 Vehicle Type: 2000p/C2500

OCDI = XXABCDEFGHI

XX = location of occupant compartment deformation

A = distance between the dashboard and a reference point at the rear of the occupant compartment, such as the top of the rear seat or the rear of the cab on a pickup

B = distance between the roof and the floor panel

C = distance between a reference point at the rear of the occupant compartment and the motor panel

D = distance between the lower dashboard and the floor panel

E = interior width

F = distance between the lower edge of right window and the upper edge of left window

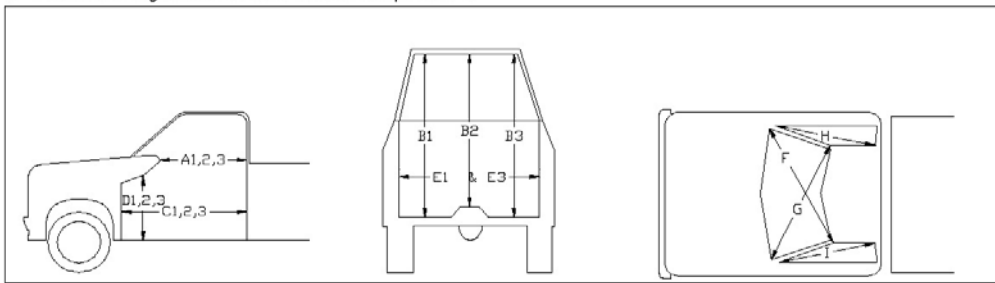
G = distance between the lower edge of left window and the upper edge of right window

H = distance between bottom front corner and top rear corner of the passenger side window

I = distance between bottom front corner and top rear corner of the driver side window

Severity Indices

- 0 - If the reduction is less than 3%
- 1 - If the reduction is greater than 3% and less than or equal to 10 %
- 2 - If the reduction is greater than 10% and less than or equal to 20 %
- 3 - If the reduction is greater than 20% and less than or equal to 30 %
- 4 - If the reduction is greater than 30% and less than or equal to 40 %



where,
 1 = Passenger Side
 2 = Middle
 3 = Driver Side

Location:

Measurement	Pre-Test (in.)	Post-Test (in.)	Change (in.)	% Difference	Severity Index
A1	41.50	41.25	-0.25	-0.60	0
A2	41.25	41.75	0.50	1.21	0
A3	40.00	40.00	0.00	0.00	0
B1	46.50	46.00	-0.50	-1.08	0
B2	42.25	40.75	-1.50	-3.55	1
B3	46.75	46.50	-0.25	-0.53	0
C1	58.00	58.00	0.00	0.00	0
C2	52.25	52.00	-0.25	-0.48	0
C3	56.75	56.50	-0.25	-0.44	0
D1	18.75	19.00	0.25	1.33	0
D2	16.25	15.75	-0.50	-3.08	1
D3	18.00	18.00	0.00	0.00	0
E1	62.50	61.00	-1.50	-2.40	0
E3	64.00	63.75	-0.25	-0.39	0
F	58.25	58.25	0.00	0.00	0
G	58.25	58.55	0.30	0.52	0
H	41.25	41.00	-0.25	-0.61	0
I	41.50	41.25	-0.25	-0.60	0

[Note: Maximum severity index for each variable (A-I) is used for determination of final OCDI value]

Final OCDI: XXABCDEFGHI
 RF 0 1 0 1 0 0 0 0 0

Figure C-6. Occupant Compartment Deformation Index (OCDI), Test MWT-5

Occupant Compartment Deformation Index (OCDI)

Test No. MWT-6
Vehicle Type: 820c/METRO

OCDI = XXABCDEFGHI

XX = location of occupant compartment deformation

A = distance between the dashboard and a reference point at the rear of the occupant compartment, such as the top of the rear seat or the rear of the cab on a pickup

B = distance between the roof and the floor panel

C = distance between a reference point at the rear of the occupant compartment and the motor panel

D = distance between the lower dashboard and the floor panel

E = interior width

F = distance between the lower edge of right window and the upper edge of left window

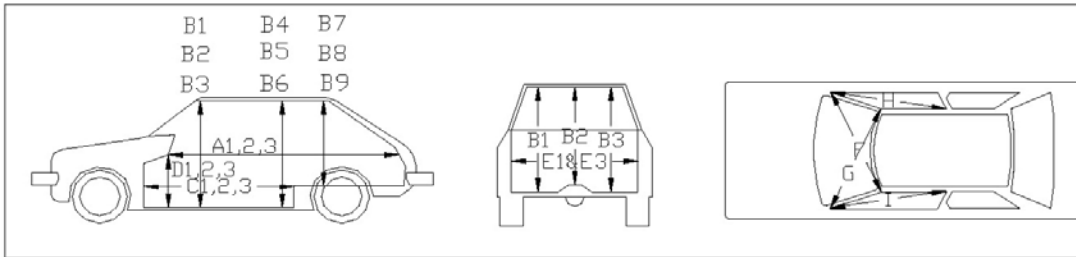
G = distance between the lower edge of left window and the upper edge of right window

H = distance between bottom front corner and top rear corner of the passenger side window

I = distance between bottom front corner and top rear corner of the driver side window

Severity Indices

- 0 - if the reduction is less than 3%
- 1 - if the reduction is greater than 3% and less than or equal to 10 %
- 2 - if the reduction is greater than 10% and less than or equal to 20 %
- 3 - if the reduction is greater than 20% and less than or equal to 30 %
- 4 - if the reduction is greater than 30% and less than or equal to 40 %



where,
 1 = Passenger Side
 2 = Middle
 3 = Driver Side

Location: RF

Measurement	Pre-Test (in.)	Post-Test (in.)	Change (in.)	% Difference	Severity Index
A1	43.25	43.50	0.25	0.58	0
A2	42.25	42.00	-0.25	-0.59	0
A3	43.00	42.00	-1.00	-2.33	0
B1	39.50	39.50	0.00	0.00	0
B2	37.00	37.00	0.00	0.00	0
B3	37.00	37.75	0.75	2.03	0
C1	56.25	56.50	0.25	0.44	0
C2	61.25	60.25	-1.00	-1.63	0
C3	56.75	54.50	-2.25	-3.96	1
D1	21.25	21.50	0.25	1.18	0
D2	21.75	22.00	0.25	1.15	0
D3	19.50	18.75	-0.75	-3.85	1
E1	49.75	46.00	-3.75	-7.54	1
E3	49.75	49.50	-0.25	-0.50	0
F	47.50	47.25	-0.25	-0.53	0
G	46.75	47.00	0.25	0.53	0
H	40.75	40.00	-0.75	-1.84	0
I	39.75	39.75	0.00	0.00	0

Note: Maximum severity index for each variable (A-I) is used for determination of final OCDI value

Final OCDI: XXABCDEFGHI
 RF 0 0 1 1 1 0 0 0 0

Figure C-7. Occupant Compartment Deformation Index (OCDI), Test MWT-6

APPENDIX D

Accelerometer and Rate Transducer Data Analysis, Test MWT-3

Figure D-1. Graph of Longitudinal Deceleration, Test MWT-3

Figure D-2. Graph of Longitudinal Occupant Impact Velocity, Test MWT-3

Figure D-3. Graph of Longitudinal Occupant Displacement, Test MWT-3

Figure D-4. Graph of Lateral Deceleration, Test MWT-3

Figure D-5. Graph of Lateral Occupant Impact Velocity, Test MWT-3

Figure D-6. Graph of Lateral Occupant Displacement, Test MWT-3

Figure D-7. Graph of Roll and Yaw Angular Displacements, Test MWT-3

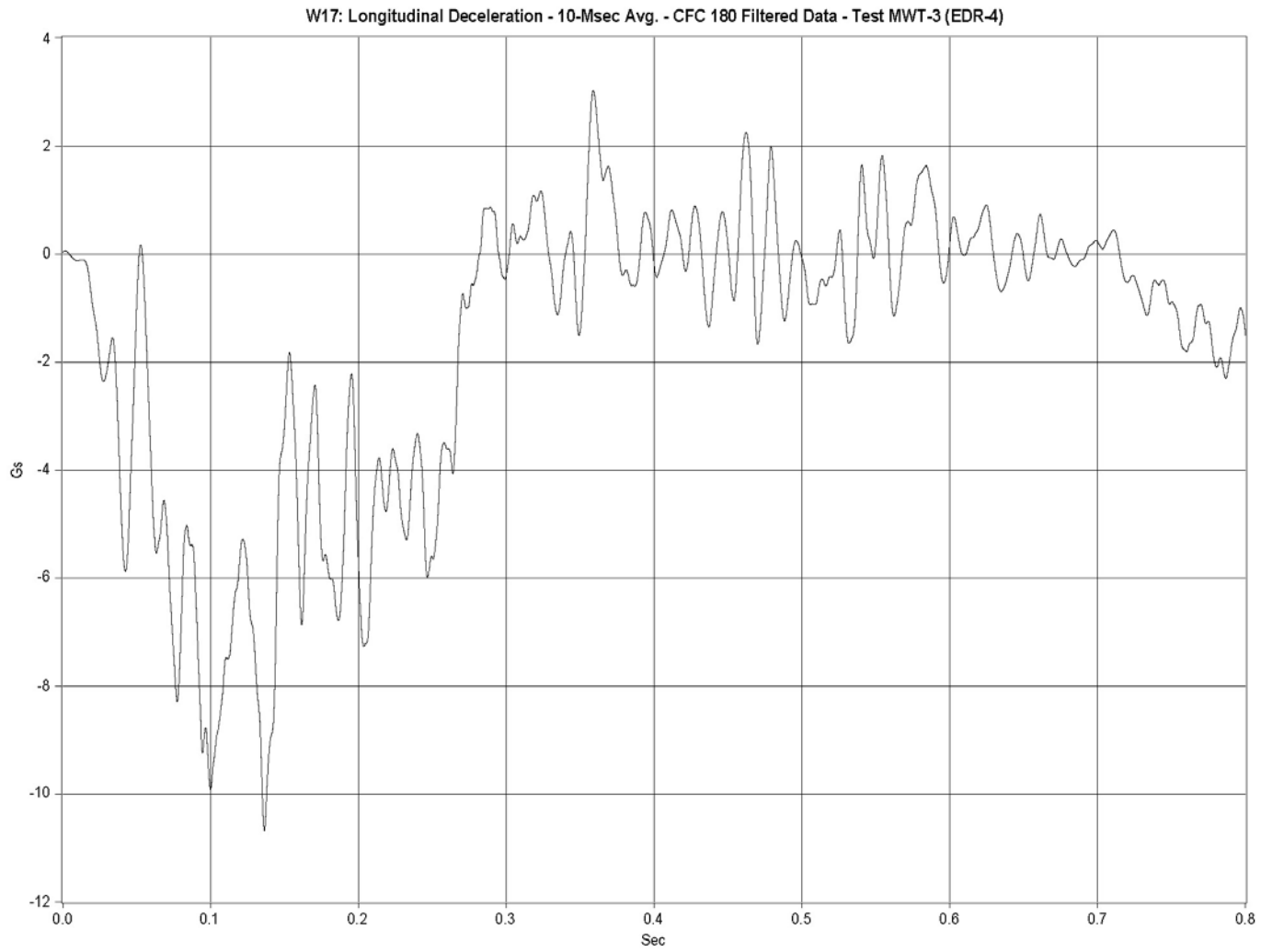


Figure D-1. Graph of Longitudinal Deceleration, Test MWT-3

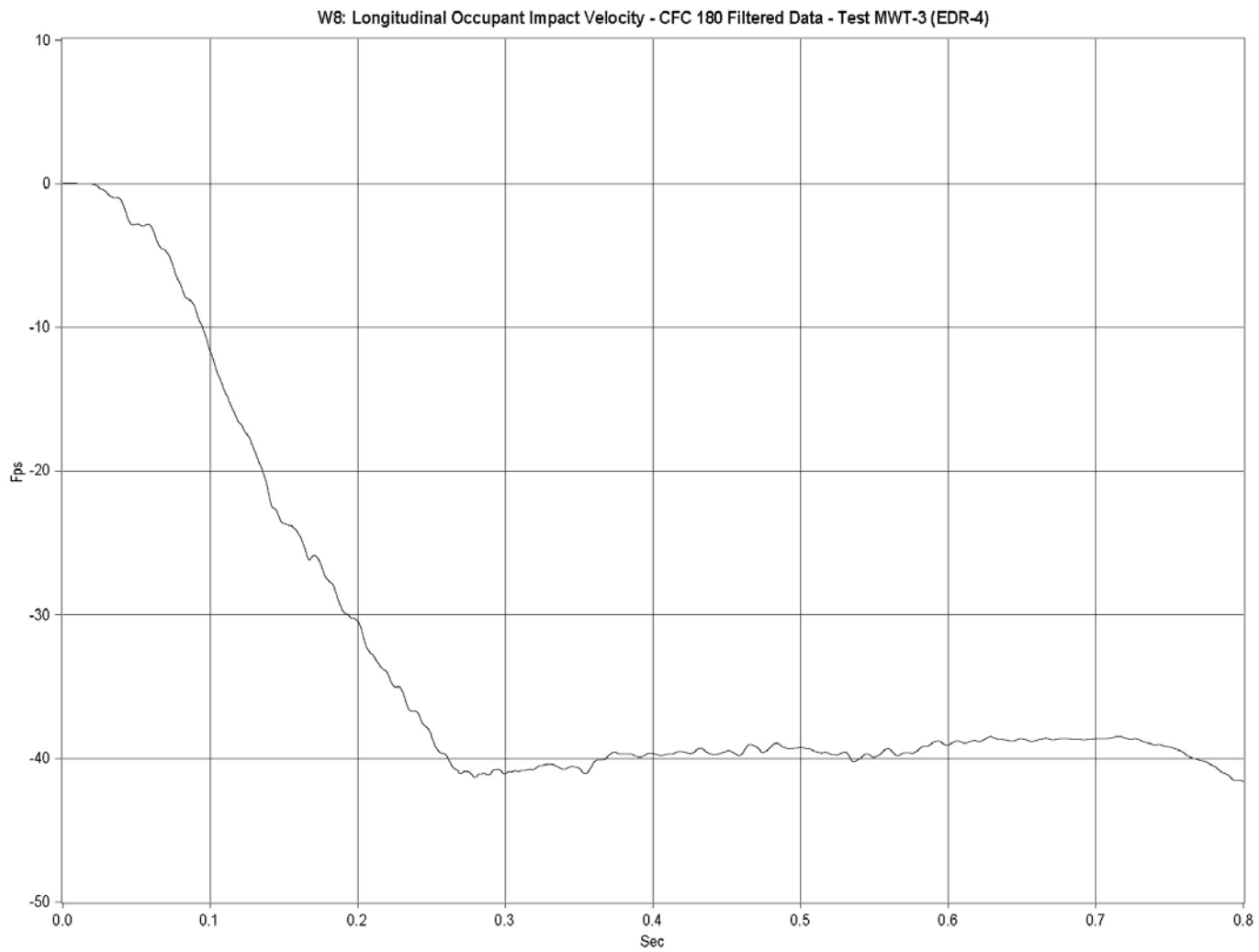


Figure D-2. Graph of Longitudinal Occupant Impact Velocity, Test MWT-3

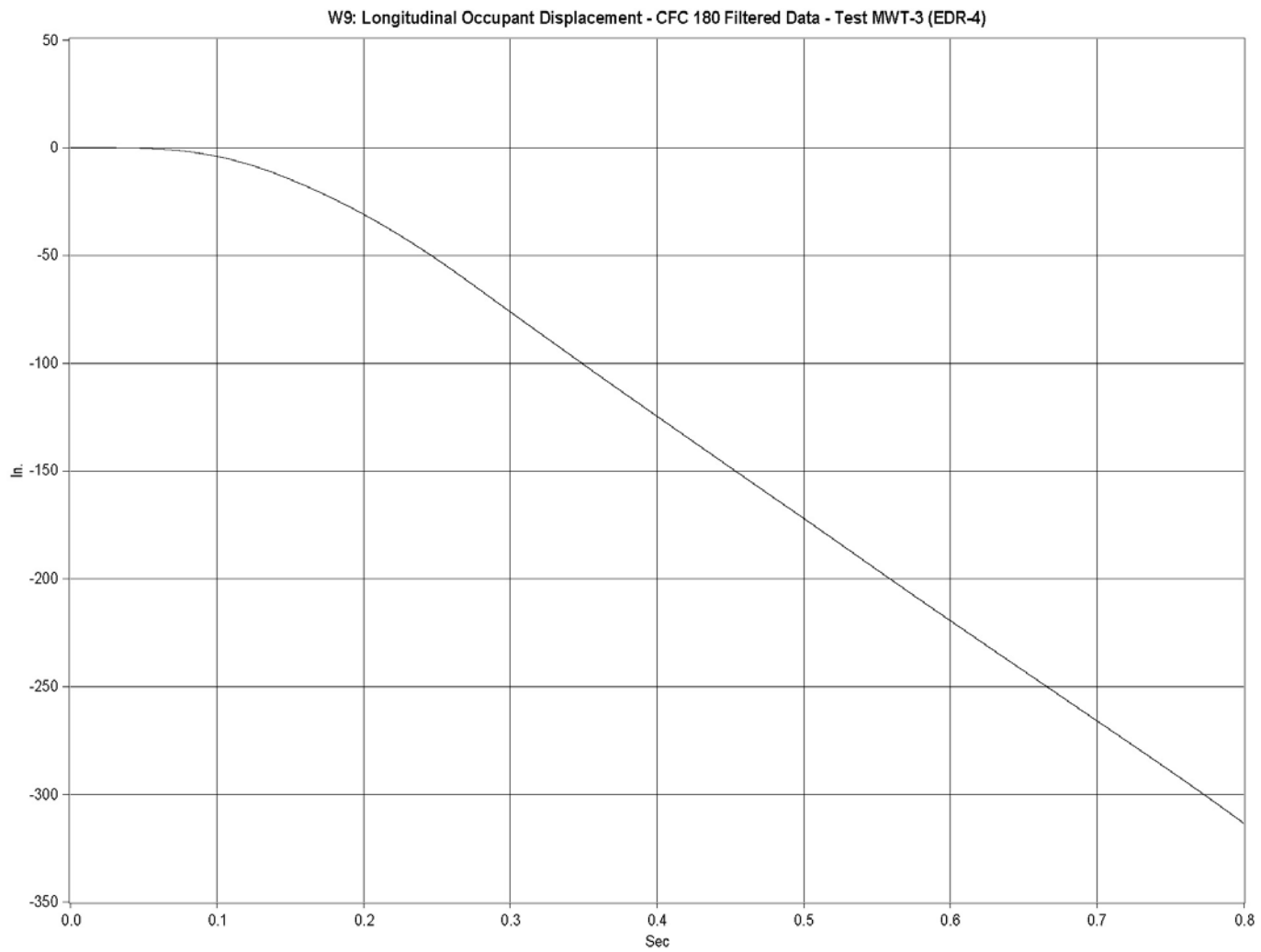


Figure D-3. Graph of Longitudinal Occupant Displacement, Test MWT-3

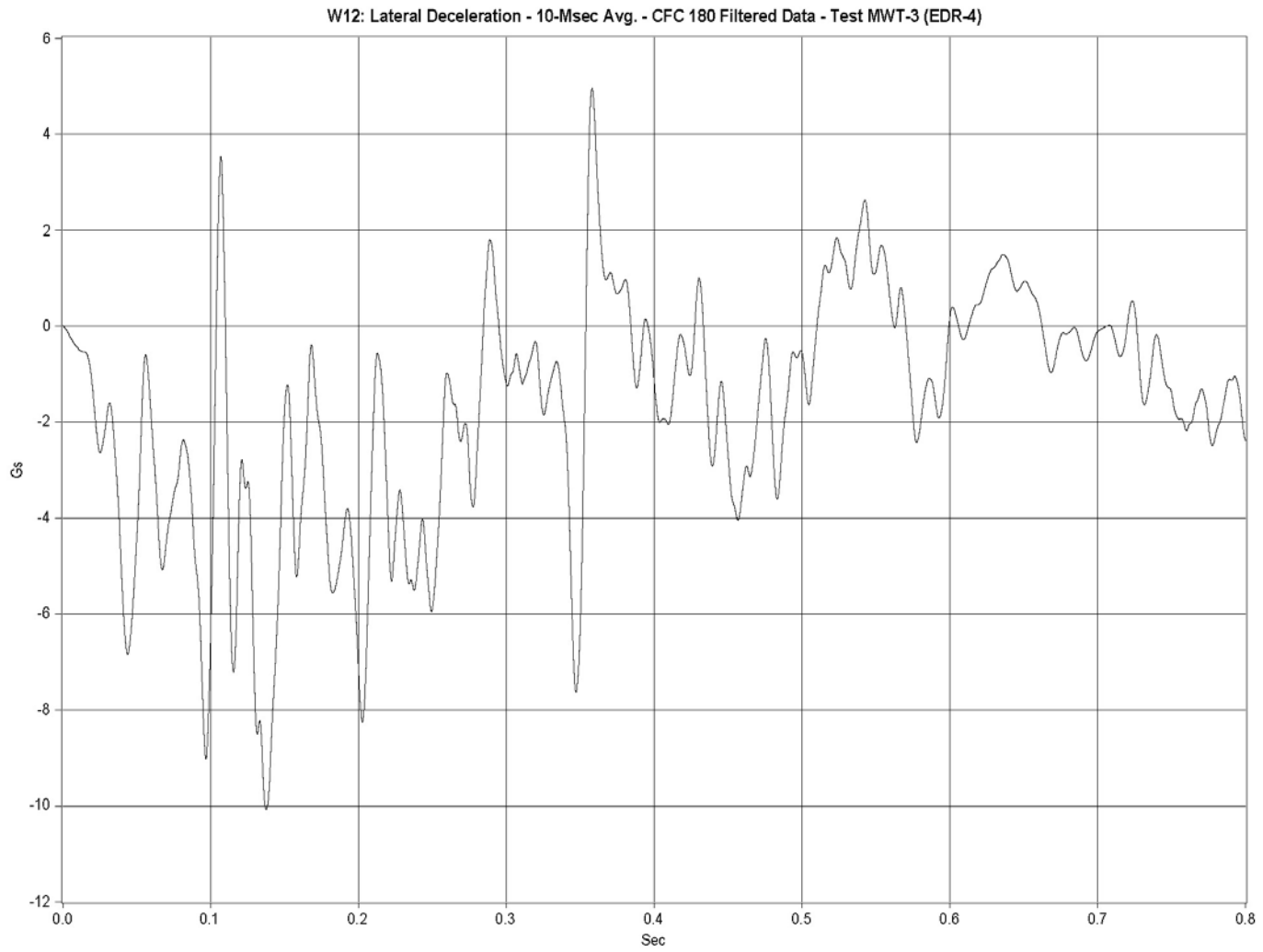


Figure D-4. Graph of Lateral Deceleration, Test MWT-3

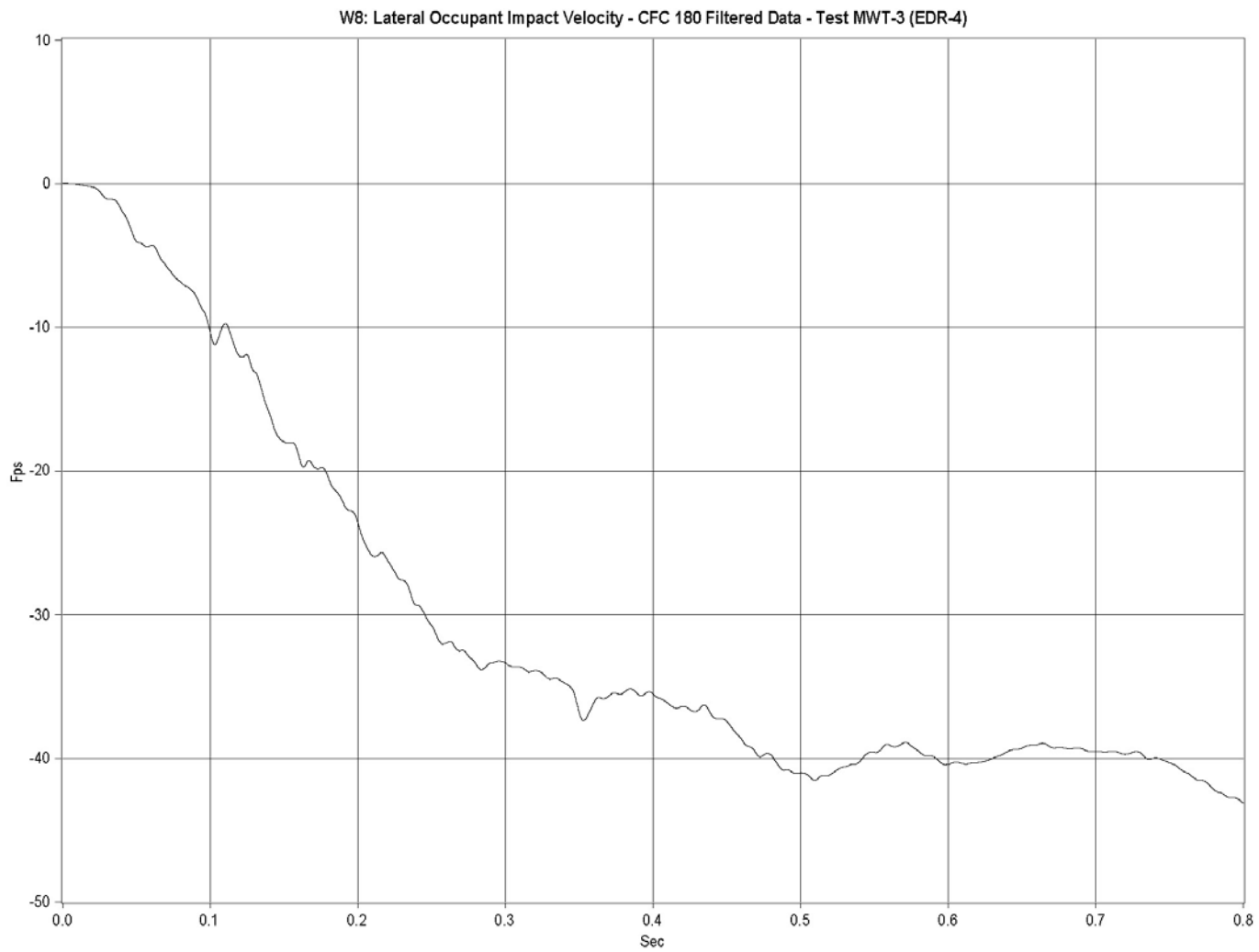


Figure D-5. Graph of Lateral Occupant Impact Velocity, Test MWT-3

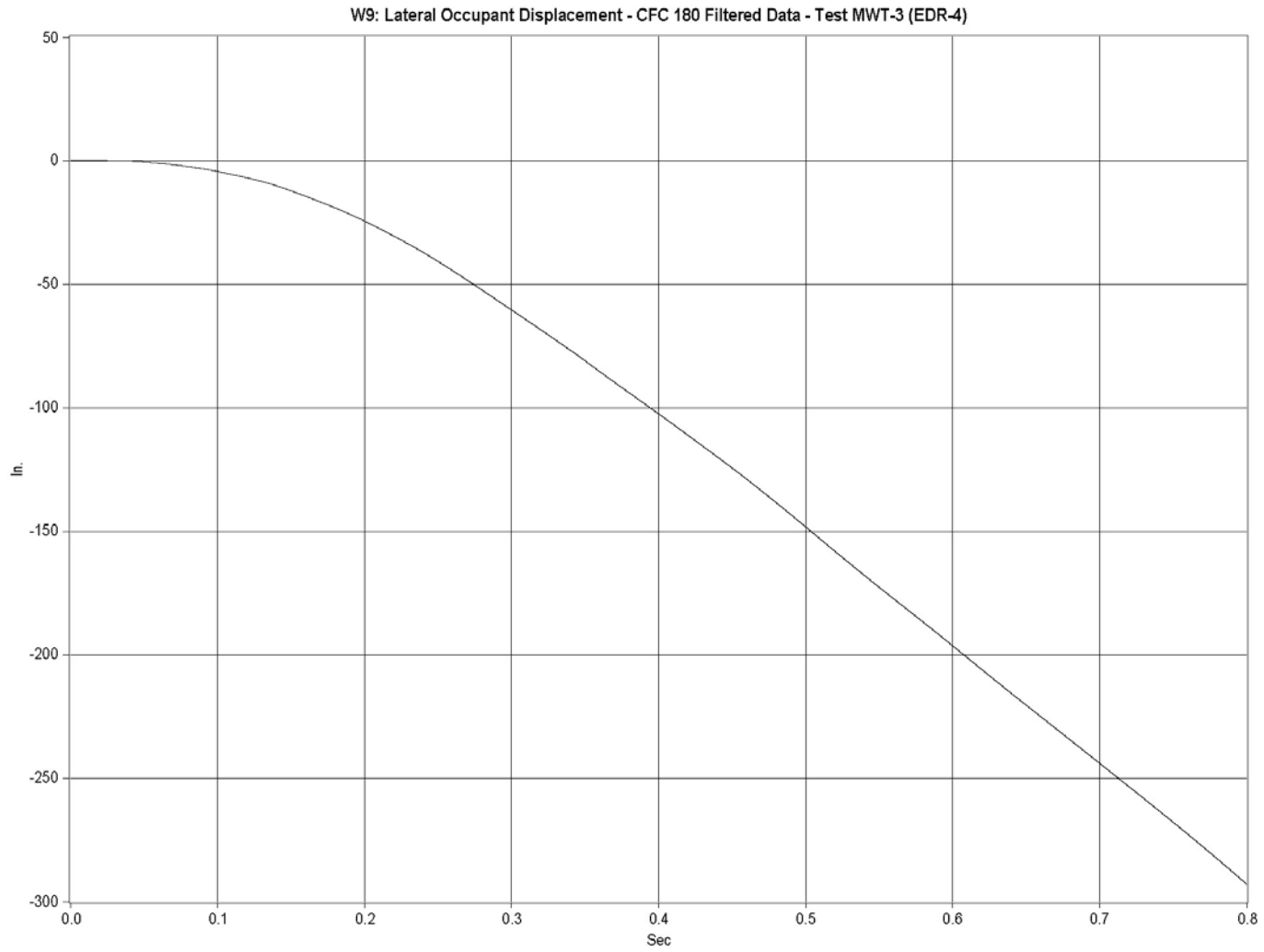


Figure D-6. Graph of Lateral Occupant Displacement, Test MWT-3

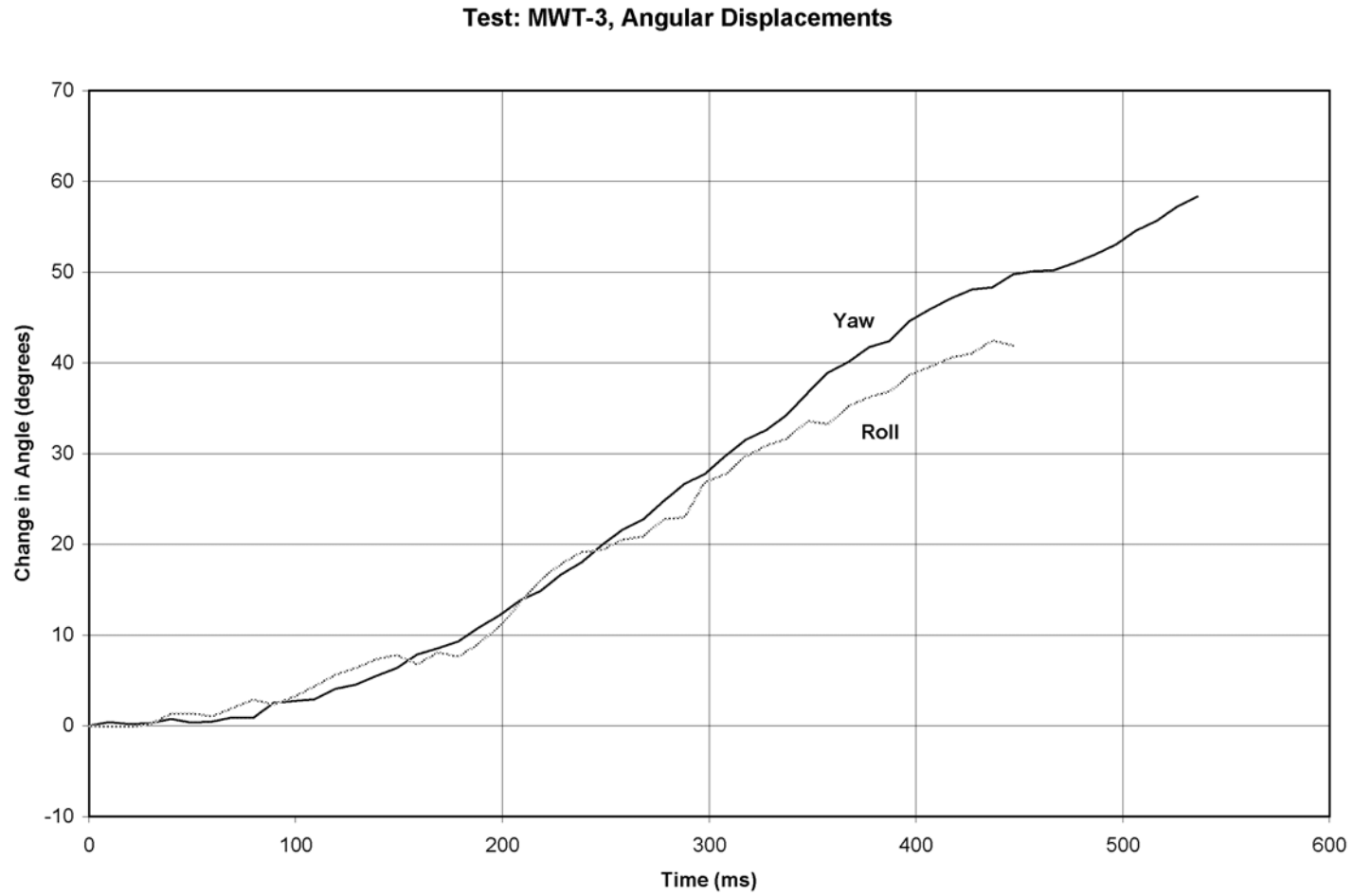


Figure D-7. Graph of Roll and Yaw Angular Displacements, Test MWT-3

APPENDIX E

English-Unit Design Details, Design No. 2

Figure E-1. Layout, Design No. 2 (English)

Figure E-2. Layout and Design Details, Design No. 2 (English)

Figure E-3. Cap Rail and Post No. 18 Details- Design No. 2 (English)

Figure E-4. Post Nos. 16 and 17 Details- Design No. 2 (English)

Figure E-5. Post Nos. 12 through 15 Details, Design No. 2 (English)

Figure E-6. Post Nos. 3 through 11 Details, Design No. 2 (English)

Figure E-7. Channel Bridge Rail Design Details, Design No. 2 (English)

Figure E-8. Channel Bridge Rail Design Details, Design No. 2 (English)

Figure E-9. Rail and End BCT Details, Design No. 2 (English)

Figure E-10. BCT Post and Tube Details, Design No. 2 (English)

Figure E-11. Cable Strut and Anchor Bracket Details, Design No. 2 (English)

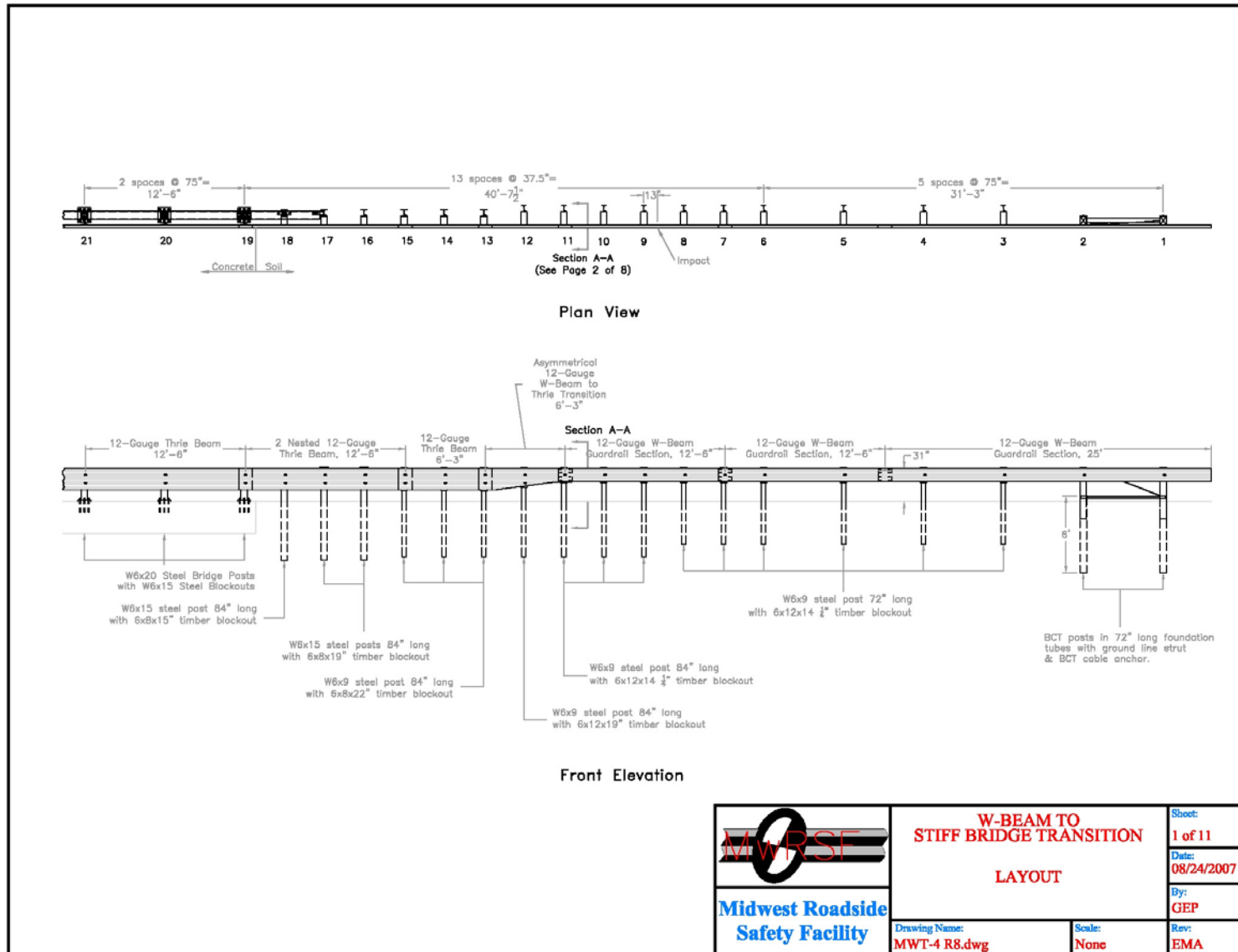


Figure E-1. Layout, Design No. 2 (English)

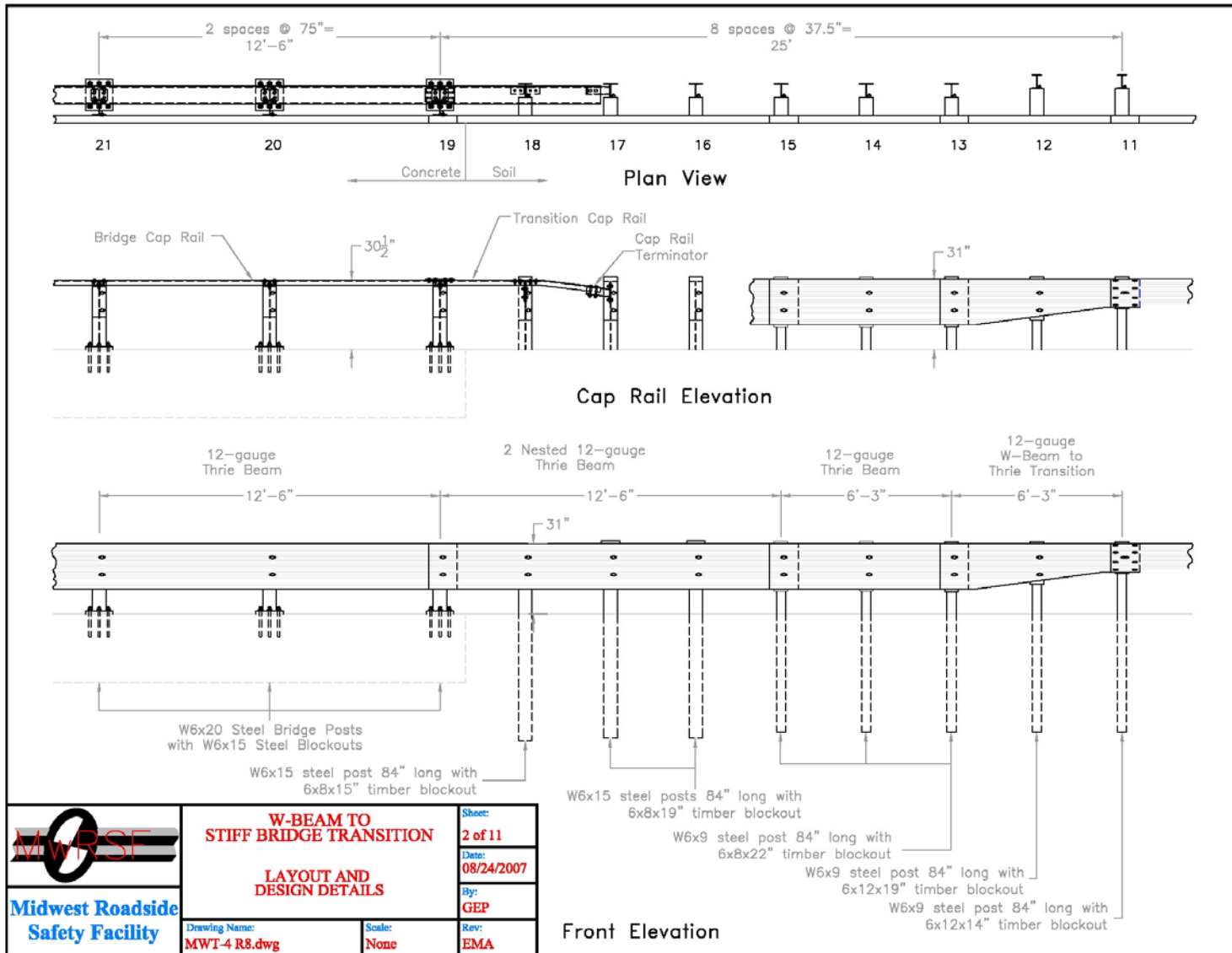


Figure E-2. Layout and Design Details, Design No. 2 (English)

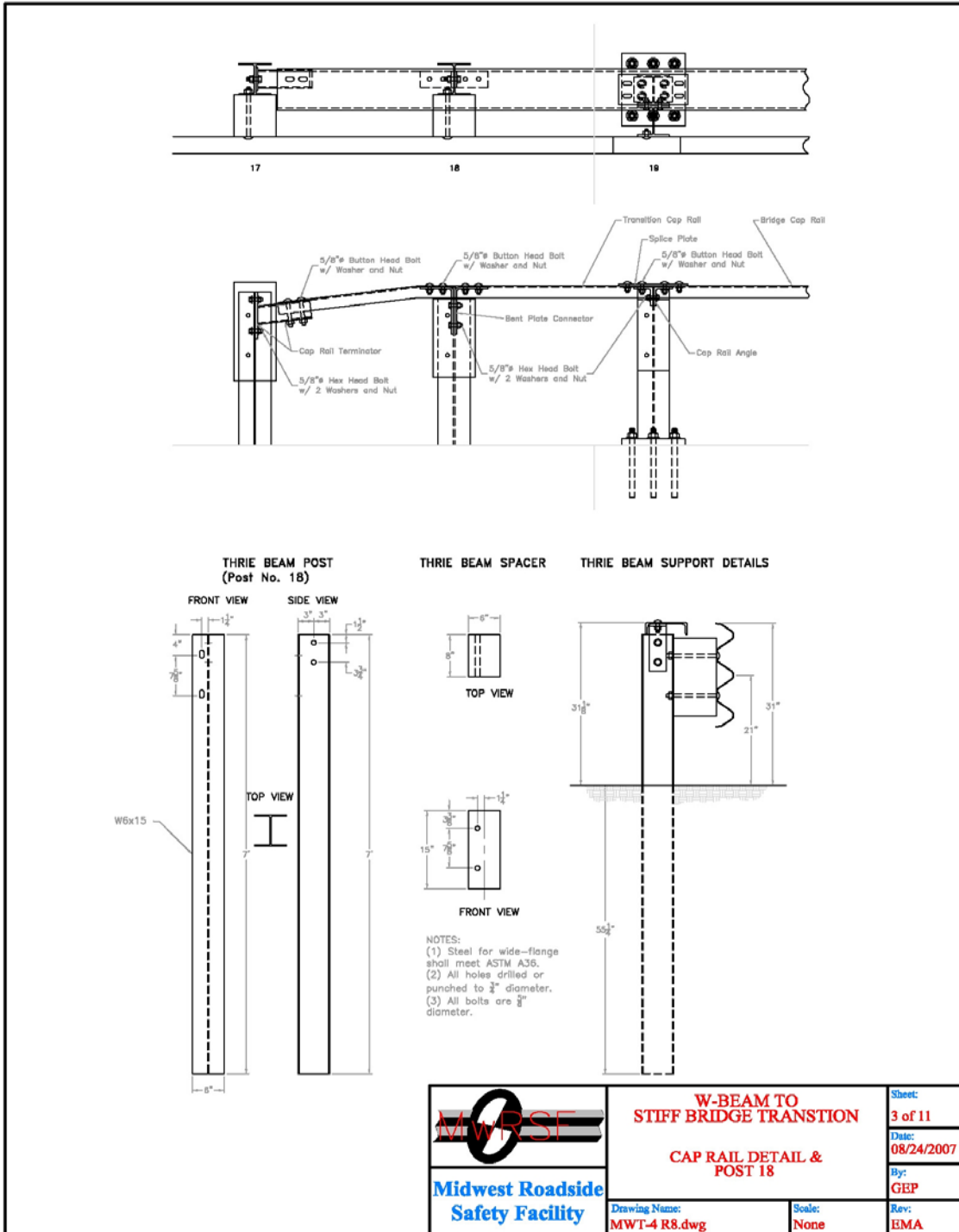


Figure E-3. Cap Rail and Post No. 18 Details- Design No. 2 (English)

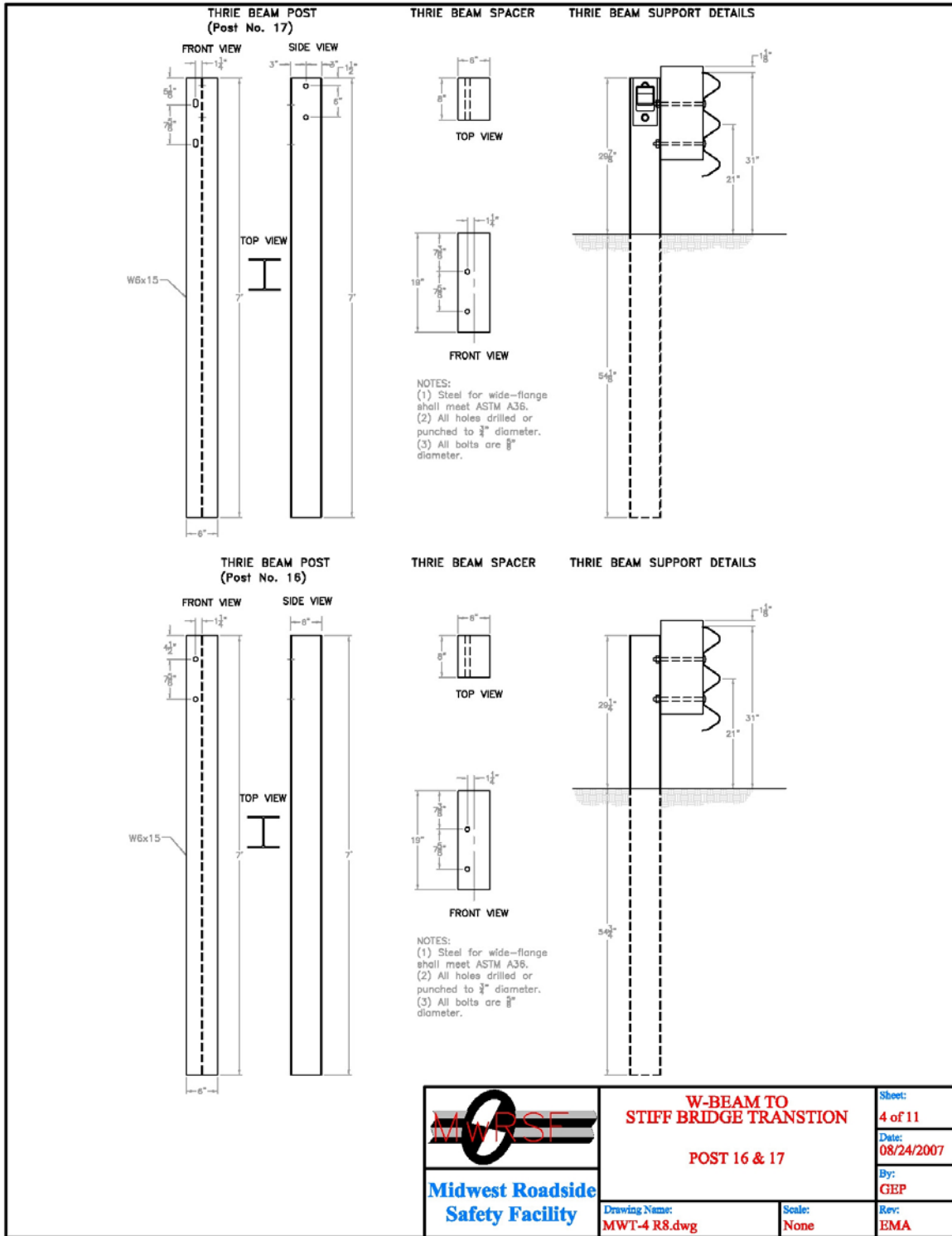


Figure E-4. Post Nos. 16 and 17 Details- Design No. 2 (English)

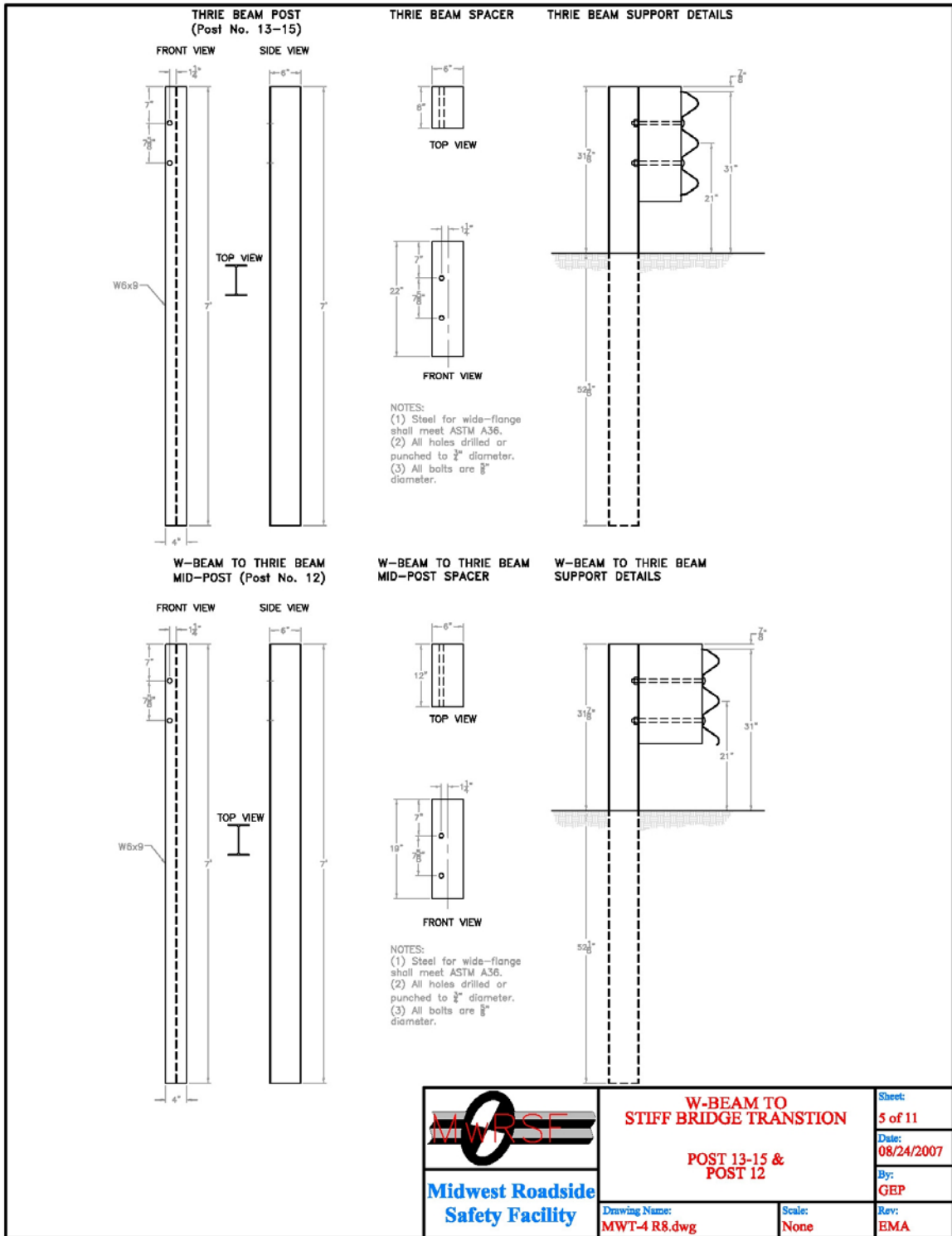


Figure E-5. Post Nos. 12 through 15 Details, Design No. 2 (English)

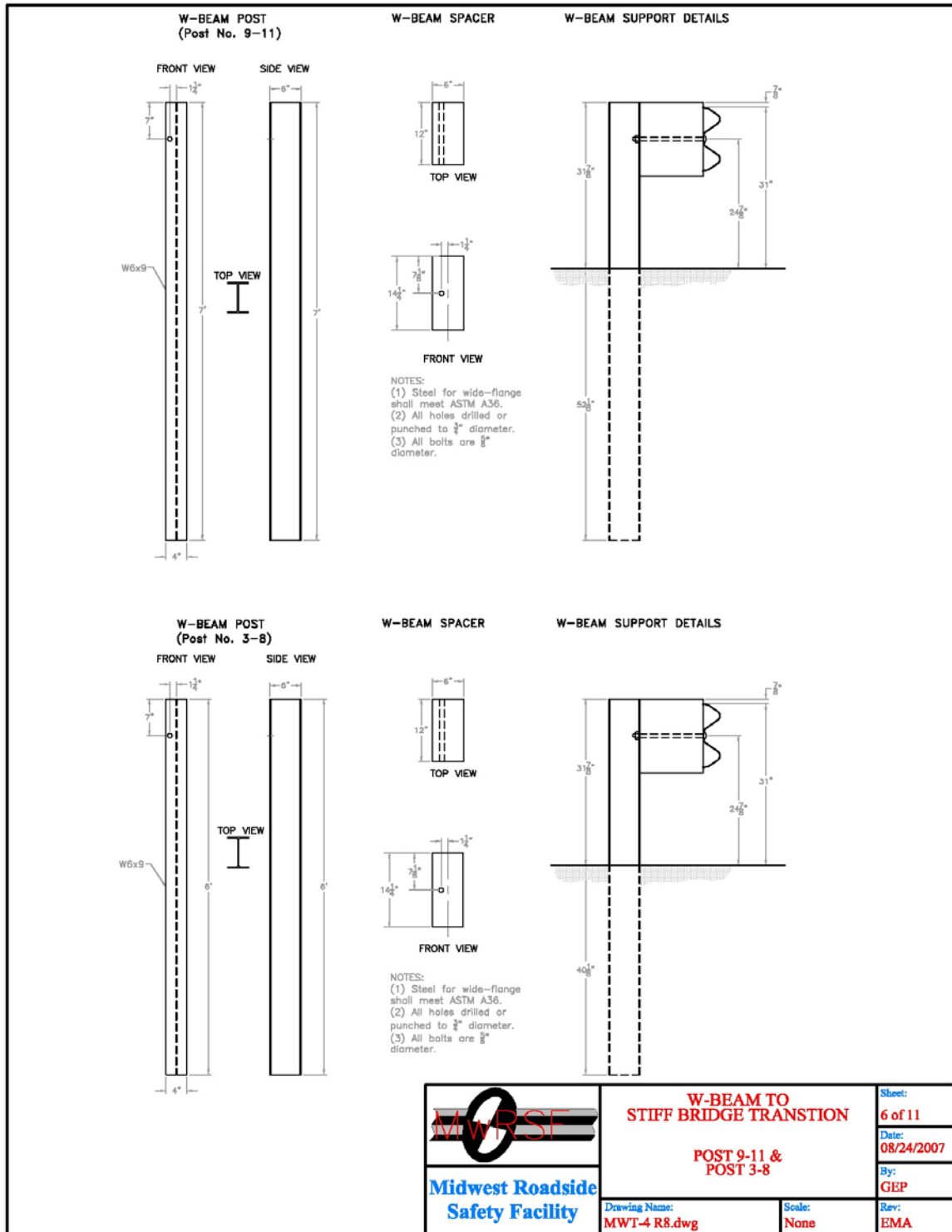


Figure E-6. Post Nos. 3 through 11 Details, Design No. 2 (English)

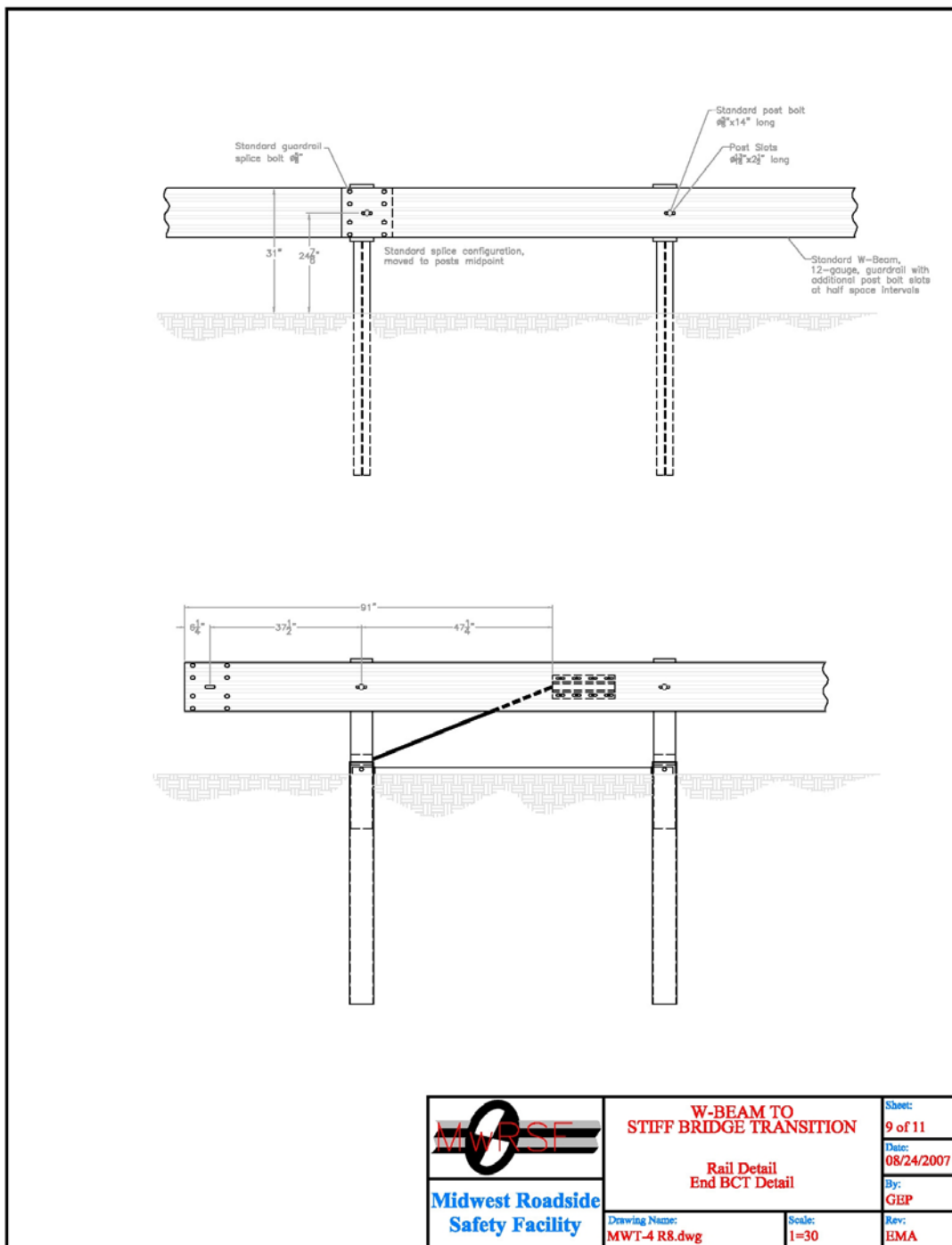


Figure E-9. Rail and End BCT Details, Design No. 2 (English)

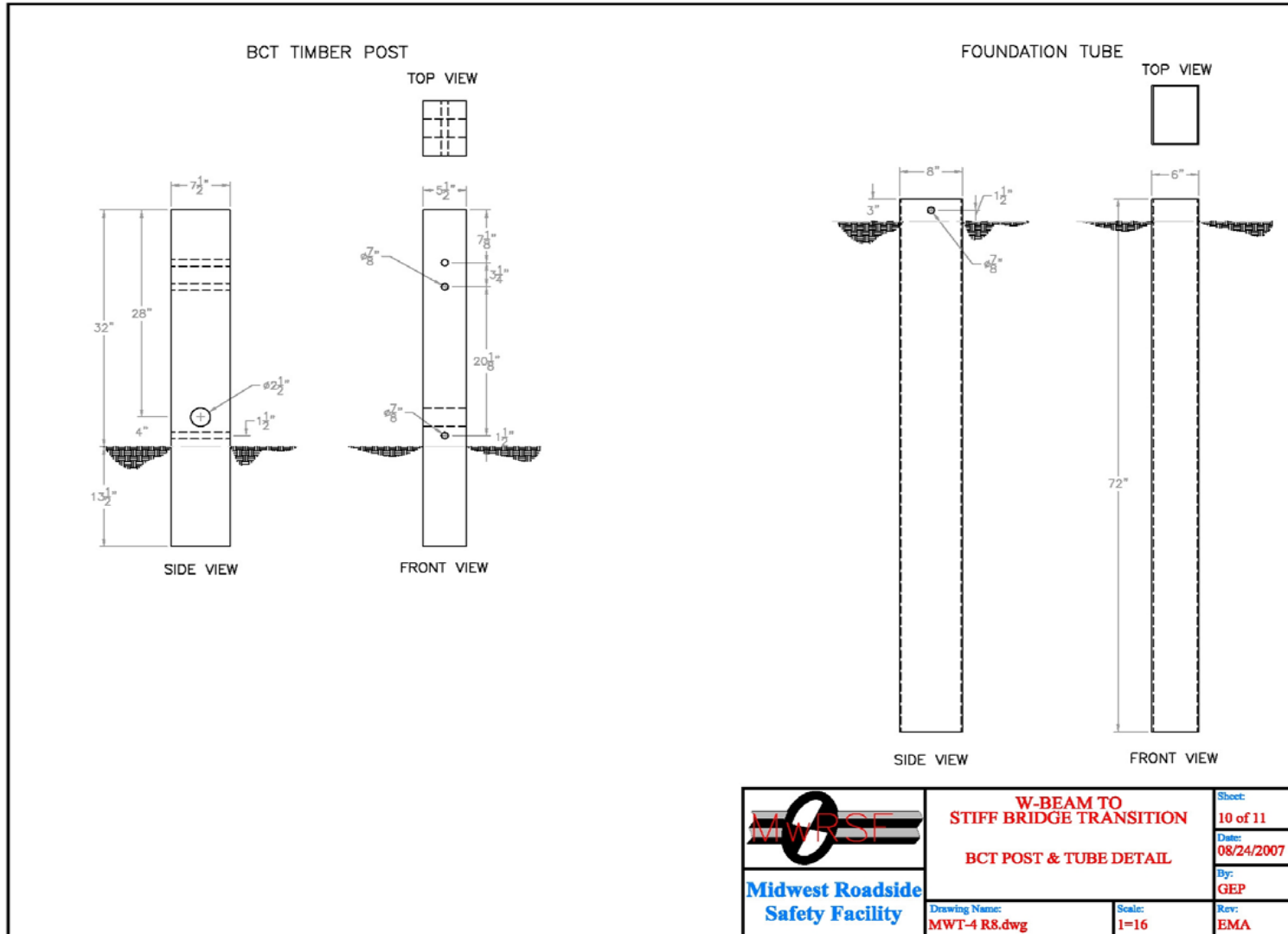


Figure E-10. BCT Post and Tube Details, Design No. 2 (English)

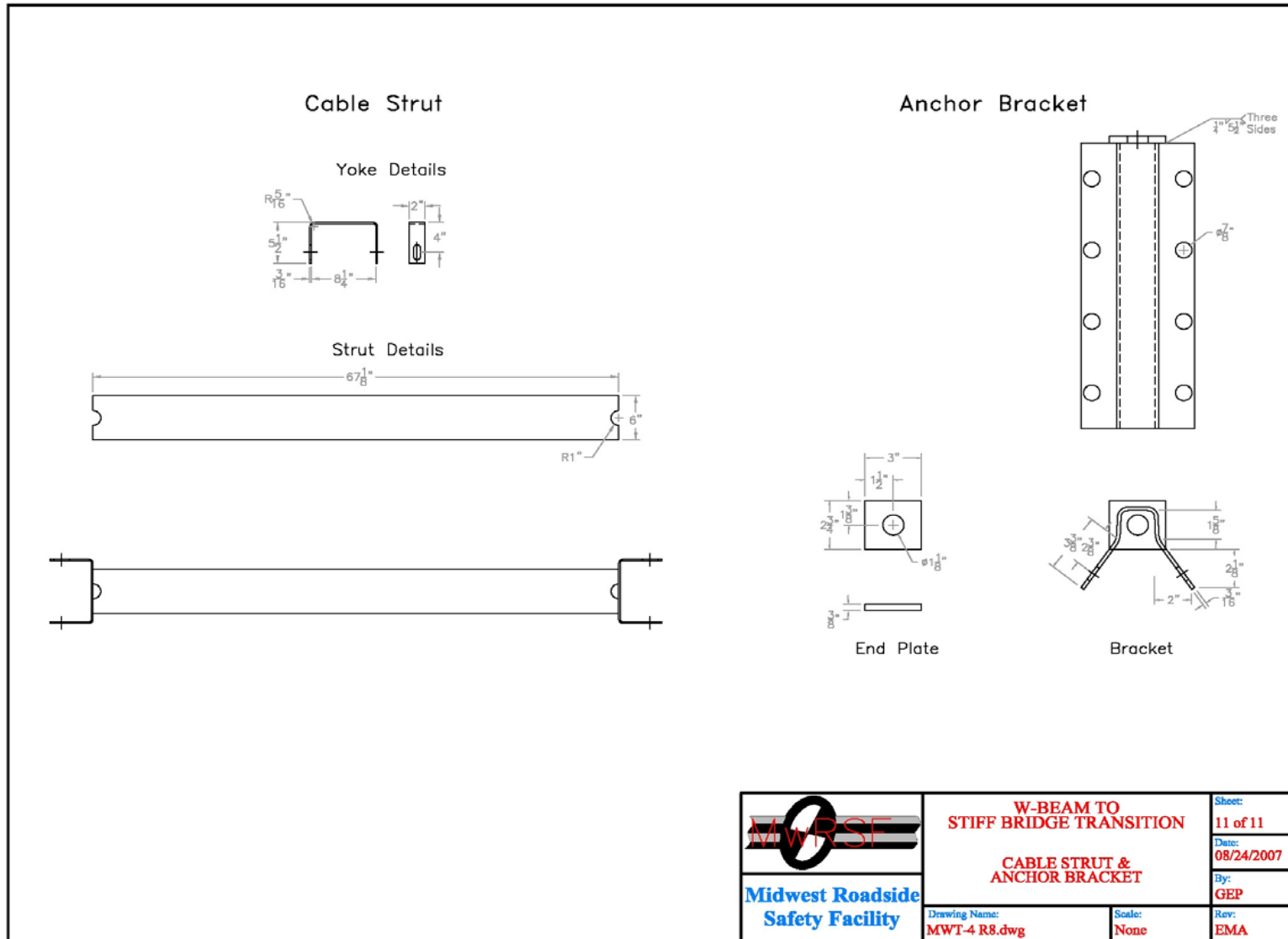


Figure E-11. Cable Strut and Anchor Bracket Details, Design No. 2 (English)

APPENDIX F

Accelerometer and Rate Transducer Data Analysis, Test MWT-4

Figure F-1. Graph of Longitudinal Deceleration, Test MWT-4

Figure F-2. Graph of Longitudinal Occupant Impact Velocity, Test MWT-4

Figure F-3. Graph of Longitudinal Occupant Displacement, Test MWT-4

Figure F-4. Graph of Lateral Deceleration, Test MWT-4

Figure F-5. Graph of Lateral Occupant Impact Velocity, Test MWT-4

Figure F-6. Graph of Lateral Occupant Displacement, Test MWT-4

Figure F-7. Graph of Roll, Pitch and Yaw Angular Displacements, Test MWT-4

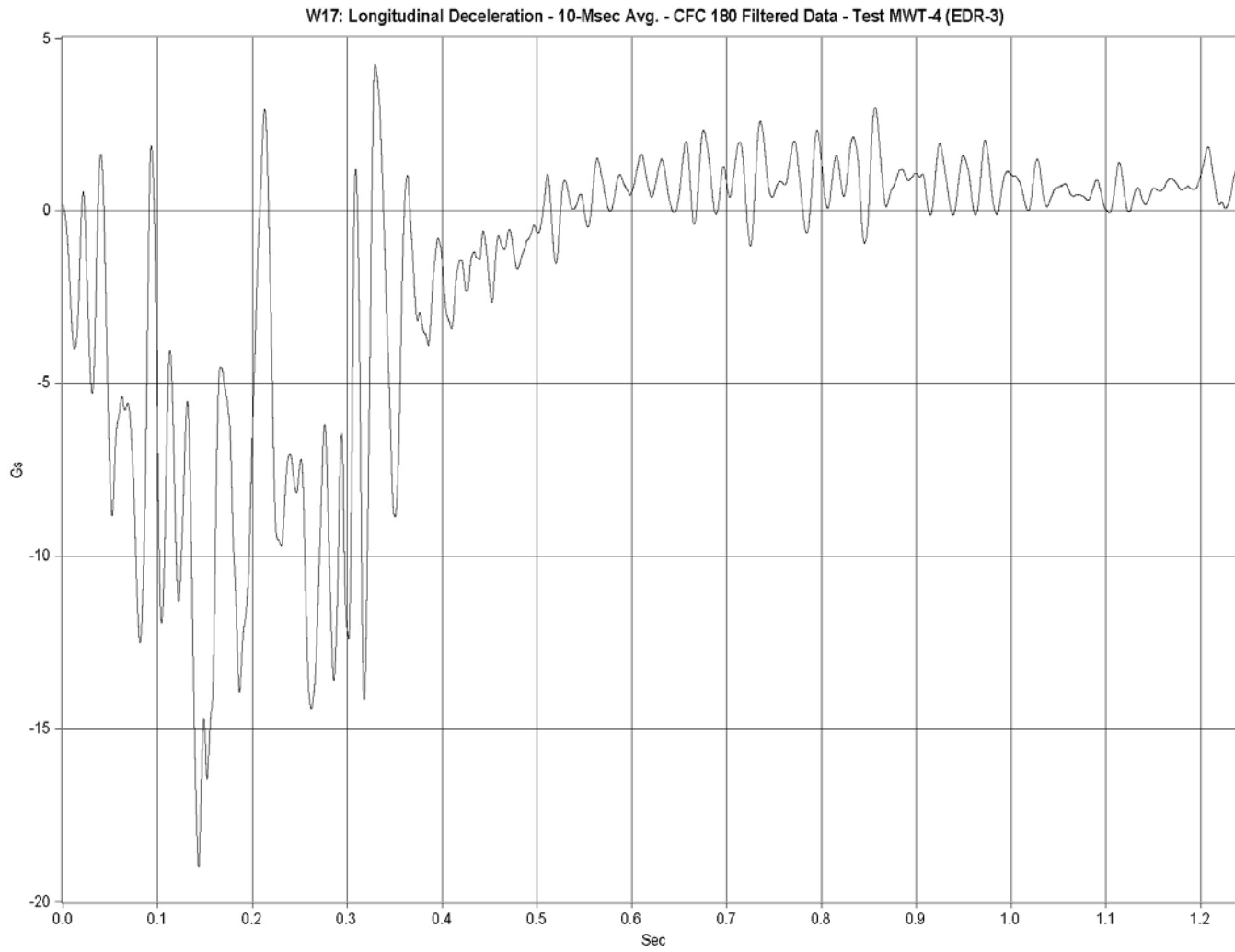


Figure F-1. Graph of Longitudinal Deceleration, Test MWT-4

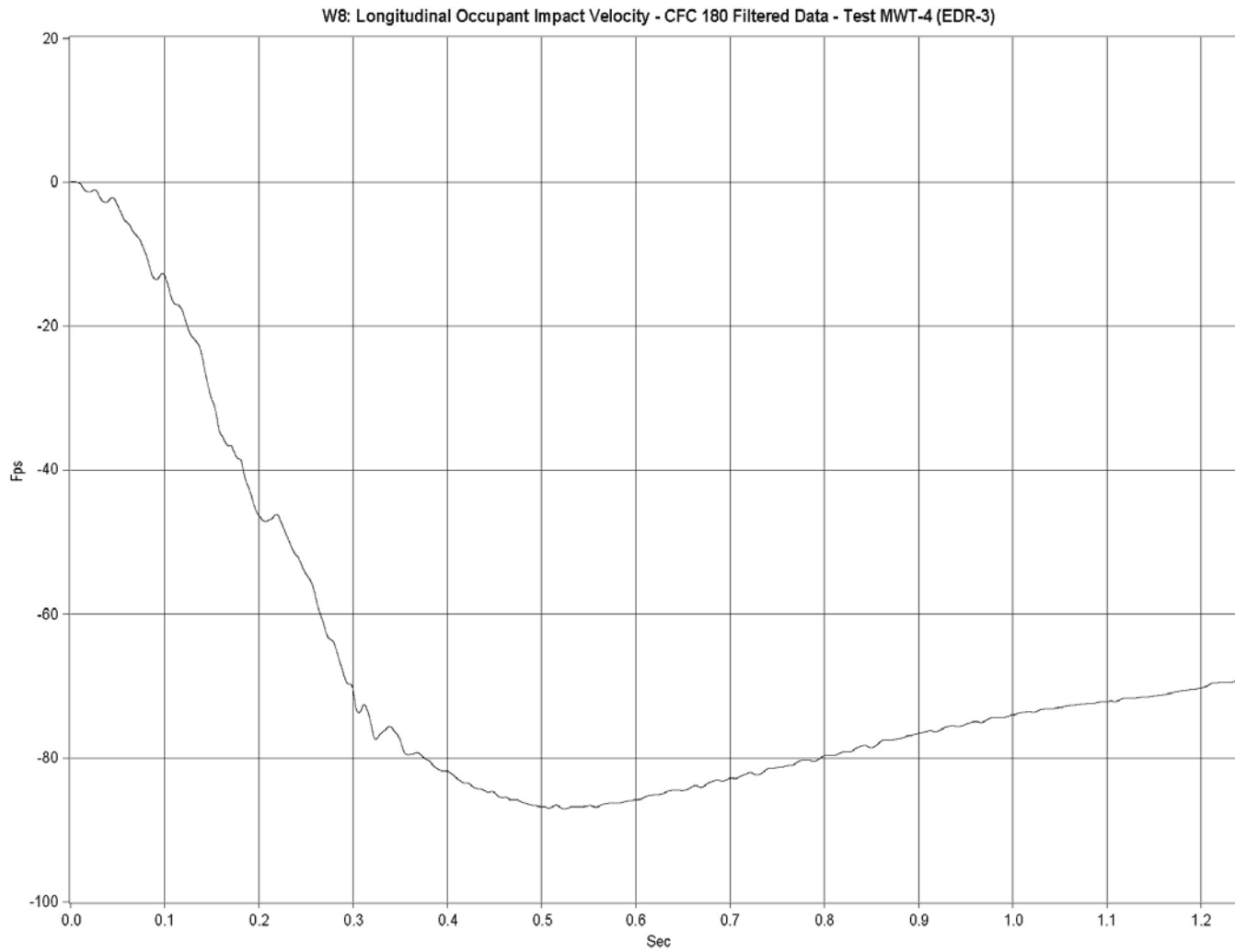


Figure F-2. Graph of Longitudinal Occupant Impact Velocity, Test MWT-4

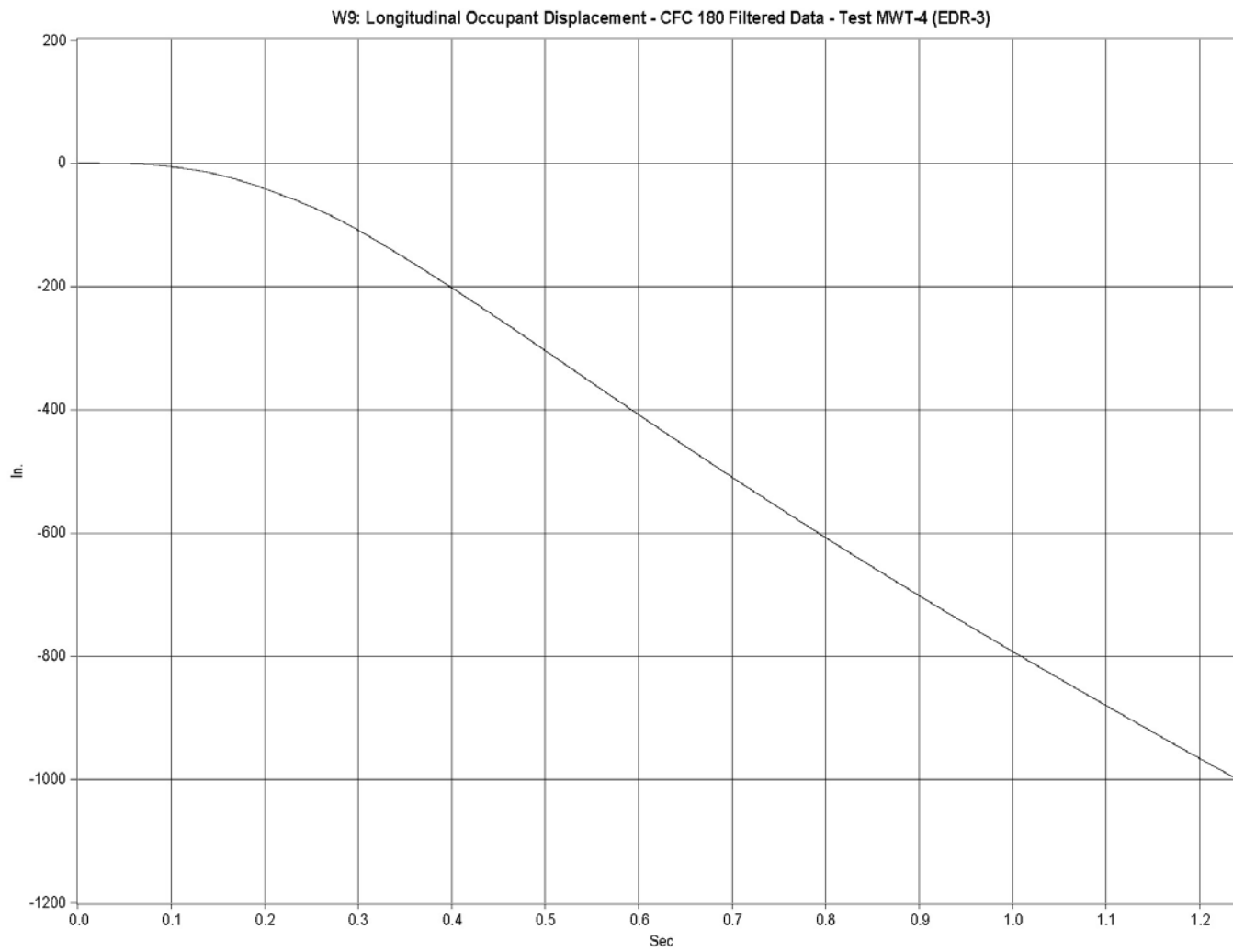


Figure F-3. Graph of Longitudinal Occupant Displacement, Test MWT-4

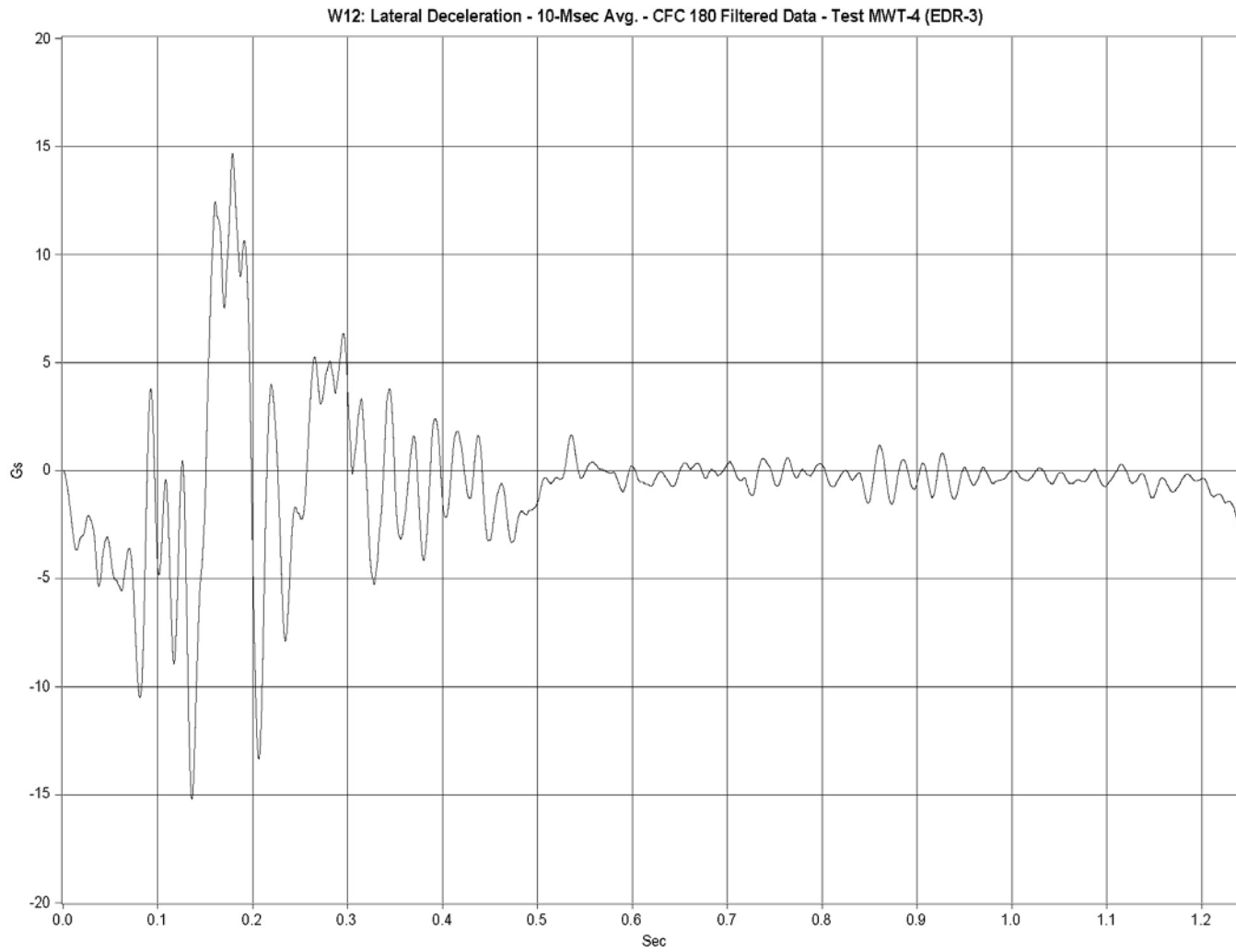


Figure F-4. Graph of Lateral Deceleration, Test MWT-4

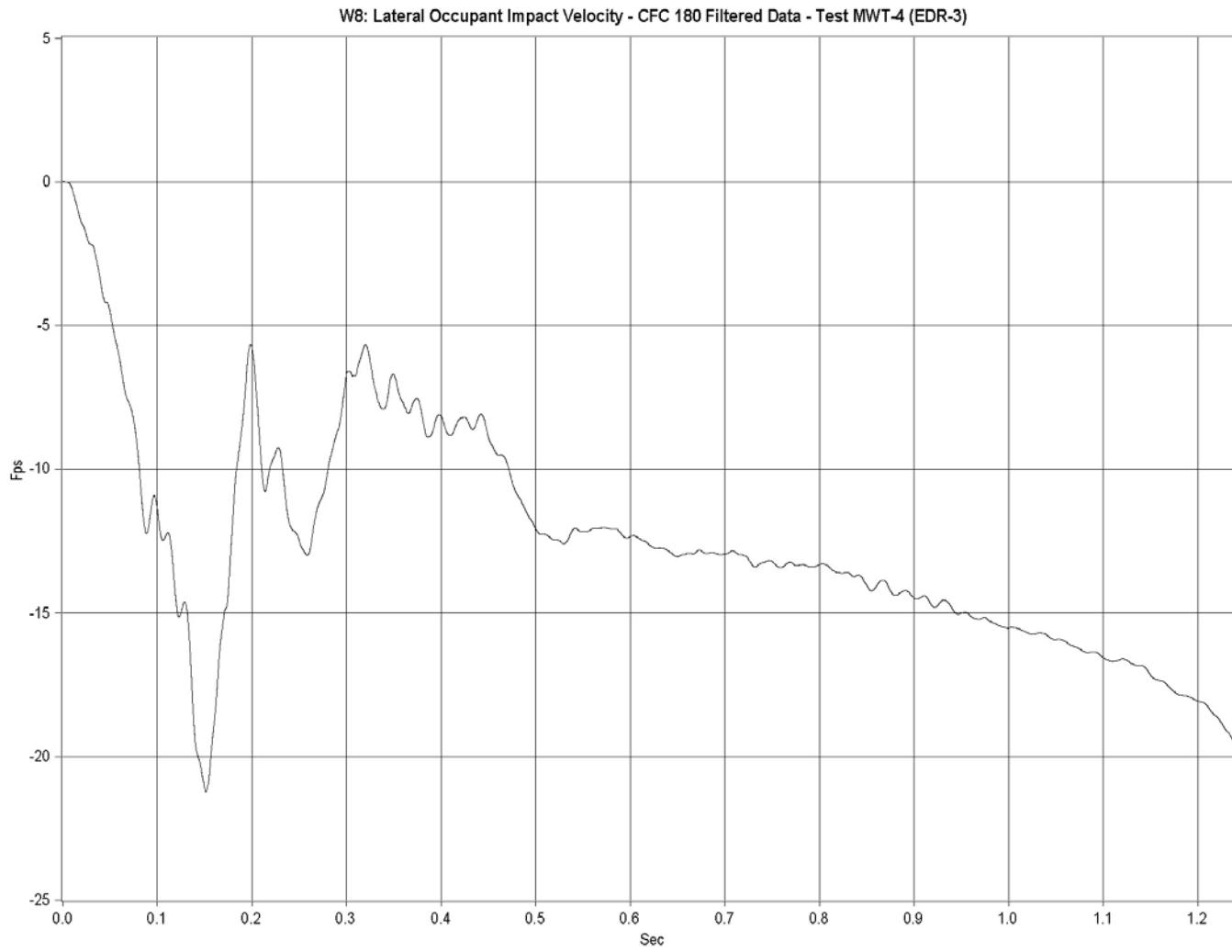


Figure F-5. Graph of Lateral Occupant Impact Velocity, Test MWT-4

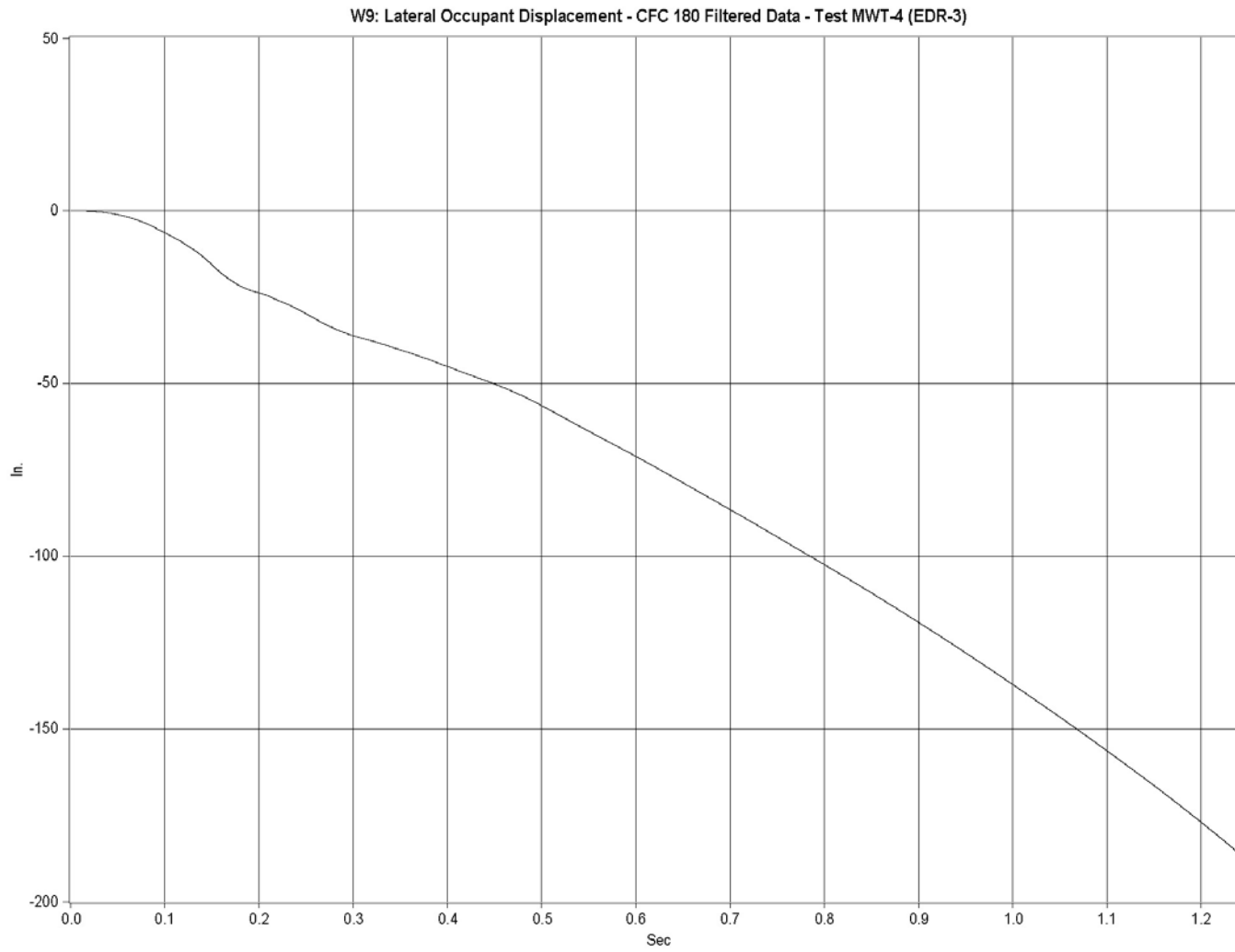


Figure F-6. Graph of Lateral Occupant Displacement, Test MWT-4

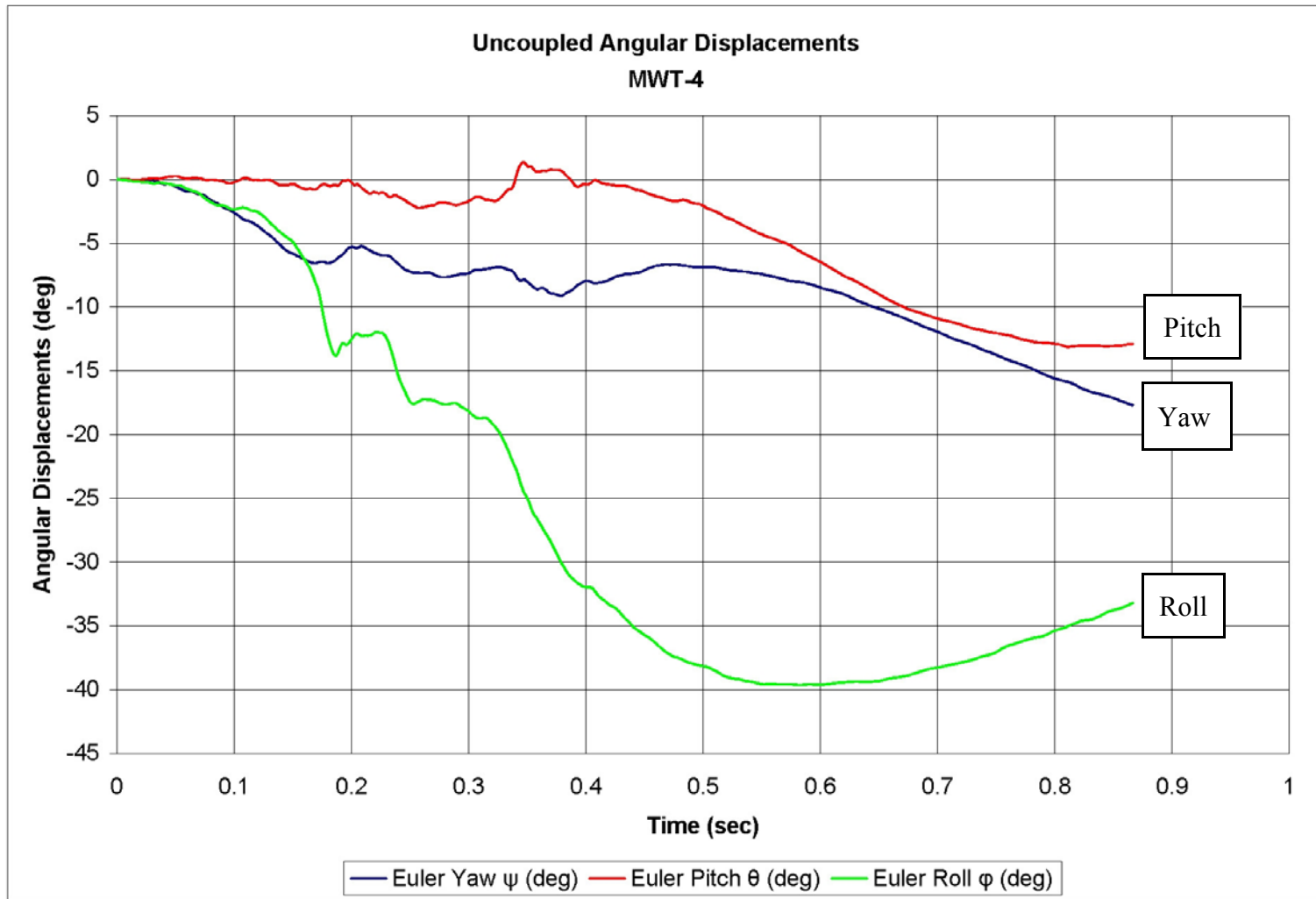


Figure F-7. Graph of Roll, Pitch and Yaw Angular Displacements, Test MWT-4

APPENDIX G

BARRIER VII Computer Model

Figure G-1. Model of the MGS W-Beam to Thrie Beam Transition

Note that the example BARRIER VII input data file corresponds with the impact point for Test MWT-5.

MWT (10 gauge W-Beam to Thrie Beam Transition) - MWT5-2a.b7

89	21	20	1	109	35	2	0			
0.0001		0.0001		0.750	3000		0	1.0	1	
10	50	50	50	50	500	10				
1		0.00		0.0						
5		75.00		0.0						
9		150.00		0.0						
13		225.00		0.0						
17		300.00		0.0						
21		375.00		0.0						
25		450.00		0.0						
29		487.50		0.0						
33		525.00		0.0						
37		562.50		0.0						
41		600.00		0.0						
45		637.50		0.0						
49		675.00		0.0						
53		712.50		0.0						
57		750.00		0.0						
61		787.50		0.0						
65		825.00		0.0						
69		862.50		0.0						
73		900.00		0.0						
81		975.00		0.0						
89		1050.00		0.0						
1	5	3	1				0.0			
5	9	3	1				0.0			
9	13	3	1				0.0			
13	17	3	1				0.0			
17	21	3	1				0.0			
21	25	3	1				0.0			
25	29	3	1				0.0			
29	33	3	1				0.0			
33	37	3	1				0.0			
37	41	3	1				0.0			
41	45	3	1				0.0			
45	49	3	1				0.0			
49	53	3	1				0.0			
53	57	3	1				0.0			
57	61	3	1				0.0			
61	65	3	1				0.0			
65	69	3	1				0.0			
69	73	3	1				0.0			
73	81	7	1				0.0			
81	89	7	1				0.0			
1	89		0.45							
89	88	87	86	85	84	83	82	81	80	
79	78	77	76	75	74	73	72	71	70	
69	68	67	66	65	64	63	62	61	60	
59	58	57	56	55	54	53	52	51	50	
49	48	47	46	45	44	43	42	41	40	
39	38	37	36	35	34	33	32	31	30	
29	28	27	26	25	24	23	22	21	20	
19	18	17	16	15	14	13	12	11	10	
9	8	7	6	5	4	3	2	1		
100	12									
1		2.29		1.99		18.75		30000.0	6.92	99.5
68.5	0.05	12-GAUGE	W-BEAM							
2		2.29		1.99		9.375		30000.0	6.92	99.5
68.5	0.05	12-GAUGE	W-BEAM							

3	3.114	2.650	9.375	30000.0	9.216	132.5
91.25	0.05	10-GAUGE W-BEAM TO THRIE BEAM				
4	3.341	2.830	9.375	30000.0	9.847	141.5
97.75	0.05	10-GAUGE W-BEAM TO THRIE BEAM				
5	3.569	3.010	9.375	30000.0	10.478	150.5
104.25	0.05	10-GAUGE W-BEAM TO THRIE BEAM				
6	3.796	3.190	9.375	30000.0	11.109	159.5
110.75	0.05	10-GAUGE W-BEAM TO THRIE BEAM				
7	4.024	3.370	9.375	30000.0	11.741	168.5
117.25	0.05	10-GAUGE W-BEAM TO THRIE BEAM				
8	4.251	3.550	9.375	30000.0	12.372	177.5
123.75	0.05	10-GAUGE W-BEAM TO THRIE BEAM				
9	4.479	3.730	9.375	30000.0	13.003	186.5
130.25	0.05	10-GAUGE W-BEAM TO THRIE BEAM				
10	4.706	3.910	9.375	30000.0	13.634	195.5
136.75	0.05	10-GAUGE W-BEAM TO THRIE BEAM				
11	3.76	3.10	9.375	30000.0	10.81	155.0
109.5	0.05	12-GAUGE THRIE BEAM				
12	7.52	6.20	9.375	30000.0	21.62	310.0
219.0	0.05	12-GAUGE NESTED THRIE BEAM				
300	9					
1	24.875	0.00	6.0	6.0	100.0	675.0
675.0	0.05	Simulated Strong Anchor Post				
100.0	100.0	15.0	15.0			
2	24.875	0.00	3.0	3.0	100.0	150.0
225.00	0.05	Second BCT Post				
50.0	50.0	15.0	15.0			
3	24.875	0.0	4.00	6.03	54.0	92.88
143.65	0.05	W6x9 BY 6-FT LONG STEEL POST (40.125" EMBEDMENT DEPTH)				
6.0	15.0	14.0	14.0			
4	24.875	0.0	4.00	6.03	63.0	108.84
303.025	0.05	W6x9 BY 7-FT LONG STEEL POST (52.125" EMBEDMENT DEPTH)				
6.0	18.75	14.0	14.0			
5	21.0	0.0	4.00	6.03	63.0	108.84
303.025	0.05	W6x9 BY 7-FT LONG STEEL POST (52.125" EMBEDMENT DEPTH)				
6.0	18.75	14.0	14.0			
6	21.0	0.0	4.00	6.03	63.0	108.84
303.025	0.05	W6x9 BY 7-FT LONG STEEL POST (52.125" EMBEDMENT DEPTH)				
6.0	18.75	14.0	14.0			
7	21.0	0.0	5.64	8.00	105.0	320.63
651.69	0.05	W6x15 BY 7-FT LONG STEEL POST (54.125" EMBEDMENT DEPTH)				
15.0	35.0	12.0	12.0			
8	21.0	0.0	5.64	8.00	105.0	320.63
645.12	0.05	W6x15 BY 7-FT LONG STEEL POST (55.25" EMBEDMENT DEPTH)				
15.0	35.0	12.0	12.0			
9	21.0	0.0	129.0	200.0	612.5	362.90
804.60	0.05	W6x20 STEEL BRIDGE POST				
20.0	45.0	2.0	2.0			
1	1	2	4	1	101	0.0
5	5	6	8	1	101	0.0
9	9	10	12	1	101	0.0
13	13	14	16	1	101	0.0
17	17	18	20	1	101	0.0
21	21	22	24	1	101	0.0
25	25	26	28	1	102	0.0
29	29	30	32	1	102	0.0
33	33	34	36	1	102	0.0
37	37	38	40	1	102	0.0
41	41	42		1	103	0.0
42	42	43		1	104	0.0

43	43	44		1	105	0.0	0.0	0.0	
44	44	45		1	106	0.0	0.0	0.0	
45	45	46		1	107	0.0	0.0	0.0	
46	46	47		1	108	0.0	0.0	0.0	
47	47	48		1	109	0.0	0.0	0.0	
48	48	49		1	110	0.0	0.0	0.0	
49	49	50	52	1	111	0.0	0.0	0.0	
53	53	54	56	1	111	0.0	0.0	0.0	
57	57	58	60	1	112	0.0	0.0	0.0	
61	61	62	64	1	112	0.0	0.0	0.0	
65	65	66	68	1	112	0.0	0.0	0.0	
69	69	70	72	1	112	0.0	0.0	0.0	
73	73	74	80	1	111	0.0	0.0	0.0	
81	81	82	88	1	111	0.0	0.0	0.0	
89	1				301	0.0	0.0	0.0	0.0
0.0									
90	5				302	0.0	0.0	0.0	0.0
0.0									
91	9	96	4	303	0.0	0.0	0.0	0.0	0.0
0.0									
97	33	99	4	304	0.0	0.0	0.0	0.0	0.0
0.0									
100	45			305	0.0	0.0	0.0	0.0	0.0
0.0									
101	49	103	4	306	0.0	0.0	0.0	0.0	0.0
0.0									
104	61	105	4	307	0.0	0.0	0.0	0.0	0.0
0.0									
106	69			308	0.0	0.0	0.0	0.0	0.0
0.0									
107	73	109	8	309	0.0	0.0	0.0	0.0	0.0
0.0									
4409.25	47400.0	20	6	4	0	1			
1	0.055	0.12	6.00	17.0					
2	0.057	0.15	7.00	18.0					
3	0.062	0.18	10.00	12.0					
4	0.110	0.35	12.00	6.0					
5	0.35	0.45	6.00	5.0					
6	1.45	1.50	15.00	1.0					
1	100.75	15.875	1	12.0	1	1	0	0	
2	100.75	27.875	1	12.0	1	1	0	0	
3	100.75	39.875	2	12.0	1	1	0	0	
4	88.75	39.875	2	12.0	1	1	0	0	
5	76.75	39.875	2	12.0	1	1	0	0	
6	64.75	39.875	2	12.0	1	1	0	0	
7	52.75	39.875	2	12.0	1	1	0	0	
8	40.75	39.875	2	12.0	1	1	0	0	
9	28.75	39.875	2	12.0	1	1	0	0	
10	16.75	39.875	2	12.0	1	1	0	0	
11	-13.25	39.875	3	12.0	1	1	0	0	
12	-33.25	39.875	3	12.0	1	1	0	0	
13	-53.25	39.875	3	12.0	1	1	0	0	
14	-73.25	39.875	3	12.0	1	1	0	0	
15	-93.25	39.875	3	12.0	1	1	0	0	
16	-113.25	39.875	4	12.0	1	1	0	0	
17	-113.25	-39.875	4	12.0	0	0	0	0	
18	100.75	-39.875	1	12.0	0	0	0	0	
19	69.25	37.75	5	1.0	1	1	0	0	
20	-62.75	37.75	6	1.0	1	1	0	0	
1	69.25	32.75	0.0	608.					

2	69.25	-32.75	0.0	608.		
3	-62.75	32.75	0.0	492.		
4	-62.75	-32.75	0.0	492.		
1	0.00	0.00				
3	512.000	0.0	25.0	62.14	0.0	0.0

1.0

APPENDIX H

English-Unit Design Details, Design No. 3

Figure H-1. Layout, Design No. 3 (English)

Figure H-2. Layout and Design Details, Design No. 3 (English)

Figure H-3. Asymmetrical W-Beam to Thrie Beam Transition Rail Detail, Design No. 3 (English)

Figure H-4. Cap Rail and Post No. 18 Details- Design No. 3 (English)

Figure H-5. Post Nos. 16 and 17 Details, Design No. 3 (English)

Figure H-6. Post Nos. 12 through 15 Details, Design No. 3 (English)

Figure H-7. Post Nos. 3 through 11, Design No. 3 (English)

Figure H-8. Channel Bridge Rail Design Details, Design No. 3 (English)

Figure H-9. Channel Bridge Rail Design Details (Continued), Design No. 3 (English)

Figure H-10. Rail and End BCT Details, Design No. 3 (English)

Figure H-11. BCT Post and Tube Details, Design No. 3 (English)

Figure H-12. Cable Strut and Anchor Bracket Details, Design No. 3 (English)

Figure H-13. Anchor Cable Details, Design No. 3 (English)

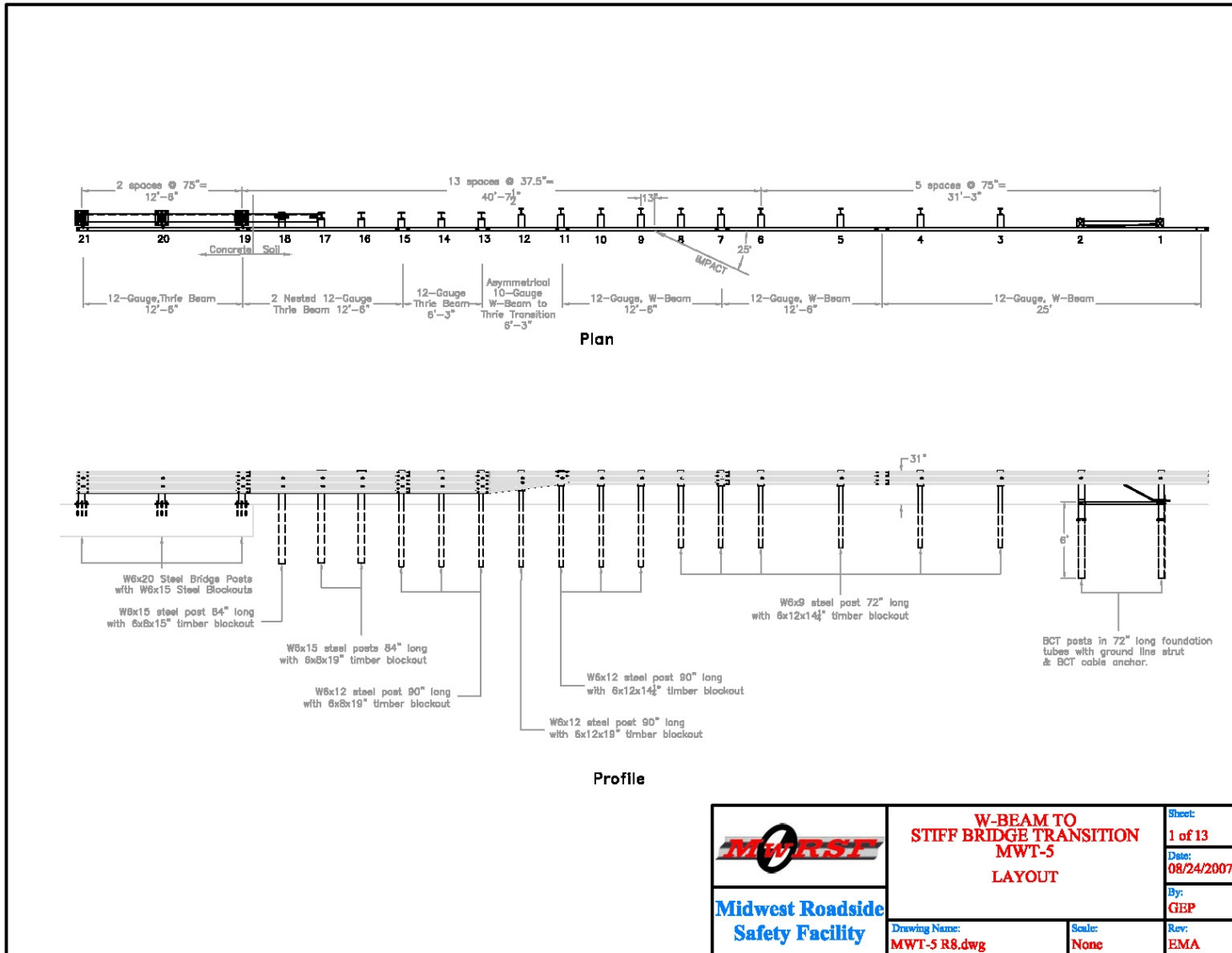


Figure H-1. Layout, Design No. 3 (English)

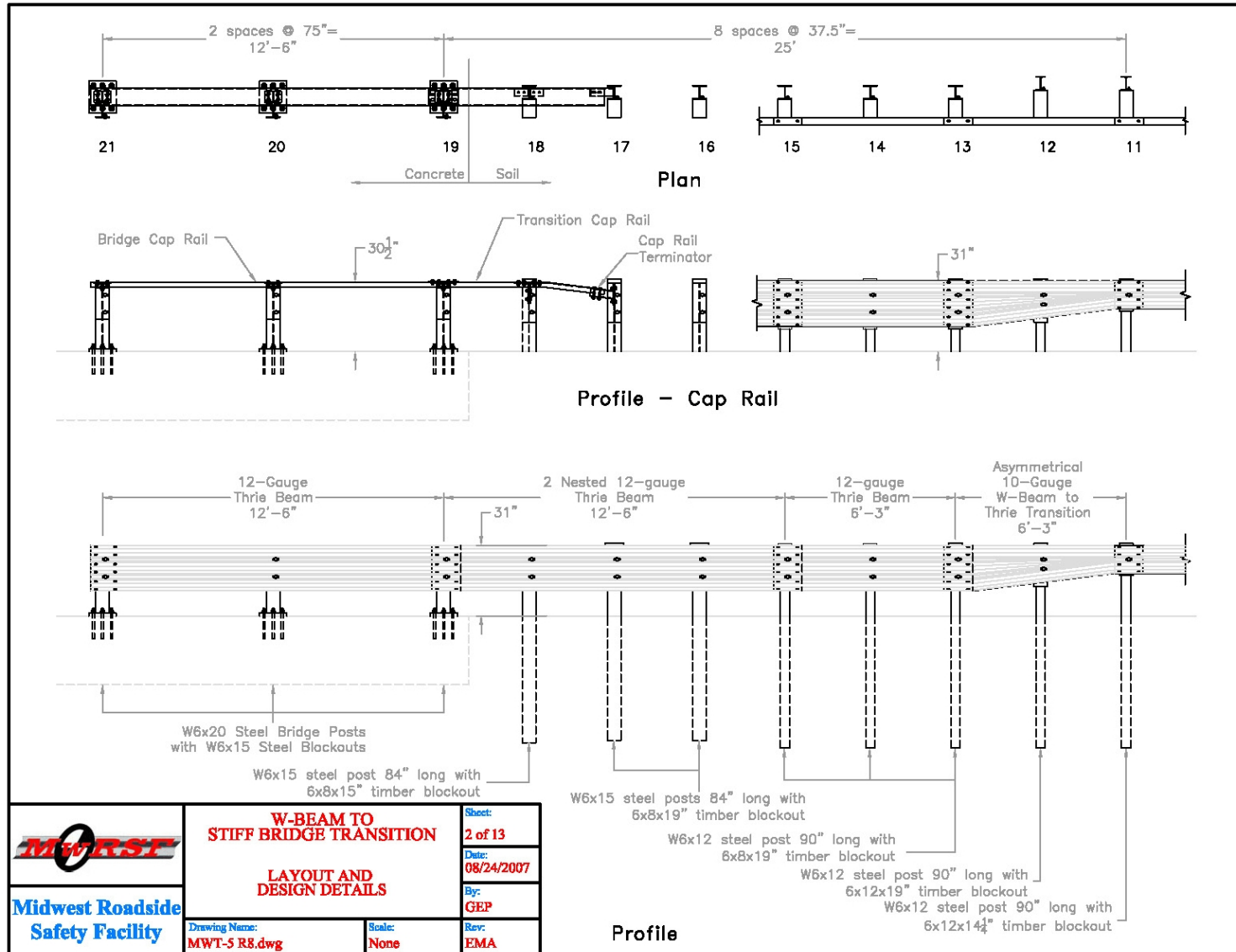
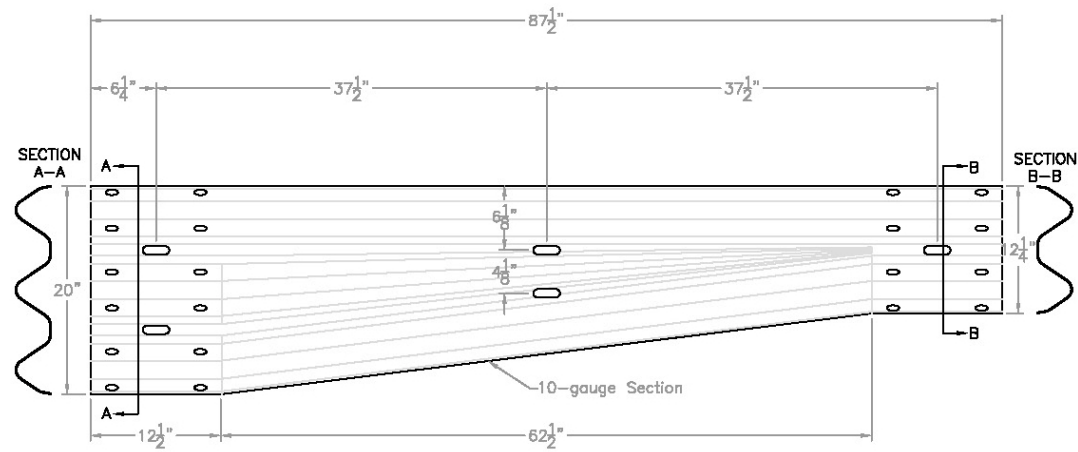


Figure H-2. Layout and Design Details, Design No. 3 (English)




 Midwest Roadside Safety Facility	W-BEAM TO STIFF BRIDGE TRANSITION	Sheet: 3 of 13
	Asymmetrical W-Beam to Thrie Beam Transition Rail Detail	Date: 08/24/2007
Drawing Name: MWT-5 R8.dwg	Scale: 1=10	By: GEP
		Rev: EMA

Figure H-3. Asymmetrical W-Beam to Thrie Beam Transition Rail Detail, Design No. 3 (English)

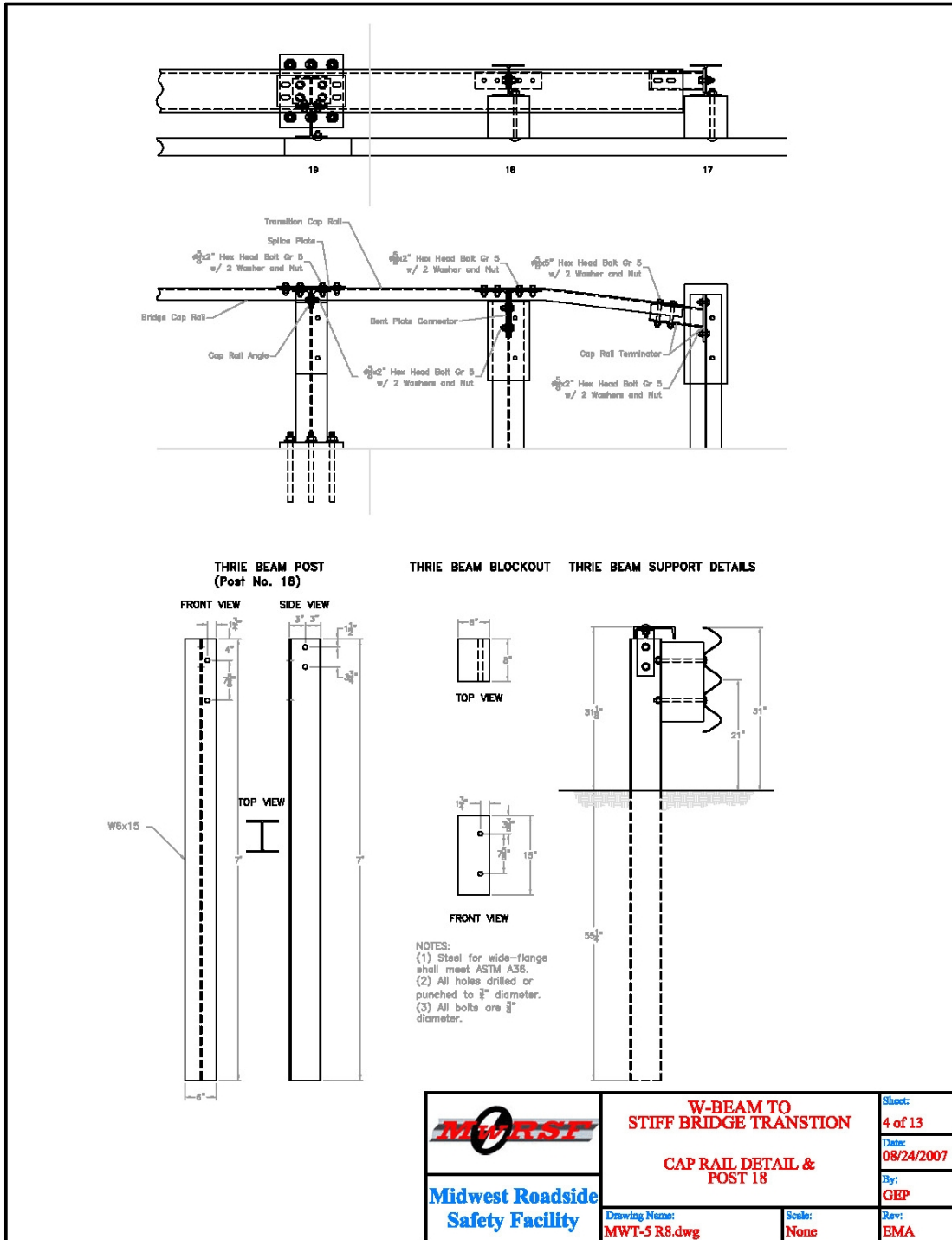


Figure H-4. Cap Rail and Post No. 18 Details- Design No. 3 (English)

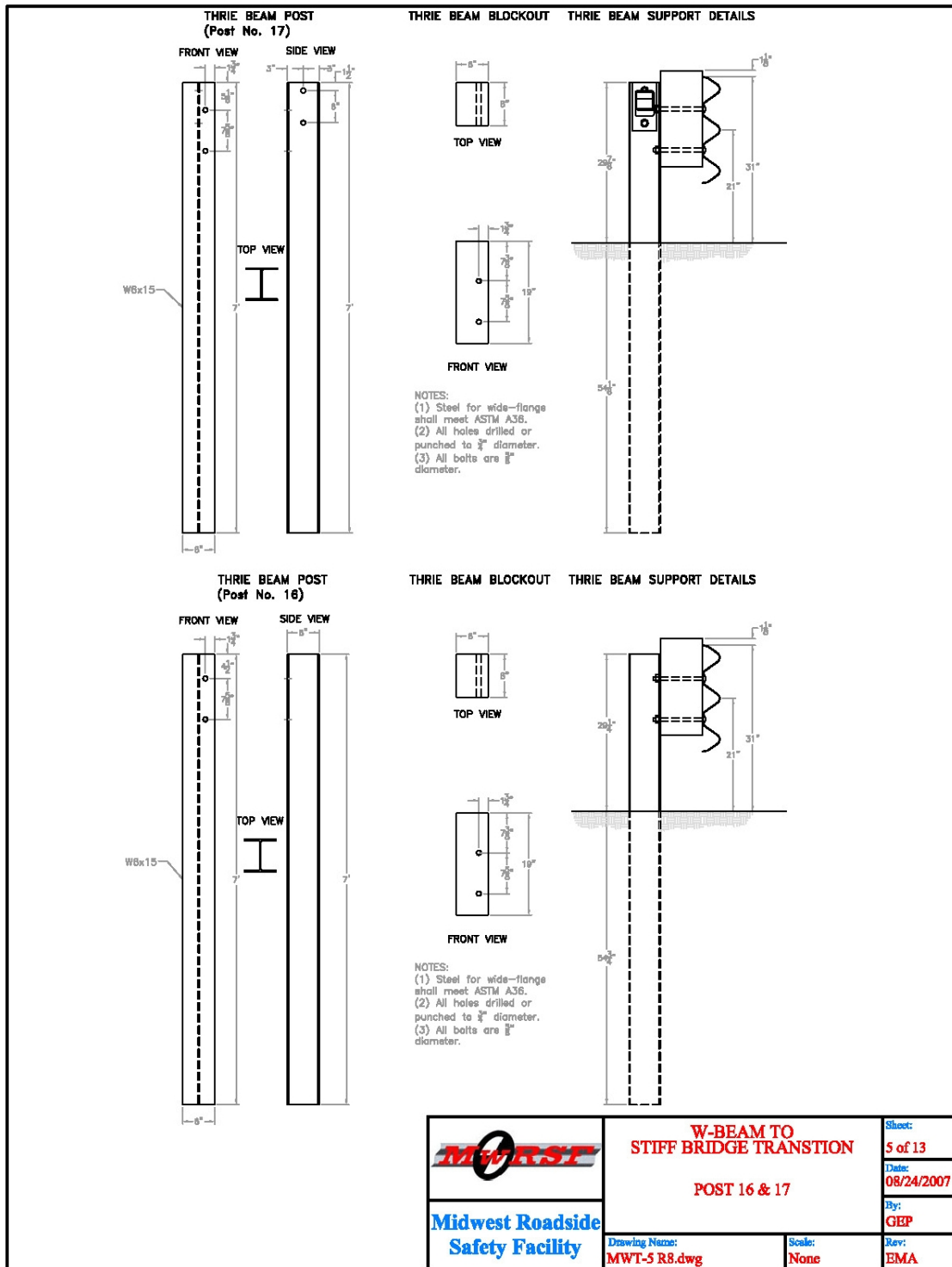


Figure H-5. Post Nos. 16 and 17 Details, Design No. 3 (English)

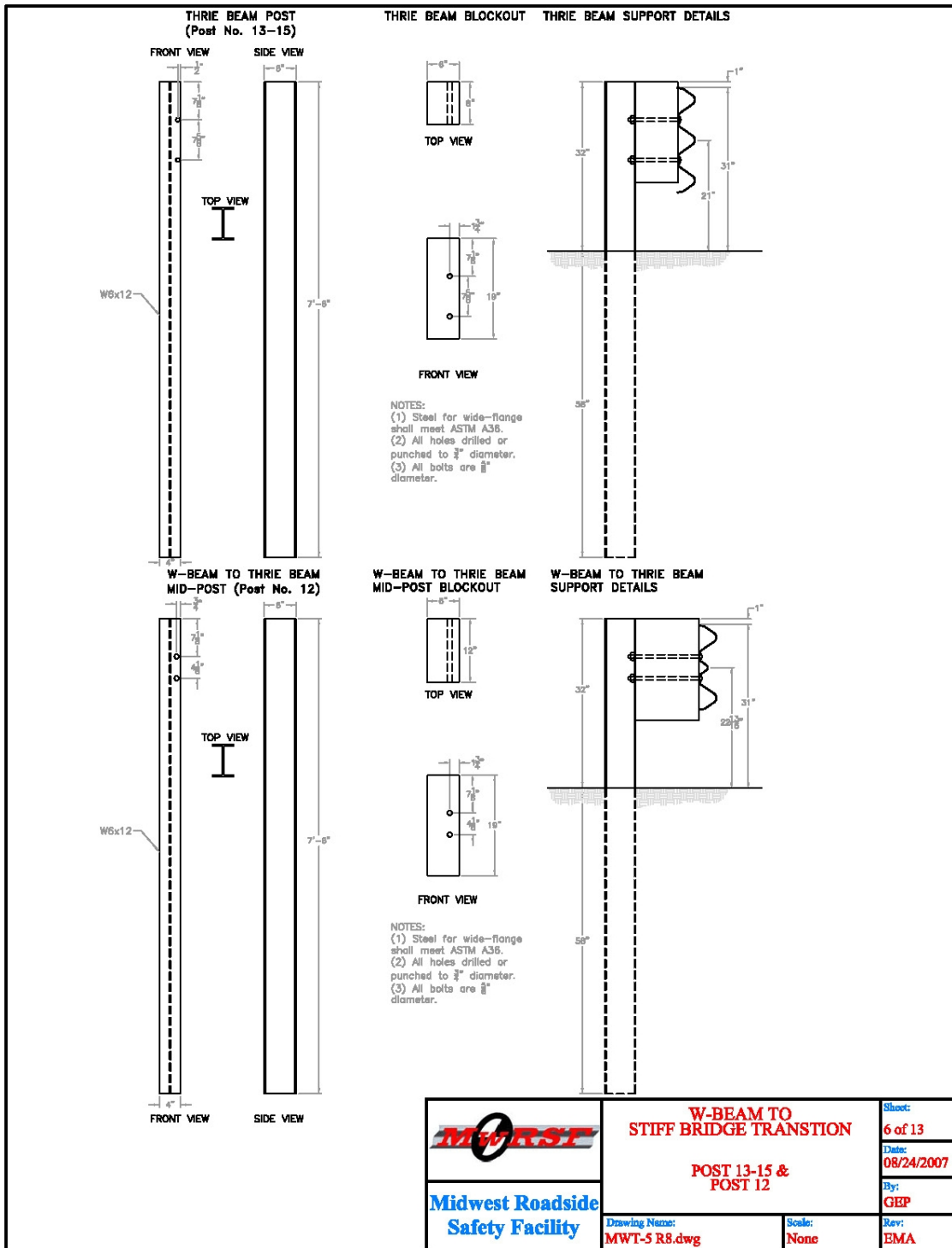


Figure H-6. Post Nos. 12 through 15 Details, Design No. 3 (English)

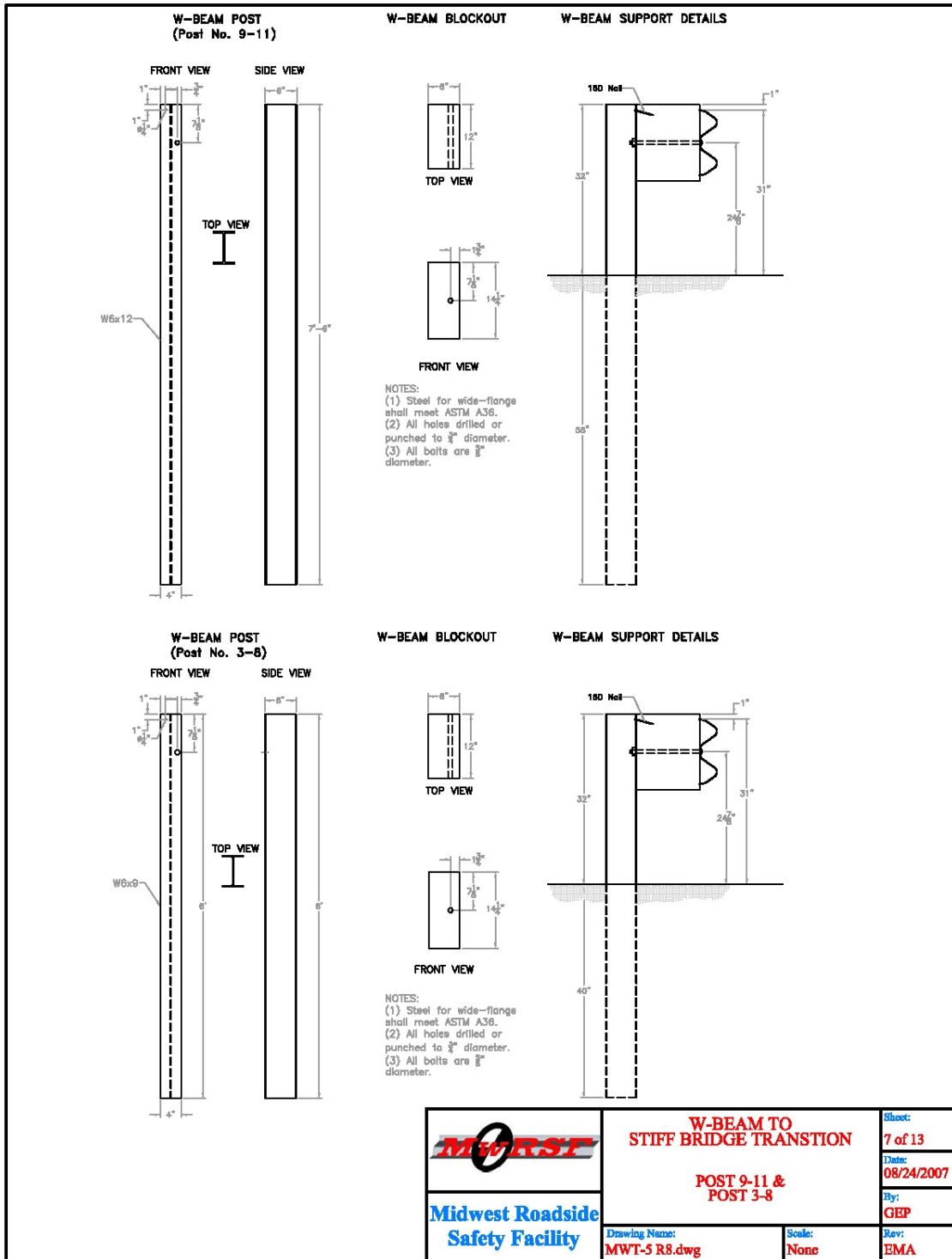


Figure H-7. Post Nos. 3 through 11, Design No. 3 (English)

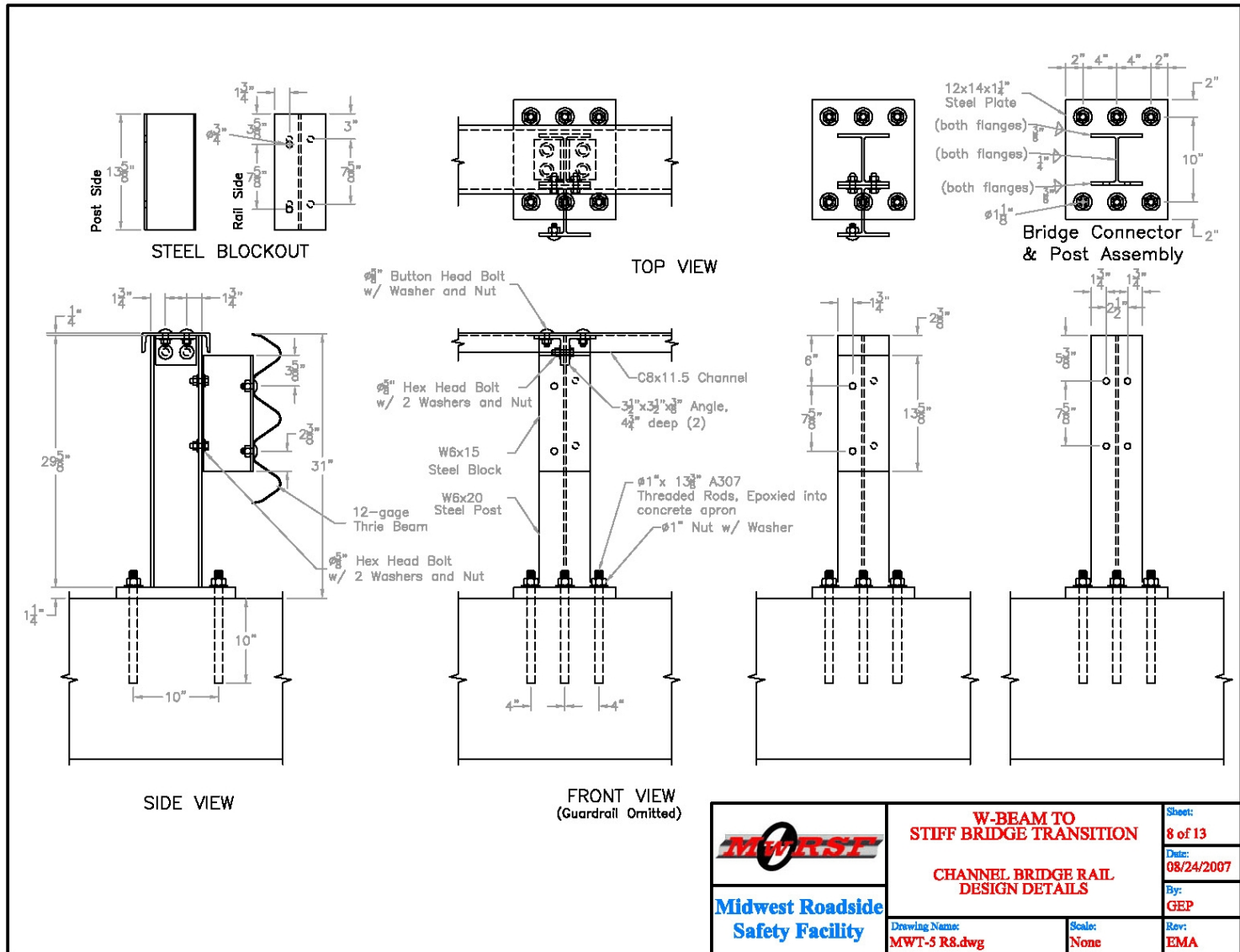


Figure H-8. Channel Bridge Rail Design Details, Design No. 3 (English)

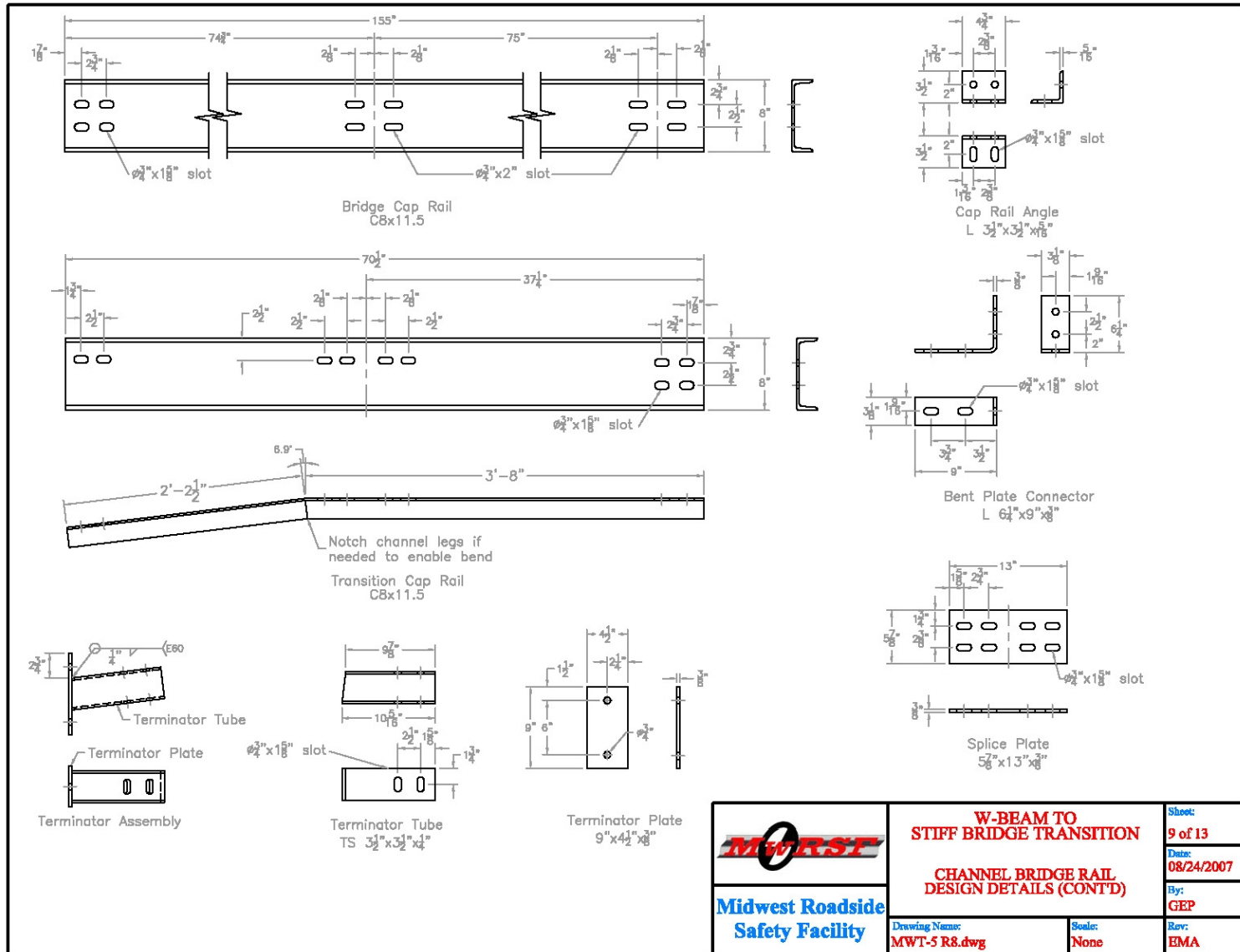


Figure H-9. Channel Bridge Rail Design Details (Continued), Design No. 3 (English)

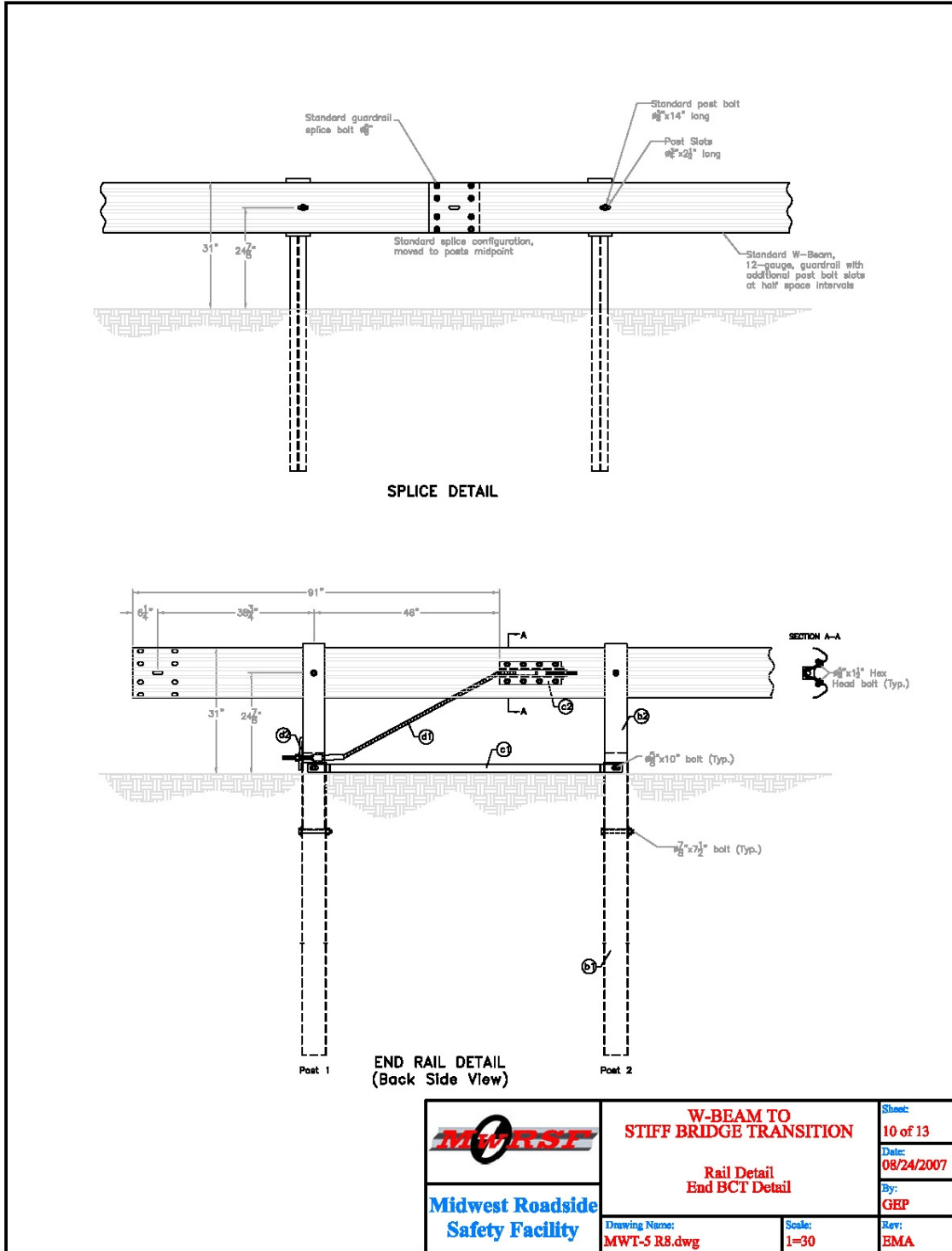
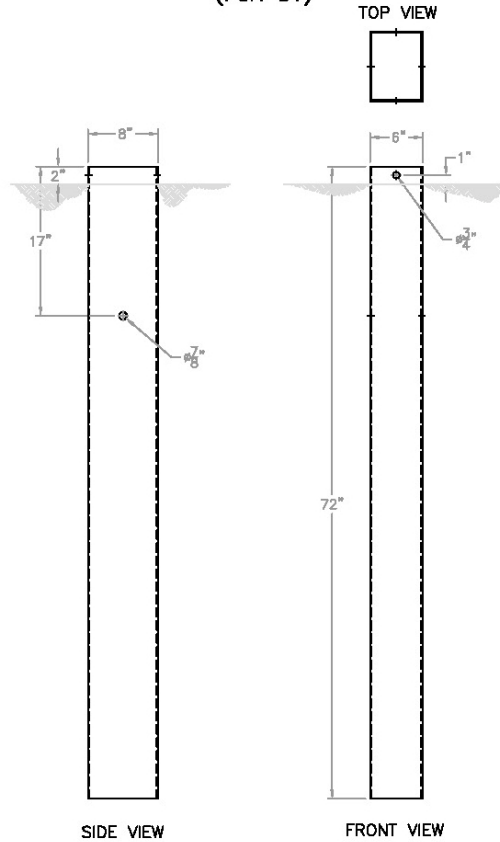


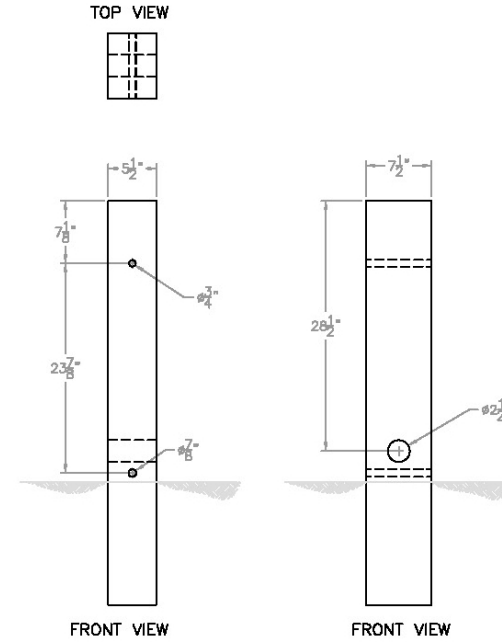
Figure H-10. Rail and End BCT Details, Design No. 3 (English)

ITEM	QTY	DESCRIPTION	MATERIAL
b1	2	Foundation Tubes	PTE05
b2	2	BCT Timber Post	PDF01

MGS FOUNDATION TUBE
(Part b1)



MGS BCT TIMBER POST
(Part b2)



	W-BEAM TO STIFF BRIDGE TRANSITION BCT POST & TUBE DETAIL		Sheet: 11 of 13
	Drawing Name: MWT-5 R8.dwg		Date: 08/24/2007
Soles: 1=16		By: GEP	Rev: EMA

11. BCT Post and Tube Details, Design No. 3 (English)

259

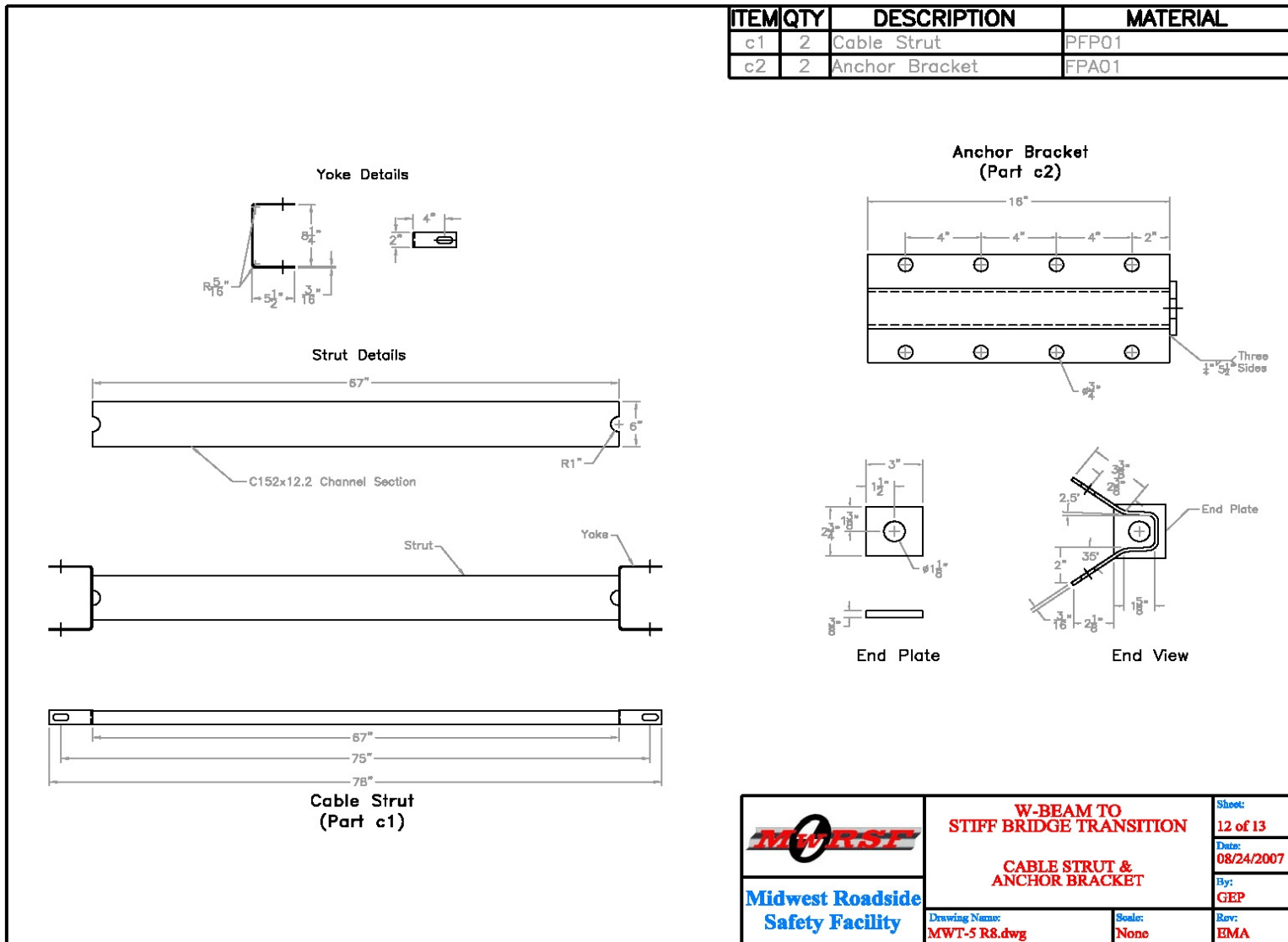


Figure H-12. Cable Strut and Anchor Bracket Details, Design No. 3 (English)

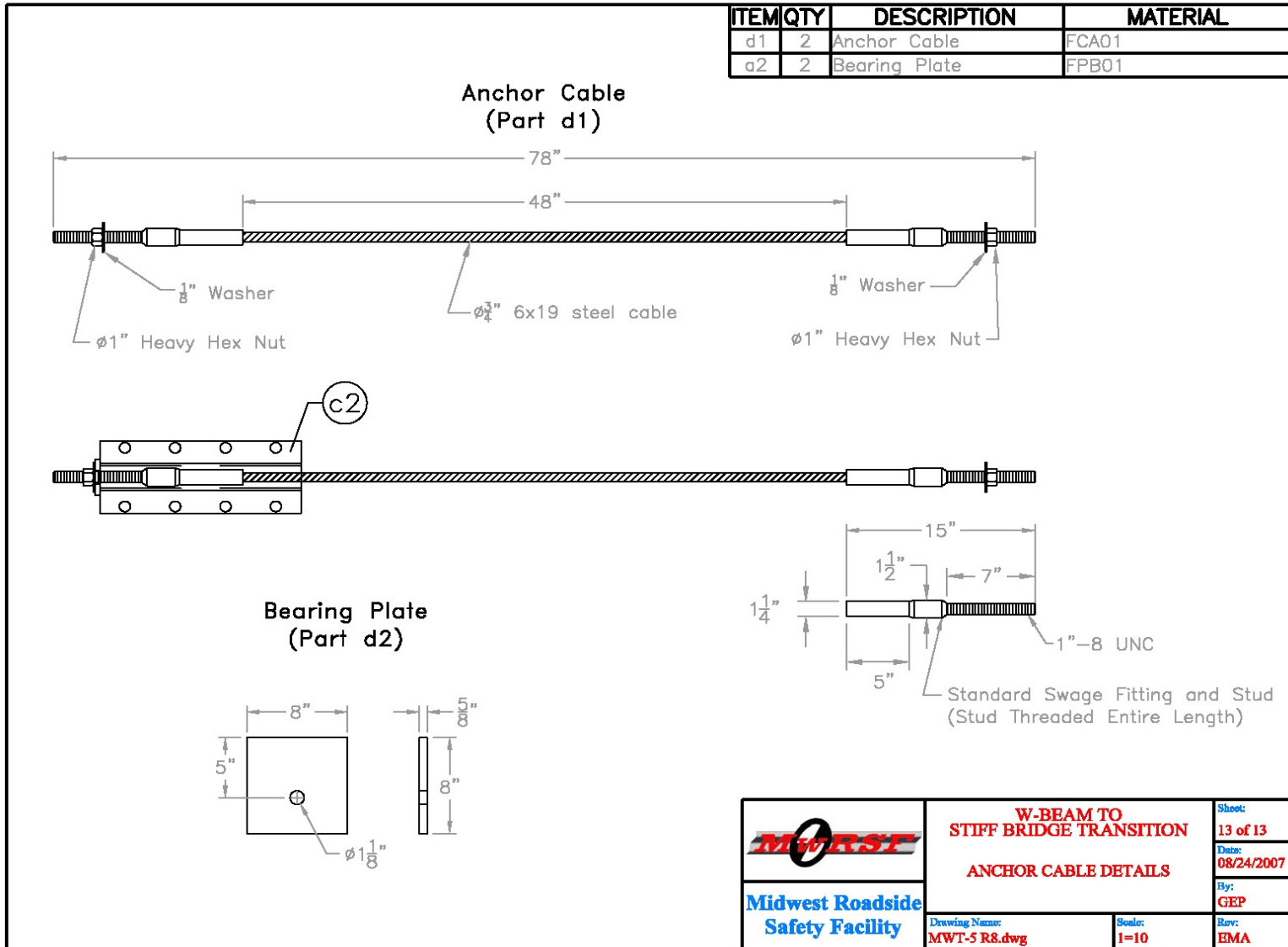


Figure H-13. Anchor Cable Details, Design No. 3 (English)

APPENDIX I

Accelerometer and Rate Transducer Data Analysis, Test MWT-5

Figure I-1. Graph of Longitudinal Deceleration, Test MWT-5

Figure I-2. Graph of Longitudinal Occupant Impact Velocity, Test MWT-5

Figure I-3. Graph of Longitudinal Occupant Displacement, Test MWT-5

Figure I-4. Graph of Lateral Deceleration, Test MWT-5

Figure I-5. Graph of Lateral Occupant Impact Velocity, Test MWT-5

Figure I-6. Graph of Lateral Occupant Displacement, Test MWT-5

Figure I-7. Graph of Roll, Pitch and Yaw Angular Displacements, Test MWT-5

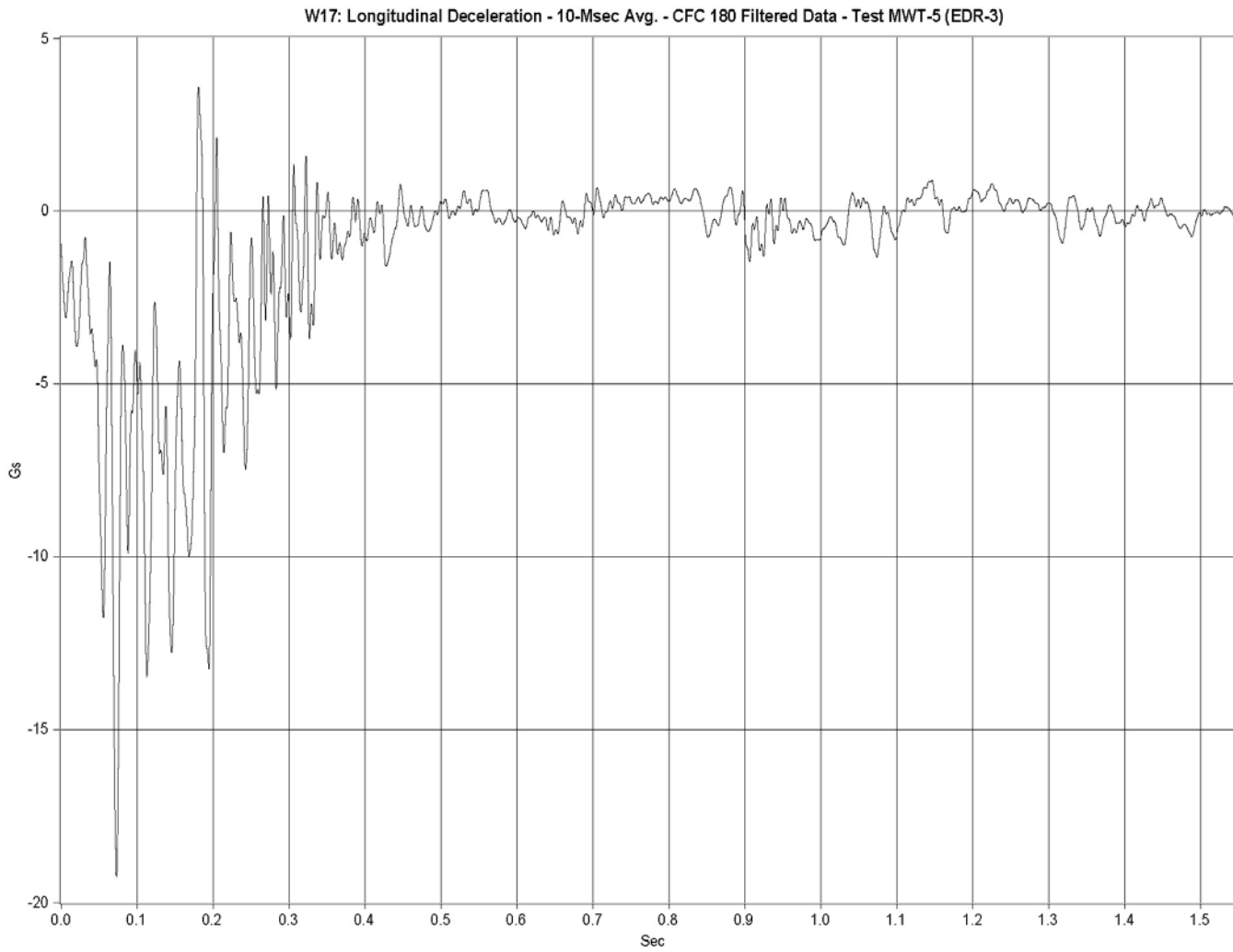


Figure I-1. Graph of Longitudinal Deceleration, Test MWT-5

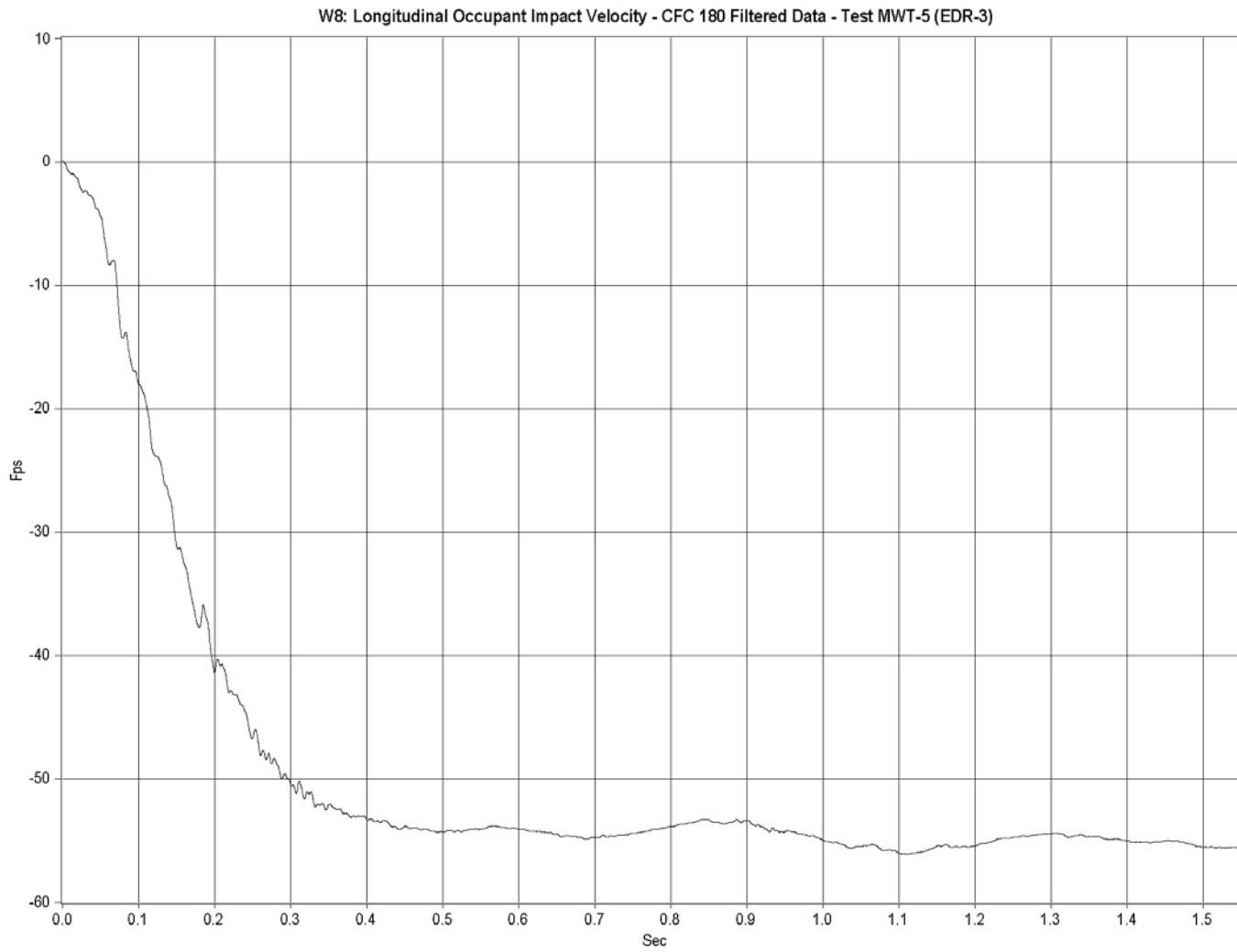


Figure I-2. Graph of Longitudinal Occupant Impact Velocity, Test MWT-5

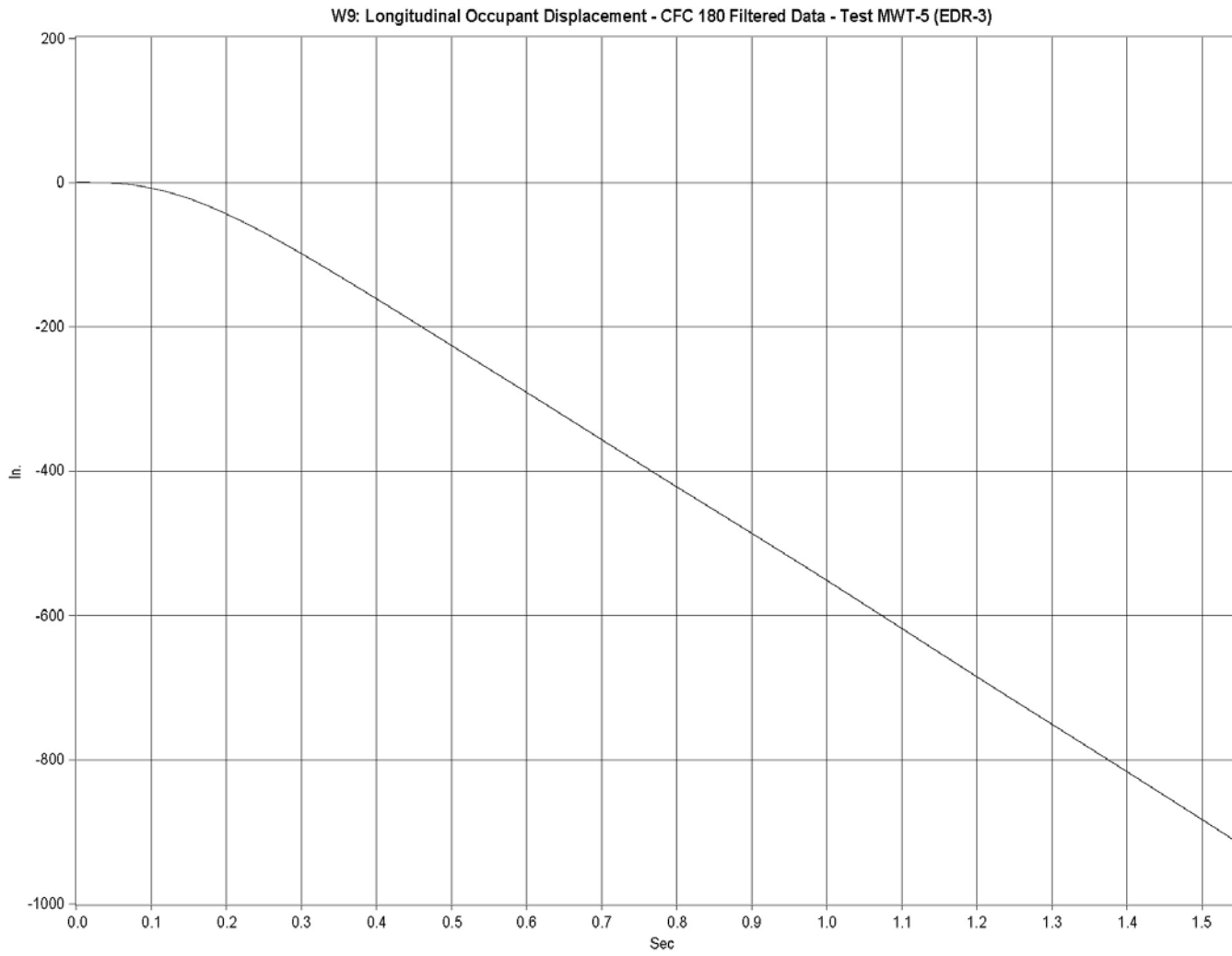


Figure I-3. Graph of Longitudinal Occupant Displacement, Test MWT-5

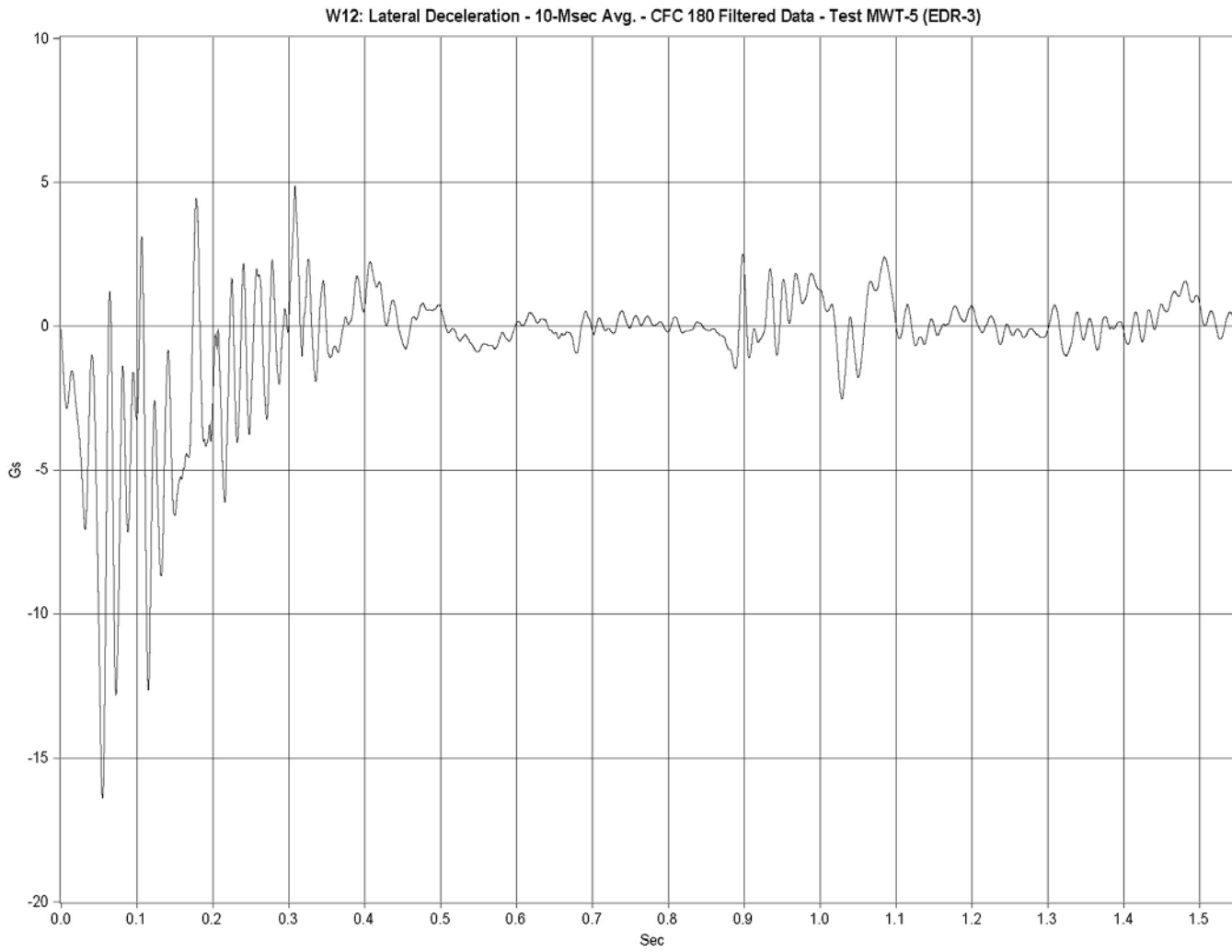


Figure I-4. Graph of Lateral Deceleration, Test MWT-5

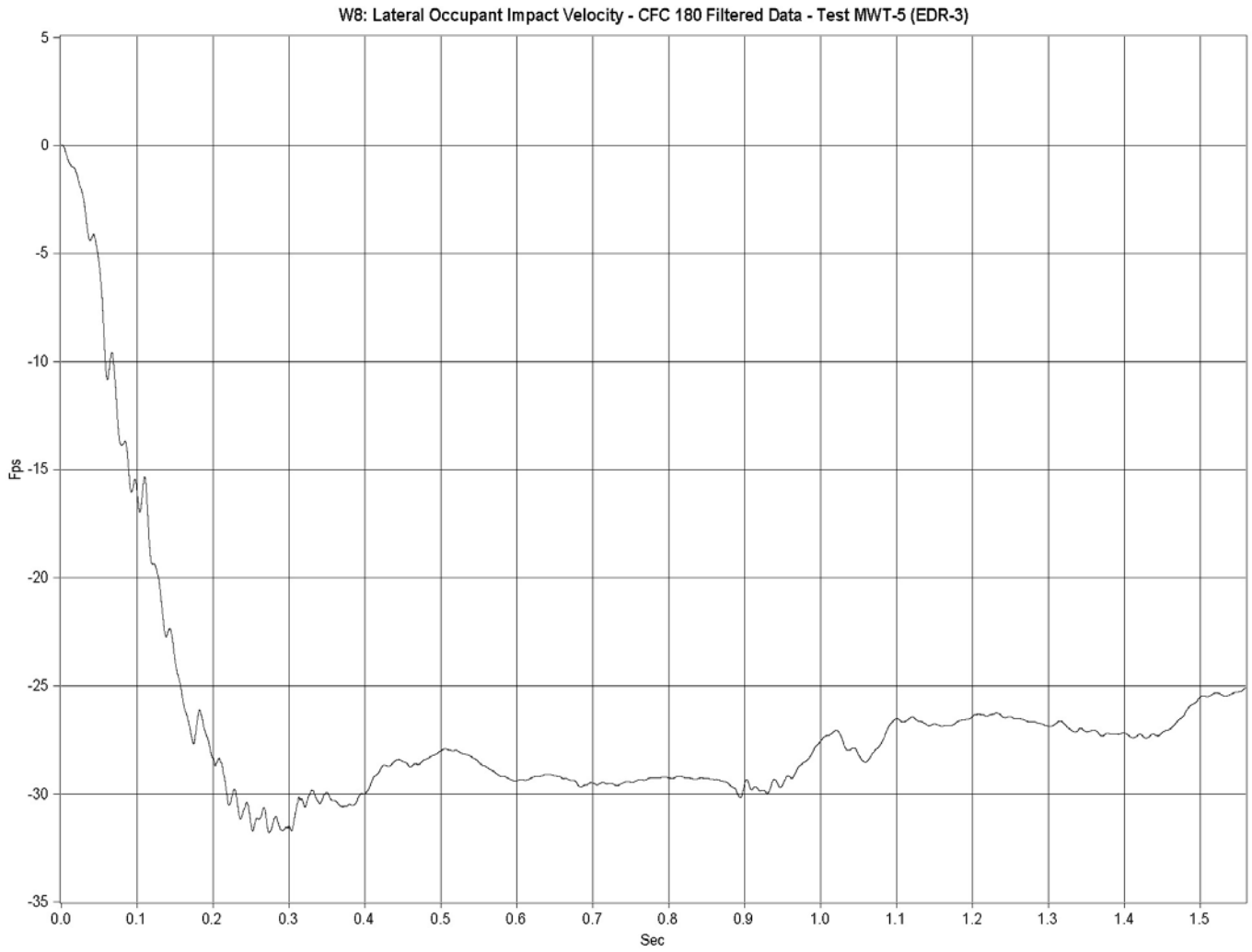


Figure I-5. Graph of Lateral Occupant Impact Velocity, Test MWT-5

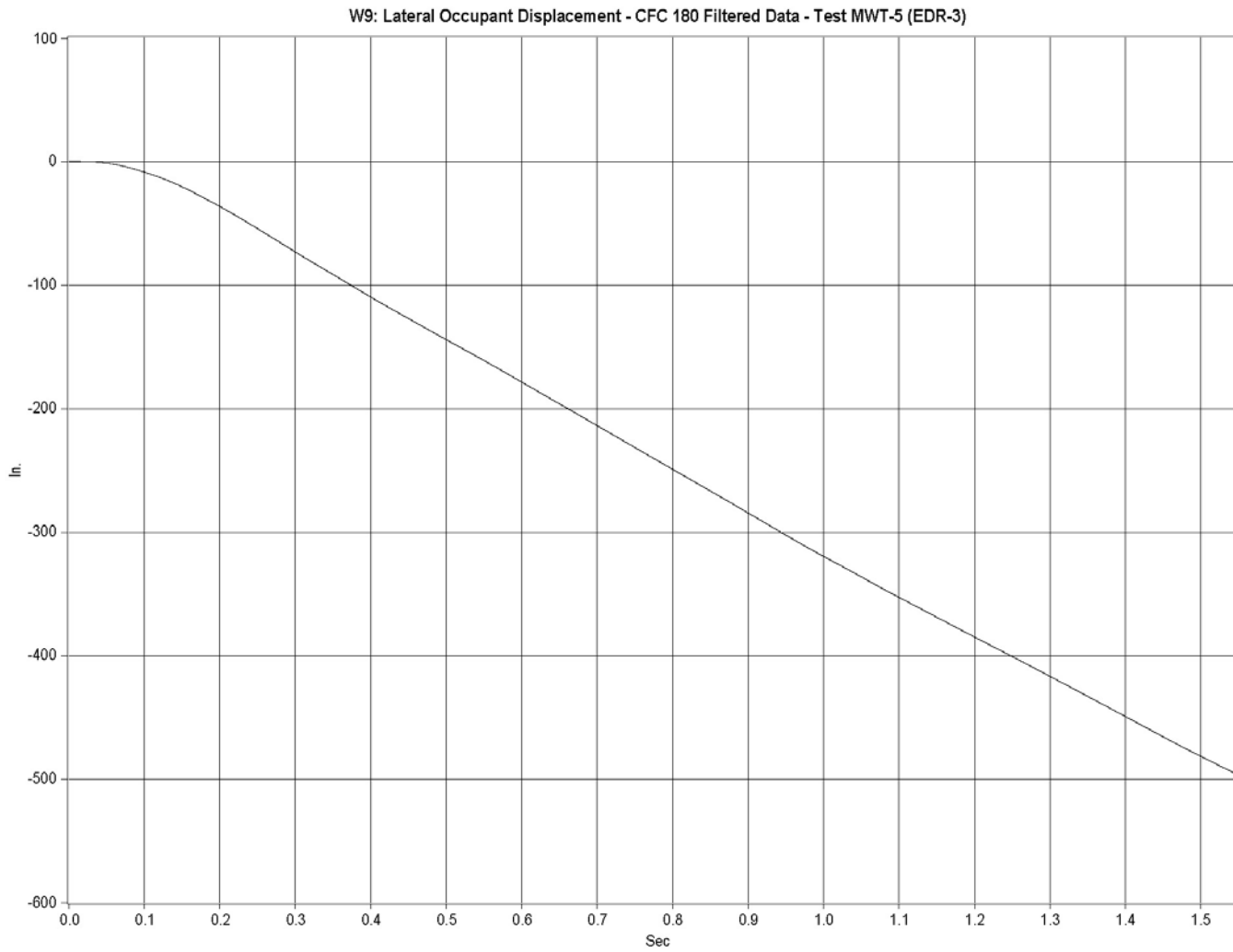


Figure I-6. Graph of Lateral Occupant Displacement, Test MWT-5

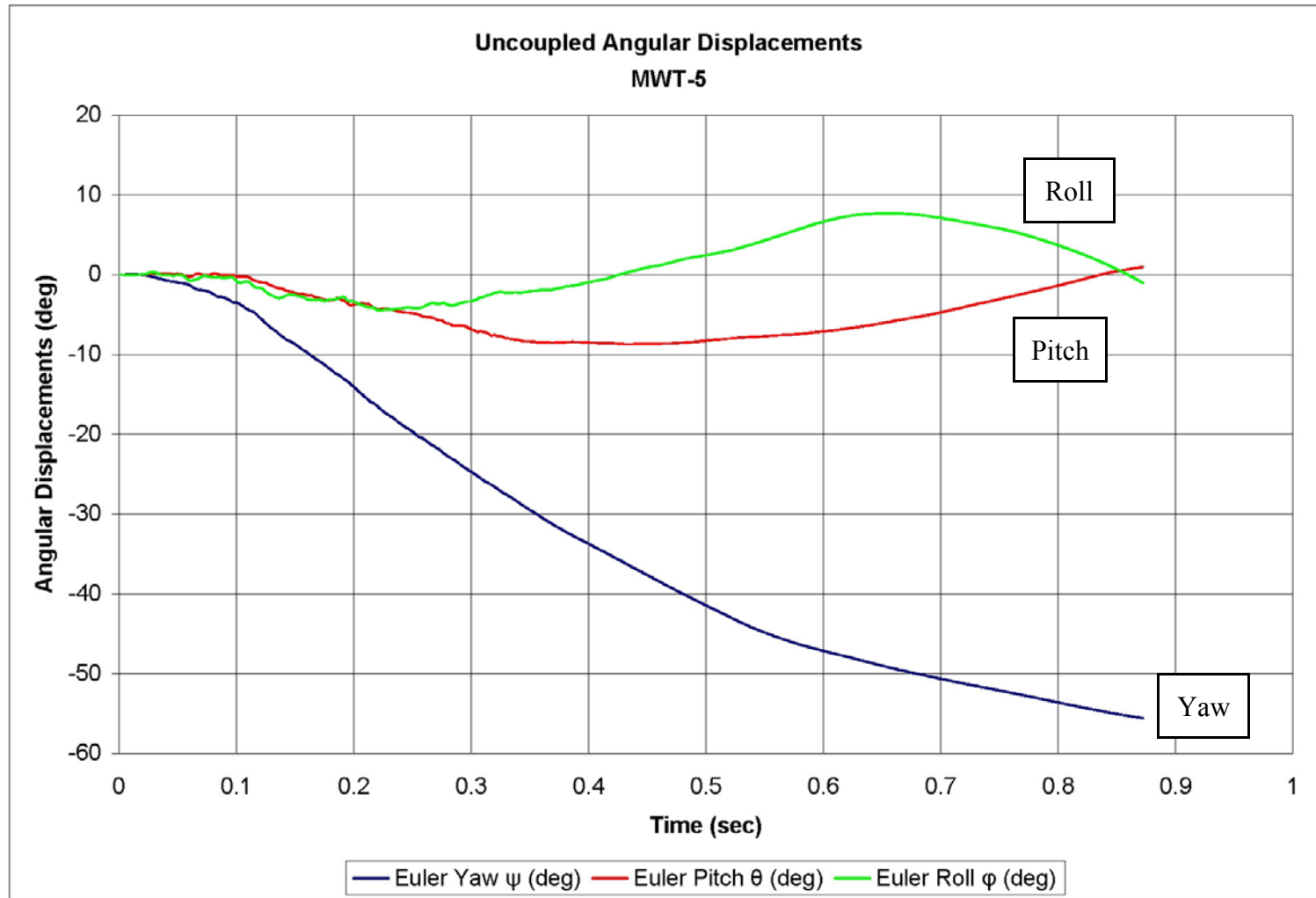


Figure I-7. Graph of Roll, Pitch and Yaw Angular Displacements, Test MWT-5

APPENDIX J

Accelerometer and Rate Transducer Data Analysis, Test MWT-6

Figure J-1. Graph of Longitudinal Deceleration, Test MWT-6

Figure J-2. Graph of Longitudinal Occupant Impact Velocity, Test MWT-6

Figure J-3. Graph of Longitudinal Occupant Displacement, Test MWT-6

Figure J-4. Graph of Lateral Deceleration, Test MWT-6

Figure J-5. Graph of Lateral Occupant Impact Velocity, Test MWT-6

Figure J-6. Graph of Lateral Occupant Displacement, Test MWT-6

Figure J-7. Graph of Roll, Pitch and Yaw Angular Displacements, Test MWT-6

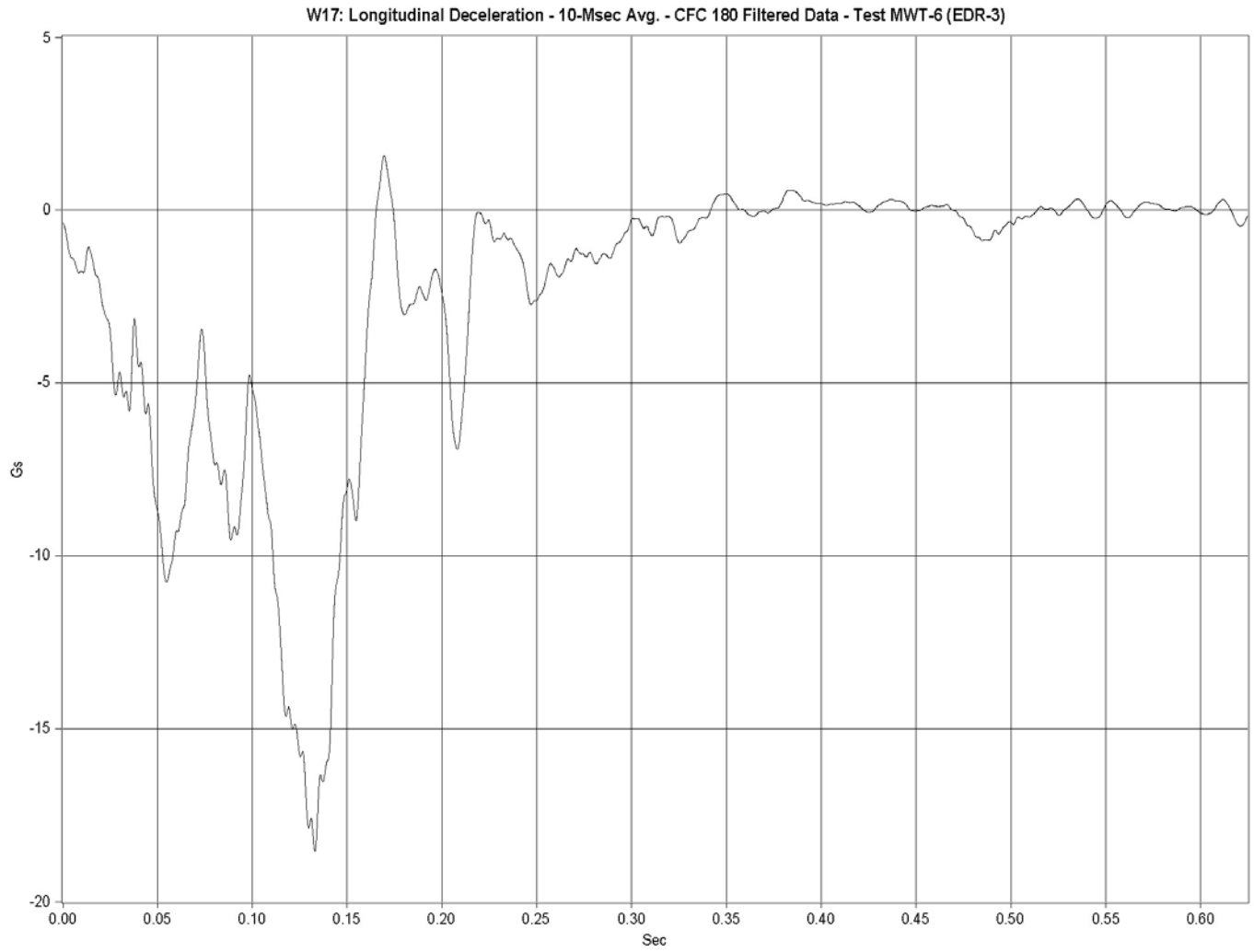


Figure J-1. Graph of Longitudinal Deceleration, Test MWT-6

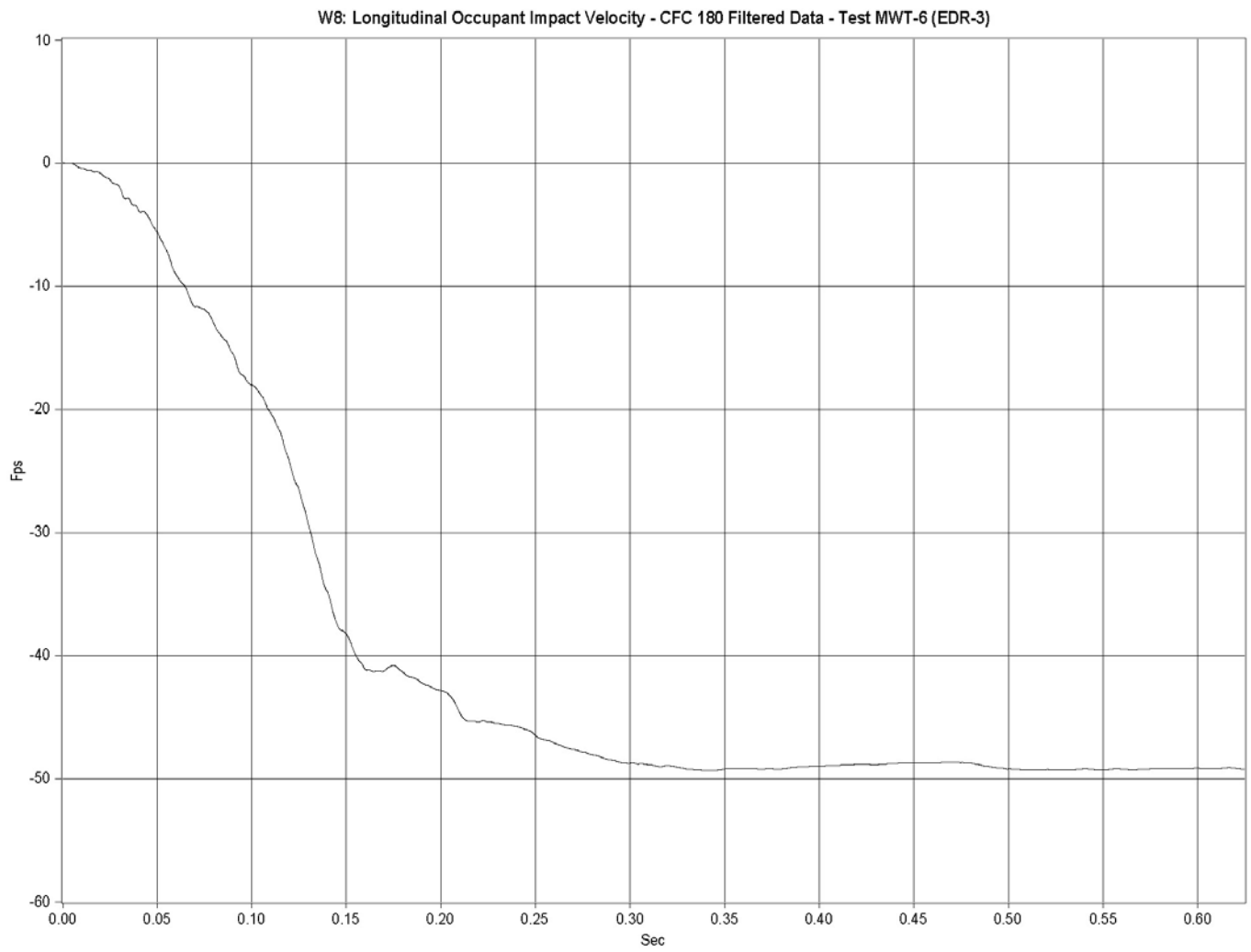


Figure J-2. Graph of Longitudinal Occupant Impact Velocity, Test MWT-6

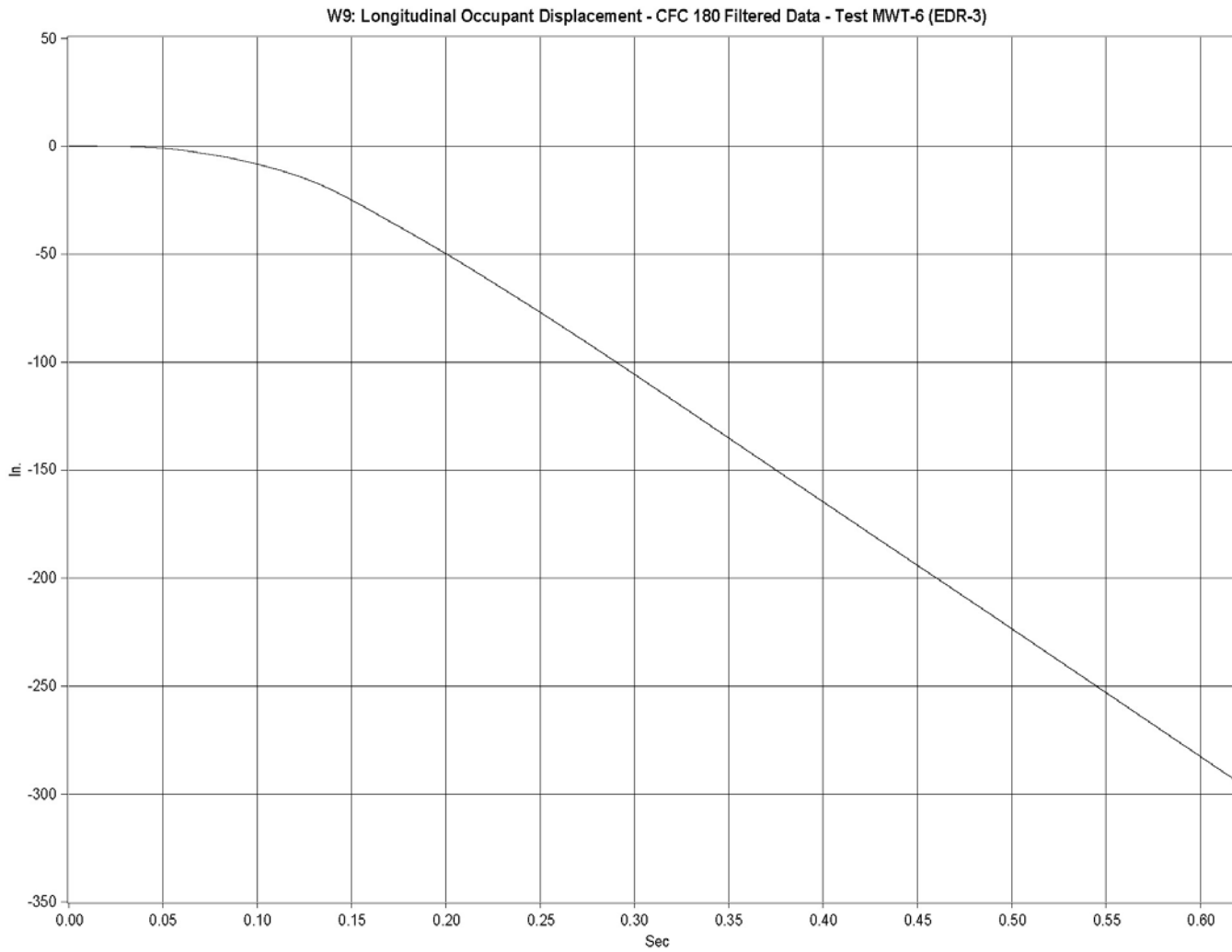


Figure J-3. Graph of Longitudinal Occupant Displacement, Test MWT-6

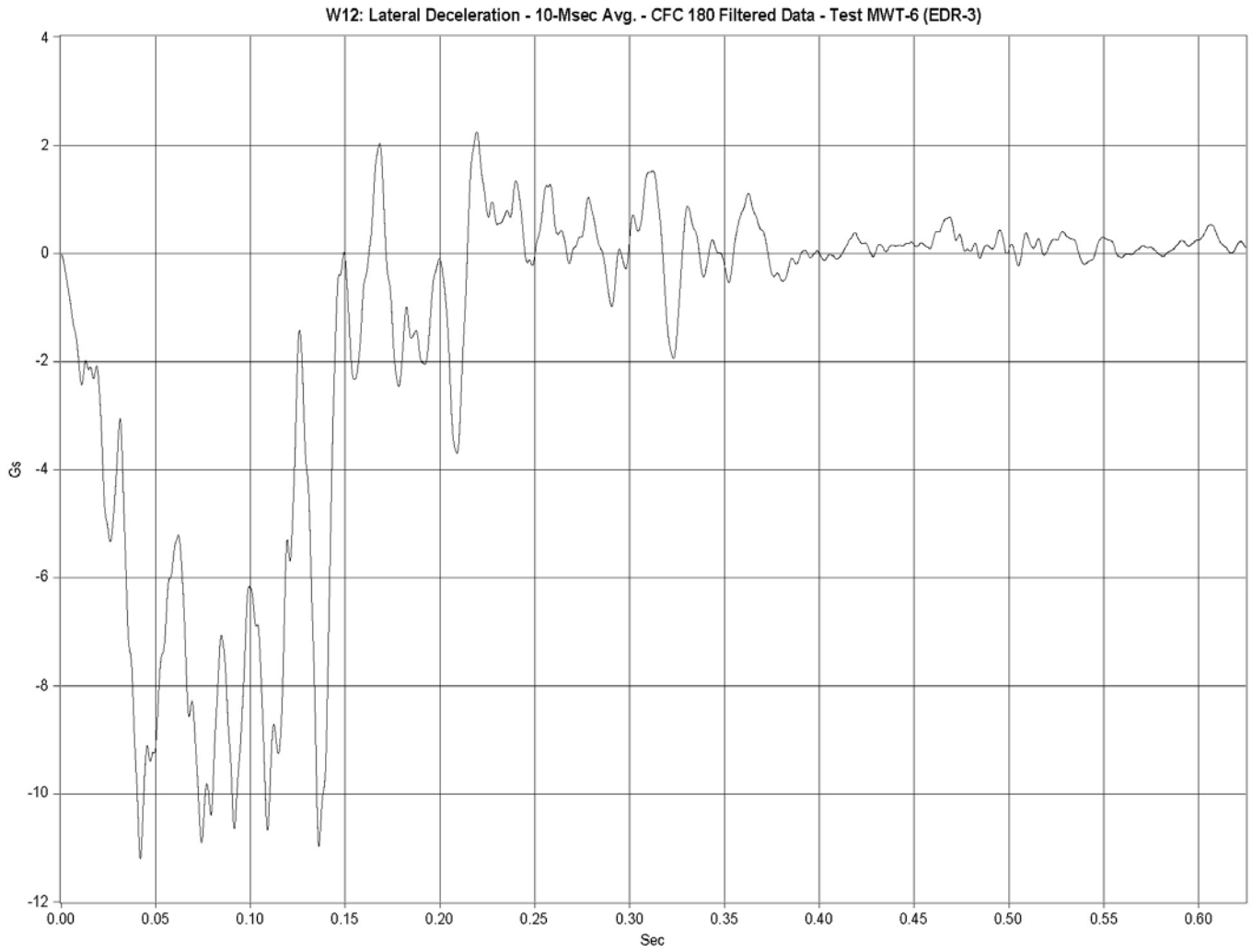


Figure J-4. Graph of Lateral Deceleration, Test MWT-6

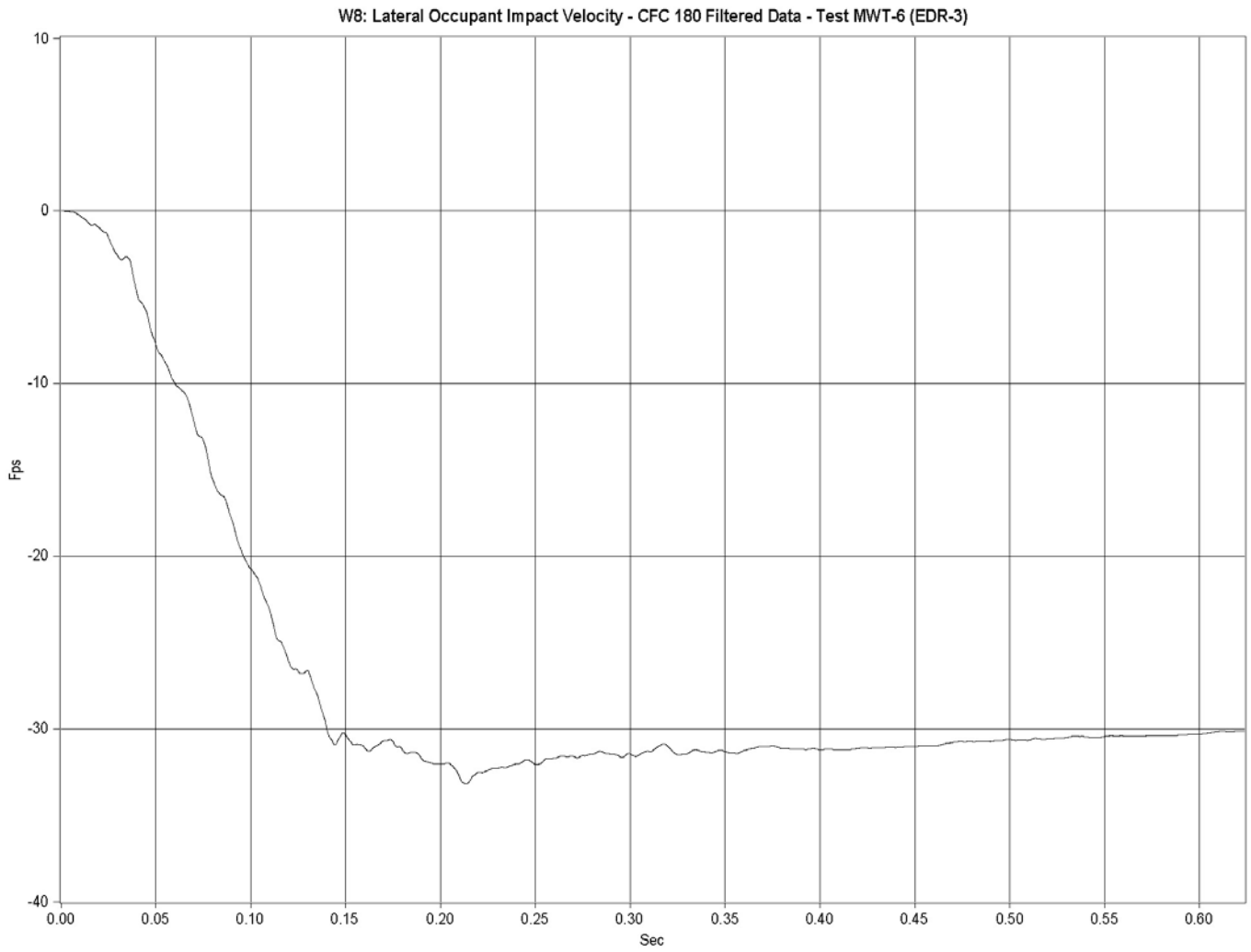


Figure J-5. Graph of Lateral Occupant Impact Velocity, Test MWT-6

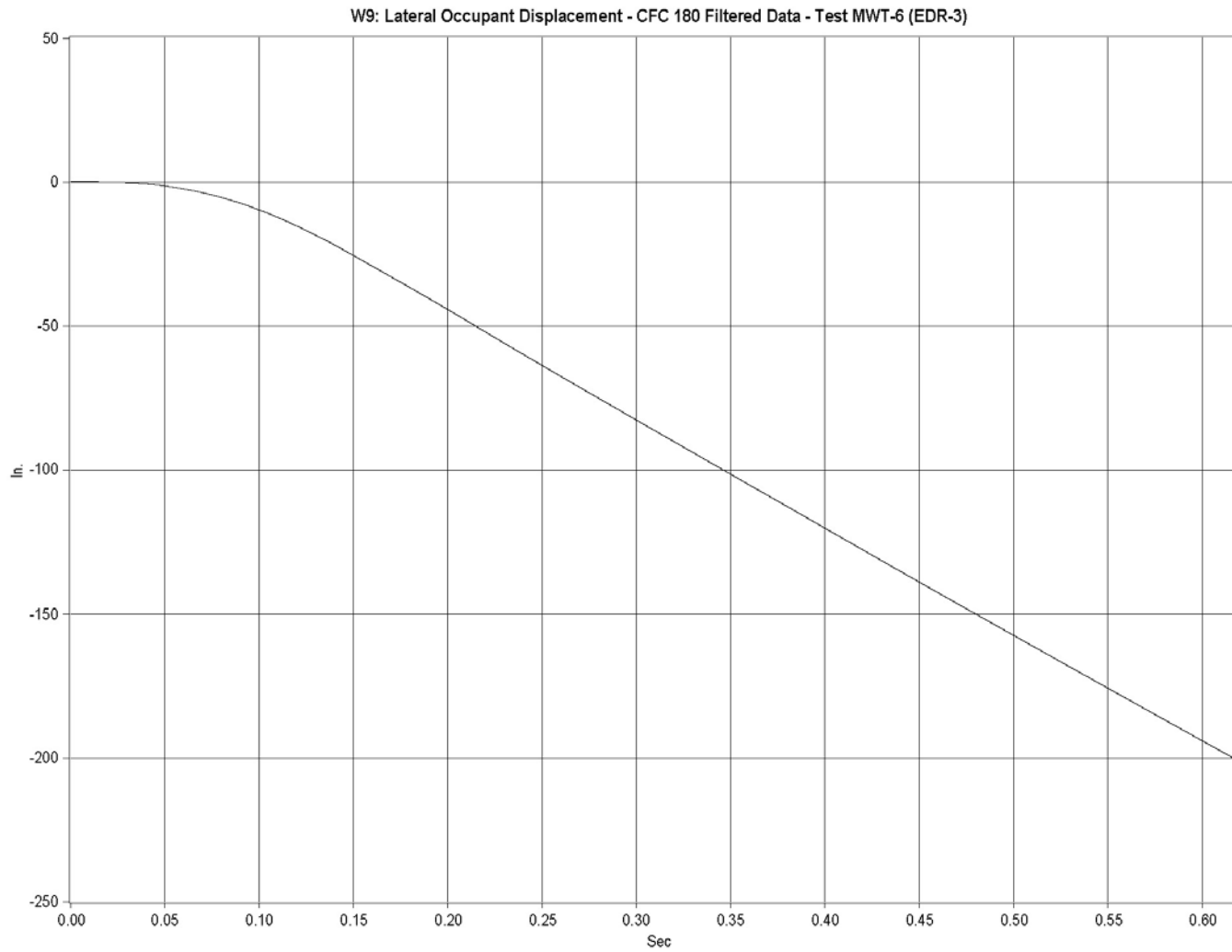


Figure J-6. Graph of Lateral Occupant Displacement, Test MWT-6

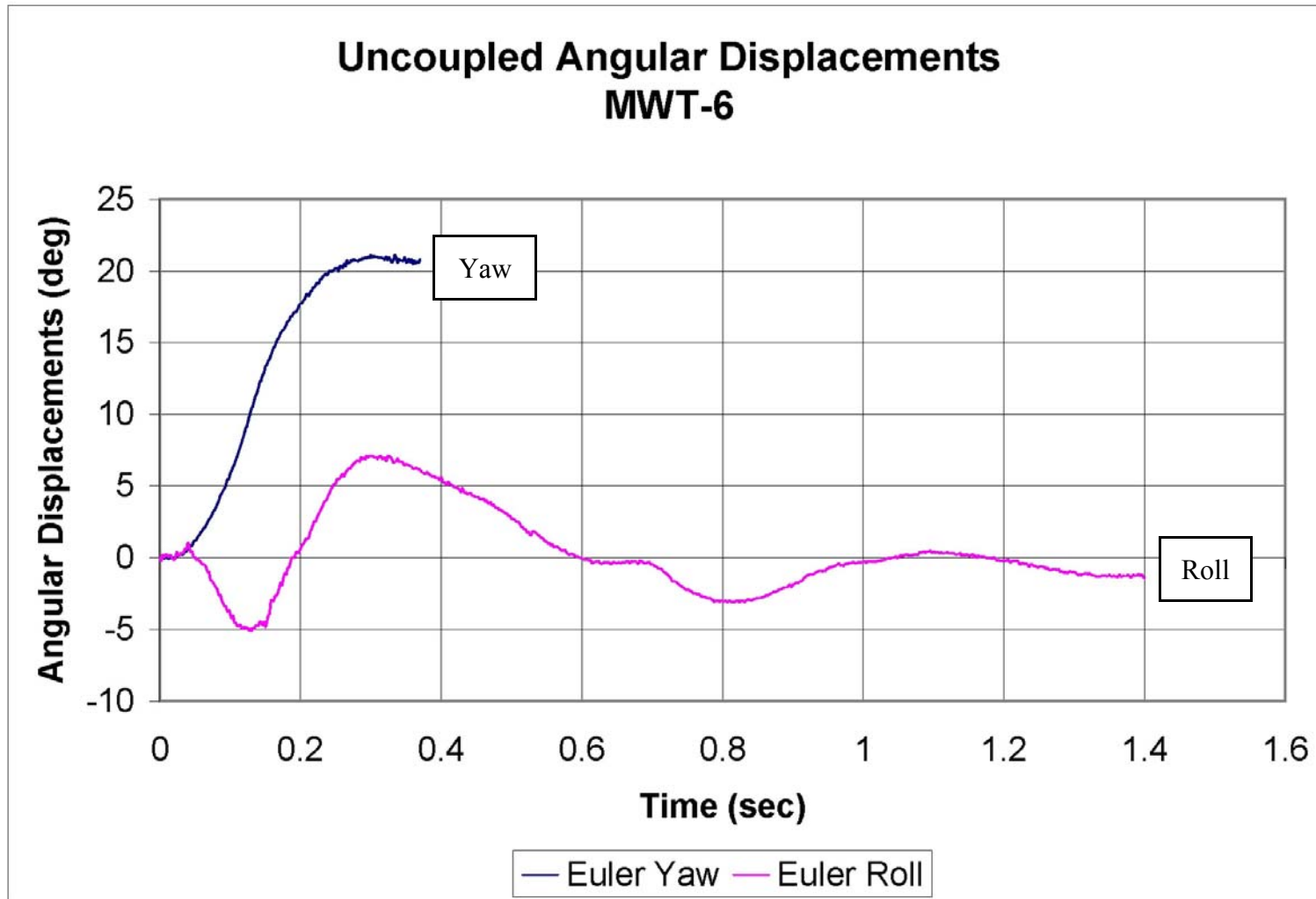


Figure J-7. Graph of Roll, Pitch and Yaw Angular Displacements, Test MWT-6